Isolation, Characterisation and Assessment of Therapeutic Potential of Bacteriophages Which Infect *P. multocida*

Ibrahim Besler

Thesis submitted to the University of Nottingham for the Degree of Doctor of Philosophy

School of Veterinary Medicine and Science,
University of Nottingham, UK

Supervisors: Dr Michael Jones, Dr Robert Atterbury

Student ID: 20129959

Signature:

Abstract

Pasteurella multocida (P. multocida) is a significant veterinary pathogen causing infections in avian and mammalian species, leading to substantial economic losses globally, particularly where multidrug-resistant (MDR) strains complicate treatment. Bacteriophage therapy presents a potential alternative to combat these infections, especially where conventional antibiotics are failing. This study aimed to isolate and characterise novel *P. multocida* phages from environmental sources and evaluate their therapeutic potential.

Fifteen distinct bacteriophages specifically targeting *P. multocida* were successfully isolated from raw sewage samples. All isolates were identified as tailed phages similar to the *Siphoviridae* like morphology, possessing icosahedral capsids and linear double-stranded deoxyribonucleic acid (dsDNA) genomes. Physiological characterisation revealed stability across a pH range of 4-10 and temperatures up to 50°C, with three phages demonstrating notable tolerance up to 60°C. The phages exhibited narrow host ranges and moderate replication kinetics, with an average latent period of 40 minutes and burst sizes ranging from 30.2 to 52.5 PFU/cell. Genomic analysis confirmed high sequence similarity among the isolates and classified them as temperate Mu-like phages (*Vieuvirus* genus), closely related to prophages found in *P. multocida* genomes but distinct from previously characterised lytic phages. *In vivo* assessment using a *Galleria mellonella* infection model with selected phages (P1 and N1) demonstrated that prophylactic administration provided significantly greater protection against lethal *P. multocida* challenge compared to therapeutic treatment.

These findings contribute novel temperate phages to the repertoire available for combating *P. multocida*. While their temperate nature requires careful consideration for therapeutic use, their stability, lack of detrimental genes and demonstrated *in vivo* efficacy, particularly prophylactically, highlight their potential. This work underscores the importance of phage characterisation and timing of administration in developing effective phage-based control strategies against *P. multocida*, adding valuable information on Mu-like phage biology and temperate phage potential in invertebrate infection models.

Declaration

I declare that the work in this dissertation was carried out in accordance with the regulations of the University of Nottingham.

The work is original and has not been submitted for any other degree at the University of Nottingham or elsewhere.

Name: Ibrahim Besler

Signature: 

Date: 29/06/2025

Acknowledgements

I would like to express my gratitude to the many valuable people who contributed to and supported the preparation of this thesis. First and foremost, I extend my heartfelt thanks to my supervisors, Dr. Michael Jones and Dr. Robert Atterbury, who guided me throughout my studies, sharing their knowledge and experience and standing by me in overcoming every challenge. Their invaluable contributions and guidance were essential to the completion of this work. Finally, I would want to express my gratitude for always expecting more from me than my best, for your honest and instructive guidance, motivating me to maintain an appearance of professionalism at all times and demonstrating how to create exceptional work that meets the high standards of scientific study.

I am deeply grateful to the Ministry of National Education of the Republic of Turkey for providing the financial support necessary to conduct this research and continue my academic career. Their scholarships and support played a significant role in making this work possible.

My family has always been my greatest source of motivation, standing by me and supporting me unconditionally. I extend my endless thanks to my beloved wife Sevgi Herek Besler, my mother Mürvet Besler, my father Ahmet Besler and my daughter Nil Besler. Their patience, understanding and love made it possible for me to complete this work. Especially, the smiles and joy of my daughter Nil gave me strength even in the most challenging moments.

And most importantly, I would like to express my gratitude to the great leader Mustafa Kemal Atatürk, who inspired me and many other young people by saying, "I am sending you as a spark; you shall return as a flame!" His vision and ideals guided me on this path and always illuminated my way.

This thesis was made possible through the contributions and support of all these valuable individuals. I thank each one of them individually and express my deepest gratitude.

Table of Contents

List of Tables

List of Figures

List of Abbreviations

Full Term	Abbreviation
Abortive Infection	Abi
Adenylate Kinase	adk
Ampicillin (10 µg/disc)	AMP10
American Type Culture Collection	ATCC
Animal and Plant Health Agency (UK)	APHA
Anti-CRISPR	ACR
Antimicrobial Resistance	AMR
Automated Tissue Lysis	ATL
Atrophic Rhinitis	AR
Average Daily Gain	ADG
Base Pairs	bp
Basic Local Alignment Search Tool	BLAST
Blood Agar Base	BAB
Blood Agar Base No.2	BAB No.2
Bovine Respiratory Disease	BRD
Bovine Serum Albumin	BSA
Brain Heart Infusion	BHI
British Society for Allergy & Clinical Immunology	BSACI
Calcium Chloride	$CaCl_2$
Capsule Gene-Specific Primers for *P. multocida*	CAPA/B/D/E/F
Capsular Gene Associated with *P. multocida* Serogroup F	fcbD
Capsular Polysaccharide Biosynthesis Gene (Serogroup E)	ecbJ
Capsular Polysaccharide	CPS
Cefotaxime (5 µg/disc)	CTX5
cGAS/DncV-like Nucleotidyltransferase	CD-NTase
Cesium Chloride	CsCl
Clustered Regularly Interspaced Short Palindromic Repeats	CRISPR
Colony-Forming Units	CFU
Cyclic Oligonucleotide-Based Anti-Phage Signalling System	CBASS
Day	d
Deionised Water	diH_2O
Degrees Celsius	°C
Digital PCR	dPCR
Dimensional Unit of Dynamic Viscosity	η
Deoxyribonucleic Acid	DNA

Full Term	Abbreviation
Double-Stranded Deoxyribonucleic Acid	dsDNA
Double-Stranded Ribonucleic Acid	dsRNA
Dodecameric Portal Protein	PP
Efficiency of Plaquing	EOP
Elution Buffer (for DNA recovery)	AE
Enzyme-Linked Immunosorbent Assay	ELISA
Enterococcus faecium, Staphylococcus aureus, Klebsiella pneumoniae, Acinetobacter baumannii, P. aeruginosa and Enterobacter spp.	ESKAPE
Epifluorescence Microscopy	EFM
Esterase	est
Exopolysaccharide	EPS
Feed Conversion Rate	FCR
Fetal (Foetal) Bovine Serum	FBS
Flow Cytometry	FCM
Fowl Cholera	FC
g (gram)	g
g (gravitational force, italicised)	*g*
Galleria mellonella (wax moth larva, in vivo model)	*G. mellonella*
Gene Transfer Agent	GTA
Genetic Modification / Good Manufacturing Practice	GMP
Glucose-6-Phosphate Dehydrogenase	gdh / zwf
Haemorrhagic Septicaemia	HS
Haemophilus influenzae Restriction Enzyme	HindIII
High-Fidelity (polymerase)	HF
High-Stringency Wash Buffer	AW2
Hydrogen Peroxide	H_2O_2
Hydroxymethylcytosine	hmC
Immature Forming Areas (in phage plaques)	IFAs
Immune Modulation Protein	Imm
Integrative and Conjugative Element	ICE
International Committee on Taxonomy of Viruses	ICTV
Ion-Exchange Chromatography	IEX
Intramuscular	IM
Intraperitoneal	IP
Intravenous	IV
Kilobase pairs	kb
Limulus Amebocyte Lysate	LAL

Full Term	Abbreviation
Lipopolysaccharide	LPS
Luria-Bertani (media)	LB
Magnesium Sulphate Heptahydrate	$MgSO_4 \cdot 7H_2O$
Malate Dehydrogenase	mdh
Mannheimia haemolytica	*M. haemolytica*
Matrix Protein (Outer Membrane)	OMP
Maximum Likelihood Sequence Typing	MLST
Microgram	µg
Microlitre	µL
Micrometre	µm
MicroMole	µM
Millilitre	mL
Millimole	mM
Minute	min
Minimum Inhibitory Concentration	MIC
Mononuclear Phagocyte System	MPS
Mole	M
Multiplicity of Infection	MOI
Nalidixic Acid (30 µg/disc)	NA30
Not Applicable / Not Available	n/a
Next-Generation Sequencing	NGS
Optical Density	OD
Optical Density at 600 nm	OD_{600}
Outer Membrane Lipoprotein TRAT	TRAT
Outer Membrane Protein	OMP
Outer Membrane Protein A	OMPA
Outer Membrane Protein H	OMPH
Pathogen-Associated Molecular Pattern	PAMP
Pasteurella multocida	*P. multocida*
Pasteurella multocida Toxin	PMT
Pasteurella Selective Media	PSM
PCR Primers Targeting kmt1 Gene	KMT1T7 / KMT1SP6
Penicillin G (1 µg/disc)	PG1
Peptidoglycan	PG
Pharmacodynamic	PD
Pharmacokinetic	PK

Full Term	Abbreviation
Phosphate-Buffered Saline	PBS
Phosphoglucose Isomerase	pgi
Phosphomannose Isomerase	pmi
Plaque-Forming Units	PFU
Plaque-Forming Units per Millilitre	PFU/mL
Polyethylene Glycol	PEG
Potassium Chloride	KCl
Quantitative Polymerase Chain Reaction	qPCR
Receptor-Binding Protein	RBP
Restriction Endonuclease	R-E
Restriction Fragment Length Polymorphism	RFLP
Restriction–Modification System	R-M system
Reverse Osmosis	RO
Ribonucleic Acid	RNA
Ribosomal Ribonucleic Acid	rRNA
Round Per Minute	rpm
Second	s
Size-Exclusion Chromatography	SEC
Sodium Chloride	NaCl
Sodium Dodecyl Sulfate	SDS
Spectinomycin (25 μg/disc)	SH25
Standard Deviation	SD
Standard Error of the Mean	SEM
Staphylococcus aureus	*S. aureus*
Streptomycin (5 μg/disc)	S5
Subcutaneous	SC
Sulfate of Magnesium Buffer	SM Buffer
Superinfection Exclusion	Sie / SIE
Tangential Flow Filtration	TTF
Tetracycline (10 μg/disc)	TE10
Toxin–Antitoxin System	TA system
Transfer Ribonucleic Acid	tRNA
Tris-Acetate-EDTA Buffer	TAE
Tris-Borate-EDTA Buffer	TBE
Tris(hydroxymethyl)aminomethane Hydrochloric Acid	Tris-HCl
Tryptic Soy Agar	TSA
Tryptic Soy Broth	TSB

Full Term	Abbreviation
Type IV Pili	TFP
Ultraviolet	UV
University of Nottingham	UoN
Volume/Volume Ratio	v/v
Whole Genome Sequencing	WGS
Approximately	~

Chapter 1. Introduction

1.1. P. multocida

The Gram-negative bacterium *Pasteurella multocida* exists as a diverse and globally significant species. This bacterium commonly resides as a commensal organism within the upper respiratory tracts of various wild and domestic animals (Rimler and Rhoades, 1989). *P. multocida* causes various diseases in economically important animals because it spreads widely throughout their populations (Wilkie *et al.*, 2012; Rimler and Rhoades, 1989). The bacterium *P. multocida* is recognised as a zoonotic pathogen which causes human infections through animal bites or scratches and close contact, leading to localised soft tissue infections that can sometimes progress to severe systemic disease (Wilson and Ho, 2013). *P. multocida* exists in four subspecies, which include *P. multocida* subsp. *multocida*, *P. multocida* subsp. *gallicida*, *P. multocida* subsp. *septica*, and *P. multocida* subsp. *tigris*, each with different characteristics (Capitini *et al.*, 2002; Mutters *et al.*, 1985).

1.1.1. Morphology and Growth Characteristics

The facultative anaerobic rod-shaped coccobacillus *P. multocida* has dimensions of 0.25 to 1 µm in diameter and 1 to 2 µm in length (Christensen and Bisgaard, 2006). The Wright's or Giemsa staining technique reveals bipolar staining in this bacterium because its cell ends stain more intensely than the central region (Christensen and Bisgaard, 2006). The bacterium grows optimally on enriched culture media that include 5% serum or blood-supplemented tryptic soy agar (TSA), brain heart infusion agar (BHIA), or blood agar (Dziva *et al.*, 2008). On blood-

supplemented agar plates it shows non-haemolytic round colonies after 18–24 hours of incubation at 37 °C. The colonies range in size from 0.2 to 2 mm and usually appear light greyish in colour (Christensen and Bisgaard, 2006). The colonies of these bacteria are typically associated with a distinct sweetish odour that appears during growth (Dziva *et al.*, 2008).

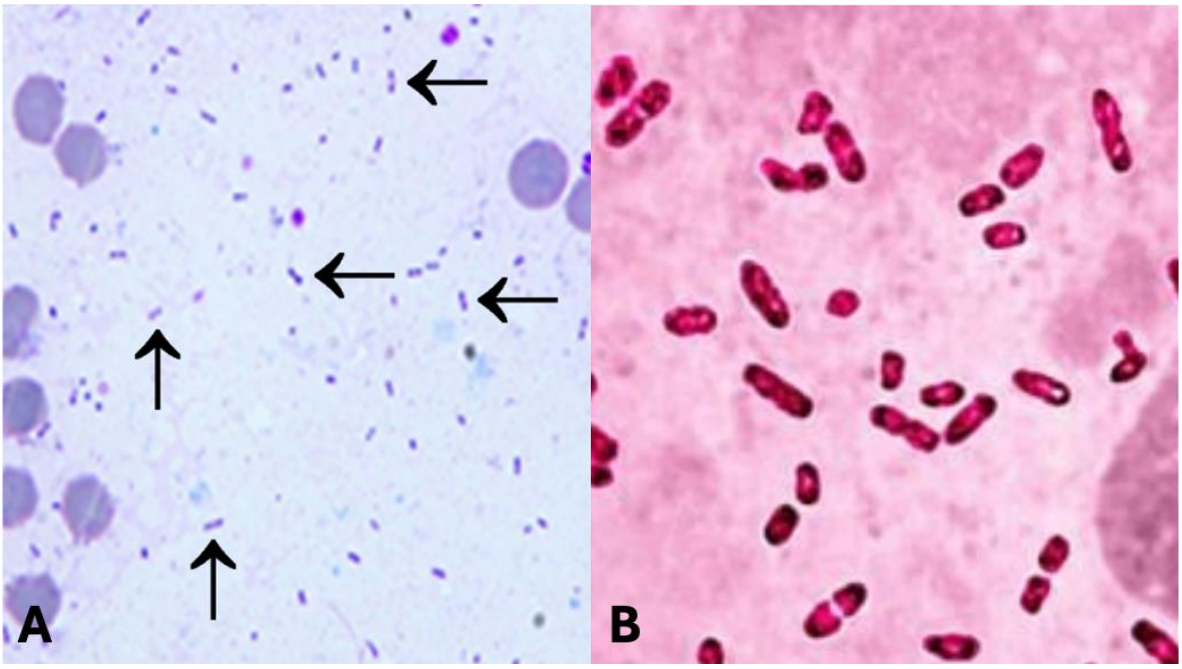

Figure 1.1. Comparative microscopic visualisation of Pasteurella species highlighting characteristic bipolar staining.
(A) *Pasteurella spp.* in a tissue impression smear stained with Leishman's stain. The arrows point to rod-shaped bacteria demonstrating a distinct bipolar ("hairpin-like") appearance (Shrivastava *et al*., 2024). (B) *P. multocida* organisms observed in a blood smear. These are Gram-negative, short bacilli exhibiting prominent bipolar staining, a morphological hallmark of the species (Kumar Sinha *et al*., 2018).

The colony morphology on culture media may be classified as mucoid or non-mucoid. Mucoid colonies are frequently obtained from pneumonic lesions in rabbits, swine, or cattle, while non-mucoid colonies are predominantly sourced from avian species, particularly chickens (Dziva *et al.*, 2008). Mucoid colonies are characterised by their considerable size, unique shape, frequently inflated or convex appearance, circular form, moist texture, and a viscous, adhesive consistency resulting from the synthesis of a capsular polysaccharide, predominantly hyaluronic

acid in serogroup A strains. These mucoid colonies may exhibit a colouration varying from yellowish green to bluish green and can have a pearlescent iridescence (Rimler and Rhoades, 1989). Serogroup A strains generally produce fluid, grey, watery mucoid colonies. In contrast, colonies of serogroups D and F tend to be pearly (Rimler and Rhoades, 1989). Strains belonging to serogroups B and E may show a bluish-green or yellowish shine when observed under transmitted light (Rimler and Rhoades, 1989). Occasionally, rough colonies, indicative of non-capsulated cells and sometimes exhibiting filaments, can be observed, typically appearing grey to blue (Rimler and Rhoades, 1989).

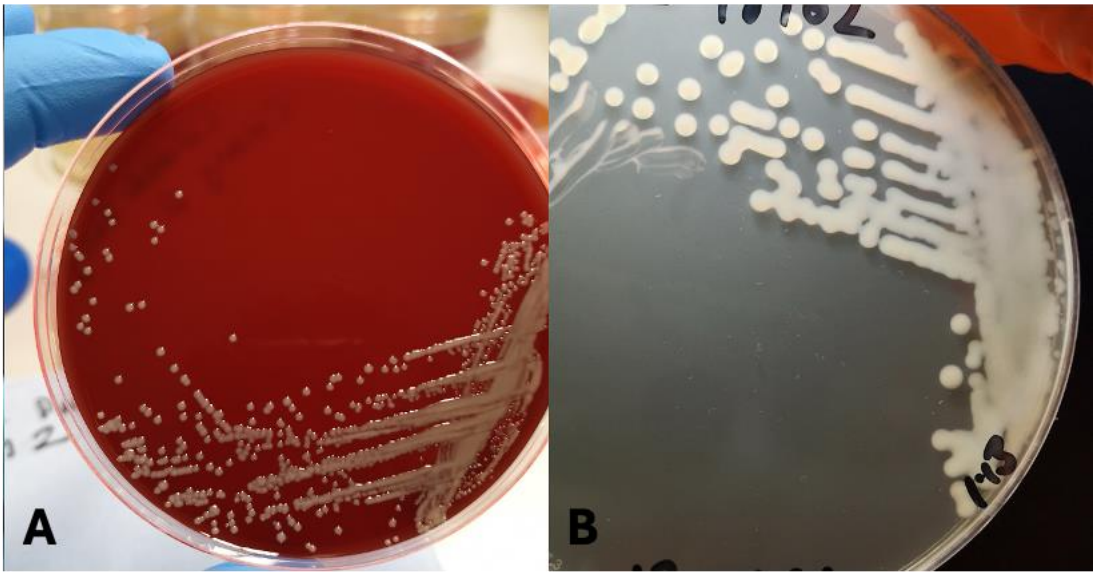

Figure 1.2. Growth characteristics of non-mucoid *P. multocida* on Tryptic Soy Agar (TSA) supplemented with different enrichments.
(A) Colonies of *P. multocida* on TSA supplemented with 5% sheep blood. The image displays characteristic non-mucoid, grey, round, and non-haemolytic colonies, aligning with typical descriptions of *P. multocida* growth on blood-enriched media after 18-24 hours of incubation. (B) Colonies of *P. multocida* on TSA supplemented with 5% Fetal Bovine Serum (FBS). This panel illustrates robust growth with similar non-mucoid, grey colonies

1.1.2. Characterisation and Typing of *P. multocida*

Various genotypic and phenotypic techniques are employed to characterise *P. multocida* isolates. These methods are essential for diverse objectives, including classification, assessment of genetic diversity, epidemiological investigations, and analysis of pathogenesis.

1.1.2.1. Phenotypic Typing Methods

1.1.2.1.1. Multi-locus enzyme electrophoresis (MLEE)

Multi-locus enzyme electrophoresis (MLEE) is a phenotypic typing method used for *P. multocida* identification. This technique relies on variations that occur when isolates are electrophoresed for their water-soluble enzymes, particularly their housekeeping enzymes (Blackall and Miflin, 2000). This method relies not on the presence or absence of enzymes but on variations in amino acid sequences that affect their mobility during electrophoresis (Blackall and Miflin, 2000). This variation is called a mobility variant. After the enzymes are separated by electrophoresis, the gel is stained with special dyes (Selander *et al.*, 1986). The resulting coloured pattern indicates enzyme activity, and isolates with similar patterns are assigned to the same electrophoretic type (ET).

1.1.2.1.2. Restriction Endonuclease Analysis (REA)

Another traditional method used for typing *P. multocida* is restriction endonuclease analysis (REA). This method utilises restriction enzymes to excise bacterial DNA at specific locations (Blackall and Miflin, 2000). The resulting DNA fragments are separated by size using electrophoresis, resulting in a pattern unique to each bacterial isolate. The complexity of the resulting pattern is determined by factors such as the DNA's G+C content and the type of enzyme used (Blackall and Miflin, 2000).

1.1.2.1.3. Ribotyping

Ribotyping is another traditional typing method used for *P. multocida* identification, very similar to REA. In this method, DNA fragments are transferred from the gel to a membrane, and the membrane is then exposed to a probe that binds to sequences containing rRNA or the genes that encode it. This produces an image with simpler patterns compared to REA (Blackall and Miflin, 2000). The main difference from REA is the restriction enzyme and probe used.

1.1.2.1.4. Pulsed-Field Gel Electrophoresis (PFGE)

Pulsed-field gel electrophoresis (PFGE) is another typing method used for the identification of *P. multocida*. Although it is essentially a type of REA, it is distinguished by the use of restriction enzymes called rare cutters to produce relatively small numbers of DNA fragments. To effectively separate these large fragments, a modified electrophoresis technique is used, in which a pulsed electric field is applied periodically (Blackall and Miflin, 2000). PFGE requires high-quality, uncontaminated DNA and is time-consuming.

1.1.2.1.5. Biochemical Characterisation

The biochemical activities of sugar fermentation involving dulcitol and D-sorbitol have been employed as conventional techniques for the identification of subgroups and biotypes within *P. multocida* (Mutters *et al.*, 1985). According to Mutters *et al.* (1985), while *P. multocida* subsp. *multocida* can ferment sorbitol but cannot ferment dulcitol, *P. multocida* subsp. *septica* cannot ferment either of these sugar alcohols; on the other hand, *P. multocida* subsp. *gallicida* shows the ability to ferment both.

1.1.2.2. Serological Typing

1.1.2.2.1. Capsular Serogroups

In 1984, Carter developed a method that aimed to identify the capsular serogroups of *P. multocida* based on the antigenic variations observed in the capsular polysaccharides. This method utilises the passive haemagglutination of erythrocytes by different antigens from the capsular polysaccharides. Through this method, *P. multocida* strains can be divided into five serogroups (A, B, D, E, and F) (Carter, 1984; Christensen and Bisgaard, 2006). Capsular typing is directly linked to disease syndromes (e.g., type B with haemorrhagic septicaemia, type A with fowl cholera), making it a practical tool for subspecies identification in veterinary settings.

1.1.2.2.2. Somatic (LPS) Serotyping

A method to type *P. multocida* strains was developed by Namioka and Murata in 1961, based on the variations in the lipopolysaccharide (LPS) structure of this bacterium. This method is called the Namioka approach, which uses the tube agglutination assay to identify different somatic serotypes. On the other hand, another method was developed by Heddleston* *et al.* (1972) based on the same variation in LPS structure to type *P. multocida* strains. However, this method used a gel diffusion technique to determine different somatic serotypes of the *P. multocida* strains. While the Namioka approach was able to identify eleven different serotypes, the Heddleston method could type sixteen serotypes (Heddleston *et al.*, 1972; Namioka and Murata, 1961).

The use of these traditional serological typing systems requires ready access to specific high-quality antisera. It is difficult to produce, standardise, and consistently use these antisera in regular clinical or diagnostic settings (Boyce *et al.*, 2010; Peng *et al.*, 2019). These procedures

have been mostly replaced by more reliable and consistent molecular methods, so many laboratories no longer use them routinely. This approach provides additional discriminatory power within capsular types, allowing epidemiologists to link strains to outbreaks and thereby refine subspecies classification.

1.1.2.3. Molecular Typing Methods

1.1.2.3.1. Traditional DNA Based Methods

Molecular methods have become increasingly popular because they are more accurate, can be repeated, and can give more detailed genetic information.

1.1.2.3.1.1. PSL PCR

PSL PCR, one of the tests developed for the typing and identification of *P. multocida*, targets the *psl* gene responsible for coding an outer membrane protein, P6-like (PSL) protein (Kasten *et al.*, 1995). This test was considered sensitive at the time, with a detection limit of 24 femtograms of purified *P. multocida* DNA, successfully detecting all 16 Heddleston somatic serovars (Kasten *et al.*, 1997). However, this protein bears a risk of cross-reactivity because it shares significant similarity with the P6 protein of *Haemophilus influenzae* (Kasten *et al.*, 1997). However, *H. influenzae* is not found in birds, making this test limited to avian *Pasteurella* species. In addition to this limitation, the method itself is also disadvantageous because it has complex and labour-intensive steps requiring both PCR and hybridisation (Kasten *et al.*, 1997).

1.1.2.3.1.2. KMT PCR Assay

The KMT PCR assay is based on a DNA sequence extracted from the KMT1 clone, which was discovered incidentally by Townsend *et al.* (1998) during their study to distinguish haemorrhagic from non-haemorrhagic septicaemia isolates. This assay was initially used to

detect positive signals from 13 field isolates of *P. multocida* and three subspecies type strains. Lee *et al.* (2000) reported that the KMT PCR assay was highly sensitive when tested on 100 *P. multocida* strains. Ongoing studies indicate that the KMT PCR assay continues to be an important tool in the identification of *P. multocida* and in molecular diagnosis. Adhikary *et al.* (2013) compared the KMT1 PCR assay with other PCR assays based on genes such as *23S rRNA* and argued that KMT1 has more sensitivity and specificity. KMT PCR is still in use today to confirm the identity of *P. multocida* isolates from various sources, such as cats or pneumonic sheep and goat samples (Ziagham *et al.*, 2025; Gorre *et al.*, 2025).

1.1.2.3.2. Capsular Genotyping

A multiplex PCR-based system for capsular genotyping was established to determine the genes involved in capsule biosynthesis (cap genes). This approach employs primers that exhibit high specificity for various serogroups: *hyaD–hyaC* for serogroup A, *bcbD* for serogroup B, *dcbF* for serogroup D, *ecbJ* for serogroup E, and *fcbD* for serogroup F (Townsend *et al.*, 2001). The method provides precise and quick identification of different capsular serogroups and has been widely used to determine *P. multocida* capsular genotypes from various host species, geographic locations, and disease presentations (Peng *et al.*, 2017; Li *et al.*, 2018). Using this method, several epidemiological studies attempted to determine a correlation between these capsular genotypes and diseases associated with *P. multocida*.

Based on the various conflicting results, capsular strains A, D, and F are generally linked with respiratory diseases, such as conjunctivitis and fowl cholera (FC) (Peng *et al.*, 2017a; Li *et al.*, 2018; Davies *et al.*, 2003). On the other hand, capsular strains B and E are associated with diseases such as haemorrhagic septicaemia (HS) in swine. Studies on capsular strain F

demonstrated its relationship with certain poultry species, especially in turkeys, which suffered from FC (Wilkie *et al.*, 2012; Rhoades and Rimler, 1987). However, other studies also found that strain F caused significant pathogenicity in non-avian species such as swine and rabbits (Peng *et al.*, 2017; Jaglic *et al.*, 2004; Jaglic *et al.*, 2008).

Moreover, strains classified as 'non-typeable', which do not amplify with primers for serogroups A, B, D, E, or F, have been identified in pneumonia cases (Peng *et al.*, 2017b; Tang *et al.*, 2009). Capsular genotyping has benefits, including speed and the ability to identify strains when serotyping is not effective, such as in cases of inadequate capsule expression. However, it is important to remember that this technique assesses genotype rather than phenotype, and there is a risk of false positives if strains have the relevant genes but do not express a capsular polysaccharide because of other genetic mutations.

1.1.2.3.2. LPS Genotyping

P. multocida strains exhibit variability in the outer core of their lipopolysaccharides (LPS) but possess only eight distinct loci for its production. Strains of LPS serovars 1 and 14 share the L1 locus; serovars 2 and 5 share the L2 locus; serovars 3 and 4 share the L3 locus; serovars 6 and 7 share the L4 locus; serovar 9 has the L5 locus; serovars 10, 11, 12, and 15 share the L6 locus; serovars 8 and 13 share the L7 locus; and serovar 16 has the L8 locus (Harper *et al.*, 2011a; Harper *et al.*, 2011b).

The genetic structure of LPS outer core biosynthetic loci led to the development of a multiplex PCR system which classified 16 *P. multocida* type strains into eight distinct genotypes (Harper *et al.*, 2015). The LPS-based genotyping system provides a fast and effective method to identify *P. multocida* LPS genotypes, which proves useful for epidemiological studies.

1.1.2.3.3. Multi-Locus Sequence Typing (MLST)

Multi-Locus Sequence Typing (MLST) is a common scheme that uses various housekeeping genes to identify bacterial species. The Rural Industries Research and Development Corporation (RIRDC) developed a method to type poultry isolates of *P. multocida* strains using the MLST system, aiming to identify seven well-conserved housekeeping genes: *adk* (adenylate kinase), *est* (esterase), *gdh* (glucose-6-phosphate dehydrogenase), *mdh* (malate dehydrogenase), *pgi* (phosphoglucose isomerase), *pmi* (phosphomannose isomerase), and *zwf* (glucose-6-phosphate dehydrogenase) (Subaaharan *et al.*, 2010).

While RIRDC developed this scheme to type poultry strains of *P. multocida*, other studies showed that it can also be used to type non-avian species of *P. multocida*, and it became widely used (Mohamed and Mageed, 2014; Turni *et al.*, 2018; Crawford *et al.*, 2019; Ujvári *et al.*, 2018). Following this, improved multi-host MLST systems were developed, allowing the investigation of evolutionary relationships of isolates from different hosts, including bovine, ovine, porcine, and avian species.

This new system also utilises seven housekeeping genes, but four of them differ slightly from the first method developed by RIRDC: *adk*, *aroA*, *deoD*, *gdhA*, *g6pd*, *mdh*, and *pgi* (Davies *et al.*, 2004; García-Alvarez *et al.*, 2017; Peng *et al.*, 2017b). MLST provides reproducible, comparable data across laboratories, enabling subspecies determination and global tracking of clonal lineages associated with different host species.

1.1.2.3.4. Core Genome Multi-Locus Sequence Typing (cgMLST)

Traditional MLST, which is used for *Pasteurella multocida* identification and relies on the analysis of a limited number of housekeeping genes, remains crucial for initial classification,

evolutionary relationships, and population biology (Smith *et al.*, 2021; Subaaharan *et al.*, 2010). However, it is somewhat limited in situations requiring high-resolution genomic typing, such as the separation of close relatives or epidemic investigations.

In such cases, a more advanced method that can be used is core genome multi-locus sequence typing (cgMLST), which employs the same principles but analyses a much larger set of genes at high resolution (Pearce *et al.*, 2018). The cgMLST system, designed for *P. multocida* identification, is publicly available in the PubMLST database, and features a robust and standardised schema that is constantly updated (Jolley *et al.*, 2018).

Compared to traditional MLST analysis of seven genes, this method utilises very high-resolution analysis of the sequences of approximately 2,100 core genes and has a more sensitive detection power. This allows for the tracking of even microevolutionary differences within a population (Myrenås *et al.*, 2024).

The web-based PubMLST platform, which can be used without extensive bioinformatics knowledge or infrastructure, provides a powerful tool that allows users to perform sensitive analyses such as tracing pathogen transmission routes, identifying epidemic clusters, and host adaptation (Jolley *et al.*, 2018).

1.1.2.3.5. Virulence Gene Profiling

Using a PCR assay and other molecular techniques, *P. multocida* strains were typed based on their virulence factors. These methods aimed to identify virulence genes, and they were generally used with other Multi-Locus Sequence Typing (MLST) methods to expand the knowledge of epidemiology and pathogenicity of this bacterium (García-Alvarez *et al.,* 2017).

1.1.2.3.6. Whole Genome Sequencing (WGS)

Advances in sequencing and *in silico* analysis, along with powerful computer technology, have made whole-genome sequencing (WGS) easier to access and enhanced its capability. Through this technique, it is possible to obtain the output of all previous typing methods in one setting, which allows for a complete characterisation. Moreover, this technique allows researchers to identify all typing determinants, such as LPS, capsule, housekeeping, virulence, and antibiotic resistance genes, while also enabling the discovery of new determinants through comparative analysis of unknown genes.

WGS represents the most comprehensive approach, as it not only allows precise subspecies classification but also supports epidemiological tracing, vaccine design, and identification of novel virulence factors.

1.1.3. P. multocida Virulence Factors

1.1.3.1. Capsule

The capsular polysaccharide in *P. multocida* is recognised as one of the main virulence factors, which led scientists to classify this bacterium into five groups: A, B, D, E, and F (Christensen and Bisgaard, 2006). The capsule appears as an outer layer surrounding the bacteria and functions as the main and first component that interacts with the host cells. The capsular materials of *P. multocida* serogroups show molecular similarities to glycosaminoglycans that occur in mammalian connective tissue structures, which enables immune evasion through molecular mimicry (DeAngelis and White, 2004).

The main composition of serogroup A capsules contains hyaluronan, whereas serogroup D capsules have heparosan as their main component, and serogroup F capsules contain mostly

unsulphated chondroitin (DeAngelis and Padgett, 2000; Rimler, 1994; Pandit and Smith, 1993). The genetic organisation for capsule biosynthesis exists in one combined unit which contains most of the necessary genes for capsule formation in a single operon (Townsend *et al.*, 2001).

The *hssB* gene (previously known as *pglA*), which is essential for heparosan synthase activity in serogroup D strains, exists outside the main capsular operon (DeAngelis and White, 2004). Research indicates that variations in heparosan-producing serogroups may result from differences in *hssB* gene expression levels, which could affect both capsular presentation and quantity (DeAngelis and White, 2004).

Multiple scientific studies have established that the capsule functions as a vital factor determining the virulence of *P. multocida*. The virulence level of *P. multocida* strains is generally increased when they possess a capsule compared to acapsular strains (Heddleston *et al.*, 1964; Snipes *et al.*, 1987; Tsuji and Matsumoto, 1989). Scientific evidence shows that laboratory-made acapsular mutants display decreased virulence. Studies have shown that acapsular mutants of serogroups A and B exhibit reduced virulence during mouse infection experiments (Chen *et al.*, 2018b).

The virulence of the capsule stems mainly from its ability to protect bacteria from phagocytic activity. Macrophages demonstrated higher efficiency in clearing intraperitoneal mouse infections with acapsular bacteria, but capsulated bacteria showed substantial resistance to macrophage engulfment and killing (Boyce and Adler, 2000; Chung *et al.*, 2001b). Acapsular serogroup A strains demonstrated no ability to cause infection in chicken muscle models, thus proving the protective function of the capsule (Chung *et al.*, 2001b).

The protective effect of phagocytic resistance depends heavily on the bacterial capsule, both in terms of presence and thickness (Harmon *et al.*, 1991; Pruimboom *et al.*, 1996). The protective role of the capsule extends beyond phagocytic defence since it provides *P. multocida* with resistance to complement-mediated lysis and subsequent serum bactericidal activity (Ataei Kachooei *et al.*, 2017; Harper *et al.*, 2012).

The research on serum resistance has produced inconsistent results across different investigations. An acapsular type A *P. multocida* strain showed reduced resistance to turkey serum compared to its capsulated parental strain, according to research findings by Snipes and Hirsh (1986) and Hansen and Hirsh (1989). Other research indicated that an acapsular serogroup A mutant showed similar resistance to avian serum when tested against its genetically modified capsule-positive counterpart (Chung *et al.*, 2001b). Acapsular mutants of serogroup B strains displayed no noticeable change in their serum resistance against murine or bovine serum compared with their capsulated parent strains (Boyce and Adler, 2000).

The exact explanations for varying results about the capsule's function in serum resistance remain unclear because they might stem from interactions between hosts and pathogens or variations in serum origins and experimental parameters. The capsule functions as the main virulence determinant, but researchers question whether it remains the key target for antibody-based protective immunity across different situations. The results of Chung *et al.* (2005) demonstrate that high-dose vaccination of chickens with acapsular serogroup A mutants triggered protective responses that protected against virulent capsulated strains. Other bacterial antigens also proved capable of triggering protective immune responses, according to this significant discovery which opened new possibilities for vaccine development.

The *P. multocida* capsule acts as a virulence factor that helps the bacteria resist phagocytosis while providing serum resistance, but its specific contribution to serum resistance may differ. Researchers have extensively studied the structural makeup of the capsule alongside its genetic properties and its ability to trigger protective immune responses, yet its absence in specific vaccine formulations demonstrates the intricate nature of host–pathogen interactions.

1.1.3.2. Lipopolysaccharide

The endotoxic compound lipopolysaccharide (LPS) exists as a primary outer membrane structural element found in all Gram-negative bacterial species (Lüthje and Brauner, 2014). The immune cells of the host identify LPS through Toll-like receptors (e.g., TLR4) because this compound functions as a major pathogen-associated molecular pattern (PAMP). Upon host cell recognition of LPS, the immune system activates innate defence mechanisms to establish the first line of microbial defence (Mogensen, 2009).

The structure of LPS consists of three distinct sections: lipid A as the outer membrane anchor with endotoxic activity, the core oligosaccharide, and the variable O-antigen polysaccharide domains (Bertani and Ruiz, 2018). Normally, in Gram-negative bacteria, the LPS contains a repeating O-antigen polysaccharide chain structure. However, in *P. multocida*, the LPS lacks this polysaccharide and instead contains an oligosaccharide. Therefore, it is generally called LOS instead of LPS.

However, this LOS structure works in the same way as LPS produced by other pathogenic bacteria and primarily infects the mucosal tissue of the host (Kahler and Stephens, 1998; Harper *et al.*, 2006). Although this LOS structure lacks an O-antigen polysaccharide, it differs in its oligosaccharide sequence. This distinction forms the basis of serological separation and

classification. Based on these serological differences, *P. multocida* has been divided into sixteen different somatic (LPS/LOS) serotypes (Rimler and Rhoades, 1989).

LOS in *P. multocida* plays an important role in disease pathogenicity. When the host immune system encounters LOS, it triggers an immune reaction because it is recognised as the main antigenic factor (Periasamy *et al.*, 2018). The immune response to LOS occurs in several ways. One of these is the activation of neutrophils and their passage through endothelial cells to the inflammatory site (Galdiero *et al.*, 2000).

A study attempting to demonstrate the pathogenic properties of *P. multocida* LOS administered endotoxin (LOS) produced by the *P. multocida* serogroup B:2 strain intravenously to buffalo. The HS symptoms observed in buffalo confirmed the pathogenicity of *P. multocida* LOS (Horadagoda *et al.*, 2002).

Studies by Harper *et al.* (2007) and El-Demerdash *et al.* (2023) show that the biological activity of *P. multocida* LOS works differently on host species. While chicken embryos and mice experience a toxic effect when exposed to LOS, turkeys were observed to be more resistant. According to Harper *et al.* (2012), *P. multocida* LOS may have many important functions. For example, LOS given as a protective antigen stimulates humoral immunity, increases antibody production, and supports the host's immune system.

Knowledge about the pathogenic properties and potential beneficial mechanisms of *P. multocida* LOS is still very limited. The claims in the literature remain controversial and require more controlled studies.

1.1.3.3. Outer Membrane Proteins

Gram-negative bacteria, including *P. multocida*, need outer membrane proteins (OMPs) to establish interaction with their external environment. The complicated functions of these proteins enable bacterial adaptation to diverse host environments and tissue invasion and colonisation, as well as iron acquisition (Garrido *et al.*, 2008; Puchalski *et al.*, 2010). The main cellular functions of OMPs include structural support of the cell membrane and molecular transport capabilities. Porins, for instance, act as essential transporters because they facilitate both general solute movement and selective ligand delivery necessary for bacterial survival (Boyce *et al.*, 2006).

Protection studies have demonstrated the crucial role OMPs play in vaccine development. Research has shown that OmpH from *P. multocida* serogroup B:2 protects mice completely when given intraperitoneally yet shows reduced effectiveness when administered subcutaneously (Tan *et al.*, 2010). Research involving the recombinant Oma87 protein showed beneficial outcomes for protecting mice from *P. multocida* serogroup A:1 infection, though these protective effects did not extend to chickens (Ruffalo and Adler, 1996; Mitchison *et al.*, 2000). The Th2-type immune response triggered by recombinant OmpA in mice failed to protect against infection (Dabo *et al.*, 2008a).

Bacterial pathogenesis depends heavily on iron acquisition mechanisms, which are controlled by iron-regulated outer membrane proteins (IROMPs) that serve as essential virulence factors (Garrido *et al.*, 2008; Puchalski *et al.*, 2010). Mutant *P. multocida* strains deficient in *fur* gene regulation produce elevated IROMPs and provide protective effects during murine infections (Garrido *et al.*, 2008).

The ability of bacteria to adhere to host cells represents a necessary step for infection establishment, while adhesins, including Cp39 and type IV fimbriae, play essential roles in this process (Hatfaludi *et al.*, 2010; Borrathybay *et al.*, 2003). A study showed that vaccination with recombinant proteins can decrease post-challenge pathogen colonisation. In mice, the *E. coli* recombinant expression of *P. multocida* B:2 fimbrial protein reduced pathogen counts during post-challenge tests (Mohd Yasin *et al.*, 2011). Encoding filamentous haemagglutinin-like proteins, the *pfhA1* and *pfhA2* virulence genes function in bacterial colonisation and adhesion (Fuller *et al.*, 2000; Tatum *et al.*, 2005).

1.1.3.4. P. multocida Toxin

Some strains of serogroup A and D have the *toxA* gene producing PMT (Pasteurella multocida toxin). Progressive atrophic rhinitis (PAR) in pigs is caused by this toxin; it is marked by nasal bleeding, bone degradation, and snout shortening or deformation. PMT increases G-protein families Gq and G12/13, acting as a mitogen for fibroblasts and osteoblasts. It also activates phospholipase Cβ (PLCβ) (Preuß *et al.*, 2009; Pullinger and Lax, 2007; Busch *et al.*, 2001).

Cells treated with PMT experience an increase in inositol and diacylglycerol levels, leading to the activation of protein kinase C (PKC) and the mobilisation of Ca^{2+} (Miyazawa *et al.*, 2006). The monomeric protein PMT has a molecular weight of 146 kilodaltons. Studies have been conducted to investigate the protective effects of mutant forms of PMT against PAR (Rajeev *et al.*, 2003; Petersen *et al.*, 1991).

1.1.4. Diseases Associated with *P. multocida.*

P. multocida is associated with several distinct disease syndromes in a wide range of animal species and can cause opportunistic infections in humans (Wilson and Ho, 2013). These

diseases display different symptoms and affect species (Wilkie *et al.*, 2012). Key diseases where *P. multocida* acts as a primary pathogen include fowl cholera (FC), haemorrhagic septicaemia (HS), and atrophic rhinitis (AR) (Harper *et al.*, 2006; Wilkie *et al.*, 2012).

1.1.4.1. Fowl Cholera (FC)

This systemic disease impacts many avian species, though turkeys are often highly susceptible (Wilkie *et al.*, 2012). While named fowl cholera (FC), the disease is predominantly caused by *P. multocida* capsular type A strains, although type F (especially in turkeys) and, infrequently, type D strains are also implicated (De Alwis, 1992; Wilkie *et al.*, 2012).

Symptoms of the acute form can include lethargy, ruffled feathers, fever, anorexia, mucous discharge from the mouth, diarrhoea, and an increased respiratory rate (Harper *et al.*, 2006). Infected animals might also exhibit swollen wattles and combs or exudative arthritis (Wilkie *et al.*, 2012). The illness is thought to progress following the colonisation of the upper respiratory tract mucosa (Harper *et al.*, 2006; Wilkie *et al.*, 2012).

Highly contagious strains subsequently spread, potentially to the lungs and air sacs, and then enter the circulation, causing bacteraemia, often late in the infection (Carter, 1955; Heddleston *et al.*, 1972; Wilkie *et al.*, 2012). The terminal stage of bacteraemia results in death through endotoxic shock, according to Harper *et al.* (2006).

The antiphagocytic capsule, together with LPS and possibly adhesins and iron acquisition systems, plays important roles in the development and progression of the disease (Boyce and Adler, 2000; Harper *et al.*, 2006; Rhoades and Rimler, 1989; Wilkie *et al.*, 2012).

Figure 1.3. Clinical Manifestation of Localized FC: Swollen Wattles in Chickens
The image shows chickens with severely swollen and inflamed wattles which is a typical clinical sign of FC caused by *P. multocida.* The localized form of the disease is often characterised by the accumulation of fibrinous caseous content within the wattles, as showed. The development of swollen wattles is a recognised symptom in infected birds (Wilkie *et al*., 2012).
Image adapted from The Poultry Site (www.thepoultrysite.com/publications/diseases-of-poultry/181/fowl-cholera).

1.1.4.2. Haemorrhagic Septicaemia (HS)

Primarily affecting ungulates such as cattle and buffalo, especially in Asia and Africa, haemorrhagic septicaemia (HS) is an acute and often fatal systemic illness (Harper *et al.*, 2006; Wilkie *et al.*, 2012; Wilson and Ho, 2013). The main causative agents are *P. multocida* capsular type B (in Asia) and type E (in Africa) strains (De Alwis and Carter, 1989; Harper *et al.*, 2006; Wilkie *et al.*, 2012).

The clinical presentation is often characterised by sudden onset of fever, decreased appetite, excessive salivation, respiratory distress, and subcutaneous oedematous swelling, especially around the head and neck (Harper *et al.*, 2006; Wilkie *et al.*, 2012; Wilson and Ho, 2013). The pathogenesis likely involves entry via the tonsils, followed by rapid bacterial multiplication in local tissues causing oedema and necrosis, and eventual invasion of the bloodstream (Wilkie *et al.*, 2012).

Although bacteraemia occurs, significant multiplication within the blood may not be the primary feature (Wilkie *et al.*, 2012). While strains sometimes responsible for bovine respiratory

disease, particularly type A, may be involved in similar syndromes (Wilson and Ho, 2013), typical HS caused by types B and E does not correlate with PMT (Pasteurella multocida toxin) production (Chanter and Rutter, 1989; Wilkie *et al.*, 2012).

Virulence factors such as the capsule, fimbriae, and potentially filamentous haemagglutinin are considered essential in the progression of disease (Chanter and Rutter, 1989; Wilkie *et al.*, 2012). Endotoxin (LPS) likely plays a significant role in the clinical signs observed during the terminal stages (Harper *et al.*, 2006; Wilkie *et al.*, 2012).

1.1.4.3. Atrophic Rhinitis (AR)

Atrophic rhinitis (AR) primarily affects swine and rabbits and is defined by the degeneration of the nasal turbinate bones, which can lead to facial deformities such as snout shortening or twisting, particularly in young animals (Harper *et al.*, 2006; Wilkie *et al.*, 2012; Wilson and Ho, 2013). This syndrome is caused by specific toxigenic strains of *P. multocida*, those belonging to capsular type D and sometimes type A (Pedersen and Elling, 1984; Harper *et al.*, 2006; Wilkie *et al.*, 2012), that produce Pasteurella multocida toxin (PMT). PMT is the primary virulence factor involved in bone lesions (Harper *et al.*, 2006; Wilkie *et al.*, 2012; Wilson and Ho, 2013).

Following bacterial colonisation of the nasal mucosa, potentially facilitated by co-infection with *Bordetella bronchiseptica* (Wilson and Ho, 2013), the toxin disrupts normal bone homeostasis by inhibiting osteoblast differentiation and promoting osteoclast-mediated bone resorption, resulting in characteristic turbinate atrophy (Horiguchi, 2012; Wilkie *et al.*, 2012). Clinical signs can include nasal deformities, sneezing, nasal discharge, epistaxis, tear staining, and potentially retarded growth (Harper *et al.*, 2006; Wilson and Ho, 2013). Other virulence factors

such as fimbriae may aid colonisation (Horiguchi, 2012). The toxin enters epithelial cells and affects underlying bone progenitor cells (Horiguchi, 2012).

In conclusion, P. multocida is a versatile pathogen capable of causing multiple diseases, each frequently associated with particular strains or subspecies of the bacterium (Harper *et al.*, 2006). While the virulence of the capsule and LPS provides an important contribution to the pathogenicity of fowl cholera (FC) and haemorrhagic septicaemia (HS), the virulence mechanism of PMT is more relevant in AR (Harper *et al.*, 2006; Wilkie *et al.*, 2012).

In conclusion, *P. multocida* is linked to distinct severe diseases in animals, often correlated with specific capsular types (Harper *et al.*, 2006). FC and HS are acute systemic infections distinguished by the critical roles of the capsule and LPS as virulence factors. In contrast, the pathogenesis of AR is mainly linked to the specific osteolytic effects of PMT (Harper *et al.*, 2006; Wilkie *et al.*, 2012). To develop effective protection strategies against these diseases, including bacteriophage therapy, virulence mechanisms must be well understood.

1.1.5. Economic Impact of *P. multocida*

As mentioned in previous sections, fowl cholera (FC), atrophic rhinitis (AR), haemorrhagic septicaemia (HS), and bovine respiratory disease (BRD) are illnesses caused by *P. multocida* that lead to serious economic losses. These effects significantly impact the livestock sector on almost every continent, but the magnitude of this effect is very difficult to calculate because of the way the disease occurs, the differences in the species it affects, and the variety of regional factors. The main causes of financial losses can be listed as mortality, morbidity, decreased production, and treatment costs (Bardhan *et al.*, 2020; Geda, 2024; Wilkie *et al.*, 2012).

One of the main illnesses linked to *P. multocida* is FC, a lethal and highly contagious disease that seriously threatens the global poultry industry (Geda, 2024; Reuben *et al.*, 2021). Sudden, large-scale die-offs may occur, with mortality rates potentially reaching 100% during acute outbreaks (Geda, 2024; Tsehay *et al.*, 2024). Documented outbreaks have occasionally led to the deaths of tens of thousands of animals in a single incident (Friend, 1999; SCWDS, 2023). The economic losses arise from elevated mortality rates, particularly in chicks; decreased weight gain; insufficient feed conversion; increased medication expenses; and carcass condemnation (Geda, 2024). A historical example from 1988 estimated the localised cost of FC in turkeys in Georgia (USA) at $634,545 (Morris and Fletcher, 1988). However, the overall impact on the contemporary global poultry sector, which includes chickens, turkeys, and waterfowl, is significant (Geda, 2024; SCWDS, 2023).

AR, induced by toxigenic strains of *P. multocida*, primarily results in economic losses due to slowed growth performance in swine (Baalsrud, 1987). Research demonstrates that AR adversely impacts the feed conversion ratio (FCR) and average daily gain (ADG), especially at the beginning of the fattening period (Donkó *et al.*, 2005). Swine with severe turbinate atrophy may exhibit 10–15% lower growth rates and require significantly more days (e.g., an average of eight extra days in one study) to reach market weight compared with unaffected swine (Baalsrud, 1987; Donkó *et al.*, 2005). Moderately affected swine (Grade 2 lesions) also show reduced growth (over 4% less) and require extra time (e.g., three days) (Baalsrud, 1987; Donkó *et al.*, 2005). The growth delay associated with AR underscores its economic significance in modern swine production (Baalsrud, 1987).

HS, a significant disease caused by *P. multocida* (serotypes B and E), presents a considerable economic risk, especially for cattle and buffalo farmers in Asian and African regions (Benkirane and De Alwis, 2002; Bardhan *et al.*, 2020). HS is associated with high mortality rates and substantial economic impacts. Recent estimates for India indicate total annual economic losses between ₹58.63 billion and ₹175.72 billion (approximately £529 million to £1.58 billion), with buffaloes, which are more vulnerable, representing the largest proportion (55%) (Bardhan *et al.*, 2020). Losses stem from high mortality (accounting for ~64% of losses in one regional study), treatment costs (~21%), reduced milk yield, increased abortions, and extra labour costs (Anandasekaran *et al.*, 2020, as cited in Bardhan *et al.*, 2020; Singh *et al.*, 2014). Estimated per-animal losses in India were ₹11,904 (£107.7) for native cattle, ₹13,044 (£118) for crossbred cattle, and ₹20,296 (£183.6) for buffaloes (Bardhan *et al.*, 2020). The data demonstrate HS as a significant threat, requiring the implementation of effective control measures such as vaccination and biosecurity (Bardhan *et al.*, 2020).

P. multocida is also a significant factor in BRD, a complex that poses a substantial economic challenge in the cattle industry, especially in feedlots (Dabo *et al.*, 2007). BRD accounts for approximately 75% of morbidity and 50–70% of mortality in North American feedlot cattle (Galyean *et al.*, 1999; Loneragan *et al.*, 2001). Early 2000s estimates indicated that annual costs to the US beef industry ranged from $800 to $900 million (Chirase and Greene, 2001). Present-day expenses are likely higher when considering declines in productivity and carcass quality (Brooks *et al.*, 2011; Wilson *et al.*, 2017). Affected cattle suffer losses resulting from treatment expenses, decreased feed efficiency, longer feeding times, a higher cost of gain, and lower carcass quality grades (Blakebrough-Hall *et al.*, 2020; Wilson *et al.*, 2017). Multiple treatments

cause a clear increase in per-animal losses (Blakebrough-Hall *et al.*, 2020; Wilson *et al.*, 2017). *P. multocida*-associated BRD remains a major obstacle despite management improvements, which emphasises the need for better strategies to minimise major economic losses (Ives and Richeson, 2015).

1.1.6. AMR in *P. multocida*

The multidrug-resistant condition that develops in bacteria with high morbidity and mortality, such as *Acinetobacter* spp., *Pseudomonas aeruginosa*, *Enterococcus* spp., *Enterobacteriaceae*, and *Staphylococcus aureus*, has attracted significant attention while causing increasing concern worldwide (Magiorakos, 2012). Research conducted in India reveals that strains of *P. multocida* derived from various animals are progressively becoming resistant to several antibiotics, including norfloxacin, chloramphenicol, lincomycin, and doxycycline (Kumar *et al.*, 2004; Shivachandra *et al.*, 2004; Maynou *et al.*, 2017).

Among these, the widespread use of tetracyclines in poultry farming worldwide is alarming, as is the development of antibiotic resistance (Endale *et al.*, 2023). Norfloxacin and enrofloxacin, which are on the WHO's list of antibiotics of critical importance for human health, continue to be frequently used in poultry farming for colibacillosis and respiratory infections (Foysal *et al.*, 2024; Azab *et al.*, 2022).

Resistance to these antibiotics has also been reported in poultry and swine isolates of *P. multocida*, posing a high-risk development (Kerek *et al.*, 2023; Bourély *et al.*, 2019). Although frequently encountered among *P. multocida* resistant strains, the use of chloramphenicol in food-producing animals has been banned in many regions due to its public health risks, making the presence of resistant findings less urgent than in veterinary practice (Wongtavatchai *et al.*, 2004).

The combination of lincomycin and spectinomycin is widely used in the poultry sector, particularly during the production phase. Studies report increasing resistance to these two antibiotics, suggesting that their therapeutic effects may diminish in the event of respiratory disease outbreaks (Jerab *et al.*, 2023; Wibisono *et al.*, 2024).

Another point worth noting is that *P. multocida* resistance to these antibiotics is frequently mediated by plasmids and integrative conjugative elements (ICEs). Numerous recent studies report this. For example, Klima *et al.* (2020) examined the antimicrobial resistance of 70 strains of *Pasteurella multocida*, the cause of bovine respiratory disease. They found resistance to multiple antibiotics, including tetracyclines, sulphonamides, macrolides, and aminoglycosides. Genome analyses showed that the genes responsible for this resistance, such as *tet(H)*, *sul2*, *floR*, *erm(42)*, and *aadA25*, are generally localised on ICEs, which facilitate horizontal gene transfer between species.

More than 500 *Pasteurellae* genomes and plasmids were examined, with particular attention paid to insertion sequences, prophages, and ICEs. More than 75% of the identified major antibiotic resistance genes, such as *tetB*, *sul2*, *floR*, *ermF*, and *blaROB-1*, were found on mobile genetic elements. Furthermore, some plasmids, such as pB1000, are shared between *P. multocida* and *Haemophilus* spp., suggesting horizontal gene transfer (da Silva *et al.*, 2022).

Another recent study found that animals suffering from bovine respiratory disease caused by *P. multocida* had more multidrug-resistant strains isolated than their host counterparts. Seventy-five strains were tested for susceptibility to 19 different antibiotics. Genome analyses of the 32 most resistant strains revealed nine different antibiotic resistance genes, and all these genes were associated with mobile genetic elements such as the ICEs Tn7407 and the novel

Tn7809, as well as prophages and transposons. These findings suggest that ICEs and other mobile genetic elements (MGEs) play a central role in the spread of antibiotic resistance in *P. multocida* (Serna *et al.*, 2025).

Overall, antibiotic resistance in *P. multocida* is increasing rapidly. This is significantly related to MGEs such as plasmids and ICEs, in addition to the selective effects of antibiotics used in poultry and livestock farming. These elements form the basis of horizontal gene transfer, allowing resistant strains to become more potent and spread rapidly among animal populations. The results of current studies demonstrate that antimicrobial resistance (AMR) of *P. multocida* is a growing veterinary and public health concern and that alternative control methods to antibiotics must be urgently developed. Among these controls, phage therapy is one promising alternative that requires intensive study.

1.2. Bacteriophages

Bacteriophages, or phages for short, are viruses that only infect and multiply within bacteria. These viruses are the most abundant organisms on Earth, far outnumbering all other life forms combined. They coexist with their bacterial hosts in almost every possible environment (Hatfull and Hendrix, 2011; Clokie *et al.*, 2011). Their large numbers and complex interactions with bacteria provide vital details on microbial ecology, evolution, and fundamental life processes.

Bacteriophages are essentially composed of a nucleic acid core, which can be DNA (single- or double-stranded) or, less often, RNA, and a capsid, a protein shell that protects this core. Phages are found in various shapes and sizes; most of them have tails that assist in recognising their hosts and injecting genetic material, while fewer have simpler filamentous, pleomorphic, or

enveloped forms (Ackermann, 2007). Bacteriophages are specific about their hosts; they usually only infect certain types of bacteria or select strains of a type. This characteristic is important for their roles in the environment and contributes to their advantages as medicines (Hyman and Abedon, 2009).

Phages interact with bacterial hosts in two main ways: the lytic cycle, which involves the rapid replication of the phage and the destruction of the bacterial cell, and the lysogenic cycle, in which the phage genome becomes part of the host genome as a prophage or exists as a plasmid, coexisting with the host without causing any immediate damage (Santos *et al.*, 2014; Weinbauer, 2004).

The effects of bacteriophages in the environments in which they exist are highly significant because they are natural predators of bacteria, and population dynamics are largely determined by phage activity. Therefore, the composition of bacterial species (biodiversity) and the evolutionary trajectory of these populations are dramatically affected by phages over time (Weinbauer, 2004). Phages do not affect these populations simply by killing some types of bacteria and allowing others to survive. The main determining factor in the evolution of bacterial populations is horizontal gene transfer established by phages. This influences many bacterial characteristics, from their responses to the environment to their virulence and antibiotic resistance genes (Brüssow *et al.*, 2004).

The effects of phages can be observed in different ways in different ecosystems. For example, in the human digestive system, they constitute the main elements of the gastrointestinal virome and directly affect the content of the microbiota. They influence many areas, from the nutritional processes of the organism in which they are found to the immune

response of the host to bacteria. Therefore, the disease and health status of the organism are also affected by phage activity (Łusiak-Szelachowska *et al.*, 2017; Cook *et al.*, 2020).

Phages can be found in almost any environment where bacteria grow. The main locations used for phage isolation are soil, aquatic ecosystems, sewage, agricultural environments (such as animal farms and plants), food products, and biological samples, including animal and human faeces (Akhtar *et al.*, 2014; Breitbart, 2012). Most phage populations have been found in seawater (Suttle, 2005). Phage diversity and abundance are significantly influenced by the condition of the environment in which they are found, including the composition of the soil and microbiome (Williamson *et al.*, 2005; Sutton and Hill, 2019). When targeting phage isolation, the sampling location is important in terms of the infection caused by the target bacteria or where they are colonised. For example, animal faeces, sewage, or wastewater may be ideal sampling areas for phage isolation specific to *Salmonella enterica*, which causes intestinal infection (Queshi *et al.*, 2018; Huang *et al.*, 2018; O'Flynn *et al.*, 2006).

Frederick Twort and Félix d'Herelle independently discovered bacteriophages in 1915 and 1917 (Letov, 2020). These discoveries marked the beginning of the field of bacteriophage research. d'Herelle immediately recognised their ability to eradicate bacteria and carefully considered their possible application in treating bacterial diseases. The findings of this study led to the introduction of phage therapy before antibiotics were discovered (d'Herelle, 1917; Summers, 2012). Early attempts at phage therapy, including the prevention of avian typhoid in 1919, produced mixed results and led to considerable controversy over their effectiveness and appropriate use, particularly in the 1930s (Summers, 2012).

The development of electron microscopy in the 1940s allowed direct observation of phage morphology (Ruska, 1940), improving knowledge of their structure and taxonomy. The first systems applied to categorise phages were based on structure (Ackermann, 2007). Later developments in molecular biology, underlined by the discovery of several types of viral nucleic acids, produced more precise classifications, best known through the Baltimore system (Koonin *et al.*, 2021). Rapid advances in sequencing technology and the rising volume of viral genome sequences have made phylogenetic and genomic techniques vital for phage classification (Satam *et al.*, 2023). These techniques help us to better understand phage evolutionary relationships. Furthermore, new technologies for microbiome analysis enable classification of bacteriophages without relying on culture techniques. Direct phage identification and classification from metagenomic data are now possible using algorithms that apply machine learning (Cook *et al.*, 2021).

However, it is imperative to apply these advanced methods with awareness of the difficulties that may arise during sample preparation, sequencing, and bioinformatic analysis, since these factors can affect interpretation of the results (Džunková *et al.*, 2023).

1.2.1. Bacteriophage Classification

As mentioned earlier, phages are the most abundant biological entities on the planet. However, they are also extremely diverse, so no single classification technique can cover all unique phage characteristics.

The establishment of the International Committee on Taxonomy of Viruses (ICTV) in 1966, which published its first report in 1971, was significant due to the importance and sometimes contentious nature of bacteriophage classification. The classification of bacteriophages involves

a complex process, and multiple aspects of phages continue to be difficult to identify. Nonetheless, as mentioned earlier, ICTV considers various factors to classify bacteriophages.

A defining feature is the kind of genetic material involved, which may include single-stranded DNA (ssDNA), double-stranded DNA (dsDNA), single-stranded ribonucleic acid (ssRNA), or double-stranded RNA (dsRNA), with a predominance of dsDNA phages (Harada *et al.*, 2018; Sharma *et al.*, 2017). Alongside their genetic composition, phages are categorised according to their physical traits. Most bacteriophage families historically belonged to the order *Caudovirales*, noted for their tail structures (Ackermann, 1998). The absence of an envelope and the presence of dsDNA molecules arranged in a linear pattern defined the *Caudovirales* (Lefkowitz *et al.*, 2018).

Classification in the order *Caudovirales* included three tail-bearing families: *Myoviridae, Siphoviridae, and Podoviridae* (Ackermann, 1998). These families exhibited distinct variations in tail morphology. The family *Myoviridae* was characterised by elongated, contractile tails. According to Leiman and Shneider (2012), phages with contractile tails were classified as lytic. *Siphoviridae* had elongated tails that were not capable of contraction, while the *Podoviridae* family was characterised by short, non-contractile tails.

In 2022, ICTV updated its methods and guidance, switching to sequence-based phylogenetic groupings and eliminating the families *Podoviridae, Myoviridae,* and *Siphoviridae*, which were previously classified based on morphology (Turner *et al.*, 2023). Although morphological classification is still used to describe phages, it is no longer considered a determining factor in taxonomic classification. Instead, according to the current ICTV framework, taxonomic classification can only be made after successful sequencing, assembly, and

annotation. These standards include phylogenetic studies and genome comparisons to establish evolutionary relationships (Simmonds *et al.*, 2023).

1.2.2. Structural Organisation of Bacteriophage

All phages consist of at least two components: a nucleic acid and a capsid that encapsulates it (Louten, 2016). The essential components known as coat proteins come together to form the capsid, a very strong and flexible structure that protects the genetic material (Louten, 2016). These proteins are usually homogeneous, and the instructions required for their synthesis and self-assembly come from the phage genome of limited length (Louten, 2016; Fokine and Rossmann, 2014). The phage genome and its capsid-surrounded compound are called a nucleocapsid (Louten, 2016).

Bacteriophage capsids are usually observed in two main forms (Louten, 2016). Both an icosahedral and helical form occur in phages; the most common is the icosahedral (Louten, 2016). Filamentous phages (Louten, 2016) exhibit a helical form. Moreover, the presence of lipid-based membranes defines several viruses in particular. According to Mäntynen *et al.* (2019), these structures are classified as envelopes. Although human or archaeal viruses typically exhibit these enclosed structures, most bacteriophages lack envelopes (Mäntynen *et al.*, 2019). The presence of the envelope shapes the interaction between the virus and its host since the proteins responsible for attachment differ depending on the virus form (Maginnis, 2018).

Bacteriophages frequently exhibit a tail structure, which is an essential component, since more than 90% of members of the order *Caudovirales* display this feature (Ackermann, 2007). The infection process depends on the tail because it enables transfer of phage genetic material into bacterial cells (Ge and Wang, 2024). The head-to-tail interface (HTI) functions as a

multiprotein complex that replaces one of the fivefold vertices of the capsid (Aksyuk and Rossmann, 2011). The dodecameric portal protein (PP) functions as the DNA-packaging motor and essential gatekeeper for genome release through its location within the capsid (Hendrix, 2002). The receptor-binding proteins (RBPs) located on the phage baseplate enable precise target-bacterium identification, leading to successful infection (Hendrix, 2002).

Myoviridae-like phages contain tail structures that function as contractile mechanisms to penetrate the outer membrane of host cells (Leiman *et al.*, 2004). The baseplate connects to the capsid through a contractile sheath (Fokine and Rossmann, 2014). The baseplate serves as a regulatory element that directs phage–bacterium interactions (Harada *et al.*, 2018; Huang and Xiang, 2020). The baseplate positions six elongated tail fibres, which act as essential components for host detection (Kostyuchenko *et al.*, 2005). The short tail fibres become active after host interaction to initiate the attachment process (Kostyuchenko *et al.*, 2005).

1.2.3. The Life Cycle of Bacteriophage

In order to infect a particular bacterium, bacteriophages from both virulent and temperate groups are highly dependent on their ability to attach to specific receptors on the surface of host cells (Birge, 2006; Salmond and Fineran, 2015). Their life cycle begins with adsorption (attachment) to the bacterial cell surface, followed by penetration of bacteriophage nucleic acid into the host cell. Subsequently, replication of the phage nucleic acid and synthesis of essential proteins occur within the host cell, leading to the assembly of new virions. Finally, the mature virions are packaged and released through lysis of the host cell, allowing the newly formed bacteriophages to infect other bacterial cells (Rakhuba *et al.*, 2010).

1.2.3.1. Adsorption and Intracellular Penetration

The initial phase in the life cycle of a bacteriophage involves its engagement with the bacterial cell through a process known as adsorption, where this connection to the host cell surface is facilitated by specific binding receptors (Adams, 1959). Numerous receptors, such as the capsule, flagella, porins, LPS, and OmpA proteins, have been thoroughly documented (Jakhetia and Verma, 2015; Zhang *et al.*, 2015; Bertozzi Silva *et al.*, 2016; Rakhuba *et al.*, 2010).

The adsorption rate is a distinctive parameter for each phage–host combination and can vary depending on the concentration of phages or hosts. As bacteriophages lack specialised mechanisms for transport, they cannot move autonomously; thus, the adsorption process results from random phage–cell collisions, as established by the law of mass action (Rakhuba *et al.*, 2010). Consequently, as the concentration of virions and bacterial cells increases, the frequency of random contacts rises, resulting in a higher adsorption rate (Sillankorva *et al.*, 2004). The adsorption rate is influenced by several non-specific physicochemical parameters such as pH, temperature, and the presence of specific substances and ions in the medium, and it also depends on the host's physiological state and culture conditions. Adsorption generally occurs in two ways: reversible and irreversible binding. The molecular mechanisms of interaction at both stages are unique to each phage–host system and may differ considerably among taxonomic families (Sillankorva *et al.*, 2004).

Nucleic acid penetration typically follows irreversible binding. Each stage of this process is unique to the phage species. The electrochemical membrane potential, ATP molecules, and the enzymatic breakdown of the peptidoglycan layer may be crucial for the incorporation of the genome into the bacterial cytoplasm.

In T4-like phages, the first stage of adsorption involves the reversible binding of long tail fibres to specific receptors. When three or more long tail fibres bind to the cell surface, the mechanism for phage tail alteration is activated. The baseplate modifies its form, leading to a stellate conformation (Crawford and Goldberg, 1977). Ultimately, six short tail fibres are generated, which irreversibly attach to the LPS core. The alteration in the baseplate synchronously triggers the contraction of tail sheaths, allowing the inner tube to penetrate the bacterial outer membrane (Montag *et al.*, 1987).

In T7-like phages, first contact occurs between the tail fibres of phage T7 and the lipopolysaccharides of the bacteria. Upon contact, the signal initiating irreversible virion binding is transmitted into the phage capsid through protein Gp13, the tail fibre, and the phage tail. This signal triggers the reorganisation of the tail proteins to form a cylindrical shape within the phage head. The genome is then coiled onto the cylinder created within the capsid. As the proteins Gp13–Gp16 cross the phage tail channel and navigate the pathway via the bacterial cell wall, the genome penetrates the cytoplasm (Molineux, 2001; Kemp *et al.*, 2004; Hu *et al.*, 2013).

Phage PRD1, recognised as a broad host-range phage, utilises different receptors for adsorption. It employs a receptor encoded by one of the conjugative plasmids N, P, or W. PRD1 can infect various bacterial species, including *E. coli, P. aeruginosa,* and *S. enterica,* if they harbour one of these plasmids (Lyra *et al.*, 1991; Olsen *et al.*, 1974). The capsid of this phage contains 24 copies of protein P3, each crowned with spikes. A membranous vesicle covering the genome is located within the capsid (Rydman *et al.*, 2000).

The initial phase of adsorption is reversible binding, which occurs between spike proteins and cell receptors. This leads to the alteration and release of three spike proteins that create a

pore in the capsid (Rydman *et al.*, 2000). The phage membrane within the capsid undergoes rearrangement, resulting in a tubular tail that penetrates the bacterial cell wall. Two proteins located at the newly developing tube degrade the peptidoglycan at the penetration sites, generating pores that facilitate the release of the phage DNA into the cytoplasm (Rydman *et al.*, 2000; Bamford and Mindich, 1982).

1.2.3.3. Nucleic acid Replication, Packaging and Release

After the bacteriophage nucleic acid enters the host cell, the process of replication begins in the lytic phage (Stone *et al.*, 2019). Following the lytic cycle, the phage genome directs the host biosynthetic machinery to replicate the nucleic acid. In addition, essential proteins are synthesised, assembled, and packaged, with new viruses released via lysis of the host cell (Shao and Wang, 2008).

Whereas some phages use alternate replication methods, they initially remain in a lysogenic relationship within the host. Subsequently, they are replicated with the genome of the host cell and then released from the cell (Birge, 2006; Dale and Park, 2013).

In some bacteriophages (*λ, P2*), the DNA is linear and has terminal pairs of complementary cohesive ends, while in other phages such as *P1* and *P22* the DNA is circularised via site-specific recombination of terminally redundant ends (Birge, 2006; Dale and Park, 2013).

1.2.4. Virulence of Bacteriophage

Two important parameters define the host-lysing capacity of bacteriophages. Firstly, bacteriophages must replicate more quickly than their host. Secondly, the emergence of phage-resistant host strains must not be significant; otherwise, they will quickly replace the phage-sensitive host population, rendering phage treatment ineffective (Levin and Bull, 2004).

In some cases, although host strains resistant to phage therapy appear to be less virulent than the parent cells, this is rare. Additionally, different resistant variants exhibit variable fitness, and their significance is difficult to determine, particularly under *in vivo* conditions (Lenski, 1988; Atterbury *et al.*, 2007). Resistant variants of *Salmonella* and *Vibrio cholerae* arose after the first phage treatment, but they constituted only a small subset of the overall bacterial population (Zahid *et al.*, 2008; Gutiérrez *et al.*, 2015).

Some bacteriophages commonly possess an enzyme called depolymerase as an integral component of their virion structure (Knecht *et al.*, 2020). Upon binding to the capsular polysaccharides of the host bacteria, these enzymes cleave the repeating polysaccharide units. Ultimately, the phage penetrates the final barrier—the bacterial cell wall—and introduces its DNA, thereby initiating infection (Knecht *et al.*, 2020). Similar enzymes have been identified in bacteriophages belonging to the *Ackermannviridae* (Plattner *et al.*, 2019). If phages do not have a depolymerase enzyme, they might not be able to infect capsulated strains (Pertics *et al.*, 2021).

1.2.5. Isolation, Purification, and Quantification of Bacteriophages

The research of bacteriophages starts with their recovery from environments which contain many bacterial hosts. The purification and quantification methods after isolation remain essential for understanding phage biology and applications in ecological research and therapeutic uses and biotechnological projects.

1.2.5.1. Isolation of Bacteriophages

The environment supports numerous bacteriophages, which can be isolated from bacterial habitats. The primary sources of bacteriophages exist in all environments where

bacteria thrive, including soil, wastewater, freshwater, marine ecosystems, sewage, animal faeces, compost, food products, and clinical samples from humans or animals (Clokie *et al.*, 2011).

The initial step of the isolation technique starts with sample processing. Solid samples are first homogenised, followed by centrifugation to remove eukaryotic cell debris and particle waste, and filtration separates phages from dominant bacteria in the original sample (Carlson, 2005).

Following initial processing, a widely used technique is enrichment. In this step, the phage-containing filtrate is incubated with a logarithmically growing culture of a suitable bacterial host in a nutrient-rich broth under favourable conditions such as appropriate temperature, pH, and aeration (Carlson, 2005). The main objective of enrichment is to selectively increase the concentration of certain phages that can infect and replicate within the targeted host, facilitating their detection (Carlson, 2005).

However, although enrichment is effective for enhancing phage titres, it may introduce substantial biases into the isolated phage population. The strategy naturally promotes the proliferation of virulent (lytic) phages that reproduce quickly and efficiently under designated laboratory conditions and on the chosen host strain (Van Twest and Kropinski, 2009). This may result in the under-representation or total absence of temperate phages, slow-replicating phages, phages with varying host specificities, or phages less robust in broth culture (Gutiérrez *et al.*, 2015). Research on phages targeting *Escherichia coli (E. coli)* and *P. aeruginosa* frequently demonstrates that enriched samples mostly produce lytic phages, attributable to their rapid replication cycles (Clokie *et al.*, 2011; Sturino and Klaenhammer, 2006).

To potentially eliminate these biases and isolate phages that may be missed during enrichment, direct plating of the processed sample (without prior enrichment) onto a lawn of the host bacteria can be utilised, especially if phages are anticipated to be present at high initial concentrations (Carlson, 2005).

The plaque assay is conventionally used to accomplish the detection and enumeration of lytic phages, regardless of whether enrichment or direct plating is employed (Adams, 1959). This method involves combining the diluted substance with the target bacteria and then spreading them on solid nutrient agar using the agar overlay technique. Lytic phages infect and lyse host cells, resulting in clearings known as plaques during bacterial growth. Theoretically, each plaque originates from a single infectious phage particle, enabling the measurement of phages as plaque-forming units (PFU) per millilitre (Carlson, 2005).

To facilitate further characterisation and guarantee a clonal phage population, individual plaques are generally selected, resuspended, and subjected to multiple rounds of purification via serial plaque isolations (Bonilla *et al.*, 2016).

1.2.5.2. Purification of Bacteriophages

After successful isolation and subsequent amplification, the purification of bacteriophage preparations is an essential multi-step procedure. The main goal is to remove unwanted materials from the host bacteria and the culture medium, such as bacterial remnants (cell walls, proteins, DNA/RNA), harmful substances (endotoxins from Gram-negative bacteria), and leftover components from the media (Carlson, 2005). This step is crucial for applications such as phage therapy, where it is important to have highly pure phage stocks to ensure they are safe, less likely

to cause immune reactions, and effective. Endotoxins are significant pyrogens that may trigger strong inflammatory reactions when introduced to patients (Pirnay *et al.*, 2018).

The initial purification procedures often include clarification of the phage lysate. This can be accomplished using low-speed centrifugation to sediment larger bacterial cells and debris, followed by filtration through membranes with pore diameters (e.g., 0.22 µm or 0.45 µm) that permit phages to pass while retaining residual bacteria and larger particles (Adams, 1959). Chloroform-resistant phages may undergo chloroform treatment at this stage to lyse any residual bacterial cells (Carlson, 2005).

Phages are subsequently concentrated. Polyethylene glycol (PEG) precipitation is a commonly employed technique. PEG, generally at concentrations of 5–10%, efficiently excludes virions from solution, resulting in their aggregation and precipitation. Phage aggregates can be pelleted using moderate-speed centrifugation and subsequently resuspended in a reduced volume of an appropriate buffer (Carlson, 2005; Green and Sambrook, 2012). However, PEG precipitation often co-precipitates host cell proteins and other contaminants, requiring further purification steps.

Tangential flow filtration (TFF), or crossflow filtration, is an effective technique for concentrating phages and facilitating buffer exchange (diafiltration), which also assists in the removal of smaller pollutants (Wickramasinghe *et al.*, 2005).

Ultracentrifugation in density gradients, such as caesium chloride (CsCl) or sucrose, is an effective but time-consuming process for attaining high-purity levels. Phages are separated according to their hydrodynamic density, enabling the collection of highly pure phage bands (Gill

and Hyman, 2010; Clark and March, 2006). CsCl gradient ultracentrifugation is frequently regarded as the gold standard for acquiring research-grade, high-purity phages.

Chromatographic techniques provide robust, scalable, and often Good Manufacturing Practice (GMP)-compatible methods for phage purification, which are crucial for producing therapeutic-grade preparations.

Size-exclusion chromatography (SEC) is a widely used method that separates particles according to their size, enabling differentiation of bacteriophages from smaller protein contaminants or larger aggregates.

Ion-exchange chromatography (IEX) is another common method, which separates components based on their surface charge. IEX is widely applied in phage purification because phages typically have a negative charge in a liquid with natural pH (Vandenheuvel *et al.*, 2018; Ackermann, 2003).

1.2.5.3. Quantification of Bacteriophages

Bacteriophage titration can be done for many purposes, such as determining their abundance in a sample, assessing their lytic properties, defining their host range, or adjusting the dose required for phage therapy. There are various methods available to detect the phage titre, but none of them are effective under all conditions. The choice depends on the specific aims of the research and the features of the samples.

The most commonly used method is the plaque assay, generally accepted as the gold standard for enumerating lytic phages. Plaque assays usually begin by diluting the sample, which is thought to contain infectious phage particles, and then mixing these dilutions with a specific bacterial culture before spreading them with a soft layer of agar on solid plates (Adams, 1959).

After incubating these plates under conditions suitable for the target bacteria, clear zones, known as plaques, appear on the bacterial lawn (Carlson, 2005). Each plaque, assumed to be formed by a single infectious phage, is counted, and the measurement of the total phages in the sample is expressed in terms of plaque-forming units (PFU) per millilitre (PFU/mL). The plaque assay is widely used because it is inexpensive, easy to perform, and considered the reference standard by many. However, the method has a significant limitation, as it only detects lytic phages and requires culturable bacterial hosts under appropriate laboratory conditions. Since it cannot detect non-lytic phages or phages that require different hosts, it is insufficient to determine the total phage count in a sample (Clokie *et al.*, 2011; Ackermann, 2003).

Direct counting techniques are available to determine the total number of phages in a sample regardless of their lytic ability. One such technique is epifluorescence microscopy (EFM), which involves staining phage nucleic acids with fluorescent dyes such as SYBR Green I or SYBR Gold and observing them under a microscope (Patel *et al.*, 2007). This staining technique also forms the basis of flow cytometry (FCM), in which stained phages in suspension are automatically counted (Heinrichs *et al.*, 2021). Transmission electron microscopy (TEM), although generally used for morphological characterisation of phages, can also be applied for direct counting; however, it is labour-intensive and not suitable for routine use (Ackermann, 2009). While these direct counting techniques are culture-independent and highly effective, they cannot distinguish between lytic and non-lytic or damaged phages (Heinrichs *et al.*, 2021).

Other approaches fall under molecular techniques. For example, quantitative PCR (qPCR) can be used to calculate the amount of different phages in a sample by targeting their genomes or specific gene sequences. This technique enables the simultaneous quantification of multiple

phages and provides useful statistical data (Yoshida *et al.*, 2010; Voorhees *et al.*, 2024). A newer method, digital PCR (dPCR), allows absolute quantification of nucleic acid targets without the need for a reference curve and offers extraordinary accuracy and reproducibility (Morella *et al.*, 2018). In environmental investigations, these molecular methods are highly advantageous for detecting phages that may be difficult to cultivate. However, molecular techniques only detect phage DNA, which does not always indicate the presence of infectious particles (e.g., free DNA or defective phage genomes). Their accuracy is dependent on primer and probe design and the availability of sequencing data, which may exclude novel or highly divergent phages.

Although not widely applied, enzyme-linked immunosorbent assays (ELISAs) can also be used to quantify phages. This technique requires specific antibodies targeting phage capsid proteins and allows phage-induced bacterial lysis to be measured over time (Khan *et al.*, 2015).

Although each technique for phage titration yields valuable results, all have limitations. It is essential to be aware of these constraints and to select the method most appropriate for the study objectives. In practice, the best results are often obtained by combining multiple techniques.

1.2.6. Bacteriophage and Host Range

The type and variety of bacteria infected are important determinants in the characterisation of phages as well as in their taxonomy. This determining factor depends on the genotype and phenotype of both the phage and the bacterium and is also significantly influenced by the environment in which they are found (Holtappels *et al.*, 2023; Chung *et al.*, 2023; Hyman and Abedon, 2010). Precise determination of this factor, called host range, is very important for examining the evolutionary processes of phages and their host bacteria, as well as for

understanding the effectiveness of phages intended for therapeutic use (Holtappels *et al.*, 2023; Chung *et al.*, 2023).

When phages are used as antibacterial agents, host range diversity can be both an advantage and a disadvantage. Phages with a narrow host range can only infect one bacterial species or strain. In phage therapy, this is advantageous because only the targeted bacteria are eliminated, with no harm done to the patient's beneficial microbiota. Situations such as microbiota disruption caused by broad-spectrum antibiotics are prevented (Chung *et al.*, 2023). Nonetheless, this specificity is also disadvantageous because the bacteria causing the infection may not fall within the host range of the phage, or the infection may be caused by the interaction of multiple bacterial species (Holtappels *et al.*, 2023; Chung *et al.*, 2023).

On the other hand, phages that exhibit a broad host range, often termed polyvalent (though definitions differ across studies), have the capability to infect multiple strains or even different species (Chung *et al.*, 2023; Fong *et al.*, 2021). The presence of these phages offers potential for empirical therapy, allowing treatment before the precise strain is identified. They are also more likely to succeed against a range of circulating strains or in cases of mixed infections (Chung *et al.*, 2023; Fong *et al.*, 2021).

Due to the host range limitations of most individual phages, it is common to recommend or design phage cocktails incorporating multiple phages. This approach aims to expand the overall host range, increase efficacy, and reduce the risk of bacterial resistance to phages (Chung *et al.*, 2023; Fong *et al.*, 2021).

Therefore, host range determination, one of the main elements of phage characterisation, should be performed with a panel containing a sufficiently diverse number of bacterial species/strains (Chung *et al.*, 2023; Fong *et al.*, 2021).

1.2.7. Bacterial Resistance to Phage

Bacteria have developed sophisticated defence mechanisms against phages. On the other hand, phages have developed counterstrategies to overcome this defence. The ongoing co-evolutionary arms race between these two microorganisms causes them and the dynamics of the environment they are in to be constantly affected (Oechslin, 2018; Hampton *et al*., 2020).

1.2.7.1. *Adsorption Inhibition*

As mentioned in previous sections, successful adsorption is essential for phage infection. In adsorption, the first step in the infection process, phage receptor recognition proteins recognise and bind to the appropriate receptor on the bacterial cell wall. Bacteria have developed several strategies to prevent this crucial initial interaction.

The first of these is modification of the receptors recognised by phages (Labrie *et al.*, 2010; Dy *et al.*, 2014). Changes in the genes encoding these receptor proteins cause significant obstruction of phage adsorption. For example, many phages infecting Gram-negative bacteria recognise the O-antigen of LPS as a receptor. *Phage P22,* which infects *Salmonella* species in particular, also recognises this O-antigen. Therefore, any change in this antigen, such as a change in its length or composition, confers P22 resistance to the bacterium (Steinbacher *et al.*, 1997; Andres *et al.*, 2013). Another example is *phage OWB,* which recognises a transmembrane protein of *Vibrio parahaemolyticus* as a receptor and does not infect mutants lacking this protein (Ho *et al.*, 2020).

The bacterial cell wall normally acts as a barrier that protects against external factors, but this barrier also contains many receptors recognised by phages. Bacteria with cell wall defects may therefore resist phage infection. Mutant *P. aeruginosa* strains lacking type IV pili were found to be resistant to *phage PA5oc* (Olszak *et al.*, 2019).

Bacteria that have modified or lost structures to prevent phage adsorption may also lose virulence. For example, changes in LPS or type IV pili have been reported to cause a reduction in virulence. A decrease in biofilm formation has also been observed following such modifications. For instance, *P. aeruginosa* PA1S ceases to encode the O-antigen used by *phage PaP1* as a receptor to develop resistance. However, the resistant mutant strain PA1RG is both less virulent and more sensitive to antibiotics due to its biofilm deficiency (Li *et al.*, 2018).

The capsule functions both as a key virulence factor and as a receptor for some phages. *Phages Phab24, ΦFG02, and ΦCO01* specifically target the capsule of *Acinetobacter baumannii*. A single nucleotide deletion in the GTR29 and GPI genes, which are responsible for capsule synthesis in these bacteria, provides effective resistance to these phages. However, all phage-resistant, capsule-deficient *A. baumannii* strains have been shown to lose their antibiotic resistance (Gordillo Altamirano *et al.*, 2021; Wang *et al.*, 2021). These findings support the therapeutic use of phages that recognise virulence factors such as capsules, LPS, and pili as receptors in combination with antibiotics. In this way, antibiotic-resistant strains can be killed by phages, while those that develop phage resistance become antibiotic-sensitive and are eliminated.

Another adsorption-inhibition method developed by bacteria is receptor masking. Bacteria form an extracellular matrix to cover receptors. This matrix is usually a capsule, an S-

layer, or an exopolysaccharide (EPS) composition, or it may include outer membrane vesicles (OMVs). This structure prevents phages from reaching their receptors (Labrie *et al.*, 2010; Rostøl and Marraffini, 2019). For example, some *E. coli* strains employ a matrix of lipoproteins and other surface components as an effective defence against *phage T4* (Labrie *et al.*, 2010). T-like phages recognise the outer membrane protein OmpA of *E. coli* as a receptor. The bacteria synthesise an outer membrane lipoprotein, TraT, which binds to OmpA and masks phage adsorption. TraT not only confers phage resistance but also aids bacterial survival under extreme environmental conditions (Riede *et al.*, 1986; Looijesteijn *et al.*, 2001).

1.2.7.2. Prevention of DNA Injection

Phage may be capable of overcoming bacterial adsorption inhibition strategies and establishing effective adsorption. However, successful infection is not always guaranteed. Bacteria can sometimes utilise strategies to prevent the later introduction of phage DNA into their cytoplasm. These include membrane proteins that actively disrupt the DNA translocation process, thereby preventing infection from progressing before the phage genome can hijack the cell's machinery (Rostøl and Marraffini, 2019).

Phage D3112 and *phage MP22* are two phages that infect *P. aeruginosa* and recognise the type IV pilus (TFP) protein as a receptor. If *phage D3112* is present as a *P. aeruginosa* prophage, it prevents reinfection by *phage MP22* by inhibiting the assembly of the type IV pilus tail fibre. This mechanism involves the prophage-encoded Gp05 protein, which interacts with an assembly inhibitory protein to block pilus formation (Chung *et al.*, 2014).

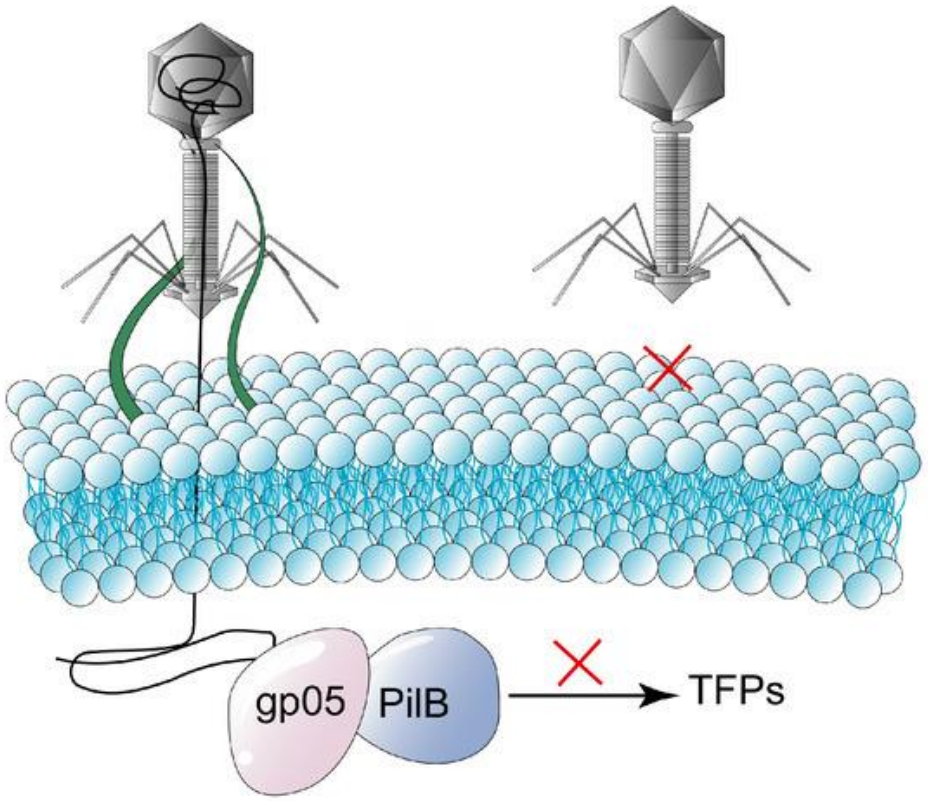

Figure 1.4. Illustration of superinfection exclusion (Sie), established by Phage D3112
Bacteria obstruct the phage's DNA injection through superinfection exclusion (Sie), as seen by the red cross symbol in the illustration, which signifies the prevention of phage adsorption. Phage D3112 encodes the protein GP05, which reduces PilB activity by interaction with PilB, hence impacting the assembly or function of TFPs and inhibiting re-infection of host cells by phage MP22, which similarly utilises *P. aeruginosa* TFPs as receptors (Wang *et al.*, 2023).

1.2.7.3. Superinfection Exclusion (Sie) Systems

Many bacteria that harbour prophages—phage genomes integrated into the bacterial chromosome or existing as plasmids—are protected from further infection by the same or closely related phages through superinfection exclusion (Sie) systems. These protective systems are typically encoded by the resident prophage itself. They frequently involve phage-derived proteins, expressed by the lysogenised bacteria and usually located in the bacterial membrane, that specifically obstruct DNA injection from incoming secondary phages (Labrie *et al.*, 2010; Seed, 2015).

This process clearly benefits the established prophage by maintaining its survival and replication within the host lineage, free from competition with other phages that could otherwise lyse the cell. The widely studied *T4 phage* encodes Sie systems that successfully hinder infection by other T-even phages (Shi *et al.*, 2020; Bucher and Czyż, 2024). *Bacteriophage P22,* which infects *Salmonella enterica* serovar Typhimurium, also employs Sie mechanisms to inhibit subsequent infections by other *P22 phages* or their relatives (Seed, 2015; Leavitt *et al.*, 2024).

The Sie mechanism has been observed most frequently in *T-like phages*. For example, after infecting a bacterium, *T4 phage* encodes two proteins, Imm and Spackle, which ensure that most foreign DNA remains trapped in the capsid while the rest is cleaved outside the host by endonuclease I if another T-like phage attempts infection. Of these proteins, Imm prevents DNA transfer by binding to a receptor protein in the inner membrane, while Spackle prevents peptidoglycan degradation. The tail spike protein Gp5 normally degrades peptidoglycan to facilitate entry into the cytoplasm; however, if the bacterium is already lysogenised by another T-like phage, the early phage produces a protein Sp that inhibits Gp5 activity by forming Sp–Gp5 complexes, thereby preventing secondary infection (Shi *et al.*, 2020).

1.2.7.4. Restriction-Modification (R-M) Systems

After phage DNA enters the bacterial cytoplasm, it encounters another significant defence mechanism: the restriction–modification (R–M) systems. These enzymatic systems function as innate immune mechanisms and are widely distributed across biological systems.

The R–M systems contain two essential enzymatic components: restriction endonucleases (REs), which identify particular short DNA sequences and cleave any DNA containing these sequences, and methyltransferases (MTases), which modify the same

recognition sequences on host DNA. The bacterial chromosome remains protected from RE cleavage through self-methylation patterns, as described by Labrie *et al.* (2010) and Tock and Dryden (2005). The host RE identifies phage DNA as foreign because it lacks the host-specific methylation patterns at recognition sites, leading to rapid degradation through cleavage and preventing infection (Sitaraman, 2016; Arias *et al.*, 2022).

The R–M systems are classified into four main types—Type I, II, III, and IV—which differ in their subunit structures, cofactor requirements, recognition sequence characteristics, and processes of DNA cleavage and methylation (Tock and Dryden, 2005).

1.2.7.5. CRISPR-Cas Systems

The Clustered Regularly Interspaced Short Palindromic Repeats (CRISPR) and CRISPR-associated (Cas) protein systems represent a sophisticated bacterial defence mechanism. Retaining genetic memories of past interactions, the system uses sequence-specific defences against phages and mobile genetic elements, functioning like an adaptive immune system in bacteria and archaea (Labrie *et al.*, 2010; Hampton *et al.*, 2020).

Immunity conferred by CRISPR–Cas operates in three sequential stages. The adaptation stage begins with an initial infection, during which the host cell captures foreign DNA fragments known as protospacers. These fragments are then integrated as new spacers into the CRISPR array within the host chromosome. This process establishes a cellular memory that protects against recurrent infections by the same pathogen, both within the present cell and among its progeny.

The expression stage involves transcription of the CRISPR array into long precursor CRISPR RNA (pre-crRNA). Cas proteins cleave the pre-crRNA to generate multiple small crRNAs containing spacer sequences derived from past invaders.

Finally, in the interference stage, the crRNAs combine with various Cas proteins to form ribonucleoprotein effector complexes. The crRNA spacer sequence serves as a molecular guide, recognising and binding to complementary DNA sequences (protospacers) in invading phages. This binding activates Cas nucleases, which cleave and inactivate the foreign DNA, halting infection (Bourgeois *et al.*, 2020; Pawluk *et al.*, 2018).

Several forms of CRISPR–Cas systems exist—Types I, II, III, V, and VI—each distinguished by unique combinations of Cas proteins and distinct operational mechanisms.

1.2.7.6. Abortive Infection (Abi) Systems

Operating as programmed cell death defence systems, abortive infection (Abi) systems benefit the surrounding bacterial population. Activation of Abi systems during phage infection leads either to bacterial cell death or to significant metabolic arrest (Labrie *et al.*, 2010; Rostøl and Marraffini, 2019). This self-destructive mechanism halts phage replication and the release of new phage progeny, thereby safeguarding the surrounding bacterial colony from widespread infection.

Abi systems manifest in diverse forms, targeting crucial stages of phage development, including DNA replication, transcription, protein translation, and virion assembly (Seed, 2015). The AbiZ system in *Lactococcus lactis* interferes with virion assembly and release mechanisms, while also inducing premature cell lysis. This mechanism significantly reduces the phage burst size, thereby protecting the bacterial population (Rostøl and Marraffini, 2019; Seed, 2015).

Since Abi activation results in bacterial death, it is considered the last line of defence against phage infection. Multiple mechanisms can activate Abi systems, which are generally examined under three main categories: CRISPR–Cas, toxin–antitoxin (TA), and cyclic oligonucleotide-based anti-phage signalling systems (CBASS) (Lopatina *et al.*, 2020).

The first mechanism is the CRISPR–Cas-mediated Abi system. If the CRISPR–Cas system of a phage-infected bacterium fails to provide complete protection, it activates Abi before phages are fully assembled. This prevents surrounding cells from being infected and triggers cell death as the bacterium sacrifices itself (Strotskaya *et al.*, 2017). An example is the Type I-F CRISPR–Cas system of *Pectobacterium atrosepticum*, which activates Abi when it fails to protect against phage infection (Watson *et al.*, 2019).

The TA system of bacteria has multiple functions, including biofilm formation, regulation of bacterial growth, maintenance of genome stability, and protection of populations from phage infections by activating Abi (Wen *et al.*, 2014). The TA system is widespread among bacteria and works by producing a toxin and a less stable antitoxin simultaneously, but at different rates, with variable effects depending on this balance. While the toxin controls bacterial growth, the antitoxin inhibits excess toxin activity (Manikandan *et al.*, 2022). As long as the antitoxin neutralises the toxin, the TA system remains inactive. During phage infection, the bacterial TA transcription mechanism is disrupted, reducing toxin–antitoxin production. The less stable antitoxin degrades before the toxin, leading to toxin accumulation, growth arrest, and eventual bacterial death (Guegler *et al.*, 2021).

Another pathway initiating Abi is CBASS, which is widely distributed among bacteria. Upon phage infection, a cGAS/DncV-like (CD-NTase) nucleotide transferase within CBASS produces

second messengers such as cyclic dinucleotides and cyclic trinucleotides (Govande *et al.*, 2021). The CD-NTase-associated protein (Cap) functions as an effector, activated upon interaction with its specific second messenger. This activation leads to cell membrane breakdown and the triggering of Abi (Fatma *et al.*, 2021).

1.2.7.7. Phage Counter-Adaptations: The Other Side of the Arms Race

In order to overcome the various defence mechanisms developed by bacteria against phages, as mentioned in previous sections, phages have evolved their own counter-mechanisms (Abdelsattar *et al.*, 2021; Hampton *et al.*, 2020).

Phages overcome adsorption inhibition through genetic mutations in their receptor-binding proteins (RBPs), located either at the distal tail fibre ends or within tail spike structures. These mutations enable phages to detect alternative host receptors or to bind to receptors presented on bacterial surfaces. Phages have also acquired enzymatic functions, such as depolymerases, which dissolve blocking capsules and exopolysaccharide (EPS) layers to expose cellular receptors.

Phages have developed multiple strategies to bypass restriction–modification (R–M) systems. One common strategy is acquiring mutations that eliminate or reduce restriction endonuclease recognition sites in their DNA sequence (Labrie *et al.*, 2010). Many phages actively modify their DNA to mimic host methylation signatures or introduce alternative modifications that prevent recognition and cleavage by host restriction enzymes. *T4 phages*, a classic example among *T-even phages,* substitute hydroxymethylcytosine (HMC) for cytosine in their DNA, which is further glycosylated to protect their genome from a wide range of host restriction enzymes (Samson *et al.*, 2013). Some phages also produce their own methyltransferases, modifying DNA

after host entry. Others synthesise proteins that directly inhibit host RE activity—for instance, the Ocr (overcomes classical restriction) protein, which functions as a molecular DNA mimic (Tock and Dryden, 2005).

The battle against CRISPR–Cas systems is met by phages through several strategic approaches. Phages develop mutations in their targeted protospacer DNA or PAM (protospacer adjacent motif) sequences, allowing escape from Cas nuclease recognition and cleavage (Labrie *et al.*, 2010; Pawluk *et al.*, 2018). The most powerful counter-defence mechanism against CRISPR–Cas immunity is the production of anti-CRISPR (Acr) proteins. These small, phage-encoded proteins form a diverse group that actively inhibits host CRISPR–Cas systems. Acr proteins interfere by blocking the DNA-binding or nuclease activity of Cas proteins, disrupting effector complex assembly, or preventing crRNA loading (Pawluk *et al.*, 2018; Stanley and Maxwell, 2018).

Phages also employ strategies to overcome abortive infection (Abi) systems. Although less studied compared with Acr proteins, some phages develop mutations in components or processes targeted by Abi systems, thereby evading their effects. It is also hypothesised that phages may produce anti-Abi proteins or establish mechanisms to block or bypass specific Abi defences, allowing them to complete their lytic cycle despite active Abi system presence (Hampton *et al.*, 2020).

The continuous interaction between bacterial resistance mechanisms and phage counter-adaptations illustrates an evolutionary arms race. This dynamic is a major driving force shaping the genetic diversity of both bacterial and phage populations, while also influencing microbial community structure and function. A complete understanding of these intricate molecular

battles provides a crucial foundation for the development and application of phage-based therapies.

1.2.8. Bacteriophage Therapy

The widespread development of antibiotic resistance (AR) across nearly every major antibiotic class is driving scientists towards the discovery of more potent antibacterial treatments and non-traditional antibiotic solutions (Ayaz *et al.*, 2017; Ayaz *et al.*, 2019). Researchers have identified bacteriophages as a promising antibacterial strategy through alternative approaches (Azizian *et al.*, 2013; Summers, 2001).

This treatment method relies either on bacterial lysis caused by phage infection or on the application of phage lysis proteins to destroy bacteria. Importantly, bacterial resistance to antibiotics does not prevent them from being infected by phages.

Research on phage structure, phage–host cellular interaction mechanisms, and the ability of phages to redirect host biochemical machinery for phage propagation will support the development of more effective phages against multidrug-resistant (MDR) pathogens (Clark and March, 2006; Duckworth and Gulig, 2002).

1.2.8.1. *Advantageous and Disadvantages of Phage Therapy*

The increasing pathogenic bacterial resistance to antimicrobials has sparked new interest in bacteriophage therapy as either an alternative or supporting method to traditional antibiotics (Levin and Bull, 2004; Wittebole *et al*., 2014). Although phages demonstrate multiple promising features for antimicrobial use, their actual utilisation encounters significant barriers.

1.2.8.1.1. Advantages of Phage Therapy

Phages demonstrate multiple inherited features that make them suitable for therapeutic applications:

Phages provide a key advantage through their targeted host specificity, as they infect particular bacterial species or strain populations. This specific targeting ability protects the host microbiota from harm, avoiding the broad-spectrum damage caused by antibiotics (Barrow and Soothill, 1997; Loc-Carrillo and Abedon, 2011; Principi *et al.*, 2019).

The bacterial hosts present at infection sites enable phages to multiply exponentially as long as contact is maintained. This auto-dosing property means a small initial dose can amplify to high concentrations exactly where required, ensuring effective bacterial elimination (Summers, 2001; Abedon *et al.*, 2011).

Phages employ distinct killing mechanisms compared with antibiotics. Due to these unique mechanisms, phages remain effective against bacteria that have acquired resistance to multiple antibiotics (Levin and Bull, 2004; Lin *et al.*, 2017). This makes treatment of ESKAPE pathogens—*Enterococcus faecium, Staphylococcus aureus, Klebsiella pneumoniae, Acinetobacter baumannii, Pseudomonas aeruginosa,* and *Enterobacter* species—possible.

Biofilm-associated bacterial infections represent a major challenge for antibiotic therapy, as these structured microbial communities are resistant to conventional antibiotics. Certain phages possess depolymerases or can be genetically engineered to produce such enzymes, breaking down biofilm matrices to facilitate penetration by phages or antibiotics and destruction of the protected bacteria (Abedon *et al.*, 2017; Pires *et al.*, 2017).

As phages are composed mainly of nucleic acids and proteins, highly purified preparations demonstrate safety for eukaryotic cells, with few adverse effects reported (Barrow, 2001; Abedon *et al.*, 2011). Their specificity also results in minimal interaction with human cells. For example, the intravenous administration of phage therapy to treat a patient with a colistin-only sensitive *P. aeruginosa* infection led to fever resolution, normalisation of liver biochemistry, and bacterial clearance confirmed by serum tests, without major adverse effects (Jennes *et al.*, 2017).

Bacteriophages are the most abundant biological entities on Earth and can be isolated from diverse environmental sources where their bacterial hosts reside (Summers, 2001). This vast natural reservoir represents a rich source for discovering novel therapeutic candidates.

1.2.8.1.2. Disadvantages and Challenges of Phage Therapy

The widespread clinical implementation of phage therapy encounters multiple obstacles despite its substantial benefits. The specific target preference of individual phages functions as a beneficial trait yet also creates an obstacle because generally phages tend to infect only a narrow range of hosts. Therapy effectiveness requires exact pathogen identification, yet this becomes difficult in emergency conditions. In the case of diseases caused by multiple pathogens, narrow-spectrum phages might not be able to eliminate all. The need to develop phage cocktails along with personalised methods complicates the process (Summers, 2001; Principi *et al.*, 2019; Kutter *et al.*, 2010).

As mentioned in Section 1.2.6, phages encounter resistance development from bacteria through different mechanisms which include adsorption inhibition, restriction–modification (R–M), CRISPR–Cas system activation, and abortive infection (Abi) system (Labrie *et al.*, 2010; Rohde *et al.*, 2018). In an early research study involving anti-K1 phage treatment for *Escherichia coli*

meningitis and septicaemia in calves and chickens, the disease symptoms disappeared at first. A calf showed disease relapse later while scientists recovered phage-resistant bacteria from its blood sample (Barrow *et al.*, 1998). Phage cocktails represent one potential solution to reduce this challenge (Payne and Jansen, 2001).

The mononuclear phagocyte system of the host detects phages when given systemically, thus leading to their elimination from circulation and reduced therapeutic impact. Phage proteins become targets for neutralising antibodies when administered multiple times to the host, which leads to decreased therapeutic outcomes (Summers, 2001; Jończyk-Matysiak *et al.*, 2017; Principi *et al.*, 2019).

The process of obtaining high-purity phage preparations involves removing bacterial debris and especially endotoxins because their parenteral administration can trigger severe inflammatory and pyrogenic reactions. The production of endotoxin-free phage preparations at commercial scale is difficult and expensive (Abedon *et al.*, 2011; Kutter *et al.*, 2010).

Many countries lack established regulatory pathways to approve phage therapy. The regulatory framework for phages faces unique challenges because these replicating biological agents differ from conventional chemical drugs regarding manufacturing consistency, quality control requirements, and clinical trial design (Principi *et al.*, 2019; Verbeken *et al.*, 2014).

The understanding of the pharmacokinetics and pharmacodynamics (PK/PD) profiles of various phages remains limited, particularly concerning their tissue distribution patterns, duration of presence, and suitable treatment protocols (Payne and Jansen, 2001; Abedon *et al.*, 2011). The effectiveness and stability of phages can be influenced by environmental conditions such as pH and temperature in the infection site (Summers, 2001).

Phage manufacturing according to Good Manufacturing Practice (GMP) standards becomes challenging when scaled up for commercial production. Phage preparations face challenges in maintaining their stability during storage and transport, which requires additional formulation solutions (Kutter *et al.*, 2010).

The use of lytic phages for therapy poses the theoretical threat of transferring unwanted bacterial genes, particularly when phages are inadequately characterised or exhibit generalised transduction capabilities (Principi *et al.*, 2019; Rohde *et al.*, 2018). Genomic analysis must be performed thoroughly to decrease this potential danger. The future therapeutic potential of bacteriophages depends on solving these challenges through ongoing research, standardised protocols, and clear regulatory guidelines.

1.2.8.2. Existing Treatment and Applications of Phage Therapy

Bacteriophage therapy, with its advantages and disadvantages, offers versatile opportunities and is increasingly being used in both clinical and veterinary medicine. The risk of global antimicrobial resistance, which jeopardises the effectiveness of traditional antibiotics, has spurred interest in phage therapy, an alternative treatment method, and its use in contemporary practice. Unlike traditional antibiotics, which are broad-spectrum and disruptive to the natural microbiota, phages hold a promising position due to their highly specific, targeted action, and their inherent ability to evolve against phage resistance if they can be developed in bacteria.

Current phage therapy can be characterised within two main frameworks: personalised phage therapy and the use of pre-prepared phage cocktails. Personalised phage therapy involves isolating phages specific to the bacterial strain infecting the patient and adapting them to target and kill the strain. An example is the personalised phage therapy used in a 62-year-old woman

with chronic prosthetic joint infection caused by *Pseudomonas aeruginosa*. Systemic administration of Pa53 phage combined with meropenem, along with local joint drainage, stopped the infection, but the bacteria were not eradicated without recurrence after two years of follow-up (Cesta *et al.*, 2023). Another case of recurrent ventilator-associated pneumonia and bacteraemia caused by a *P. aeruginosa* strain with a strong MDR profile, following a severe burn, was cured with personalised phage therapy. In this case, phages were administered nebulised and intravenously along with imipenem–relebactam, resulting in successful treatment within a short time (Teney *et al.*, 2024). Another promising result was observed in a paediatric case. A 3-month-old baby with very severe bronchitis due to multiresistant *P. aeruginosa* and *Dolosigranulum pigrum* was initially reported to have decreased antibiotic resistance and complete eradication of the bacteria after inhalation of Pyobacteriophage, a commercial phage preparation, along with antibiotics (Morozova *et al.*, 2024). These examples illustrate the potential of the synergistic use of personalised phage therapy with antibiotics.

In addition to personalised phage therapy, the use of pre-prepared phage cocktails is also an important option in some cases. Cocktails formulated to target the most prevalent strains, previously isolated against strains known to be resistant to antibiotics, have a broader application potential without the delays associated with the specialised phage isolation step in personalised phage therapy. For example, a 2019 study demonstrated the potential of phage cocktails against prosthetic joint infection caused by multi-resistant *Staphylococcus aureus*. In the study, various treatment regimens were tested in the adult male Sprague–Dawley rat model, a clinically relevant animal model. While the phage cocktail alone reduced bacterial load by fivefold, vancomycin alone caused an approximately sixfold reduction. However, the combined use of the

phage cocktail and this antibiotic resulted in an approximately 23-fold reduction and resolution of joint swelling and inflammation (Morris *et al.*, 2019). These findings further emphasise the potential of the synergistic use of phage and antibiotic in cases untreatable with antibiotics alone. In a study investigating the efficacy of the AB-SA01 cocktail, consisting of three *Myoviridae* phages, against diabetic foot ulcers caused by MRSA multi-resistant *S. aureus*, the effects of the phage cocktail, saline, and vancomycin were compared in mice. No improvement was observed in the mice treated with saline; in fact, purulent ulcers were observed as the infection worsened. In contrast, phage cocktail AB-SA01 reduced bacterial load similarly to or even better than vancomycin results, while promoting wound healing without any observed side effects (Kifelew *et al.*, 2020).

Phage therapy is gaining increasing importance in veterinary practice, as well as in human medicine. In animal husbandry, where antibiotics have been extensively used for a long time, phage therapy is an important alternative to antibiotics, reducing the risk of antibiotic resistance and allowing pathogens to be eliminated without leaving residues. *Staphylococcus aureus*, the causative agent of bovine mastitis, one of the most serious problems in dairy farms, has been one of the primary agents studied. Studies have shown that phage preparations are effective in bovine mastitis. For example, Srujana *et al.* (2022) isolated the agent and its bacteriophages from cows with mastitis caused by antibiotic-resistant *S. aureus*. In the study, 32 of the agents isolated from farm wastewater were multidrug resistant, and 19 lytic phages were isolated against them. Isolate A2, one of the most promising phages, had a broad host range in the broth. Topical application of similar phages is suggested as an alternative or supplementary approach to antibiotics in controlling mastitis and may play an important role in reducing antibiotic resistance.

In another example of the use of phages against mastitis, Cho *et al.* (2025) conducted a study in Southern Korea. The team isolated three novel phages (OPT-SA02, OPT-SC01, and OPT-SX11) specific for *S. aureus* and *S. xylosus*, the main agents of bovine mastitis, from chicken faeces and sewage. Phages from the *Herelleviridae* family have been observed to be resistant to extreme environmental conditions and to be effective even at low MOI. Genetic analyses have shown that the phages possess holin–endolysin lytic cassettes and have high antibacterial properties. In a milk model, the phages significantly eliminated bacteria, suggesting they are a promising alternative to antibiotics in the treatment of mastitis.

There are also studies demonstrating the benefits of phage therapy in pig production. For example, Thanki *et al.* (2022) examined the prophylactic use of a two-phage cocktail against *Salmonella enterica* in pigs. SPFM10 and SPFM14 phages were sprayed, along with preservatives, onto commercial pig feeds before pelleting. It was noted that the phages remained active in pelleted feeds for up to six months and based on the challenge model of piglets fed these feeds, significant inhibition of *Salmonella* colonisation in various intestinal regions was reported without damaging the intestinal microbiota. This study demonstrates that phages can effectively protect against intestinal pathogens when formulated with feed. It also serves as an example of phage application in food safety.

Poultry farming is another application area where phage activity is extensively tested. An example is Atterbury *et al.* (2007), who attempted to control *S. enterica* colonisation in broiler chickens using phage applications. After characterising 232 phages isolated from poultry farms and abattoirs, three were determined to have a broad host range and were tested *in vivo* and *in vitro*. Oral administration of high doses of these phages resulted in a 2–4 log CFU reduction in the

bacterial load of *S. Enteritidis* and *S. Typhimurium* colonising the caecum within 24–48 hours. Although small amounts of phage resistance were observed, it was noted that it was not stable and did not persist for long periods. This study demonstrates that carefully prepared phage preparations, when applied at adequate doses, significantly reduce *Salmonella* colonisation and that phage applications are a significant alternative to antibiotics in the poultry sector and animal food production. A more recent example is the study conducted by Wanasawaeng *et al.* (2025) in Thailand, where they evaluated the potential of phage applications for *Salmonella* control in broiler chickens. The SEpBS-1 phage they isolated was found to be stable under varying pH, salinity, and temperature conditions and to have a very broad host range, infecting *S. Enteritidis, S. Typhimurium, S. Hadar, S. Dublin,* and *S. Poona*. A high burst size of 973 PFU/cell also indicated high lytic activity. *In vivo* studies reported a significant reduction in *Salmonella* in the caecum and internal organs of treated animals. Microbiota analyses reported that, in addition to pathogen reduction, gut health was supported, and villus development was observed.

Given the heavy burden of bacterial diseases in fish, phage applications in aquaculture are observed to be promising. Akmal *et al.* (2020) suggest that phage therapy against *Aeromonas hydrophila*, the cause of motile Aeromonas septicaemia, is promising. The Akh-2 phage they isolated had a burst size of approximately 140 PFU/cell, a latent period of approximately 50 minutes, and was stable at pH 6–8 and temperatures from –80 to 37 °C. After genome analysis revealed no lysogeny-related genes and confirmed its safety for therapeutic use, they conducted animal testing. Phage application significantly reduced mortality, from nearly 100% in controls to ~57%, and recovered fish reported with no clinical signs.

Phage use in companion animals has targeted multidrug-resistant bacteria, and many successful studies have yielded positive results. Wei *et al.* (2025)'s study testing the efficacy of phage application against a multidrug-resistant strain of *P. aeruginosa*, the cause of canine pyoderma, is an example. Characterisation of the target bacteria (GDPA-01) revealed that it possesses numerous antibiotic resistance and virulence genes, making it challenging to treat. The isolated phage, HJ01, was found to be suitable for *in vivo* application due to its stability under varying pH and temperature conditions, a 20-minute latency period, and a burst size of 53 PFU/cell. Genome analysis revealed that the phage did not carry any virulence or resistance genes, and therefore, phage therapy was deemed reliable. Subcutaneous phage administration following *in vivo* analyses significantly improved pruritus, lesion severity, cytology scores, and histopathological healing compared with controls. This study, while representing the first trial of phage application against canine pyoderma, suggests that phage use in companion animals may be a potential way to reduce antibiotic dependence. In another successful application in companion animals, Braunstein *et al.* (2024) treated a chronic infection caused by zoonotic *P. aeruginosa* and associated with an implant in a Siamese cat undergoing orthopaedic surgery with phage. After testing numerous antibiotics for the infection caused by a multidrug-resistant strain and failing to achieve successful results, the research team decided to obtain the phage ΦpasB7 from an Israeli Phage Bank, which may be counteractive to the pathogen. Topical application of the phage in conjunction with intramuscular ceftazidime resulted in complete wound healing on the second iteration. The study emphasises that while either phage or antibiotic used alone failed, their combined use achieved success through synergistic effects. This study shows that phage application is an important alternative and supportive factor against zoonotic and

multidrug-resistant bacteria and may be an effective factor in protecting animal owners and veterinary staff against zoonoses.

In conclusion, phage therapy is gaining increasing acceptance in both clinical and veterinary medicine as an alternative to antibiotics, as well as a complementary one. Their specific mechanisms of action, their ability to co-evolve with their hosts, and their applicability in personalised or cocktail forms make phage therapy a versatile tool against antibiotic-resistant bacteria. Recent studies in clinical and veterinary medicine demonstrate that phages not only reduce pathogen loads but also enable much more successful outcomes through their synergistic effects with antibiotics.

1.2.8.3. Application of Phages for Treatment Purposes

1.2.8.3.1. Oral Administration

The administration of phages through oral routes has proven to be effective for treating intestinal diseases as well as certain systemic infections. Phage delivery through food and beverages enables better user experience because it enables phages to enter the system. Pathogenic bacteria that colonise the larynx can be targeted by phages which move from the mouth to the intestines after oral delivery. To defend phages from stomach acidity and proteolytic enzymes, researchers use polymer microencapsulation and anti-acid applications. Research indicates that several phages taken orally can penetrate the bloodstream, thus extending their therapeutic capabilities (Ryan *et al*., 2011; Keen and Adhya, 2015).

1.2.8.3.2. Local and Topical Application

Phage applications through local and topical routes have established effectiveness in medical treatments. Bacteriophages are commonly used to treat infections caused by bacteria

such as *Staphylococcus, Klebsiella, Pseudomonas, Proteus* and *Escherichia* species. The therapeutic applications of phage cocktails extend to treating infections of the ear and eye, as well as skin infections like furunculosis, gingivitis, ulcers, wound infections and osteitis from fractures and chronic suppurative fistulas. The product PhagoBioDerm works against *Streptococcus spp., Staphylococcus aureus* and *P. aeruginosa*. Wound treatment with this product requires its application as small pieces or in powder form to open wounds. PhagoBioDerm serves two functions by helping wounds heal and debriding necrotic tissue, which enables better phage penetration to bacterial multiplication sites (Goodridge, 2010; Kutter *et al*., 2010).

1.2.8.3.3. Aerosol Administration

The use of aerosolised phage therapy represents a promising treatment approach for respiratory infections. Traditional spray methods have been used in avian species (Oliveira ***et al.***, 2009), but nebulisation provides superior delivery of phages to the respiratory system. The *in vitro* study shows that aerosolised phages effectively eliminate bacterial pathogens. Phage titration represents an essential requirement for successful treatment because it determines the appropriate phage concentration required to reach the infection site effectively (Le Guellec *et al.*, 2023).

Nebulised phage therapy demonstrates its effectiveness beyond laboratory-based *in vitro* research. Scientific evidence shows beneficial results in both laboratory-based preclinical and clinical investigations. Aslam *et al.* (2019) present three case studies of lung transplant recipients who received bacteriophage treatments. The treatment administered to the patient involved nebulised phages, yet two other patients received theirs intravenously. The study shows phage

applications in difficult-to-treat situations where treatment choices are limited and reveals the safety profile together with potential therapeutic outcomes of phage therapy in this particular patient group. Although this study does not restrict itself to nebulisation methods, it proves the approach can be used in medical practice. The paper presents case studies but lacks controlled clinical trial design, which limits the ability to draw broader conclusions. Wang *et al.* provide an extensive analysis about using inhaled phage therapy for treating pulmonary infections. This study examines the obstacles and possibilities of this therapeutic method together with techniques for better phage delivery. Wang *et al.* (2021) analyse sophisticated nebulisation methods, which combine liposomes with individualised controlled inhalation systems. The article examines preclinical and clinical research that demonstrates how inhaled phage therapy should be implemented.

Several aspects determine the success rate of aerosolised phage therapy. The dimensions of the nebulised droplets determine their ability to penetrate the lower respiratory tract, according to Wang *et al.* (2021). The size of lung penetration varies based on droplet dimensions because small droplets penetrate deeper while larger droplets tend to deposit in upper airways (Wang *et al.*, 2021).

1.2.8.3.4. Rectal Administration

Phage administration through the rectal route, specifically with *E. coli* strains KH1 and SH1, demonstrates its ability to decrease O157 bacteria counts in cattle intestines. Commercial rectal suppositories exist in Russia, but the pharmacokinetic aspects of this delivery method need additional research (Letarov *et al*., 2010).

1.2.8.3.5. Parenteral Administration

Parenteral administration techniques enable bacteriophages to bypass the gastrointestinal tract when treating systemic or deep-seated infections that cannot be reached through topical or oral delivery methods. The delivery methods, including intravenous (IV), intraperitoneal (IP), intramuscular (IM) and subcutaneous (SC), provide different pharmacokinetic profiles that match various clinical needs for patient treatment. The phage therapy routes have proven effective in treating infections according to historical records and various animal studies (Abedon *et al.*, 2011; Ryan *et al.*, 2011). IP administration enables rapid phage distribution throughout the body because phages can target bacteria in the peritoneal space before entering the bloodstream, thus providing an effective treatment for abdominal sepsis (Bogovazova *et al.*, 1991). The phage agents applied through IM or SC injections enter the systemic circulation at a slower rate than IV or IP routes, which creates a localised phage depot that slowly releases the agents. The phage delivery method allows the agents to stay active throughout time while targeting muscle and subcutaneous infections before the agents distribute systemically (Smith and Huggins, 1982; Barrow *et al.*, 1998). The intravenous delivery method delivers phage agents to the body at the fastest rate, thus making it the best choice for treating severe bacteraemia infections and sepsis (Speck and Smithyman, 2016). The historical standard of intravenous phage administration can be traced to the early 20th century. Modern studies in phage therapy indicate potential with purified phage preparations (Abedon *et al.*, 2011; Speck and Smithyman, 2016), countering earlier assumptions regarding the lack of literature or application (Clark and March, 2006). The intravenous administration of phages, in contrast with other techniques, encounters considerable obstacles due to their rapid clearance from the

bloodstream. When phages enter blood circulation, the immune system identifies them as foreign particles, which leads to their clearance through the mononuclear phagocyte system (MPS) located in the liver and spleen (Kurzepa *et al.*, 2019). The clearance process substantially lessens the effective dosage and shortens the circulation duration of phages. Multiple variables, including phage size, surface properties, dose amount and host immune response, determine the speed of clearance (Kim *et al.*, 2008). The host immune system encounters phages after parenteral administration, leading to the generation of both innate and adaptive immune reactions. The immune responses which help eliminate bacteria tend to produce neutralising antibodies against phages, especially when repeated administrations occur. Antibodies produced by the body reduce the effectiveness of phage treatments in repeated therapy sessions (Kim *et al.*, 2008; Kurzepa *et al.*, 2019). Research into PEGylation of phages along with encapsulation methods is ongoing to address rapid clearance and immunogenicity issues, but these techniques bring their set of challenges (Kim *et al.*, 2008). The safety of administering phages through parenteral routes depends on the purity standards of phage preparations. To guarantee both patient safety and regulatory acceptance, every parenteral application must use endotoxin-free high-titre phage lysates which require rigorous purification protocols (Carlson, 2005; Abedon *et al.*, 2011). Parenteral phage therapy is becoming more practical thanks to ongoing clinical trials and controlled use cases that show it can help treat difficult infections (LaVergne *et al.*, 2018; Nir-Paz *et al.*, 2019; Schooley *et al.*, 2017).

1.2.8.4. Animal Models of Phage Therapy

Various animal models have been conducted *in vivo* to assess the effectiveness of phage therapy. Three invertebrate species widely used in research are the nematode *Caenorhabditis*

elegans together with *Drosophila melanogaster* and *Danio rerio* zebrafish. The scientific community conducts research with *Gallus gallus* chickens and *Oryctolagus cuniculus* rabbits as well as *Mesocricetus auratus* hamsters and *Mus musculus* mice as their higher vertebrate models (Brix *et al.*, 2020).

Bacteria serve as the primary food source for nematodes, so infection becomes simple to establish because pathogens naturally settle in the intestine, while phages can use the same route for transmission. Researchers have studied phage treatment of *S. aureus* and *S. enteritidis* infections using *C. elegans* models. The application of bacteriophages led to improved survival outcomes of infected worms in both research scenarios. The recovery of nematodes produced healthy offspring, which proved their wellness after undergoing phage therapy 100 hours post-treatment (Głowacka-Rutkowska *et al.*, 2019; Augustine *et al.*, 2014). The findings indicate *C. elegans* serves as a valuable animal model to assess phage treatment effectiveness.

Insects have two aspects that make them suitable for use as non-vertebrate infection models: a complex innate immune system and their biological resemblance to mammals. The research of Buchon *et al.* (2014) and Lindberg *et al.* (2014) used *D. melanogaster* as their model organism to study phage efficacy in *P. aeruginosa* infections.

The larval stage of zebrafish has emerged as a valuable model for studying host–bacterial interactions during this developmental phase (Neely *et al.*, 2002; Pont *et al.*, 2021; Nguyen *et al.*, 2020; Virgo *et al.*, 2024). Zebrafish embryos provide valuable models to study specific aspects of infectious diseases that are difficult to investigate with traditional animal models. Their advanced innate immune system, genetic manipulability, and optical clarity render them especially valuable. Zebrafish models have been established to investigate bacterial infections like

Enterococcus faecalis and *P. aeruginosa* within the framework of phage therapy (Al-Zubidi *et al.*, 2019; Cafora *et al.*, 2019).

Rabbits naturally acquire *Staphylococcus aureus* infections, which makes them suitable models for studying human infection transmission patterns. Nale *et al.* (2016) showed that hamsters who received an oral phage cocktail after *Clostridium difficile* infection survived better. Nonetheless, given the restricted access to virulent lytic phages that specifically target *C. difficile*, this study utilised temperate phages, consistent with previous investigations. This, however, was deemed unsuitable for therapeutic applications. Nonetheless, the authors demonstrated that a combination of various phage strains could reduce bacterial pathogenicity (Nale *et al.*, 2016).

The larval stage of *Galleria mellonella*, also known as the greater wax moth, has emerged as an alternative invertebrate model recently (Tsai *et al.*, 2016; Blasco and Tomás, 2024). The use of this model helps to resolve ethical issues with mammalian testing while offering several practical benefits, including affordability, ease of handling, short experimental time, and the possibility of culturing at 37 °C, which helps in the study of human pathogens and temperature-dependent virulence factors (Tsai *et al.*, 2016; Blasco and Tomás, 2024). Although *G. mellonella* does not have adaptive immunity, it has a well-developed innate immune system that includes both cellular (phagocytosis and encapsulation mediated by haemocytes, antimicrobial peptides, melanisation) and humoral (antimicrobial peptides, melanisation) components that are functionally equivalent to vertebrate innate immunity (Tsai *et al.*, 2016; Blasco and Tomás, 2024; Mirza *et al.*, 2024). *G. mellonella* has been successfully used to study the pathogenesis of several bacterial species, including ESKAPE pathogens (*Enterococcus faecium, Staphylococcus aureus, Klebsiella pneumoniae, Acinetobacter baumannii, P. aeruginosa* and *Enterobacter* species) and

the *Burkholderia cepacia* complex, and to evaluate the efficacy of antimicrobial agents (Tsai *et al.*, 2016; Blasco & Tomás, 2024). This model has been shown to be particularly useful in the assessment of phage therapy efficacy (Blasco and Tomás, 2023; Tsai *et al.*, 2016). Research shows that larvae carrying different pathogens, including the *Burkholderia cepacia* complex (Seed and Dennis, 2009), *E. coli* K1 (Antoine *et al.*, 2021) and *S. enterica* (Kosznik-Kwaśnicka *et al.*, 2022), survive better after phage treatment. This model is a valuable tool for studying phage pharmacokinetics, phage–antibiotic synergy and phage treatment regimens (Tsai *et al.*, 2016; Blasco and Tomás, 2023). Despite some limitations, such as the lack of standardised strains and possible variability (Tsai *et al.*, 2016), *G. mellonella* presents a strong platform for the preclinical assessment of phage therapeutics (Blasco and Tomás, 2023). This study (Chapter 6) presents a new application of the *G. mellonella* model to study *P. multocida* infection and evaluate phage therapy for this specific veterinary pathogen.

Animal models have improved our understanding of bacteriophage effectiveness and their *in vivo* mechanisms of action. The use of medications in vertebrates and invertebrates for demonstrating their usefulness compared to human clinical trials has the advantages of being faster, cheaper and more ethical. Phage activity has been tried in several ways, demonstrating the potential of bacteriophages or their enzymes in human therapeutics. Phage cocktails are used in phage therapy, and phages are mixed with antibiotics and used for preventive treatments. Phage transport can be increased to enhance the antibacterial effect. These methods may be tested in animal models affordably before being applied to humans (Brix *et al.*, 2020).

1.2.8.5. Selecting Bacteriophage for Phage Therapy

The selection of appropriate bacteriophages stands as a critical step for developing safe and effective phage therapy applications following successful isolation and purification (Gill and Hyman, 2010; Carlson, 2005; Pirnay *et al.*, 2011). The evaluation process for candidate phages depends on various essential criteria to verify desired biological features and safety requirements for therapeutic applications.

Phages that are obligately lytic represent the standard for therapy applications in phage selection. Obligately lytic phages exclusively enter a lytic life cycle by invading host cells to use cellular machinery for reproduction before causing cell destruction, which releases new virus particles (Adams, 1959). Phage therapy seeks direct bacterial elimination through this killing mechanism because it serves as the main therapeutic objective (Abedon *et al.*, 2011). Therapeutic use of temperate phages is avoided because of their inherent safety risks. The life cycle of temperate phages includes two distinct pathways where they can either insert their DNA into the host genome as prophages or exist as plasmids to form lysogenic relationships (Lwoff, 1953). The use of these phages presents multiple risks, which makes them less suitable for direct therapy applications. Firstly, there exists the problem of inadequate lysis, as the phage may not promptly eliminate the bacteria but instead reside together with it, perhaps failing to address an acute infection. Secondly, lysogenic conversion may occur, where prophages possess genes that modify the host's phenotype, occasionally augmenting its virulence unfavourably by encoding toxins (e.g. Shiga toxin in *E. coli*, diphtheria toxin in *Corynebacterium diphtheriae*) or other fitness determinants (Brüssow *et al.*, 2004; Waldor and Mekalanos, 1996; Gummalla *et al.*, 2023). The primary function of temperate phages as gene transduction agents enables them to spread

antibiotic resistance genes together with undesirable traits between bacteria, which creates a major safety risk (Cieślik *et al.*, 2021; Gummalla *et al.*, 2023). Bacteria that become lysogenised gain phage immunity because they develop resistance to both identical and closely related phage infections, which reduces therapeutic effectiveness (Lwoff, 1953; Gummalla *et al.*, 2023). The activation of a prophage into a lytic cycle is unpredictable, as it results in cell lysis but does not provide the same reliability and control as direct lytic phage action (Hyman, 2019).

The preference remains strong for lytic phages, although researchers sometimes work with temperate phages because these might be the only available isolates for specific bacterial targets. Researchers have established methods for using temperate phages while minimising their risks through genetic engineering techniques (Park *et al.*, 2017). The solution of genetic modification for phage engineering stands as the most promising approach because it has received extensive research attention. Scientists accomplish this transformation by making precise genetic modifications that disable lysogeny in the genomes of temperate phages, resulting in the production of obligately lytic viruses (Lu and Collins, 2007; Park *et al.*, 2017; Chen *et al.*, 2019). This is achieved through gene identification followed by inactivation or deletion of essential lysogeny-related genes. Researchers target integrase genes for site-specific phage DNA insertion into host chromosomes and repressor genes that suppress lytic cycle genes (Lee *et al.*, 2018; Borges *et al.*, 2018). They also modify regulatory elements of the lysis–lysogeny decision pathway to create a phage with purely lytic properties (Hyman and Abedon, 2009). The method requires permanent genetic alterations, which must be proven to prevent the engineered phage from returning to its lysogenic state (Gill and Hyman, 2010). Complete phage characterisation through genomic and phenotypic analysis (Hyman, 2019) is required to validate strong lytic

efficiency and eliminate unwanted toxin-encoding or antibiotic resistance genes from the original temperate phage genome. Research studies demonstrate that engineered temperate phages possess therapeutic potential by showing their ability to combat various pathogens (Zhou *et al.*, 2023; Chen *et al.*, 2020; Sumrall *et al.*, 2019).

Reliable conversion of temperate phages into obligately lytic derivatives followed by thorough safety assessment through genomic and phenotypic analysis makes them suitable for phage cocktails alongside naturally lytic phages (Li *et al.*, 2022). The fundamental principles of cocktail design, such as broadening the host range and reducing the likelihood of resistance development, would still apply. The essential requirement is that their temperate nature has been definitively and irreversibly eliminated through genetic engineering and verified by appropriate testing (Monteiro *et al.*, 2019). The use of unmodified temperate phages in therapeutic cocktails remains generally discouraged because of the major risks linked to lysogeny, virulence gene transfer and unpredictable lytic activity.

A phage used for therapy must meet multiple essential criteria regardless of its original nature as lytic or temperate. The host range and specificity of the phage need to be defined, which refers to the range of bacterial strains or species that the phage can infect and kill (Hyman, 2019). The lytic capability and efficiency of the phage must be evaluated through quantitative measures that include efficiency of plaquing (EOP) on target strains, burst size determination (the number of progeny phages produced per infected cell), and evaluation of bacterial killing dynamics (Hyman and Abedon, 2009). Genomic sequencing needs to be performed for complete characterisation and safety evaluation to confirm the lytic state (or modification success for engineered phages) and to ensure the phage does not harbour dangerous elements like toxins,

antibiotic resistance genes or lysogeny-related genes (Zaki *et al.*, 2023). Additionally, the phage needs to be stable and formulable to maintain its viability and activity under required storage parameters (e.g. temperature, pH, duration) as well as throughout the formulation process for the planned administration route (Merabishvili *et al.*, 2009). Determining its resistance generation potential is also vital and can be evaluated using *in vitro* co-evolution experiments or resistance emergence rate monitoring against target pathogens (Chan *et al.*, 2013).

1.2.9. *P. multocida* Phages

Research on *P. multocida* bacteriophages has grown significantly because scientists want to explore their therapeutic potential as agents that target this important zoonotic pathogen. The study of *P. multocida* phages started many years ago, when scientists reported lysogeny and phage isolation (Gadberry and Miller, 1978; Kirchner and Eisenstark, 1956; Chen *et al.*, 2019), but recent research involving detailed morphological, genomic, and functional analyses has been undertaken. Phages of *P. multocida* display a wide variety of morphologies. Studies using electron microscopy have identified phages belonging to the three major tailed phage families within the order *Caudovirales*: *Myoviridae*-like (contractile tails), *Siphoviridae*-like (long, non-contractile tails), and *Podoviridae*-like (short tails) (Ackermann and Karaivanov, 1984; Abdulrahman and Davies, 2021). Ackermann and Karaivanov (1984) examined 21 phages, classifying them into three morphological types: type AU (*Myoviridae*-like, resembling coliphage P2), types C-2 and 32 (*Siphoviridae*-like), and type 22 (*Podoviridae*-like, resembling coliphage T7). Phage B932a, described by Gadberry and Miller (1978), possesses a hexagonal head (approx. 57 × 55 nm) and a long (151 nm), non-contractile, filamentous tail, consistent with the *Siphoviridae*-like group. Temperate phage F108 was classified as *Myoviridae*-like (Campoy *et al.*, 2006), while phage PMP-

GAD-IND was identified as a lytic virus (Qureshi *et al.*, 2018). Phages PHB01 and PHB02 were characterised as T7-like podoviruses (Chen *et al.*, 2018a; Chen *et al.*, 2019), and the recently described vB_PmuM_CFP3 is a myovirus (Chen *et al.*, 2024). Abdulrahman and Davies (2021) also found diverse *Siphoviridae*-like and *Myoviridae*-like morphotypes upon inducing temperate phages from various *P. multocida* isolates.

Genomic sequencing has revealed further diversity. F108, the first temperate *P. multocida* phage sequenced, has a 30.5 kb dsDNA genome with cohesive ends and integrates into a host transfer RNA (tRNA) gene (Campoy *et al.*, 2006). Phage PMP-GAD-IND possesses a 46.3 kb dsDNA genome (Qureshi *et al.*, 2018). The lytic T7-like phages PHB01 (37.3 kb) and PHB02 (38.7 kb) contain linear dsDNA genomes which have terminal redundancy and G+C contents resembling those of their host (Chen *et al.*, 2018a; Chen *et al.*, 2019). The myovirus vB_PmuM_CFP3 contains a genome of 32.7 kb (Chen *et al.*, 2024). Prophage induction research on *P. multocida* strains has revealed that these bacteria can harbour various phage strains with distinct genetic characteristics, reflecting horizontal gene transfer processes (Abdulrahman and Davies, 2021).

Differentiating between temperate and lytic phages is crucial for research. The temperate phages F108 and B932a exhibit lysogenic behaviour by integrating into the host genome (Campoy *et al.*, 2006; Gadberry and Miller, 1978). The use of temperate phages in therapy presents risks because they can potentially transfer bacterial virulence or resistance genes (Abdulrahman and Davies, 2021). The lytic phages PHB01, PHB02, PMP-GAD-IND, and vB_PmuM_CFP3 show promising traits for therapy because they replicate inside host cells and cause lysis. Sequenced lytic phages PHB01, PHB02, and vB_PmuM_CFP3 are suitable for therapeutic applications

because they do not contain detectable antibiotic resistance or virulence genes (Chen *et al.*, 2018a; Chen *et al.*, 2019; Chen *et al.*, 2024).

P. multocida phages demonstrate a wide range of variability regarding host specificity. Phage F108 only infects serogroup A strains, but PHB02 exhibits broad host range activity (Chen *et al.*, 2018a, 2018b). PHB01 shows preference towards non-toxigenic type D strains (Chen *et al.*, 2019), but PMP-GAD-IND can lyse both type A and B strains (Qureshi *et al.*, 2018). Phage vB_PmuM_CFP3 successfully lysed only a portion of the tested avian type A strains, representing 28.2% of the total number (Chen *et al.*, 2024). The primary components responsible for phage interactions are surface structures, including bacterial capsules, which serve as key receptors (Rakhuba *et al.*, 2010).

The capsular polysaccharide-degrading enzymes known as depolymerases, which reside on tail fibres or spikes, have been found in different phages (Łątka *et al.*, 2017). Depolymerase activity enables phages to penetrate bacterial cells but often produces visible plaques with surrounding halos on bacterial lawns (Chen *et al.*, 2018a; Łątka *et al.*, 2017). The tail fibre protein (Dep-ORF8) of PHB02 displays depolymerase activity against type A capsules, and mutants lacking capsules proved resistant to both the phage and the recombinant enzyme (Chen *et al.*, 2018b). These depolymerases have potential applications in biocontrol because of their ability to degrade protective capsules, making bacteria more susceptible to immune responses or other antimicrobial treatments (Majkowska-Skrobek *et al.*, 2016; Guo *et al.*, 2017; Hsieh *et al.*, 2017; Chen *et al.*, 2018b).

According to Gadberry and Miller (1978), phage B932a survived at 4°C but lost its infectivity at 60°C after 10 min and was completely inactivated at 70°C within the same period.

The lytic phages PHB01 and PHB02 demonstrated high stability across a broad pH range from 5 to 9 and at temperatures of 50°C for PHB01 and 40°C for PHB02 (Chen *et al.*, 2018a; Chen *et al.*, 2019). The stability of phage vB_PmuM_CFP3 was confirmed in the temperature range of 30–40°C and pH 4–10 (Chen *et al.*, 2024). Stability profiles determine the feasibility of developing therapeutic preparations as well as their practical implementation.

Lytic phages serve as therapeutic agents because they provide an alternative method to combat bacterial infections while effectively targeting multidrug-resistant (MDR) strains. This has been demonstrated in both animal models and human subjects (Cheng *et al.*, 2018). The therapeutic advantages of phages PHB01 and PHB02, as well as their derived depolymerase, were shown in mouse studies where lethal *P. multocida* doses were used, resulting in improved survival rates (Chen *et al.*, 2018b; Chen *et al.*, 2019). The therapeutic potential of phage Pas-MUP-1 was demonstrated through its ability to reduce IL-1β, IL-6, and MUC1 expression levels and inflammation in swine cell cultures infected with *P. multocida* (Park *et al.*, 2020). Research also focuses on bacteriophage-derived endolysins as standalone antibacterial therapeutic agents (Ha *et al.*, 2018).

Phages that infect *P. multocida* exhibit multiple virus types with various morphologies, as well as diverse host specificity and genomic features, summarised in Table 1.1. The therapeutic capabilities of lytic phages, along with their depolymerase derivatives, are increasingly demonstrated for this significant pathogen. Phage-based solutions to combat *P. multocida* diseases require a systematic workflow: phage isolation, full characterisation, stability assessment, host range determination, genomic safety evaluation, host–phage interaction studies, and comprehensive *in vivo* experiments.

Table 1.1. Previous *P. multocida* Phage Isolation Works.

Phage	Host	Genome size (bp)	Morphology	Source	Reference
PHB02	*P. multocida A*	38,670 dsDNA	*Podoviridae*-like short noncontractile tail.	Wastewater of a swine farm / China	(Chen *et al.*, 2018a)
PHB01	*P. multocida D*	37,287 dsDNA	*Podoviridae* short noncontractile tail.	Sewage/swine farm/ China	(Chen *et al.*, 2019)
PMP-GAD-IND	*P. multocida B:2*	46,335 dsDNA	*Siphoviridae*-like long noncontractile tail	Sewage/India	(Qureshi *et al.*, 2018)
F108	*P. multocida A*	30,505 dsDNA	*Myoviridae-like* long contractile tail	natural collection / Spain	(Campoy *et al.*, 2006)
Pasteurella phage AFS-2018a	*n/a*	33,296 dsDNA	n/a	inducible chromosomal	(Fillol-Salom *et al.,* 2018)
Pasteurella phage Pm86	*n/a*	56048 dsDNA	*n/a*	inducible chromosomal	(Fillol-Salom *et al.,* 2018)
B932a	*P. multocida B932a donor*	*n/a* dsDNA	*Siphoviridae*-like *Long, non-contractile*	Lysogenic *P. multocida* (Bison isolate)	(Gadberry and Miller, 1978)
Type AU (10 phages)	*Various*	*n/a*	*Myoviridae*-like *Contractile*	Lysogenic *P. multocida*	(Ackermann and Karaivanov, 1984)
Type 32 (3 phages)	*Various*	*n/a*	*Siphoviridae*-like *Long, non-contractile*	Lysogenic *P. multocida*	(Ackermann and Karaivanov, 1984)
Type 22 (7 phages)	*Various*	*n/a*	*Podoviridae*--like *Short, non-contractile*	Lysogenic *P. multocida*	(Ackermann and Karaivanov, 1984)
Pas-MUP-1	*P. multocida*	*n/a*	*n/a*	*n/a*	(Park *et al*., 2020)
Induced Phages	*Various hosts*	N/A	*Siphoviridae & Myoviridae*-like	Induced from *P. multocida* isolates	(Abdulrahman and Davies, 2021)
vB_PmuM_CFP3	*P. multocida A (Avian)*	32,696 dsDNA	*Myoviridae*-like *Contractile*	Chicken farm faces/wastewater	(Chen *et al.,* 2024)

1.3. Aims and Objectives of Project

The overall aim of the project was to investigate the potential of bacteriophages as an alternative treatment method to antibiotics for the control of P. multocida infections, particularly in the context of increased antibiotic resistance.

To achieve this aim, the project has been designed in line with the following specific objectives.

1. Isolation of circulating P. multocida strains from environmental and clinical sources for use in phage studies.
2. Isolation and purification of P. multocida-specific phages.
3. Phenotypic, morphological, and physiological characterization of isolated phages and bacterial strains.
4. Genetic analysis of phages to determine genetic diversity, phylogenetic relationships, and safety for therapeutic use.
5. Evaluation of the therapeutic potential of selected bacteriophages using an in vivo Galleria mellonella larvae infection model, including both prophylactic and therapeutic applications.

Chapter 2. Materials and Methods

2.1. Pasteurella Selective Media

Pasteurella selective media (PSM) was used for isolation of *Pasteurella* from field water samples. Lab-Lemco powder 10 g (Oxoid, UK), peptone 10 g (Oxoid, UK), 5 g of sodium chloride (Sigma, UK) and 15 g of select agar (Sigma, UK) were added to 950 mL RO (reverse osmosis) water. The medium was then cooled down to 45°C before adding 50 mL defibrinated sheep blood (VWR International), 0.002 g Neomycin (Apexbio, US) and 0.0035 g Bacitracin (Apexbio, US) mixed gently by swirling and poured into 90 mm standard Petri dishes. Plates were air-dried in a class 2 microbiological safety cabinet until the agar set. Plates were stored at 4°C and used within 8 weeks.

2.2. *P. multocida* Isolates and Growth

Field isolates of *P. multocida* were obtained from Ridgeway Biologicals (UK) and the APHA (Animal and Plant Health Agency, UK) and are listed in Table 2.3.1. The strains from Ridgeway Biologicals were all field isolates from the livers of free-range chickens that had died of FC and were isolated from different farms. A range of more recent strains from different conditions were obtained from APHA (Table 2.3.1). Additionally, five capsular type strains from Robert Davies, University of Glasgow, were obtained to be used as a control in capsule typing experiments.

All routine cultures of and experiments with *Pasteurella* strains were carried out on trypticase soy broth (TSB; Oxoid, UK) or trypticase soy agar (TSA; Oxoid, UK) supplemented with 10% of foetal bovine serum (FBS) (Sigma, UK). All culture media used for incubation was pre-warmed to 37°C unless stated otherwise. Strains were resuscitated from frozen stocks on TSA

agar supplemented by 10% defibrinated sheep blood (Thermo Scientific, UK). Liquid cultures were prepared by inoculating a single colony from TSA plate into 5 mL of TSB broth and then incubating aerobically for 3 h at 37°C. Then 30 µL of this liquid culture were inoculated in TSB broth which was supplemented with 10% v/v FBS and then incubated aerobically until the culture reached the mid-exponential point where the optical density reached around 0.5 *OD*600.

For long-term storage, bacteria were cultured on plates, and multiple colonies were inoculated by loop from the plate into TSB with 33% v/v glycerol and frozen at -20°C (short-term stocks) and -80**°**C (long-term stocks).

Table 2.1. Bacterial Strains Used in This Study.

P. multocida **Strains Name**	**Name in this study**	**Sample source and details**	**Isolation Date**	**Source**
TW222/11	Pm*222*	Poultry liver from FC	n/a	Ridgeway Biologicals
TW13/12	Pm13	Poultry liver from FC	n/a	Ridgeway Biologicals
TW48/12	Pm48	Poultry liver from FC	n/a	Ridgeway Biologicals
TW52/12	Pm52	Poultry liver from FC	n/a	Ridgeway Biologicals
TW106/12	Pm106	Poultry liver from FC	n/a	Ridgeway Biologicals
ATCC 43137	Pm43	Swine	n/a	Thermo Scientific
Y8962	PM2Y	Swine, joint swab	05-Mar-21	AHPA
Y8925	PM3Y	Swine, lung	10-Feb-21	AHPA
Y8841	PM4Y	Swine, pericardial swab	24-Dec-20	AHPA
Y8197	PM6Y	Swine, pus	06-Mar-20	AHPA
Y7417	PM8Y	Swine, abscess	18-Sep-18	AHPA
Y6986	PM12Y	Swine, lung	17-Jun-17	AHPA
Y6714	PM13Y	Swine, pericardial fluid	14-Dec-16	AHPA
Y02780	PM16Y	Swine, nasal swab. Toxin positive	20-Oct-99	AHPA
Y01391	PM17Y	Swine, nasal swab. Toxin positive	24-Oct-95	AHPA
B2308	PM18B	Swine, spleen swab	08-Feb-21	AHPA
B2283	PM19B	Pg, bone marrow	07-Aug-20	AHPA
B2252	PM22B	Swine, liver swab	02-Oct-19	AHPA
B2226	PM24B	Swine, sinus	05-Nov-18	AHPA
B2222	PM25B	Swine, spleen	08-Oct-18	AHPA
B2217	PM26B	Swine, liver swab	29-May-18	AHPA
B2212	PM27B	Swine, spleen swab	06-Dec-17	AHPA
B2167	PM28B	Swine, liver	24-Mar-16	AHPA
B01707	PM29B	air sac	22-Oct-07	AHPA
X73	X73	Poultry	n/a	University of Glasgow
P1235	P1235	Poultry	n/a	University of Glasgow
P3881	P3881	Poultry	n/a	University of Glasgow
P4769	P4769	Poultry	n/a	University of Glasgow
M1404 Check this	M1404	Poultry	n/a	University of Glasgow

Note. This table lists the bacterial isolates used for phage host range and characterisation studies. Strain names include both original identifiers and simplified nomenclature used throughout this study. Details include the anatomical source of isolation, host species (poultry or swine), date of isolation (where available), and the supplying institution. Isolates were sourced from Ridgeway Biologicals (UK), Animal and Plant Health Agency (AHPA), Thermo

Scientific, and the University of Glasgow. Poultry isolates were largely obtained from cases of FC, while swine isolates were collected from various clinical presentations including lung, liver, abscesses, and toxin-producing strains. n/a : not available.

Not all P. multocida strains were used in every experiment. Some were used in the experiment, while others were stored at -20°C. In experiments requiring the use of all strains, they were removed from -20°C two days prior and inoculated onto suitable plates. The strains that recovered on the plate were inoculated into broth and prepared for the experiment. Strains that did not recover from -20°C that day were not used in that experiment, indicating that the number of bacteria used in the experiments varied from experiment to experiment.

2.3. Determination of Optimum Media Condition for Pasteurella Isolates

Optimisation of culture media was initially performed using *P. multocida* reference strains (PM13 and ATCC43137), which were also employed as host strains during phage isolation experiments. These strains were selected as representative models since the media and supplement combinations tested have all been successfully applied in previous *P. multocida* studies. The optimum condition identified was subsequently applied across all 31 isolates in this study to ensure consistency and comparability between experiments. While minor strain-specific differences in growth performance cannot be excluded, the use of literature-validated media and a standardised condition provided both reliability and experimental continuity, allowing robust comparisons across the dataset. An assessment was made to optimise the media for use in this study. The base media assessed were Tryptic Soy Agar (TSA), Brain Heart Infusion (BHI) agar, Blood Agar Base No.2 (BAB No.2), and Mueller-Hinton (MH) agar. Common additions to media used in previously published studies, summarised in Table 2.2, were assessed. These included

Foetal Bovine Serum (FBS; 10% v/v), Calcium Chloride ($CaCl_2$; 10 mM), sterile defibrinated sheep blood (5% v/v), and sterile defibrinated horse blood (5% v/v).

Table 2.2. Media And Supplement Used in Previous *P. multocida* Studies.

Media	**Supplemented with**	**Reference**
TSA	10 % v/v FBS	(Chen *et al.*, 2018a)
BHI, TSA	+10 mM *CaCl2*	(Qureshi *et al.*, 2018)
Blood Agar Base No.2	5 % v/v sheep blood	(Zagkic, 2006)
Selective Medium (CGT)	10 % v/v horse blood	(Knight *et al.,* 1983)
Mueller-Hinton agar	10 % v/v horse blood	(Avril *et al.,* 1990)
BHI, Blood Agar Base No.2	10 % v/v horse blood	(Pullinger., 2004)

All media were prepared following the manufacturers' protocols, and each specified supplement was added to each base medium individually to create all possible combinations, as detailed in Table 2.3.

Table 2.3. Combination of Media and Supplemented Assessed.

Base	Supplement	Base	Supplement
TSA +	10 % v/v FBS	Blood Agar Base No.2 +	10 % v/v FBS
TSA +	+10 mM $CaCl_2$	Blood Agar Base No.2 +	+10 mM $CaCl_2$
TSA +	5 % v/v sheep blood	Blood Agar Base No.2 +	5 % v/v sheep blood
TSA +	10 % v/v horse blood	Blood Agar Base No.2 +	10 % v/v horse blood
BHI +	10 % v/v FBS	Mueller-Hinton agar +	10 % v/v FBS
BHI +	+10 mM $CaCl_2$	Mueller-Hinton agar +	+10 mM $CaCl_2$
BHI +	5 % v/v sheep blood	Mueller-Hinton agar +	5 % v/v sheep blood
BHI +	10 % v/v horse blood	Mueller-Hinton agar +	10 % v/v horse blood

Agar plates were prepared as described in section 2.1, and *P. multocida* strains were streaked on these plates before incubating aerobically at 37°C for 20 h. After incubation, colonies were observed, and the growth of *P. multocida* was scored as large colonies (+++), medium colonies (++), small colonies (+), or no growth (0). The combinations where *P. multocida* strains produced large colonies (+++) were also assessed for additional features. Media clarity and background, particularly the potential of FBS and $CaCl_2$ to provide a clearer background compared to blood for subsequent plaque visualisation, were noted. Combinations of media and supplements where *P. multocida* strains grew with better confluence and optimal colony size were chosen for further experiments.

2.4. Plaque Assay (Double Agar Overlay Method)

Plaque assays were performed as described by Kropinski (2009). In this assay, TSB was used as the base liquid medium, and agarose was added into it in two different concentrations to make plate 1.5% agar (bottom agar) and 0.35% top agar (soft agar), respectively, by 15 g/litre and 3.5 g/litre.

Bottom agar plates were poured in Petri dishes and air dried in a class 2 microbial safety cabinet for 1 h or stored at room temperature for 1 d. Starter cultures of *Pasteurella* were prepared by adding 250 µL of a stationary phase culture to 25 mL of prewarmed TSB supplemented with 10% FB. The mix was incubated for *ca*. (circa (approximately)) 2 h until the *OD*600 reached 0.5. Molten top agar was maintained at 45°C in a water bath just prior to use. To prepare the phage for plating, decimal dilutions (10^{-1} to 10^{-6}) of the phage suspension were prepared in SM buffer. Volumes (100 µL) of each phage dilution and 100 µL of *Pasteurella* bacteria culture at 0.5 OD_{600} were mixed in sterile bijou tubes. After mixing of phage and bacteria, 3 mL of molten top agar was added to the tubes, mixed, then poured onto a prewarmed bottom agar plate and swirled to form an even overlay. The plates were allowed to set at room temperature for 15 min. Additional control tubes were inoculated with bacteria or phage individually to control for contamination.

The plates were then inverted and incubated aerobically at 37°C overnight, at which point they were visually inspected for plaques. For enumeration, dilution plates with distinct countable plaques (30-300) were chosen to calculate the titre in PFU/mL (plaque-forming units per millilitre). Phage titres were determined with the following calculation.

.

Number of plaques on plate x $\frac{1000ul}{100ul}$reciprocal of dilution on counted plate = PFU/mL

2.5. Bacteriophage Enumeration by Using Small Drop Test (Spot Test)

Enumeration of bacteriophages was performed based on the previously described method by Mazzocco (2009). TSA top agar (soft agar) supplemented with 10% FBS was prepared and kept at 47°C. A bacterium at the mid-exponential growth (0.5 OD_{600}) was diluted 50 µL per millilitre into top agar, mixed and immediately poured on the agar plate to form an overlay. The overlay was then allowed to set for 40 min at room temperature. Spots of 10 µL of individual phage lysates or a liquid sample to be screened for phage presence were spotted on the dry top agar seeded with bacteria. The spots were allowed to dry into the agar by air drying in a class 2 microbial safety cabinet. At that point, the plates were inverted and incubated aerobically at 37°C overnight. The formation of lysis zones and/or individual plaque formation were observed by eye the next day and used to calculate the original plaque-forming units (PFU) of samples.

2.6. Isolation and Purification of *P. multocida* and Phage

2.6.1. Collection and Preparation of Environmental Water Samples

Environmental samples were collected to isolate *P. multocida* and phages (Table 2.4). These samples included water from lakes, rivers, ponds and marinas, as well as sewage samples from wastewater treatment centres, cattle faeces and samples from a dairy farm slurry tank. Except for cattle faeces, each sample was collected in sterile, 500-mL Nalgene bottles (Sigma, UK). After collection, the samples were transported to the laboratory in insulated polystyrene boxes and stored at 4°C until processing. When feasible, samples were transported on the same day (within a few hours, typically 1 hour). The precise collection location was determined using Google Maps and recorded, along with the date, time and ambient temperature.

Environmental samples were prepared differently for phage isolation based on the physical consistency of the liquid. Samples with large quantities of bulk debris, such as slurry from dairy farms, were first mixed with SM buffer in the ratio of 1% v/v and then incubated at room temperature, shaking at 200 (rounds per minute) rpm for 15 min. If the samples contain a high level of debris, crude filtration was performed through a 70 µm cell strainer (Falcon, UK). All samples were centrifuged at 4°C at 5,000 *g* for 20 min, then the supernatants were filtered through a 0.22 µm nylon syringe filter (Sartorius, UK). If the supernatant was still too viscous to filter through from a 0.22 µm filter, the next finest filter item was used: a 0.45 µm nylon syringe filter (Sartorius, UK), a 1.2 µm nylon syringe filter (Sartorius, UK), a 5 µm filter paper (Whatman, UK) and a 13 µm filter paper (Whatman, UK). The filtrates were stored at 4°C until further processing.

Table 2.4. Source of Water Samples

Site	Location	Collection Date / Time	Local temperature[1]	Transferred to SVMS UoN/ +4°C
Lake 2	**Highfield Park, Nottingham** 52°56'17.8"N 1°11'26.6"W	13.08.2020 09:00 am	18°C	13/08/2020
Lake 3	**Attenborough Nature Reserve** 52°54'01.3"N 1°14'07.0"W	13.08.2020 09:30 am	18°C	13/08/2020
Pond 1	**Black Pool, Sutton Bonington** 52°50'06.5"N 1°15'45.9"W	18.03.2021 13:30	11°C	18.03.2021
River 1	**River Trent, Stoke Bardolph, Nottingham** 52°58'24.7"N 1°02'14.3"W	21.03.2021 14:40	11°C	21.03.2021
Lake 4	**Colwick Country Park, Nottingham** 52°57'08.7"N 1°05'29.6"W/ 52°57'07.9"N 1°05'27.2"W / 52°57'07.6"N 1°05'25.6"W	21.03.2021 15:05	11°C	21.03.2021
Pond 2	**Martin's Pond, Nottingham** 52°57'23.8"N 1°13'03.5"W	21.03.2021	n/a	24.03.2021
Lake 4	**Harrison's Plantation Nature Reserve Lake**	21.03.2021	n/a	21.03.2021
Lake 5	**Wollaton Park Lake** 52°56'42.1"N 1°12'54.8"W / 52°56'34.8"N 1°12'53.5"W 52°56'41.7"N 1°12'50.4"W	28.03.2021 14:40 / 14:50 / 15:00	°9°C	28.03.2021
Lake 6	**Attenborough Nature Reserve Lake 2** 52°54'00.3"N 1°14'05.0"W/ 52°54'00.5"N 1°14'06.9"W/ 52°54'01.5"N 1°14'07.0"W	31.03.2021 15:30 / 15:35 / 15:40	21°C	31.03.2021
Lake 7	**Jubilee Campus Lake** 52°57'08.8"N 1°11'15.5"W	09.04.2021 16:00	6°C	10.04.2021
Pond 3	**Arboretum, Nottingham** 52°57'37.3"N 1°09'28.2"W	09.04.2021 16:30	5°C	10.04.2021
River 2	**Toton Bridge** 52°53'50.5"N 1°14'43.8"W	10.04.2021 16:40	6°C	10.04.2021
Sewage into River 3	**Derby Sewage into River Derwent** 52°54'11.4"N 1°25'26.4"W	24.04.2021 17:00	13°C	26.04.2021
Sewage into River 4	**Chapel Farm Marina Sewage into** 52°52'15.9"N 1°19'38.1"W	24.04.2021 17:30	13°C	26.04.2021
Marina 1	**Shardlow Marina** 52°51'59.5"N 1°20'11.5"W	01.05.2021 11.55	15°C	01.05.2021
Slurry 1	**Dairy Farm Slurry, UoN** 52°50'23.8"N 1°15'02.2"W	11.06.2021 08:00	9°C	11.06.2021

[1]www.metoffice.gov.uk, n/a not available, SVMS UoN School of Veterinary Medicine and Science University of Nottingham.

2.6.2. Isolation of *P. multocida* from Water Samples

Unfiltered water samples (100 µL) were spread onto 90 mm Pasteurella selective medium plates (Oxoid, UK). The plates were dried at room temperature before being inverted and incubated aerobically at 37°C for 24-48 h. Presumptive positive colonies (grey, non-haemolytic, diameter of 1 to 3 mm) were picked and streaked on TSA plates supplemented with 10% defibrinated sheep blood. These subcultures were incubated aerobically at 37°C for 24-48 h. After incubation, single colonies were further streaked on MacConkey (MAC) agar and TSA sheep blood agar and incubated aerobically at 37°C for 24 h. Isolates which did not grow on MAC agar were assayed with their oxidase and catalase activity.

Catalase assay: A small amount of growth from the culture was placed on a clean microscope slide, and a few drops of H_2O_2 were mixed with the culture smear with a toothpick. Catalase is the enzyme that converts hydrogen peroxide (H_2O_2) to water (H_2O) and oxygen (O_2). The observed bubbling is caused by the formation of O_2 gas, which is considered catalase positive.

Oxidase Assay: For oxidase tests, oxidase test strips (Sigma Aldrich, UK) were used. These strips are rapid detection materials for the oxidase-cytochrome enzyme. Strips have been impregnated with tetramethyl-p-phenylene-diamine, which is reduced to blue when exposed to oxidase-positive bacteria. With a sterile plastic loop, a small amount of organism was obtained from an agar plate and swiped on oxidase strips. Positive reactions change the colour of the bacteria instantly, from violet to purple, or within 10 to 30 s. Delayed responses were rejected.

2.6.2.1. PCR Confirmation of Pasteurella Isolates

Presumptive *Pasteurella* isolates were confirmed by PCR with a primer targeting the KMT1 gene, which only amplifies a conserved sequence present in *P. multocida*. The PCR was

carried out using a TC-512 thermocycler (Techne, UK), with an initial denaturation at 95°C for 4 min, followed by 30 cycles of denaturation at 95°C for 1 min, annealing at 55°C for 1 min, extension at 72°C for 1 min and final extension at 72°C for 10 min. Resulting amplicon products were run on an agarose gel (2% v/v agarose) electrophoresis in 1x TAE, which was prepared from 50x TAE buffer (Millipore, UK) for 1 h and stained with Nancy-520 (Sigma-Aldrich, UK). A Bio-Rad UV gel doc imager was used to visualise the bands.

2.6.3. Characterisation of *P. multocida* Strains

2.6.3.1. Determination of Capsule Presence of P. multocida strains by Indian Ink Staining

To evaluate the capsule presence and size of *P. multocida* strains, bacteria were grown in two different culture conditions: plate and liquid media. For plate cultures, bacteria were grown on solid TSA plates supplemented with 5% FBS, while liquid cultures were prepared in TSB supplemented with 5% FBS. Capsule sizes were visualised using the India ink staining method as described by Hansen and Hirsh (1989). For each sample, 10 µL of bacterial suspension was mixed with 4 µL of India ink (Talens, UK) on a microscope slide. The smear was air-dried for 5–6 min, dipped in distilled water and flooded with 1% crystal violet for 1 min. Slides were rinsed with distilled water, air-dried again and observed at 100× magnification using immersion oil.

2.6.3.2. Measurement of Capsule Size of P. multocida Strains Using a Leica 500b Microscope

Slides prepared for each strain as described in section 2.7.3.1 were observed using a Leica 500b microscope. The light intensity, field of view, and aperture were adjusted, and a scale bar was added to the captured images using the LAS (Leica Application Suite) software. Images were exported in JPG (Joint Photographic Experts Group) format and using ImageJ software (IJ 1.46r,

National Institutes of Health). For each slide, multiple bacteria were imaged. Capsule thickness was measured at three distinct points around the capsule of each bacterium. The average of these three values represented the capsule thickness for that bacterium. Capsule size data were then summarised across bacteria to obtain a mean and standard deviation for each strain under each condition.

These measurements reflect technical variability within a single preparation per strain and condition, rather than biological replication. Statistical comparisons between strains (one-way ANOVA with Tukey's HSD post-hoc test) and between conditions (independent-sample t-test) were therefore interpreted. A scatter plot was generated to visualise the relationship between capsule sizes in plate and liquid cultures, with strain names annotated and a line of equality ($y = x$) included to indicate deviations.

2.6.3.3. Capsule Typing of P. multocida Strains by PCR

Capsule typing of *P. multocida* strains was performed using a multiplex PCR method previously described by Townsend *et al*. (2001), using primer pairs (CAPA, CAPB, CAPD, CAPE and CAPF) specific for capsule genes (*HYAD-HYAC, BCBD, DCBF, ECBJ* and *FCBD*) presented in Table 2.5. *P. multocida* strains of X73 (CAPA), M1404 (CAPB), P3881 (CAPD), P1235 (CAPE) and P4679 (CAPF), which were kindly provided by Dr Robert Davies, were used as capsular reference strains. A primer set of KMT1T7 and KMT1SP6 (Townsend *et al*., 2001), which are *P. multocida*-specific, was also added to the reaction to confirm that the isolates that were negative for these capsular types were *P. multocida*. All primers were synthesised by EasyTM Oligos (Sigma-Aldrich, UK). PCR amplification was carried out using the Qiagen Multiplex PCR kit (Qiagen, UK). PCRs were performed in a TC-512 thermocycler (Techne, UK). Application parameters were 15 min initial

heat activation at 95°C, 30 cycles of 30 sec denaturation at 94°C, annealing at 60°C and extension at 72°C with a final extension for 10 min at 72°C. Running the final products of PCR on agarose gel and visualisation of the bands were performed as previously described in section 2.7.2.2.

Table 2.5. *P. multocida*-specific primers and primers set specific for serogroups A, B, D, E and F

Serogroup	Gene	Primers	Sequence 5`to 3`	Amplicon size
All	*kmt1*	KMT1T7 F	ATCCGCTATTTACCCAGTGG	460
		KMT1SP6 R	GCTGTAAACGAACTCGCCAC	
A	*hyaD-hyaC*	capA F	TGCCAAAATCGCAGTCAG	1044 bp
		capA R	TTGCCATCATTGTCAGTG	
B	*bcbD*	capB F	CATTTATCCAAGCTCCACC	760 bp
		capB R	GCCCGAGAGTTTCAATCC	
D	*dcbF*	capD F	TTACAAAAGAAAGACTAGGAGCCC	657 bp
		capD R	CATCTACCCACTCAACCATATCAG	
E	*ecbJ*	capE F	TCCGCAGAAAATTATTGACTC	511 bp
		capE R	GCTTGCTGCTTGATTTTGTC	
F	*fcbD*	capF F	AATCGGAGAACGCAGAAATCAG	851 bp
		capF R	TTCCGCCGTCAATTACTCTG	

2.6.3.4. LPS Typing of P. multocida Strains by PCR

The LPS genotypes of *P. multocida* isolates were determined according to prior descriptions (Townsend *et al.,* 2001); Cap-PCR was used to identify the isolates' capsular types. The presence of certain LPS outer core biosynthesis loci, such as *PCQ, NCTA, GATF, LATB, NCTB, RMLA, PPGB* and *NATG* genes, was then checked in the isolates. The associated precise primers were those that have been previously published (Harper *et al.,* 2014). The oligonucleotide primer sequences and the anticipated size of each amplicon for the loci involved in LPS production are shown in Table 2.6.

The PCRs were performed in a final volume of 50 µL at the following reagent concentrations: 25 µL of 2x GIAGEN Multiplex PCR Master Mix, 0.4 µM of each primer, 50 ng of DNA, 10 of 5X Q-Solution, and a variable amount of RNAse-free water. Amplification was

performed at 30 cycles. The PCR conditions were initial denaturation at 95°C for 5 min, followed by 30 cycles of denaturation at 96°C for 30 s, annealing at 52°C for 30 s and extension at 72°C for 2.5 min. The final cycle was completed by a final extension at 72°C for 5 min.

The amplicons from the 50 µL reaction volume were mixed with 10 µL of 6X gel loading dye (NEB, UK) and loaded into the wells of a 1% agarose gel. The gel was run for 240 min at a voltage of 75 V and 400 mA to separate the amplified products. Nancy-520 (Sigma, UK) was used to stain the agarose gel. By using a UV transilluminator (Bio-Rad UV gel doc imager), DNA fragments were imaged. GeneRuler Express DNA Ladder (SM1551, Thermo Scientific, UK) was used to compare the size of the amplified fragments.

Table 2.6. Primers Specific to Eight LPS Types of *P. multocida*.

Locus	Primer	Sequence (5'-3')	Location	Predicted product size (bp)
L1	BAP6119-F	ACATTCCAGATAATACACCCG	*pcgD*	1107
	BAP6120-R	ATTGGAGCACCTAGTAACCC	*pcgB*	
L2	BAP6121-F	CTTAAAGTAACACTCGCTATTGC	*nctA*	810
	BAP6122-R	TTTGATTTCCCTTGGGATAGC	*nctA*	
L3	BAP7213-F	TGCAGGCGAGAGTTGATAAACCATC	*gatF*	474
	BAP7214-R	CAAAGATTGGTTCCAAATCTGAATGGA	*gatF*	
L4	BAP6125-F	TTTCCATAGATTAGCAATGCCG	*latB*	550
	BAP6126-R	CTTTATTTGGTCTTTATATATACC	*latB*	
L5	BAP6129-F	AGATTGCATGGCGAAATGGC	*rmlA*	1175
	BAP6130-R	CAATCCTCGTAAGACCCCC	*rmlC*	
L6	BAP7292-F	TCTTTATAATTATACTCTCCCAAGG	*nctB*	668
	BAP7293-R	AATGAAGGTTTAAAAGAGATAGCTGGAG	*nctB*	
L7	BAP6127-F	CCTATATTTATATCTCCTCCCC	*ppgB*	931
	BAP6128-R	CTAATATATAAACCATCCAACGC	*ppgB*	
FL8	BAP6133-F	GAGAGTTACAAAAATGATCGGC	*natG*	255
	BAP6134-R	TCCTGGTTCATATATAGGTAGG	*natG*	

2.6.3.5. AMR Profiling by Disk Diffusion Method

The antibiotics examined in this study were chosen for their documented relevance to *P. multocida* infections in poultry and livestock as well as their accessibility. They are essential for

assessing resistance patterns in veterinary isolates because prior research has documented resistance to tetracyclines, aminoglycosides, penicillin, and fluoroquinolones (such as norfloxacin and enrofloxacin). Given that spectinomycin and streptomycin are frequently used in combination therapies and that rising resistance has been documented in poultry production, their inclusion was also needed. In addition to covering clinically and agriculturally relevant antibiotics, testing every disc available allowed for the identification of new or unexpected resistance patterns, giving researchers a more comprehensive understanding of the changing AMR situation of *P. multocida.*

The antibiotic sensitivity profiles of *P. multocida* strains were determined using the Kirby-Bauer disc diffusion method (Hudzicki, 2009), following the British Society for Antimicrobial Chemotherapy (BSAC) guidelines (Version 14, January 2015). Mueller-Hinton (MH) (Fisher, UK) agar, supplemented with 5% mechanically defibrinated horse blood (EO Labs, UK) and 20 mg/L β-NAD (Fisher, UK), was used as the testing medium. Three replicates were performed per strain against seven antibiotics: ampicillin, penicillin G, cefotaxime, nalidixic acid, tetracycline, spectinomycin and streptomycin. A sterile cotton swab was dipped into a freshly grown culture ($1–2 \times 10^8$ CFU/mL) and spread evenly across the plate surface using an L-shaped spreader with a plate rotator. Antibiotic discs (AMP10, NA30, SH25, S5, TE10, CTX5, PG1; Oxoid, UK; Table 2.7.4) were applied within 15 min of inoculation. Plates were incubated at 36°C in an air incubator for 20 h. After incubation, the plates were examined, and the zones of inhibition were measured with a calliper. The concentration of the antibiotic disc and the interpretation of the zone diameters are shown in Table 2.7.

Table 2.7. Diameter Breakpoints for Interpreting the Antibiotic Susceptibility of *P. multocida* by BSAC Methodology.

		Interpretation of Zone Diameters (mm)				
Disk Name	**Antibiotics**	Resistant(R) (≤mm)	Intermediate (I) (mm)	Sensitive(S) (≥mm)	**Std. BSAC Disk Conc. (µg/unit)**	**Disk Conc. (µg/unit) Applied**
AMP10	Ampicillin	29	N/A	30	10 (µg)	25 (µg)
PG1	Penicillin G	21	N/A	22	1 unit	1 unit
CTX5	Cefotaxime	35	36-40	41	5 (µg)	30 (µg)
NA30	Nalidixic acid	27	N/A	28	30 (µg)	30 (µg)
TE10	Tetracycline	29	30-33	34	10 (µg)	30 (µg)
SH25	Spectinomycin SH	N/A		N/A	N/A	25 (µg)
S5	Streptomycin S	N/A		N/A	N/A	5 (µg)

Note 1 (For Ampicillin, Cefotaxime, Tetracycline): "A disk concentration higher than the standard BSAC recommendation was used for this antibiotic due to availability. The 'Resistant' interpretation (e.g., ≤29mm for Ampicillin) is applied tentatively, based on the rationale that a zone diameter falling within the resistant range of the lower (standard) disk concentration, despite using a higher concentration disk, strongly indicates resistance. This is a deviation from standard BSAC interpretive criteria for the disk concentration used. Intermediate and Sensitive categories cannot be determined (ND) with these non-standard disk potencies using BSAC breakpoints."

2.6.3.6. Growth Curve of P. multocida Strains

Starter cultures of *Pasteurella* were prepared by inoculating a single colony from an overnight incubated TSA plate into 5 mL of TSB liquid media supplemented with 10% FBS in a 30 mL universal tube. Cultures were incubated aerobically at 37°C for 3 to 4 h until the absorbance reached the stationary phase, which was taken as an *OD*600 of 1.5. Then 25 mL of prewarmed TSB media was inoculated with 250 µL of this starter culture and incubated aerobically at 37°C. At 10-min intervals, a 1 mL sample of this culture was taken to measure *OD*600 from 0 to 210 min with a spectrophotometer. At the same time points, 10 µL of this culture were decimally diluted to 10^{-6}. Volumes of 10 µL of each dilution were spotted three times on the surface of an air-dried TSA plate, and this was done by three replicates. The spots were allowed to dry prior to incubating aerobically overnight at 37°C. Following incubation, individual colonies for each dilution were enumerated, and the original bacterial count of the cultures was determined as colony-forming units (CFU) per mL.

2.6.4. Isolation of Phage for *P. multocida*

Volumes (50 mL of 3×TSB) were mixed with 150 mL of each filtered water sample in a 500 mL Erlenmeyer flask. The flask then was inoculated with 0.5 mL of a mid-exponential broth culture of 6 different *P. multocida* strains (PM13, ATCC 43137, PM48, PM52, PM106, PM222). After overnight (18-20 h) aerobic incubation at 37°C with 150 rpm shaking, 50 mL of this culture was transferred to a 50 mL Falcon tube and centrifuged at 10,000 × *g* for 20 min. The resulting supernatant was filtered before using in the plaque assay described in section 2.5.

2.6.5. Plaque Purification

To ensure that a single phage was isolated, they were plaque purified. The centre of each plaque was picked using a sterile pipette tip and transferred into 100 µL of SM buffer in a microfuge tube. The tubes were vortexed at a medium speed for 5 seconds. The suspension of phage was then plated with the host bacteria using the double agar overlay method, which was described in section 2.5. This purification procedure was repeated a minimum of 5 times, or the morphology of all plaques on a plate was similar. The suspension was left at 4°C until further use.

2.6.6. Preparation of High Titre Phage Stock by Full Plate Lysate

Phage amplification using the full plate lysate method was performed according to the protocol described in Swanstrom and Adams (1951). Following plaque purification, mid-exponential bacteria were inoculated with undiluted phage lysate to achieve just less than confluent lysis on the plates. For a negative control, top agar was prepared by adding bacteria only. The plates were incubated at 37°C overnight. Then 5 mL of SM buffer was added to each plate and swirled gently. The plates were sealed with paraffin film and placed on a plate rocker

at 20 rpm and incubated at room 4°C overnight. Following incubation, the SM buffer containing phage was removed with a 5 mL syringe and transferred to 50 mL Falcon tubes. The suspensions were then centrifuged at 10,000 × *g* for 15 min at 4°C. The supernatant was then filtered through a nylon syringe filter with a pore size of 0.22 µm (Sartorius, UK). Phage lysates were enumerated by plaque assay and stored short-term at -20°C in a 33% w/v glycerol stock. For long-term storage, the samples were kept at -80°C with added glycerol to achieve a final concentration of 50% (w/v).

2.6.7. Preparation of High Titre Phage Stock by PEG Precipitation

To prepare high-titre and pure phage stocks, PEG (polyethylene glycol) precipitation was performed following the protocol described in Green and Sambrook (2012). A single colony of *P. multocida* was inoculated in 100 mL of TSB medium in a 500 mL flask. The culture was incubated overnight at 37°C with shaking at 150 rpm under aerobic conditions. The OD_{600} of this culture was adjusted to 1 by diluting it in TSB to achieve a titre of ~1×10^9 CFU/mL. The diluted culture was centrifuged at 5,000 × *g* for 15 min at 4°C. The supernatant was discarded, and the pellet was resuspended in 3 mL of SM buffer. The multiplicity of infection (MOI) was adjusted to 0.1 by adding 1 mL of 1×10^9 PFU/mL phage lysate. The tubes were incubated at 37°C at 100 rpm for 20 min before adding to 500 mL of TSB broth in 2 L conical flasks. The cultures were then incubated at 37°C at 200 rpm for up to 12 h, or until the culture clarified, indicating phage lysis. Each tube received 10 mL of chloroform, which was then incubated for 10 min at 37°C at 200 rpm. Following room temperature cooling, DNase and RNase (Sigma, UK) were added to the cultures at a final concentration of 1 µg/mL each. Before adding NaCl (29.2 g, 1 M) to each 500 mL of lysate, the lysate was allowed to sit at room temperature for 30 min. Suspensions were mixed with a magnetic stirrer until the NaCl had dissolved, then incubated on ice for 1 h. The suspension was

decanted into 250 mL polypropylene centrifuge tubes and centrifuged at 12,000 × *g* for 15 min at 4°C. The supernatant was transferred to another sterile 250 mL polypropylene centrifuge tube, to which 20 g of PEG 8000 was added. The tubes were agitated until the PEG had dissolved and then incubated on ice for at least 1 h.

Following incubation, the tubes were centrifuged at 12,000 × *g* for 15 min at 4°C. The supernatant was discarded, and the tubes were inverted and drained of residual fluid. For each 200 mL supernatant, phage pellets were precipitated by adding 4 mL of SM buffer. The pellets were gently resuspended with the aid of a wide-bore serological pipette with a bulb. An equal volume of chloroform was added to each suspension before vortex mixing for 25 seconds and centrifugation at 4,000 × *g* for 10 min at 4°C to separate the aqueous and organic phases. The aqueous phase, which was expected to contain phage particles, was recovered using a pipette and transferred to a sterile 1.5 mL microfuge tube before enumeration and storage.

2.6.8. Purification of Phage Stock by Ammonium Acetate

Purified high titre phage lysates were prepared by the ammonium acetate method as described by Ackermann (2001). High titre phage lysates (1 mL), which contain a minimum of 10^9 PFU/mL, were prepared in 1.5 mL conical bottom centrifuge tubes. These tubes were centrifuged at 25,000 × *g* for 60 min at room temperature. The supernatant was discarded, and the phage pellet was resuspended with 0.1 M ammonium acetate solution (pH 7). The tubes were centrifuged again at the same speed for the same duration, and the procedure was repeated three times to generate purified phage lysate.

.

2.6.9. Purification of Phage Stock by CsCl (Caesium Chloride) Density Gradient Centrifugation

To obtain the highest purity bacteriophage particles, free from bacterial contaminants, the CsCl density gradient centrifugation method described by Green and Sambrook (2012) was used. Three solutions with different densities (1.45 g/mL, 1.50 g/mL, 1.70 g/mL) were prepared by adding varying amounts of solid CsCl (60 g, 67 g, 95 g) to SM buffers (85 mL, 82 mL, 75 mL). These solutions achieved refractive indexes of 1.3768 η, 13815 η and 1.3990 η, respectively. A step gradient was made by precisely layering three CsCl solutions of decreasing density on top of one another, with equal amounts in a 5 mL ultra-clear tube (Beckman Coulter, UK). After adding the 1.45 g/mL density solution, a mark was made with a permanent marker pen on the exterior of the tube at the solution's level where the bacteriophage particles were assumed to be accumulated as an aqueous band. After making the density gradient by adding three solutions, PEG-precipitated bacteriophage suspensions were layered over the step gradient. Tubes were ultracentrifuged (CP80 NX, Hitachi) at 120,000 x *g* for 20 h at 4°C in an RPS55T-2 bucket. Bacteriophage particles were collected with a 21-gauge hypodermic needle by puncturing the marked spot.

2.6.10. Purification of Phage Stock by OptiPrep (Iodixanol) Density Gradient Centrifugation

OptiPrep (Iodixanol 60% (w/v) in water; Sigma-Aldrich, UK) was substituted for CsCl in the CsCl density gradient centrifugation protocol to obtain highly pure and concentrated phage particles. Similar to the CsCl protocol, three solutions of varying densities were prepared by combining OptiPrep and SM buffer in varying proportions. To prepare a 10 mL stock of each solution containing 40%, 35% and 30% concentrations, 6.7 mL, 5.8 mL and 5 mL of OptiPrep were added to 3.3 mL, 4.2 mL and 5 mL of SM buffer, respectively. In 5 mL ultra-clear tubes (Beckman

Coulter, UK), 1 mL of each solution with different densities was layered, starting from the highest concentration to the lowest. Then, 1 mL of phage lysate was loaded on top of the layers. Finally, a thin layer of mineral oil was added to the top. Tubes were centrifuged at 200,000 *x g* for 2 h at 4°C. Phage particles were collected as described in section 2.6.9.

2.6.11. Purification of Phage Stock by Molecular Weight Cut-off

To obtain high-purity and concentrated phage particles, an Amicron Ultra-15 Centrifugal Filter Device (Merck, UK) was used, following the manufacturer's instructions. For each phage, 45 mL of high-titre phage lysates, prepared using the full plate lysate method described in section 2.7.6, were processed. Of these stocks, 15 mL of lysate was loaded into the Amicron filter device. The devices were placed in a swing rotor and centrifuged at 4,000 × *g* for 25 min. It is important not to dry the ultrafiltration membrane of the device; therefore, centrifugation must be stopped just before 1.5 mL of the sample remains in the sample loading part. After discarding the infranatant from the collection tube, another 15 mL of phage lysate was added to the filtration part of the device. These steps were repeated until all 45 mL of the sample had been processed. The remaining 1.5 mL of concentrated sample was collected using a pipette.

2.6.12. Host Range Profiling

The host range of each bacteriophage was assessed using the agar overlay method as described by Kutter (2009). A total of 28 *P. multocida* strains were tested for susceptibility to phage infection. Bacterial strains were cultured in TSB supplemented with 10% FBS and incubated at 37°C with shaking until reaching the mid-exponential phase ($OD_{600} \approx 0.5$). Bioassay plates were prepared using a solid base agar, as detailed in section 2.5. To create an overlay, molten top agar was inoculated with 50 µL/mL of bacterial culture, mixed thoroughly, and poured onto pre-

warmed base agar plates. The plates were allowed to solidify at room temperature for 30 min before phage application.

Phage susceptibility was determined by spotting 10 µL of high-titre phage lysate (1×10^9 PFU/mL) onto the prepared bacterial lawns. A 10 µL drop of SM buffer served as a negative control to account for any spontaneous bacterial lysis. After drying, plates were incubated aerobically at 37°C for 18 to 20 h. Plaque formation was assessed qualitatively based on the efficiency of bacterial lysis, with the extent of clearing scored as follows: ++++ (complete lysis), +++ (semi-confluent lysis), ++ (numerous plaques too many to count), + (few individual plaques) and – (no plaques observed). The experiment was performed in triplicate, with three independent biological replicates to ensure reproducibility and minimise variability.

To statistically evaluate phage effectiveness and host susceptibility patterns, lysis scores were converted into numerical values (++++ = 4, +++ = 3, ++ = 2, + = 1, – = 0) for quantitative analysis. The percentage of bacterial strains lysed by each phage was calculated by dividing the number of susceptible strains by the total number tested. Statistical comparisons among phages were conducted using one-way analysis of variance (ANOVA) to determine whether significant differences existed in lysis efficiency. To determine which phage groups had significantly different host ranges, Tukey's HSD post-hoc test was used. Ward's approach was used to visualise associations between phages based on their lytic spectra through hierarchical clustering analysis. The similarity in host range patterns between several phages was evaluated using Pearson's correlation analysis, and correlation coefficients were interpreted to ascertain functional redundancy or distinctiveness. To assess variations in phage lysis efficiency, statistical analyses were conducted using JMP 18 software, including one-way analysis of variance (ANOVA) and

Tukey's HSD post-hoc test. JMP-18 was also used to visualise the data, creating correlation matrices, heatmaps, and dendrograms to show host range relationships and statistical correlations between phages.

2.6.13. Efficiency of Plating

Using the guidelines outlined by Kutter (2009), the relative efficiency of plating (EOP) for every phage on various susceptible *P. multocida* strains was calculated. EOP measures a phage's titre on a particular test strain in relation to its titre on a reference strain. The susceptible host strain on which a phage produced the highest plaque titre (PFU/mL), as established by preliminary titrations, was designated as the reference strain for each phage (results presented in Table 4.3).

To calculate EOP, accurate phage titres were determined using the double agar overlay plaque assay method (detailed in Section 2.5). Briefly, serial dilutions of the phage stock were prepared in SM buffer. For each test strain and the corresponding reference strain, aliquots of appropriate phage dilutions were mixed with mid-exponential phase host bacteria and plated using the soft agar overlay technique. Plates were incubated aerobically at 37°C overnight. Following incubation, plates exhibiting countable plaques (typically 30–300 plaques) were used to calculate the phage titre (PFU/mL) on the test strain ($Titre_{test}$) and the reference strain ($Titre_{ref}$).

The EOP was then calculated as the ratio:

EOP= $Titre_{test} / Titre_{ref}$

Experiments were performed in triplicate, using three independent biological replicates.

2.6.14. pH Sensitivity

pH sensitivity tests were performed according to a previously described method (Capra, Quiberoni and Reinheimer, 2006). The pH of aliquots of SM buffer were adjusted using either NaOH or HCl to pH 2, pH 4, pH 6, C (pH 7.5), pH 8, pH 10 and pH pH12. After sterilising by autoclave and cooling down to room temperature, 900 µL of each pH solution was transferred to 1.5 mL centrifuge tubes. A high titre phage lysate (100 µL) was added into these tubes and gently inverted to mix. After incubation at room temperature for one hour, each suspension was decimally diluted to 10^{-6} in SM buffer. Volumes of each dilution (10 µL) were spotted onto bacterial lawns and incubated as above before enumerating plaques. Three biological and three technical repeats were performed for each phage.

2.6.15. Thermal Stability

With a few adjustments, thermal stability tests were conducted using the methodology Chen *et al*. (2019) outlined. In short, 1.5 mL microcentrifuge tubes were filled with 900 µL of high-titre lysate (1×10^9 PFU/mL) for every phage. A heating block that had been previously set to 40°C, 50°C, 60°C, 70°C, and 80°C was used to hold each tube. Every ten min from the beginning to the end, 100 µL of the heat-treated phage lysate was extracted and decimally diluted to 10^{-6} in SM buffer. Before counting plaques, volumes of each dilution (10 µL) were spotted onto bacterial lawns and incubated as previously mentioned. For every phage, three technical and three biological replicates were carried out.

2.6.16. Chloroform Sensitivity

To evaluate the phage's stability in chloroform, 100 µL of chloroform was added to 900 µL of high-titre lysate (1×10^9 PFU/mL). After 30 min at 100 rpm at ambient temperature, the

suspension was centrifuged at 10,000 × g for 10 minutes at 4°C. The aqueous phase was decimally diluted to 10^{-6} in SM buffer after being decanted into a different tube. The spot assay was utilised to ascertain the shift in phage titre. Three biological and three technical replicates were used for the tests, as previously mentioned.

2.6.17. Transmission Electron Microscopy Visualisation

Five phage samples in SM buffer (P1, P8, N1, N3 and N4) were visualised by Transmission Electron Microscopy (TEM) at the Electron Microscopy Facility, Core Biotechnology Service, College of Life Sciences at the University of Leicester, with the assistance of Natalie Allcock. All chemicals and consumables were obtained from Agar Scientific (www.agarscientific.com/). In the first run, 5 µL of undiluted P1, P8, N1, N3 and N4 samples were applied onto a carbon film copper grid, which was glow-discharged in a Quorum Gloqube Plus at 20 µA for 15 s. The samples were allowed to absorb for 3 min, blotted with filter paper, and a drop of distilled deionised water was applied. After further blotting, 5 µL of 1% uranyl acetate was applied. The grids were allowed to dry before being viewed on a JEOL JEM-1400 TEM with an accelerating voltage of 120 kV. Digital images were collected using an EMSIS Xarosa digital camera with Radius software. In the second run, P1 and N3 samples were diluted 1:5 and 1:10, respectively, and stained as described above. Phage tail and head dimensions were measured using ImageJ software. The tail length was measured from the base of the head to the end of the tail sheath, and the head diameter was determined at its widest point.

All statistical analyses were performed using JMP Pro 18 (SAS Institute Inc., Cary, NC, USA). Descriptive statistics, including mean, standard deviation (SD) and standard error of the mean (SEM), were calculated for each phage group. A one-way analysis of variance (ANOVA) was

conducted to assess differences in tail and head dimensions among the five phages (N1, N3, N4, P1 and P8). When a significant effect was detected ($p < 0.05$), Tukey's Honestly Significant Difference (HSD) test was applied for multiple pairwise comparisons. Results were considered statistically significant at $p < 0.05$. For visualisation, Tukey's HSD comparison plots were generated within JMP 18 to display confidence intervals for each pairwise comparison.

2.6.18. Genome Extraction by Phenol Chloroform and Isoamyl Alcohol Method

Phage genomes were extracted as follows: DNase (Thermo Scientific, UK) and RNAse (Thermo Scientific, UK) were added to 750 µL of high-titre phage lysate to achieve a final concentration of 15 mg/mL and incubated at 37°C for 60 min. Then, 30 µg of proteinase K (MC5005, Promega, UK), 35 µL of SDS (10% w/v) (Promega, UK) and EDTA (V6551, Promega, UK) at a final concentration of 40 mM (pH 8.0) were added. The mixture was gently mixed and incubated for 60 min at 60°C.

After incubation, the solutions were cooled to room temperature, and an equal volume of phenol:chloroform:isoamyl alcohol (25:24:1) (Invitrogen, UK) was added and gently mixed. The sample was then centrifuged at 10,000 × *g* for 5 min. The pellet was discarded, and the aqueous phase was transferred to another sterile centrifuge tube. An equal volume of phenol:chloroform (1:1) was added to the aqueous phase, mixed, centrifuged, and the aqueous phase collected again. The same steps were repeated once more with an equal volume of chloroform.

Next, a 1 in 10 dilution of 3 M sodium acetate and 2.5 × the volume of ice-cold 100% ethanol were added to the aqueous solution. This was gently mixed and stored at -20°C overnight. The tubes were then centrifuged at 10,000 × *g* for 30 min, and the supernatant was discarded. The nucleic acid pellet was washed twice with ice-cold 70% v/v ethanol, then

centrifuged again at 10,000 × *g* for 5 min, and the supernatant was removed. The nucleic acid pellets were air-dried for 30 min. The nucleic acids were then dissolved in TE buffer (pH 7.6) (Invitrogen, UK) and stored at -20°C.

The quality and quantity of the extracted genomes were assessed by TAE (tris-acetate-EDTA) agarose gel electrophoresis and NanoDrop. A 2 µL aliquot of 6× loading dye (NEB, UK) was mixed with 10 µL of the extracted nucleic acid before loading 10 µL into each well of the gel. The gel was prepared with 1% agarose (Thermo Scientific, UK) in 1× TAE buffer and stained with Nancy-520 (Sigma, UK). The gel was run at 100 V and 100 mA for 120 min. Quick-Load 1 kb Plus (NEB, UK) was used as a control DNA marker.

2.6.19. Genome Extraction by DNeasy Blood and Tissue Kit

The bacterial culture was grown to an OD_{600} of 0.6 for PM13 and 0.65 for ATCC 43137, respectively, to obtain approximately 2 × 10^9 CFU/mL, according to the growth curves of *P. multocida* strains in Section 3.2.6. To collect the cells, 1 mL of the culture (2 × 10^9) was centrifuged at 5,000 × *g* for 10 min in a microcentrifuge tube. The supernatant was discarded, and the pellet was resuspended in 180 µL of buffer ATL. Then, 200 µL of buffer AL was added, and the mixture was thoroughly mixed by vortexing before incubation at 56°C for 10 min. After incubation, 200 µL of ethanol (100%) was added, and the solution was vortexed thoroughly until a homogeneous solution was obtained. After that, the DNeasy Mini Spin Column was put in a 2 mL collection tube, and the solution was pipetted into it. The collection tube was disposed of with the flow-through after the tube was centrifuged for one min at 6,000 × g.

Prior to centrifugation at 6,000 × g for one min, 500 µL of Buffer AW1 was added to a fresh 2 mL collection tube containing the DNeasy Mini Spin Column. The column was put in a

fresh 2 mL collection tube, and the old collection tube was thrown away. The DNeasy membrane was then spin-dried after 500 µL of buffer AW2 was added and centrifugation was run for three min at 20,000 × g. The spin column was put in a sterile 1.5 mL microcentrifuge tube, and the collection tube was disposed of as before. After pipetting 200 µL of buffer AE straight onto the DNeasy membrane, the column was allowed to sit at room temperature for one min. The tube was centrifuged at 6,000 x g for one min in order to elute.

2.6.20. Restriction Digestion Analyses of Extracted Phage Genomes

Seven high-fidelity (HF) restriction enzymes (NEB, UK) were used to digest each sample: BamHI, BmtI, EcoRI, HindIII, KpnI, NcoI and PstI. Lambda DNA (NEB, UK), which is cut by all these enzymes, was used as a control. For each reaction, 1 µg of DNA, 5 µL of 10X rCutSmart Buffer (NEB, UK), 1.0 µL of the restriction enzyme, and nuclease-free water were mixed to a final volume of 50 µL. The mixture was incubated at 37°C for 30 min, after which 10 µL of 6X loading dye was added to stop the reaction before cooling to room temperature. The resulting products were tested on an agarose gel, as described in the previous section.

2.6.21. Sequencing and Primary Phage Contig Assembly

Phenol-extracted DNA from each phage was sent to the University of Leicester, where whole-genome sequencing was performed at the Department of Genetics on an Illumina sequencer. Low-quality reads were assessed using FastQC (www.bioinformatics.babraham.ac.uk/projects/fastqc/), and then filtered and eliminated using the Trimmomatic tool (Bolger *et al.,* 2014) according to the following criteria: reads with a certain proportion of low-quality bases (20) and/or a certain proportion of Ns were removed. Adapter contamination and duplication were also removed. The high-quality reads were then *de novo*

assembled into the genome using SPAdes (Prjibelski *et al.,* 2020). The terminal sequences of the viral genome were determined using Geneious Prime software. Glimmer 3.0 and tRNAscan-SE 2.0X (Chan and Lowe, 2019) were used to predict open reading frames (ORFs) and transfer RNAs (tRNAs) encoded by the phage genomes, respectively, with default parameters.

2.6.22. Contig and Phage Sequence Assessment

Raw sequence data from Illumina NGS in FastQ formats were first quality-checked using the FastQC quality control tool (Andrews, 2023). This tool provides information on basic statistics, per-base sequence quality, per-sequence quality scores, per-base sequence content, per-base GC content, per-sequence GC content, per-base n content, sequence length distribution, sequence duplication levels, overrepresented sequences and K-mer content. After quality control, Trimmomatic (Bolger *et al.,* 2014), a read trimming tool for Illumina NGS data, was used to perform several steps, including the removal of adaptors and other Illumina-specific sequences from the read (ILLUMINACLIP), trimming the read when the average quality in a sliding window falls below a specified threshold (SLIDINGWINDOW), discarding reads shorter than a defined length (MINLEN), removing low-quality bases at the beginning or end of a read (TRIMMING and TRAILING), truncating reads to a predetermined length (CROP), removing a specified number of nucleotide bases from the start of a read (HEADCROP), discarding reads with an average quality below a threshold (AVGQUAL) and adaptively trimming reads to optimise the balance between read length and error rate (MAXINFO).

Reads were assembled into contigs using SPAdes following an additional round of quality testing with FastQC (Prjibelski *et al*., 2020). FASTA files containing the correctly assembled readings were extracted. In order to determine whether these sequences had been previously

reported or were closely linked to any organisms, they were then compared to the NCBI BLAST database. To anticipate transfer RNAs (tRNAs), phage sequences were analysed using tRNAscan (Lowe and Eddy, 1997) and ARAGORN (Laslett, 2004).

The virulence and antimicrobial resistance genes contained in the sequences were then found using the AMRFinderPlus and ABRicate tools. The sequences of the *P. multocida* phages in this study were aligned using the Clustal Omega 1.2.2 tool in Geneious Prime software (version 2024.0.4). Similarities were noted, and differences at the beginning and end were extracted for further analysis. Phage genomes were analysed using the PHASTEST web-based tool (Wishart *et al.,* 2023), which is dedicated to detecting phage genomes and proteins. Previously annotated genes and the organisms they were found in were recorded. After detecting phage genes, remaining phage-like proteins, hypothetical proteins and bacterial proteins were extracted for further analysis.

These extracted sequences were translated into amino acid sequences and then searched for domains using the BLASTp tool on the NCBI database, the InterProScan tool (www.ebi.ac.uk/interpro/) and the UniProt (UniProt.org) databases. Publicly available *P. multocida* phage genomes, genetically similar phage genomes and representatives of other phage genomes from different families were downloaded from the NCBI database. A comparative analysis was performed by multiple sequence alignment, building phylogenetic trees and gene cluster comparisons using the following tools: Geneious Prime, ngphylogeny.fr, the Clinker tool (cagecat.bioinformatics.nl) and the VirClust tool (rhea.icbm.uni-oldenburg.de/virclust/).

2.6.23. One Step Growth Experiment

The phage preparation was diluted to 10^7 PFU/mL. A *P. multocida* subculture grown in BHI medium supplemented with 2 mM $CaCl_2$ to the mid-exponential phase, at an OD_{600} of approximately 0.5. Four flasks were labelled as "adsorption flask", "flask A", "flask B" and "flask C", and placed in a water bath at 37°C. A volume of 9.9 mL of the log-phase culture was transferred into the adsorption flask using a pipette, and the flask was immersed in the water bath for 5 min. Following this, the flask was quickly centrifuged, and the cell pellet was resuspended in 9.9 mL of fresh, pre-warmed medium.

Flask A, flask B and flask C each received 9.9 mL, 9 mL and 9 mL of broth, respectively. Phage preparation (0.1 mL) was added to the 9.9 mL culture in the adsorption flask, which was gently swirled and incubated for 5 min in the water bath (= 1/100, 1×10^5 PFU/mL).

After 5 min of adsorption, 0.1 mL was removed from the adsorption flask and added to flask A (containing 9.9 mL broth), which was then gently mixed (1/100, 1×10^5 PFU/mL). One millilitre from flask A was transferred to a tube containing 50 µL chloroform, vortexed for 10 sec, and placed on ice; this served as the adsorption control. Subsequently, 1 mL was transferred from flask A to flask B (a 1:10 dilution), and 1 mL was transferred from flask B to flask C (a 1:10 dilution).

Every 5 min, for up to 120 min, 0.1 mL samples were removed from each flask and added to 4.5 mL of molten overlay BHI agar supplemented with 5% FBS and inoculated with 0.2 mL of the plating host culture. The mixture was then poured onto the surface of underlay agar plates.

After 12 min from the start of adsorption, two 0.1 mL samples from the chloroform-treated tube (adsorption control) were plated using the same overlay method. Once the overlays solidified, the plates were inverted and incubated in an air incubator at 37°C for 18 hours. After

incubation, plaques were counted on each plate. Plaque counts were used to calculate PFU/mL at each time point, considering the dilution factors of the plated samples (typically from flasks B and/or C). The PFU/mL was then plotted against time.

2.6.24. LD_{50} Dose of *P. multocida* Strains

To evaluate the therapeutic effectiveness of the *P. multocida* phages against different *P. multocida* strains, this work utilised *G. mellonella* wax moth larvae as an in vivo model. With few modifications, the assessment procedure adhered to a previously defined protocol (Abbasifar *et al*., 2014). Commercial *G. mellonella* larvae were acquired from Livefoods UK Ltd. (www.livefoods.co.uk; Somerset, UK). A precision scale and ruler were used to measure each larva's weight and length once they were received. The larvae chosen to participate in the infection studies weighed roughly 250 mg and ranged in length from 2 to 3 cm. The larvae were kept in the dark, without food or water, at 4°C for a maximum of 7 days. Healthy larvae can be identified by their vigorous movement and uniform cream colour, which is free of any melanisation, spots, or markings (Li *et al*., 2018).

The larvae were frozen at -20°C for at least 24 hours after being exposed to 4°C for 1 hour to euthanise. At an *OD*600 of 0.5, cultures of *P. multocida* strains were incubated until they reached the mid-exponential phase. After that, the cultures were diluted to the appropriate concentrations and cleaned with PBS (phosphate-buffered saline) to obtain rid of any remaining media. The leftover supernatant was also injected with PBS in order to evaluate the bacterial lysate's pathogenicity effect on the larvae.

At different concentrations, 1.7×10^4, 1.7×10^5, 1.7×10^6, 1.7×10^7, 1.7×10^8 or 1.7×10^9 CFU per larva, the larvae were infected with bacterial cultures. With a final volume of 10 µL, the

infection was introduced into the last left proleg. Ten microlitres of PBS were injected into the vehicle control groups, whereas no injection was given to the negative control group. Placing the colonies onto blood-supplemented BHI agar allowed for the verification of the inoculum dosage.

The larvae were incubated at 37°C for 48 h. Throughout this period, they were regularly observed for melanisation and survival, with assessments taken every 12 h from 24 h to 48 h post-injection. Mortality was determined by the absence of a motor response after gentle stimulation with a sterile pipette tip. A minimum of 10 larvae per group were used, with data pooled from at least three independent trials. The bacterial strain's virulence on *G. mellonella* and the LD_{50} value for *G. mellonella* were determined using the Miller and Tainter technique, as described by Randhawa (2009), with some modifications.

To determine the LD_{50} dose, the log of actual concentrations was plotted against the resulting mortality. The regression equation was obtained by performing linear regression using GraphPad Prism (Version 10.2.0 (392)). Injections were made using sterilised Hamilton 10 µL 700-series microlitre syringe needles. Each experiment was performed independently three times. The chosen dosage used to induce colonisation for each bacterial strain in *in vivo* phage therapy experiments was determined based on the calculated LD_{50} values.

2.6.25. Phage Therapy

The host bacteria for phage therapy, *P. multocida* PM13 and ATCC 43137, were selected based on their efficiency of plating results, virulence activity on *G. mellonella* and consistent plaque-forming performance over time. The host bacteria were grown at 37°C until they reached the mid-exponential phase. The cultures were then centrifuged at 8,000 × *g* for 15 min, and the

supernatant was transferred to a new tube. The resulting pellet was resuspended in PBS at 37°C, washed twice, and diluted to the LD_{50} dose.

Phages, purified by molecular weight cut-off, were used in phage therapy. The first injections were administered into the last left proleg of the larvae. After 30 min, a second injection was made into the last right proleg. For the injection control, 10 µL of PBS was injected into both prolegs at 30-min intervals. Two phage therapy regimens were used: therapeutic and prophylactic (Table 2.8).

For the therapeutic treatment, the first injection consisted of 10 µL of bacteria, followed by the second injection of 10 µL of phage. For the prophylactic treatment, the injection order was reversed. For the bacterial, supernatant and phage controls, only 10 µL of the sample was injected 30 minutes before the PBS injection. The assay was conducted as previously described (Blasco and Tomás, 2023)

Table 2.8. Time Course of Phage Treatment Regimens on *G. mellonella* Used in This Study.

Groups		**Time (h)**				
n=10*	**Treatments**	**0**	**0.5**	**24**	**36**	**48**
1	No injection Control	-	-	-	-	-
2	Injection Control	PBS	PBS	-	-	-
3	Supernatant Control	S	PBS			
4	Bacterial Control	B	PBS	-	-	-
5	Therapeutic	B	P	-	-	-
6	Prophylactic	P	B	-	-	-
7	Phage Control	PBS	P	-	-	-

**A total of ten larvae were utilized for each designated time point and treatment regimen. Each larva was subjected to treatment using a Hamilton syringe, with 10 µL of phage (P), bacteria (B), supernatant of bacteria (S) or PBS (as an injection control). The experiment was conducted independently on three separate occasions.*

2.2.27. Data and Statistical Analyses

Data analysis and visualisation were conducted via various software packages suitable for the data type. Image analysis, encompassing the determination of bacterial capsule dimensions

and phage plaque diameters, was performed with ImageJ software (IJ 1.46r, National Institutes of Health) and Leica Application Suite (LAS) software.

The main statistical approach for comparing means between groups included one-way analysis of variance (ANOVA) for studying capsule sizes between different strains and phage virion diameters. The Tukey's Honestly Significant Difference (HSD) post-hoc test followed ANOVA when the analysis showed significant differences ($p < 0.05$) for multiple pairwise comparisons. The analysis of two related conditions, such as capsule sizes in different media or phage titres before and after chloroform treatment, used paired t-tests or the non-parametric Wilcoxon signed-rank test as appropriate.

The host range relationships of phages were studied by hierarchical clustering analysis (Ward's method) and Pearson's correlation analysis. JMP Pro 18 software (SAS Institute Inc., Cary, NC, USA) was used for the analyses.

The Lethal Dose 50 (LD_{50}) for *P. multocida* strains in the *Galleria mellonella* model was determined by linear regression analysis of log-transformed bacterial concentrations against mortality effects, utilising GraphPad Prism (Version 10.2.0, Build 392). Survival data from the in vivo phage therapy experiments were examined using Kaplan-Meier survival curves, and differences across treatment groups were evaluated using the Log-rank (Mantel-Cox) test in GraphPad Prism.

In all statistical analyses, a p-value below 0.05 was considered statistically significant. Data in graphs are typically presented as mean ± standard deviation (SD) or mean ± standard error of the mean (SEM), based on at least three independent biological replicates, as indicated in the figure legends. Bioinformatic analyses for genome assembly, annotation, comparison, and

phylogenetics utilised specific tools detailed in the relevant sections, including SPAdes (Bankevich *et al*., 2012) , Geneious Prime (version 2024.0.4)., PHASTEST (Wishart *et al., 2023*), BLAST tools (Altschul *et al*., 1990), Clinker (Gilchrist and Chooi, 2021), VirClust (Moraru, 2023), and ngphylogeny.fr (Lemoine *et al.,* 2019).

Chapter 3. *Isolation and Phenotypic Characterisation of P. multocida Strains*

P. multocida is a Gram-negative pathogen that causes FC in poultry and HS in cattle and AR in swine, according to Harper *et al*. (2006). The virulence of this bacterium depends on its capsular polysaccharides and lipopolysaccharides (LPS), which function as main targets for host immune evasion and phage adsorption (Knecht *et al*., 2020; Chen *et al*., 2024). The clinical relevance of *P. multocida* is challenging to determine in environmental water systems near poultry farms, largely due to its fastidious growth requirements and competition with other microbial species (Bredy and Botzler, 1989; El-Sayed *et al*., 2021).

The emergence of AMR in *P. multocida* makes phage therapy an essential alternative treatment option. Effective phage therapy depends on well-characterised host strains with defined surface receptors (e.g., capsule/LPS types) and growth dynamics (Labrie *et al*., 2010). Prior they have successfully isolated *P. multocida* from clinical specimens, but environmental sources, including water systems near poultry farms, remain understudied for phage discovery (Abdulrahman and Davies, 2021). The existing knowledge gap is essential because environmental strains possess distinct characteristics which affect phage-host interactions. The proposed research aimed to obtain and characterise different *P. multocida* strains through their physical attributes, including growth patterns, antibiotic resistance and capsule and LPS features. The characteristics of these strains will be distinct from one another, which will enable the selection of appropriate strains for phage isolation and therapy experiments through detailed characterisation.

3.1. Aims of Chapter

This chapter focuses on attempts to isolate *P. multocida* from environmental water and farm samples, which was limited due to Covid-19 restrictions. In order to better understand the role of wetlands in FC outbreaks, researchers have examined the viability of *P. multocida* in both water and sediment (Botzler, 1991). Previous studies have identified *P. multocida* in areas with major outbreaks, but analysis of these isolates was often inconclusive due to limited serotyping or virulence testing (Botzler, 1991).

The specific aims of this chapter were:

1. To isolate, confirm and characterise multiple *P. multocida* strains for use in subsequent phage isolation and characterisation studies.

2. To identify the probable binding sites (capsule and LPS) of these strains and evaluate whether they are suitable for further phage investigations.

3. To assess, optimise and select media for bacterial growth and phage isolation and characterisation.

4. To identify and characterise suitable *P. multocida* strains for use in future phage therapy experiments.

To achieve these objectives, optimisation of media was performed. *P. multocida* isolates were tested step-by-step, including capsule staining and PCR typing of their capsule and LPS groups. Antibiotic susceptibility tests were carried out to establish antimicrobial resistance (AMR) profiles, ensuring that results would not interfere with phage therapy experiments. Various growth parameters of host strains were assessed to determine the optimal conditions for phage timing and infection.

3.2. Isolation of *P. multocida*

To acquire a panel of contemporary *P. multocida* strains suitable for subsequent phage isolation and host range studies, an attempt was made to isolate this species from environmental reservoirs potentially harbouring the bacterium. The objective was to screen diverse environmental samples, focusing on water sources and faecal matter from locations considered high-risk for *P. multocida* presence, using established selective culture techniques.

Ninety-one environmental samples were collected from sixteen distinct locations, which include various water bodies such as lakes, rivers, ponds, and marinas, as well as faecal matter. The initial culture on *Pasteurella* selective medium produced 97 presumptive isolates, identified by colony morphology characteristic of *Pasteurella* species. Subsequent screening indicated that 51 of these isolates exhibited growth inhibition on MacConkey agar. Among the 51 MAC-negative isolates, 31 exhibited positive results for both oxidase and catalase activity, which are characteristic biochemical markers of Pasteurella. Thirty-one presumptive isolates went through species-specific PCR targeting the kmt1 gene to confirm their identification as *P. multocida*.

Despite screening numerous environmental samples using selective isolation and biochemical testing protocols, no *P. multocida* strains were successfully isolated from the targeted locations. This outcome necessitated the use of previously acquired reference and clinical strains (obtained from Thermo Scientific, Ridgeway Biologicals, APHA and the University of Glasgow) for subsequent phage isolation and characterisation experiments within this study.

3.2.1. Biochemical Characterisation of Presumptive Isolates

To narrow down the candidate isolates obtained from selective plating (both environmental samples and sourced strains) towards those likely belonging to the genus

Pasteurella or closely related genera, standard preliminary biochemical tests were performed. Specifically, isolates unable to grow on MacConkey agar were assessed for positive oxidase and catalase activity, characteristics typical of *P. multocida*.

After initial culture and screening for growth inhibition on MacConkey agar, 58 isolates, including six strains obtained from Ridgeway Biologicals, were evaluated for catalase activity. Forty-two of the isolates exhibited a positive catalase reaction. Forty-two catalase-positive isolates were tested for oxidase activity, resulting in 38 positive outcomes. The 38 isolates exhibited both catalase and oxidase positivity while failing to grow on MacConkey agar, leading to their classification as presumptive *Pasteurella* or *Pasteurellaceae* species. Appendix Table 7.1 presents a comprehensive breakdown of these results by isolate.

The sequential biochemical screening successfully identified 38 isolates possessing key characteristics (MAC-negative, oxidase-positive, catalase-positive) consistent with the target genus. These 38 presumptive isolates were therefore selected for definitive species confirmation using *P. multocida*-specific PCR.

3.2.2. PCR Confirmation of *P. multocida* Isolates

To definitively determine if the 38 presumptive isolates (selected based on growth characteristics and biochemical tests) were indeed *P. multocida* and to confirm the identity of the sourced reference and clinical strains, species-specific PCR targeting the *kmt1* gene was performed. This step was crucial for finalising the panel of confirmed *P. multocida* strains to be used in subsequent experiments.

The 38 presumptive isolates obtained from environmental samples, exhibiting suitable biochemical profiles (MAC-negative, oxidase-positive, and catalase-positive), went through *P.*

multocida-specific PCR analysis. All 38 isolates tested negative for *P. multocida*, as evidenced by the absence of positive PCR results. In contrast, all strains acquired from external collections—six from Ridgeway Biologicals, one from Thermo Scientific, eighteen from APHA, and six from the University of Glasgow—yielded positive results in the same PCR assay, thereby confirming their identification as *P. multocida*.

Representative gel electrophoresis images confirming these results are provided in the Appendix (Figures 7.4-7.7), and a summary is presented in Table 3.3.

Species-specific PCR analysis conclusively demonstrated that none of the isolates obtained from the environmental sampling were *P. multocida*. However, the identity of all 31 sourced strains from Ridgeway Biologicals, Thermo Scientific, APHA and the University of Glasgow was confirmed as *P. multocida*, thus establishing the final panel of bacterial strains used for the phage isolation, characterisation and therapy experiments described in the following chapters.

Table 3.3. Characterisation Results of *P. multocida* Strains Used in This Study.

Strain	Source	PSM	MAC	OX/CAT	PCR kmtp1	CAP +	CAP type	LPS	*TOX-A*	AMR profile
PM13	Poultry	✓	×	✓	✓	✓	U	L3		AMP. NA, S, TE, CTX, PG
ATCC 43137	Swine	✓	×	✓	✓	✓	U	L3		AMP. NA, S, TE, CTX, PG
PM48	Poultry	✓	×	✓	✓	✓	U	L3		n/a
PM52	Poultry	✓	×	✓	✓	✓	U	L3		AMP. NA, TE, CTX, PG

PM106	Poultry	✓	×	✓	✓	✓	U	L3		n/a
PM222	Poultry	✓	×	✓	✓	✓	U	L4		n/a
X73 (A)	Poultry	✓	×	✓	✓	✓	U	L5		AMP. NA, TE, CTX, PG
M1404 (B)	Poultry	✓	×	✓	✓	✓	B	L2		NA, TE, CTX, PG
P3881 (D)	Poultry	✓	×	✓	✓	✓	D	L6		NA, TE, CTX, PG
P1235 (E)	Poultry	✓	×	✓	✓	✓	E	L2		AMP. NA, TE, CTX, PG
P4679 (F)	Poultry	✓	×	✓	✓	✓	F	L1		AMP. NA, TE, CTX, PG
PM2Y	Swine	✓	×	✓	✓	✓	n/a	L6		S, TE, CTX, PG
PM3Y	Swine	✓	×	✓	✓	✓	U	L6		NA, TE, CTX, PG
PM4Y	Swine	✓	×	✓	✓	✓	U	L4		AMP. NA, TE, CTX, PG
PM6Y	Swine	✓	×	✓	✓	✓	U	L4		AMP. NA, S, TE, CTX, PG
PM12Y	Swine	✓	×	✓	✓	✓	U	L3		AMP. NA, TE, CTX, PG
PM13Y	Swine	✓	×	✓	✓	✓	U	L4		AMP. NA, S, TE, CTX, PG
PM16Y	Swine	✓	×	✓	✓	✓	D	L4	✓	NA, TE, CTX, PG
PM17Y	Swine	✓	×	✓	✓	✓	D	L4	✓	NA, S, CTX, PG
PM19B	Swine	✓	×	✓	✓	✓	B	U		n/a
PM22B	Swine	✓	×	✓	✓	✓	U	L1		AMP. NA, TE, CTX, PG
PM24B	Swine	✓	×	✓	✓	✓	B	L3		NA, S, SH, TE, CTX, PG
PM25B	Swine	✓	×	✓	✓	✓	U	U		AMP., NA, SH, TE, CTX, PG
PM26B	Swine	✓	×	✓	✓	✓	U	U		NA, TE, CTX, PG
PM27B	Swine	✓	×	✓	✓	✓	U	U		AMP, NA, S, SH, TE, CTX, PG

This table summarises the overall characterisation results of *P. multocida* strains used in the study.
PSM: Growth on *Pasteurella* selective medium (✓ = growth, × = no growth).
MAC: MacConkey agar growth (✓ = growth, × = no growth).
OX/CAT: Oxidase and catalase test (✓ = positive).
PCR kmt1: *P. multocida*-specific PCR test (✓ = positive).
CAP +: Detection of capsule production (✓ = positive).
CAP Type: Capsule type determined by multiplex PCR (A, B, D, E, F, U = untypable, n/a = not applicable).
LPS: Lipopolysaccharide genotype (e.g., L1, L2).
TOX-A: Presence of *TOXA* gene (✓ = present).
AMR Profile: Antimicrobial resistance profile: AMP = ampicillin, NA = nalidixic acid, S = streptomycin, SH = spectinomycin, TE = tetracycline, CTX = cefotaxime, PG = penicillin G,

3.3. Optimisation of Media for Pasteurella Growth.

Considering the initial finding that the *P. multocida* strains utilised in this investigation displayed variable growth on regular, non-supplemented TSA, it became essential to identify a more reliable and effective growth medium. The objective of this experiment was to evaluate different combinations of base media (TSA, BHI, BAB No.2, and MH agar) and supplements (10% v/v FBS, 10 mM $CaCl_2$, 5% v/v sheep blood, and 5% v/v horse blood) to identify an optimal formulation that facilitated robust bacterial growth and enabled clear visualisation of bacteriophage plaques in subsequent assays.

The proliferation of *P. multocida* on the evaluated combinations is shown in Table 3.1. The findings demonstrated that combinations of TSA with FBS, TSA with sheep or horse blood, BHI with sheep or horse blood, and BAB No.2 with horse blood produced the most abundant bacterial growth, classified as large colonies (+++). The incorporation of 10 mM $CaCl_2$ led to small growth of colonies (+) in all tested base media. Although blood-enriched media facilitated large colony growth (+++) and enabled the evaluation of haemolytic activity, the dark characteristics of the media complicated the observation of phage plaques. Media supplemented with FBS provided the clearest background for observing distinct phage plaques compared to blood-supplemented media; $CaCl_2$-supplemented media, despite being somewhat brighter than blood agar, did not offer the same clarity as FBS and supported poorer growth.

Based on these observations, TSA supplemented with 10% v/v FBS, which supported large colony growth (+++) of the *P. multocida* strains and offered superior clarity for the accurate visualisation and enumeration of phage plaques, was selected as the primary medium.

Table 3.1. Combination of media and supplements.

Medium	Supplement	Comment	Result*
TSA	10 % v/v FBS	Large colonies, suitable of phage work	++++
TSA	+10 mM $CaCl_2$	Small colonies	+
TSA	5 % v/v sheep blood	Large colonies, haemolytic activity can be assessed	++++
TSA	10 % v/v horse blood	Large colonies, haemolytic activity can be assessed,	++++
BHI	10 % v/v FBS	Medium colonies,	++
BHI	+10 mM $CaCl_2$	Small colonies	+
BHI	5 % v/v sheep blood	Medium colonies, haemolytic activity can be assessed	+++
BHI	10 % v/v horse blood	Medium, haemolytic activity can be assessed	+++
BAB No.2	10 % v/v FBS	Medium colonies,	++
BAB No.2	+10 mM $CaCl_2$	Small colonies	+
BAB No.2	5 % v/v sheep blood	Medium colonies,	++
BAB No.2	10 % v/v horse blood	Large colonies, haemolytic activity can be assessed	++++
MH agar	10 % v/v FBS	Small colonies	+
MH agar	+10 mM $CaCl_2$	Small colonies	+
MH agar	5 % v/v sheep blood	Small colonies	+
MH agar	10 % v/v horse blood	Small colonies	+

Scoring Key:
Large colonies = +++
Medium colonies = ++
Small colonies = +
No growth = 0
Suitable for phage work (clear background) = +
Haemolytic activity can be assessed = +
Note for 'Result' column: The score in this column represents a composite assessment. It was calculated by summing the '+' values for each observed characteristic, based on the individual scores detailed in the Scoring Key above. For instance, a medium supporting large colony (+++) and allowing assessment of haemolytic activity (+) received a total score of ++++.

3.4. Characterisation of *P. multocida* Strains

3.4.1. Determination and Measurements of Capsules

The bacterial capsule serves as a crucial virulence factor for *P. multocida* and could function as a key interaction site or barrier for bacteriophages. Consequently, the presence and dimensions of the capsule on the provided *P. multocida* strains were examined microscopically

to characterise this essential phenotypic characteristic. The study aimed to ascertain whether capsule thickness exhibited considerable variation among strains or was affected by growing circumstances (solid versus liquid media).

Microscopic analysis subsequent to India ink staining verified the existence of a capsule on all examined *P. multocida* strains (Figures 3.1 and 3.2). Quantitative image analysis revealed considerable and statistically significant variation in capsule thickness among the different strains when grown under identical conditions (Figures 3.3, 3.4 and 3.5). For instance, under plate culture conditions, capsule sizes ranged from approximately 181 nm (strain X73) to 903 nm (strain 3Y) (Figure 3.4), with one-way ANOVA indicating significant differences between strains ($F = 73.70$, $p < 0.0001$).

Considerable inter-strain variation was detected in liquid culture ($F = 11.96$, $p < 0.0001$), with diameters varying from 240 nm (strain P1235) to 613 nm (strain 22B) (Figure 3.5). Although individual strains occasionally exhibited varying capsule thicknesses based on growth conditions—either on plates or in liquid culture—statistical analyses using paired t-tests and Wilcoxon signed-rank tests revealed no significant difference in capsule size between the two conditions across the strain panel ($p > 0.05$) (Figure 3.6).

All the analysed *P. multocida* strains presented a capsule, however the thickness of this layer exhibited considerable variation across various isolates. The natural inter-strain variability in capsule size, rather than the culture conditions (solid versus liquid), seems to be the primary factor affecting capsule thickness. The variability in a crucial surface structure may affect both virulence and susceptibility to phage infection in future tests.

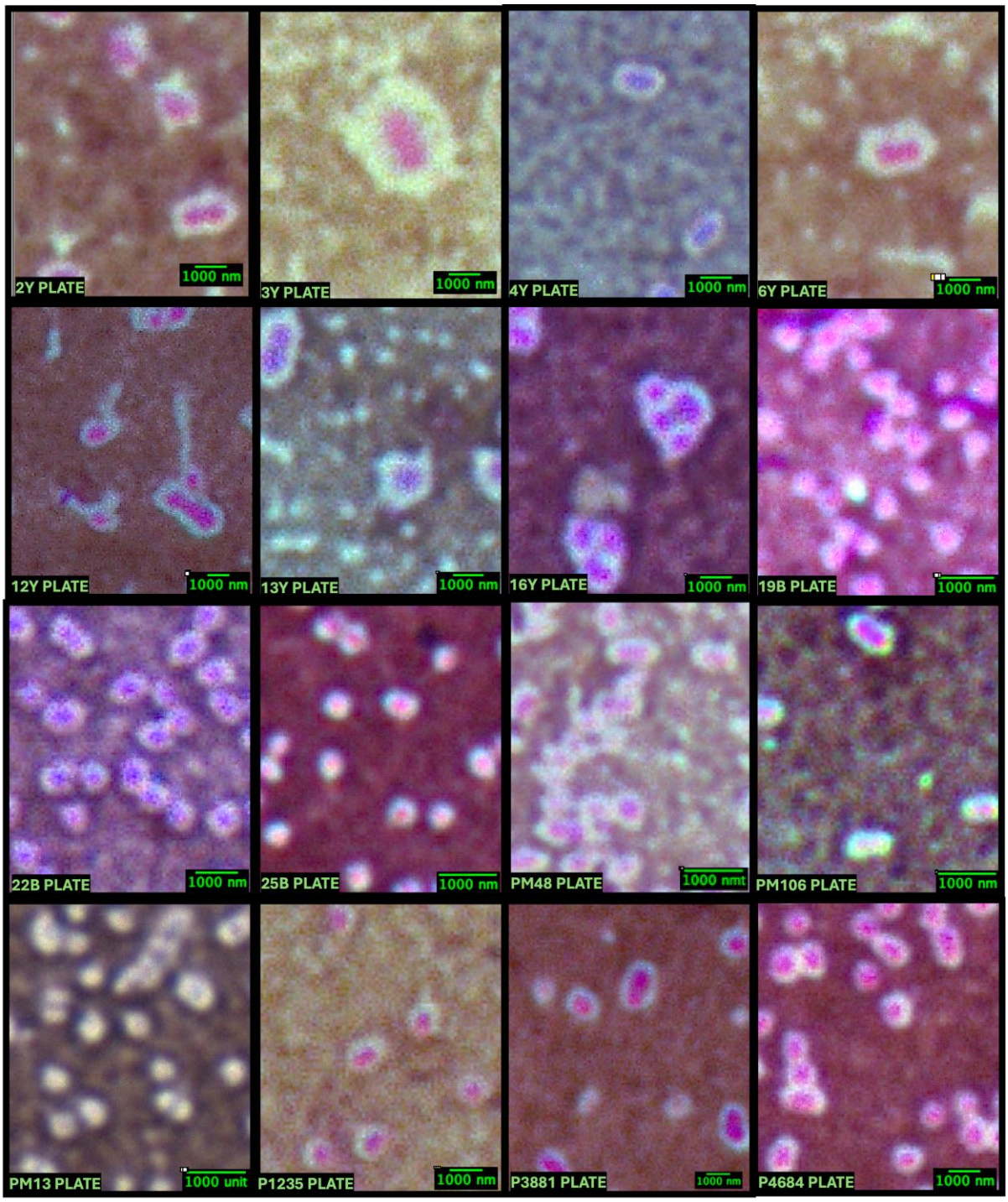

Figure 3.1. Microscopic Visualisation of *P. multocida* Strains Stained with India Ink to Demonstrate Capsule Presence on Solid Agar.

India ink staining was performed to visualising the capsules of *P. multocida* strains grown on solid agar. Strains were grown on TSA supplemented with 5% FBS. Smears were prepared by mixing bacterial suspensions with India ink, followed by staining with 1% crystal violet. Specimens were observed using a light microscope at 100× magnification with immersion oil. Scale bars represent 1,000 nm.

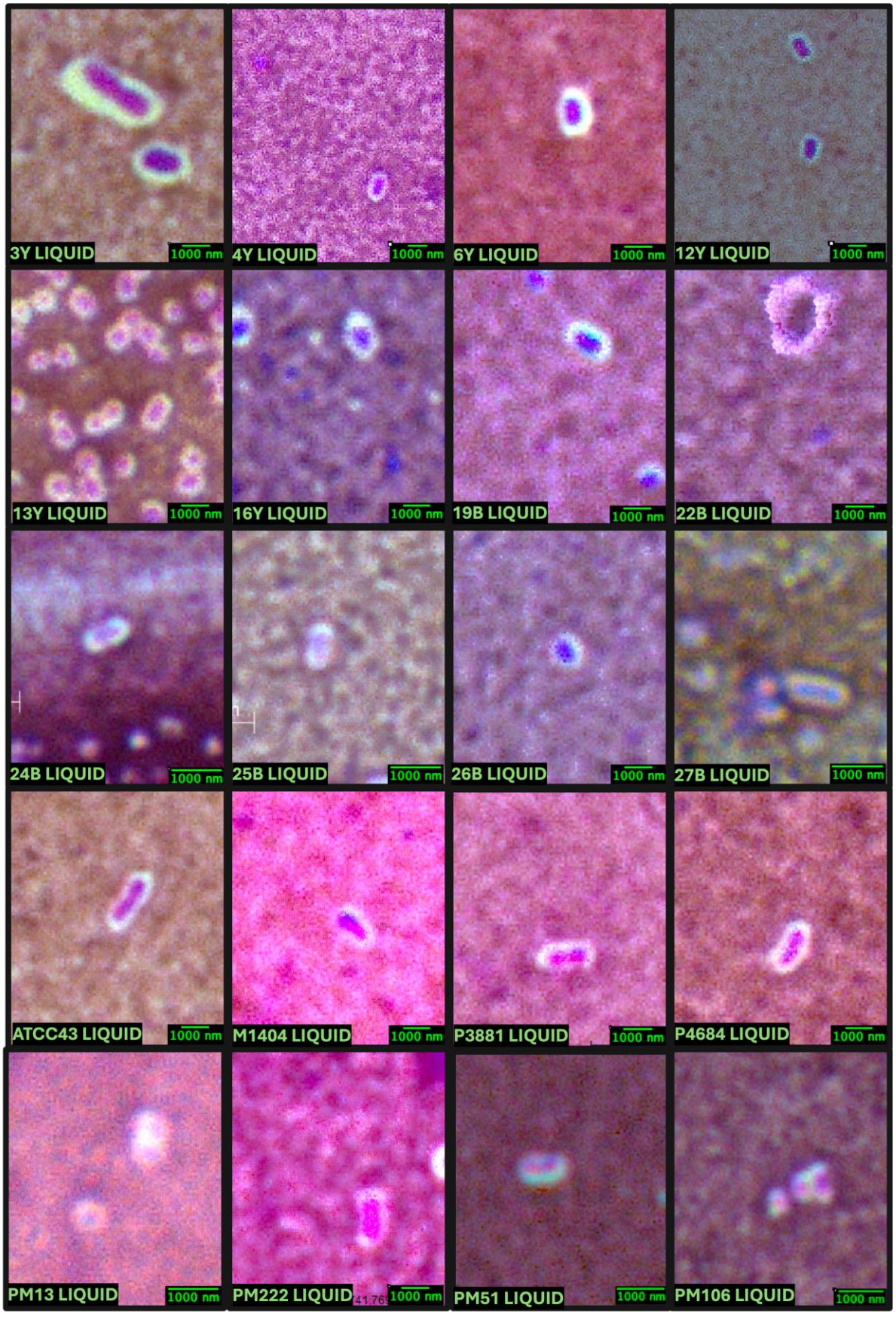
3Y LIQUID
1000 nm
4Y LIQUID
1000 nm
6Y LIQUID
1000 nm
12Y LIQUID
1000 nm
13Y LIQUID
1000 nm
16Y LIQUID
1000 nm
19B LIQUID
1000 nm
22B LIQUID
1000 nm
24B LIQUID
1000 nm
25B LIQUID
1000 nm
26B LIQUID
1000 nm
27B LIQUID
1000 nm
ATCC43 LIQUID
1000 nm
M1404 LIQUID
1000 nm
P3881 LIQUID
1000 nm
P4684 LIQUID
1000 nm
PM13 LIQUID
1000 nm
PM222 LIQUID
1000 nm
PM51 LIQUID
1000 nm
PM106 LIQUID
1000 nm

Figure 3.2. Microscopic Visualisation of *P. multocida* Strains Stained with India Ink to Demonstrate Capsule Presence in Liquid Media.

India ink staining was performed to visualise the capsules of *P. multocida* strains grown in liquid media. Strains were grown on TSB supplemented with 5% FBS. Smears were prepared by mixing bacterial suspensions with India ink, followed by staining with 1% crystal violet. Specimens were observed using a light microscope at 100× magnification with immersion oil. Scale bars represent 1,000 nm.

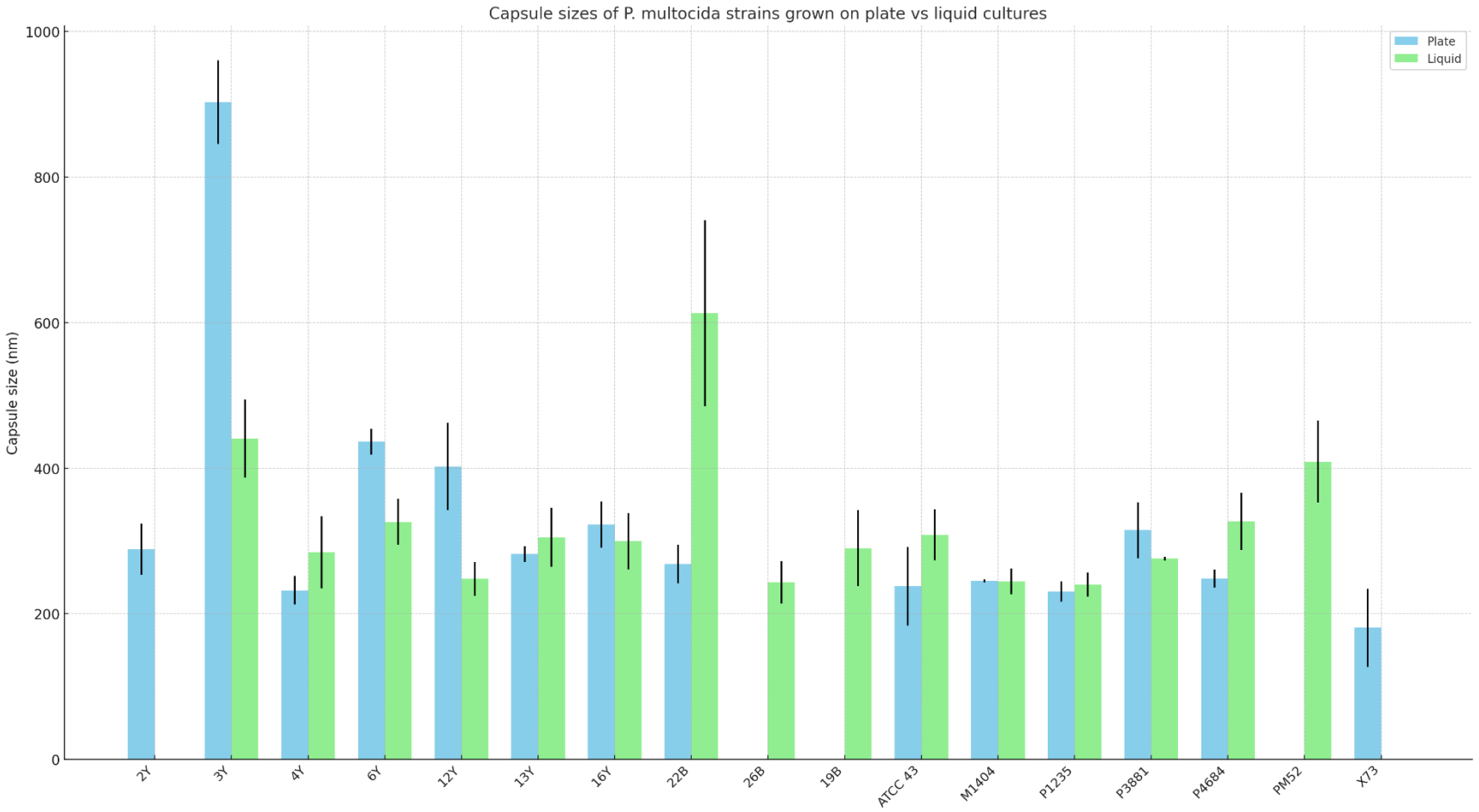

Figure 3.3. Comparison of Capsule Sizes of Different Strains of *P. multocida* When Grown in Plate and Liquid Culture Media.
The bar chart shows the mean capsule size (nm) ± standard deviation for each strain under two growth conditions: plate (sky blue) and liquid (light green). Zero-height bars indicate missing data for a given condition.

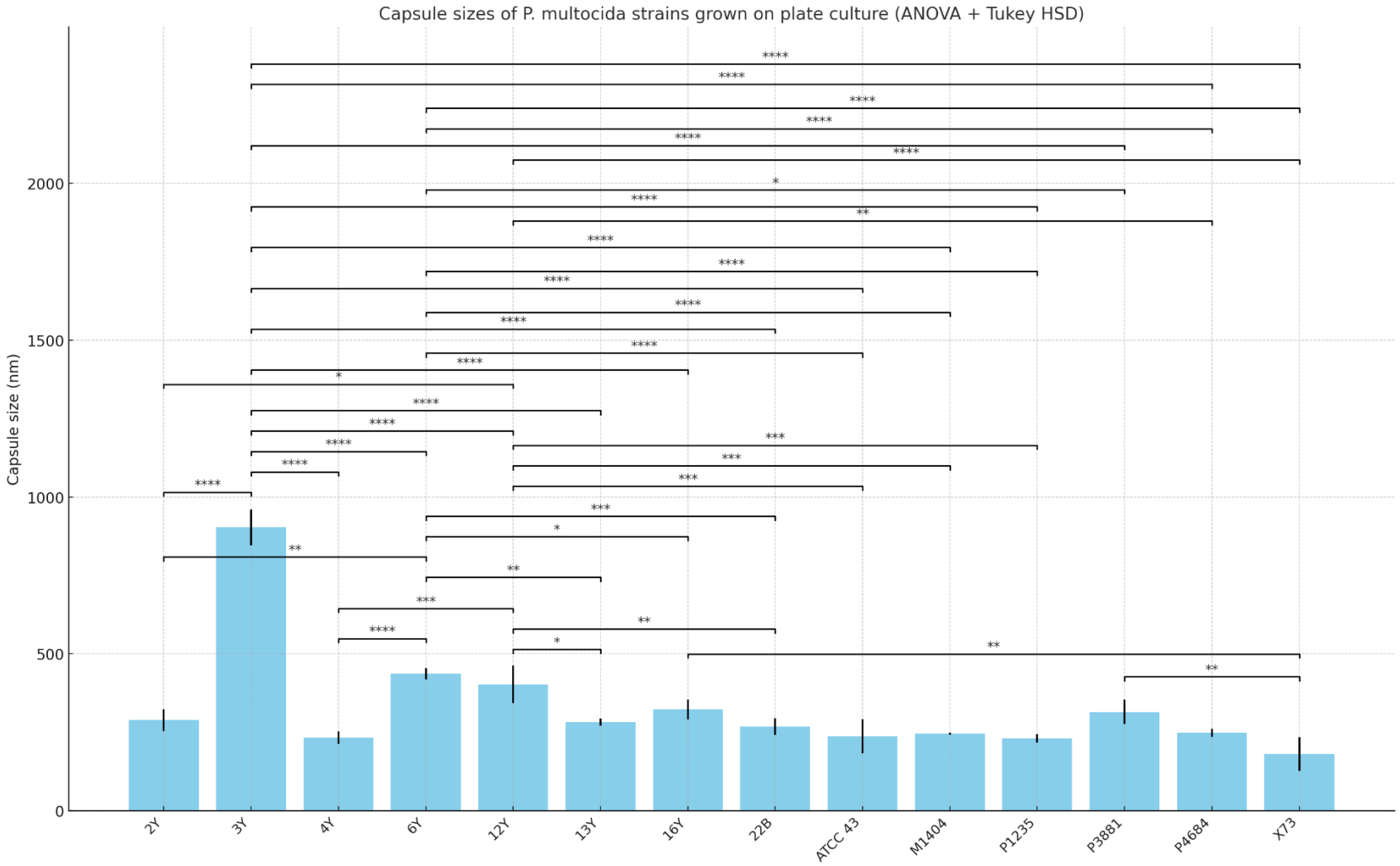

Figure 3.4. Capsule Sizes of *P. multocida* Strains Grown on Plate Culture with Significant Differences Annotated.

Bars represent mean capsule sizes (nm) ± standard deviation. Statistical differences between strains were determined using one-way ANOVA followed by Tukey's HSD post-hoc test. Levels of significance are denoted as $p < 0.05$ (*), $p < 0.01$ (**), $p < 0.001$ (***), and $p < 0.0001$ (****).

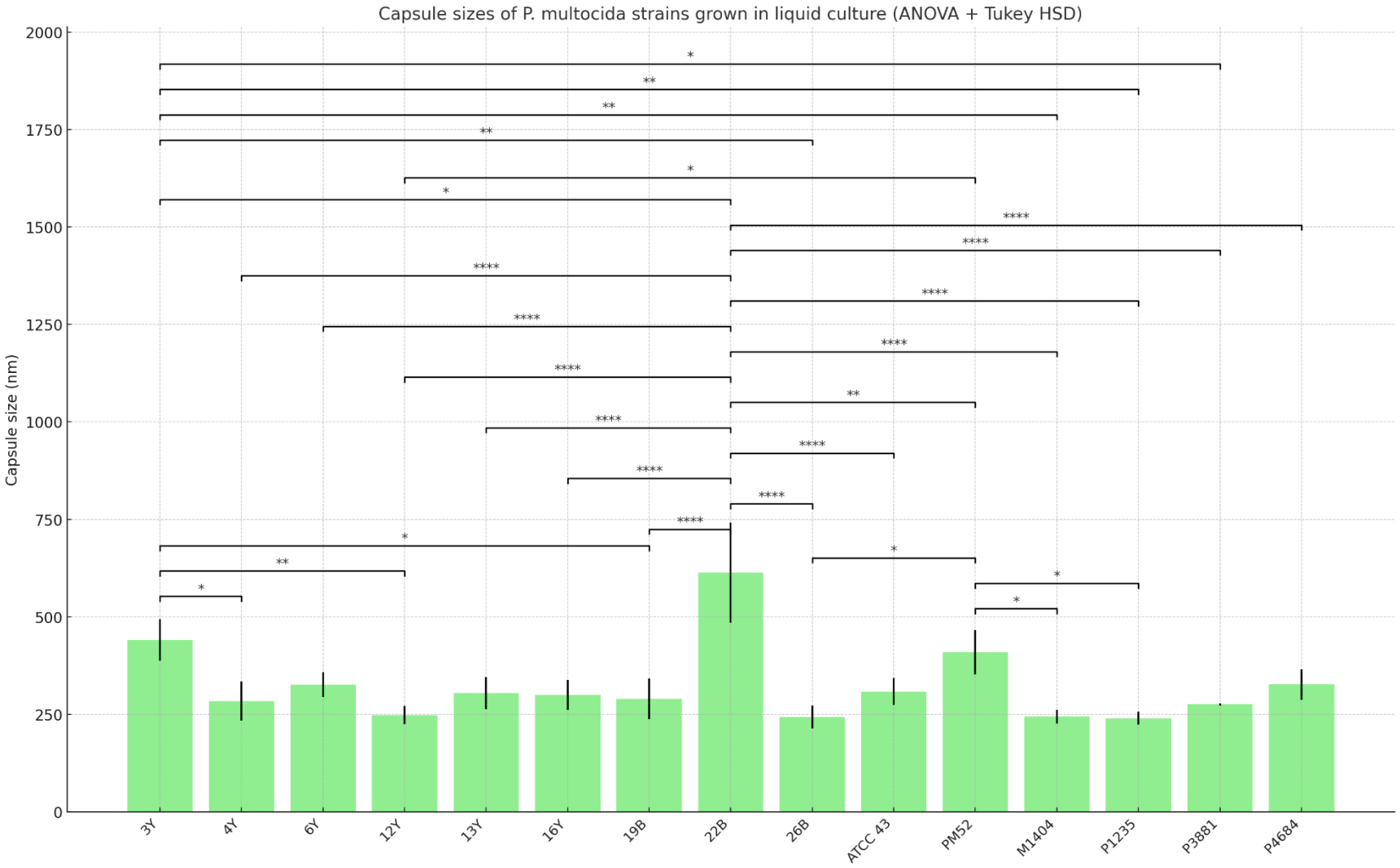

Figure 3.5. Capsule Sizes of *P. multocida* Strains Grown in Liquid Culture with Significant Differences Annotated.
Bars represent mean capsule sizes (nm) ± standard deviation. Statistical differences between strains were determined using one-way ANOVA followed by Tukey's HSD post-hoc test. Levels of significance are denoted as $p < 0.05$ (*), $p < 0.01$ (**), $p < 0.001$ (***), and $p < 0.0001$ (****).

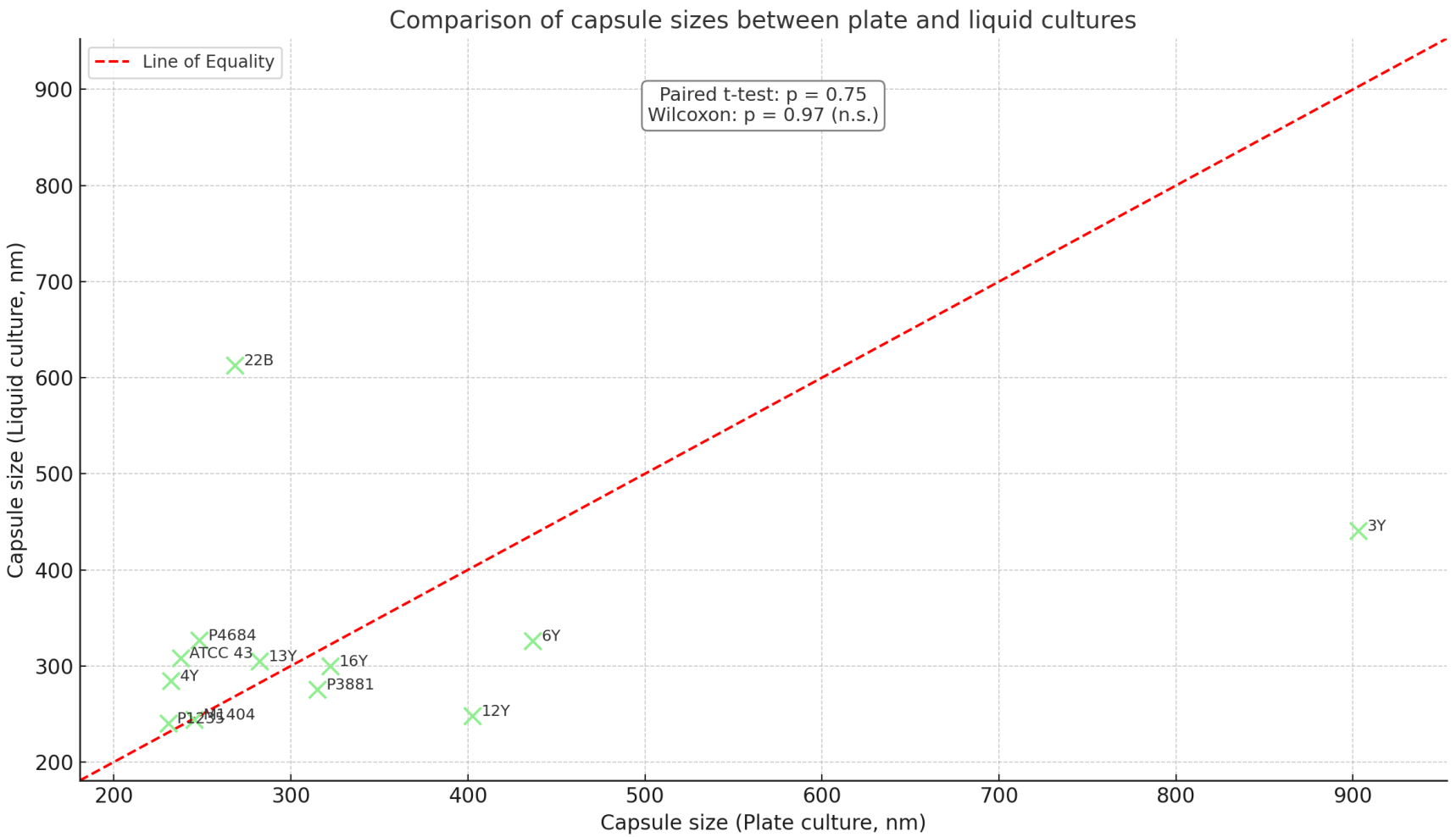

Figure 3.6. Comparison of Capsule Sizes of *P. multocida* Strains Between Plate and Liquid Cultures.
The scatter plot compares average capsule sizes (nm) of strains under the two conditions. Each point represents the mean capsule size for a strain. The dashed red line indicates the line of equality (y = x). Statistical comparison using a paired *t*-test (t = 0.33, *p* = 0.75) and Wilcoxon signed-rank test (W = 38.0, *p* = 0.97) showed no significant overall difference between capsule sizes in plate and liquid cultures.

3.4.2. Capsule Typing by PCR

Subsequent to the verification of capsule presence using microscopy, the following step was identifying a specific capsular serogroup (A, B, D, E, or F) for each isolate, as various capsular types correlate with unique host ranges and disease pathologies in *P. multocida*. Multiplex PCR targeting capsule biosynthesis genes was used for this genetic classification.

The capsular types for 22 confirmed *P. multocida* isolates were determined using multiplex PCR, with the outcomes presented in Figures 3.7 and 3.8. This analysis revealed a distribution of several capsular types among the isolates: one strain (P4679) was identified as type F, three strains (P3881, 16Y and 17Y) were type D and three strains (M1404, 19B and 24B) were type B. Notably, no isolates were identified as capsular type A using this PCR method, and a significant portion (14 isolates) could not be typed, remaining designated as untypable despite confirmation of physical capsule presence via microscopy.

Multiplex PCR effectively identified capsular genotypes B, D, and F in a subset of *P. multocida* strains, offering significant insights into their potential origins and facilitating subsequent phage host range analysis. The majority of isolates were untypable by this method, indicating either the existence of capsule types not addressed by the standard primer set or possible limitations in the PCR assay employed, especially regarding the detection of type A.

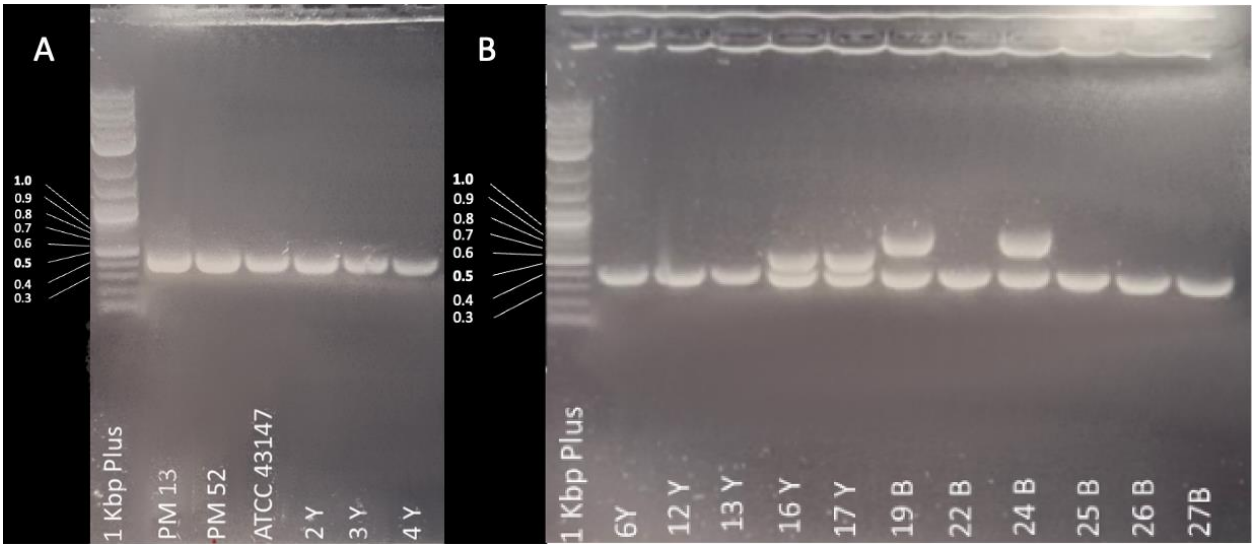

Figure 3.7. Gel Electrophoresis of Multiplex PCR Products for Capsule Typing of *P. multocida* Strains 1

The figure presents the results of agarose gel electrophoresis for multiplex PCR amplification of capsule-specific genes from *P. multocida* strains. (A): PCR products from strains PM13, PM52, ATCC 43137, PM2Y, PM3Y and PM4Y. (B): PCR products from strains PM6Y, PM12Y, PM13Y, PM16Y, PM17Y, PM19B, PM22B, PM24B, PM25B, PM26B and PM27B. Bands were visualised under UV light following gel electrophoresis, with a 1 kb plus DNA ladder included for reference. Band sizes correspond to the amplicon sizes listed confirming the presence of capsule-specific genes: Bands at 460 bp indicate *P. multocida* specific gene (*kmt1*), bands at 1044 bp indicate serogroup A (*hyaD-hyaC*), bands at 760 bp indicate serogroup B (*bcbD*), bands at 657 bp indicate serogroup D (*dcbF*), bands at 511 bp indicate serogroup E (*ecbJ*) and bands at 851 bp indicate serogroup F (*fcbD*).

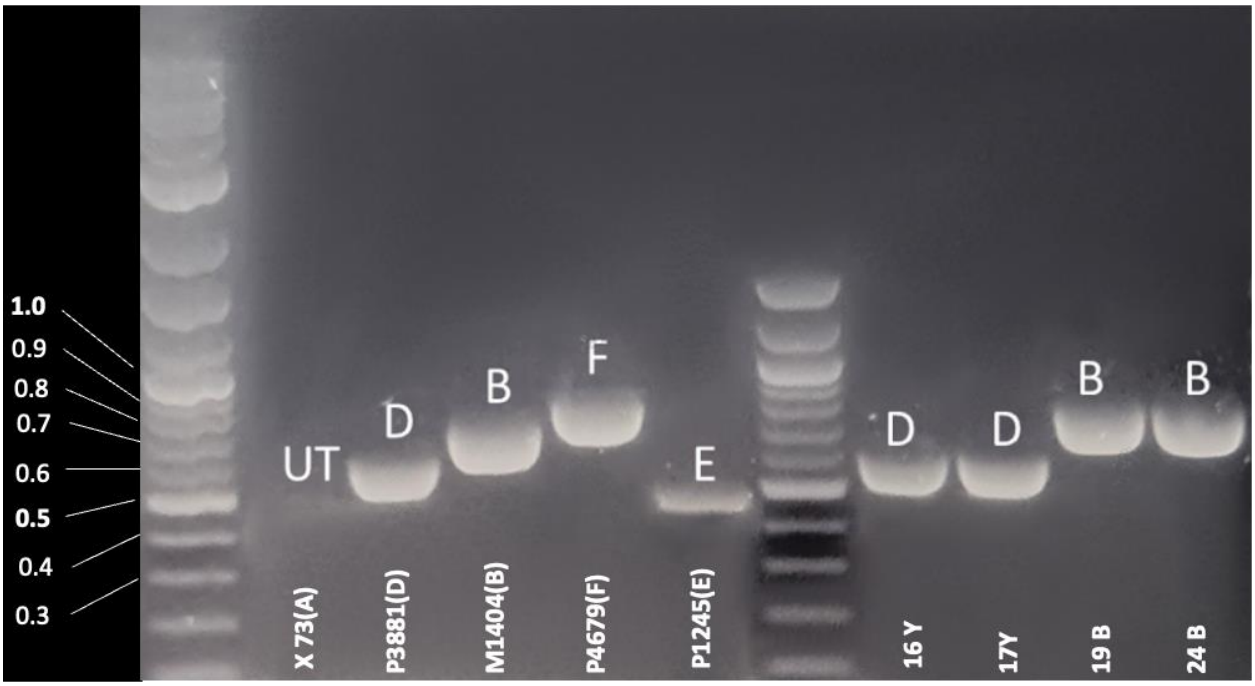

Figure 3.8. Gel Electrophoresis of Multiplex PCR Products for Capsule Typing of *P. multocida* Strains 2.
The strains presenting in the gel were selected from typeable ones except X73 which was type strain for capsule A. Band sizes correspond to the amplicon sizes listed confirming the presence of capsule-specific genes: Bands at 1044 bp indicate serogroup A (*hyaD-hyaC*), bands at 760 bp indicate serogroup B (*bcbD*), bands at 657 bp indicate serogroup D (*dcbF*), bands at 511 bp indicate serogroup E (*ecbJ*) and bands at 851 bp indicate serogroup F (*fcbD*). Amplified fragments were separated on a 1% agarose gel at 75 V for 240 minutes, stained with Nancy-520, and visualised under UV light with a 1 kb plus DNA ladder included for reference.

3.4.3. LPS Typing by PCR

As LPS is another major surface antigen and a known determinant of phage interaction in Gram-negative bacteria, the LPS genotype of each *P. multocida* isolate was determined. This classification aimed to identify the distribution of the eight known *P. multocida* LPS outer core biosynthesis loci within the strain panel, providing further context for potential phage specificities.

Multiplex PCR targeting genes specific to the eight recognised LPS outer core biosynthesis loci (L1–L8) was performed on 22 *P. multocida* strains. The analysis revealed a variety of LPS genotypes within the panel. Eight strains demonstrated the L3 profile (PM13, PM48, PM106,

ATCC 43137, PM52, PM12Y, and PM24B), establishing it as the most common type in this collection. Seven strains were classified under genotype L4: PM222, PM4Y, PM6Y, PM13Y, PM16Y, and PM17Y. Genotypes L1, L2 and L6 were also represented by two (P4679, PM22B), two (P1235 and M1404) and three (P3881, PM2Y and PM3Y) strains, respectively. One strain (X73) possessed the L5 LPS genotype. No strains corresponding to LPS genotypes L7 or L8 were detected among the tested isolates. In a few cases, such as in figure 3.9 lane 11 (PM4Y), band migration was close to the expected size for more than one locus (e.g. L3 vs. L4), and these assignments should therefore be regarded as tentative. Representative gel images are shown in the Appendix (Figures 3.9 and 3.10).

LPS genotyping revealed considerable diversity within the *P. multocida* strain collection, with six of the eight known LPS types (L1–L6) represented. The prevalence of types L3 and L4 and the absence of L7 and L8 characterises this specific panel and provide a basis for investigating potential correlations between LPS structure and phage susceptibility in subsequent experiments.

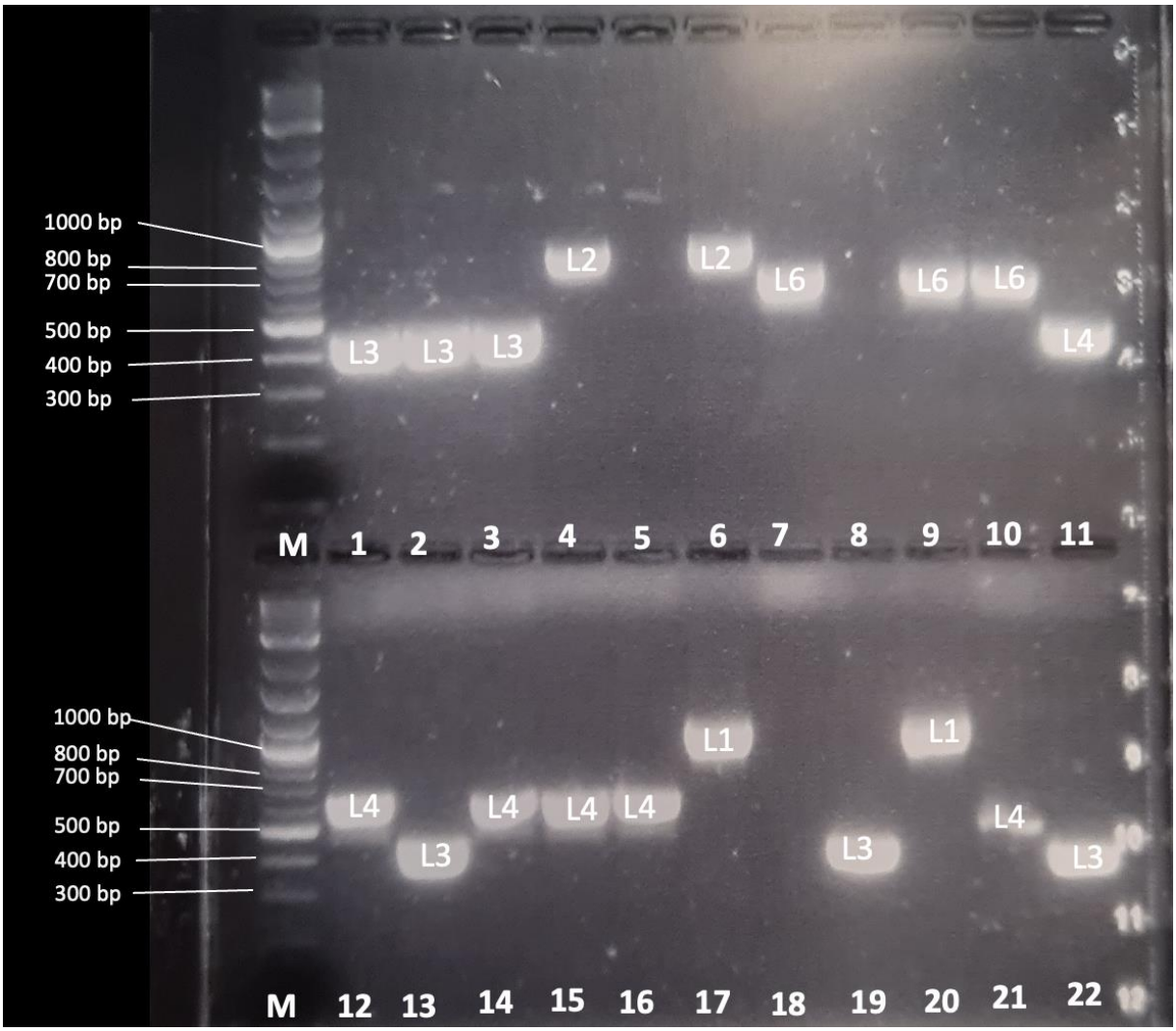

Figure 3.9. PCR Amplification of LPS Outer Core Biosynthesis Loci in *P. multocida* Isolates 1.

This figure shows agarose gel electrophoresis results of PCR products targeting LPS outer core biosynthesis loci in *P. multocida* isolates. DNA fragments were amplified using primers specific to loci pcgD (L1~1107 bp), nctA (L2~810 bp), gatF (L3~474 bp), latB (L4~550 bp), rmlA (L5~1175), nctB (L6~668 bp), ppgB (L7931~) and natG (L8~255). Amplified fragments were separated on a 1% agarose gel at 75 V for 240 minutes, stained with Nancy-520, and visualised under UV light. M: DNA ladder (GeneRuler Express DNA Ladder, Thermo Scientific, UK) with sizes marked in base pairs (bp). Lanes 1–22: *P. multocida* isolates. Labelled bands: 1= PM13, 2=ATCC 43137 (L3), 3=PM52, 4=P1235, 5=P4679, 6=M1404 (B.2), 7=P3881, 8=X73 (L1), 9=PM2Y, 10=PM3Y, 11=PM4Y, 12=PM6Y, 13=PM12Y, 14=PM13Y, 15=PM16Y, 16=PM17Y, 17=PM19B, 18=PM22B, 19=PM24B, 20=PM25B, 21=PM26B, 22=PM27B.

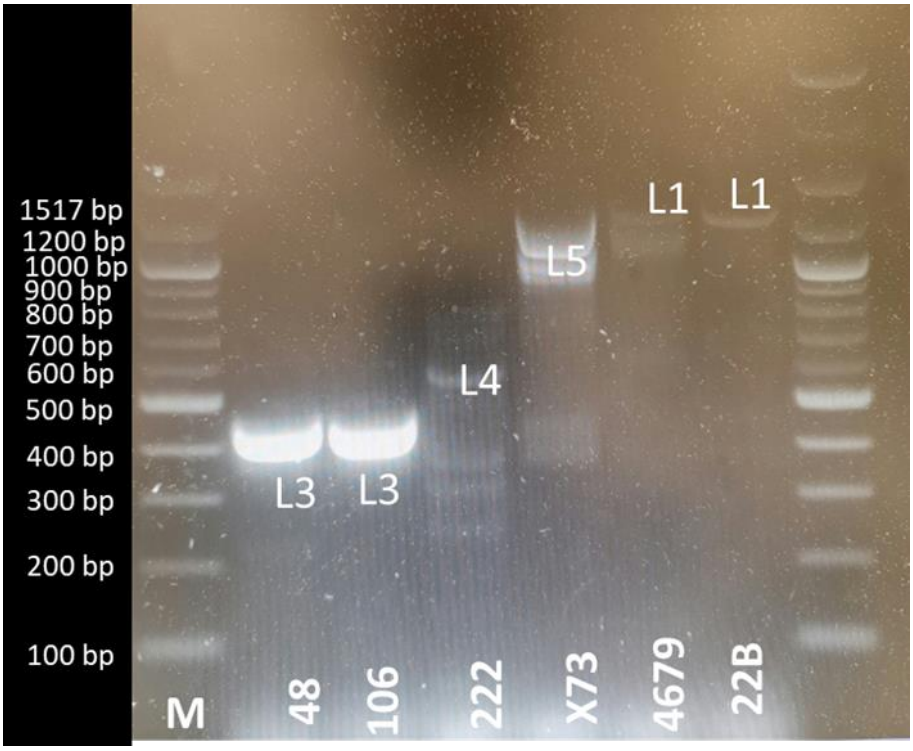

Figure 3.10. PCR Amplification of LPS Outer Core Biosynthesis Loci in *P. multocida* Isolates 2.
This figure shows agarose gel electrophoresis results of PCR products targeting LPS outer core biosynthesis loci in *P. multocida* isolates of PM48, PM106, PM222, X73, P4679 and PM22B. DNA fragments were amplified using primers specific to loci pcgD (L1~1107 bp), nctA (L2~810 bp), gatF (L3~474 bp), latB (L4~550 bp), rmlA (L5~1175), nctB (L6~668 bp), ppgB (L7931~) and natG (L8~255). Amplified fragments were separated on a 1% agarose gel at 75 V for 240 minutes, stained with Nancy-520, and visualised under UV light. M: DNA ladder (GeneRuler Express DNA Ladder, Thermo Scientific, UK) with sizes marked in base pairs (bp).

3.4.4. AMR Profiling of *P. multocida* Strains

To further characterise the panel of *P. multocida* isolates and understand their potential resistance to common antimicrobial agents, their susceptibility profiles were determined against seven relevant antibiotics using disc diffusion. This information provides context regarding the background resistance levels present in these strains. Detailed inhibition zone diameters for all isolates against each antibiotic are presented in Table 3.2.

Twenty-one *P. multocida* isolates were evaluated. For antibiotics tested using standard disc concentrations and interpreted with BSAC/EUCAST 2015 criteria for *P. multocida*, widespread resistance was observed. All isolates (100%, 21/21) were resistant to penicillin G (1

unit). High rates of resistance were also observed for nalidixic acid (30 µg), with 95%, 20/21 isolates found to be resistant.

Interpretation for streptomycin (5 µg) and spectinomycin (25 µg) using standard clinical breakpoints for *P. multocida* was challenging. Therefore, isolates exhibiting a complete absence of an inhibition zone (0 mm diameter) around these discs were operationally defined as resistant for this study. Based on this criterion, seven strains (33%, 7/21) were resistant to streptomycin, and two strains (9.5%, 2/21) were resistant to spectinomycin.

For ampicillin, cefotaxime, and tetracycline, disc potencies higher than those for which standard [BSAC/EUCAST] interpretive breakpoints for *P. multocida* are established were utilised due to laboratory availability (ampicillin: 25 µg disc used vs. 10 µg standard; cefotaxime: 30 µg disc used vs. 5 µg standard; tetracycline: 30 µg disc used vs. 10 µg standard; see Materials and Methods for full details). Consequently, interpretations for these agents were made with specific considerations. Resistance was tentatively inferred if an isolate's zone diameter, obtained with the higher potency disc, was less than or equal to the established resistant (R) breakpoint for the respective standard (lower) potency disc. Using this approach: all isolates (100%, 21/21) were considered resistant to cefotaxime. For ampicillin, 62% of strains (13/21) were tentatively classified as resistant. For the remaining 8 strains (38%), sensitive or intermediate status could not be determined due to the use of the non-standard disc potency, and their interpretation was therefore classified as 'Not Determined' for these categories. It must be emphasised that, for ampicillin, cefotaxime, and tetracycline, this method of inferring resistance is a deviation from standard interpretive practice. Furthermore, because higher potency discs were used, isolates

could not be reliably classified as 'sensitive' or 'intermediate' to these three agents using the established breakpoints for standard potency discs.

Overall, the antimicrobial susceptibility testing revealed significant levels of resistance or tentatively inferred resistance among the characterised *P. multocida* isolates. Resistance was particularly prevalent for beta-lactams (penicillin G and tentatively for cefotaxime and ampicillin) and tetracycline. These findings suggest notable multi-drug resistance profiles within this collection of strains.

Table 3.2. Disk Diffusion Diameter and Resistance Profiles of *Pasteurella* Strains Used In This Study.

	Disk diffusion Diameter (mm)*						
Strain/AB	**AMP (25 µg)**	**NA (30 µg)**	**SH (25µg)**	**S (5µg)**	**TE (30 µg)**	**CTX (30 µg)**	**P 1 unit**
PM13	25	23	11	0	25	27	0
ATCC 43137	25	22	9.11	0	26	25.9	11
PM52	23.9	24	12.5	11.3	27.1	32	0
X73 (A)	23.5	21.8	10.2	14.6	24.77	30.3	12.4
M1404 (B)	31.7	22	10.5	10.1	25	25.2	0
P3881 (D)	34.4	24.7	11.6	10	27.1	25.5	10
P1235 (E)	25	22	11.7	16	25.5	21.1	0
P4679 (F)	23.2	25.6	13.1	14.3	22.9	19.5	0
PM2Y	29.2	29	12.8	0	22.8	26.7	0
PM3Y	33.8	23.2	11.3	9.9	26.3	24.5	0
PM4Y	26.7	21.25	11.5	12.7	24.5	27.3	0
PM6Y	27.55	26.5	9.6	0	26.8	26.6	0
PM12Y	26.7	23.9	12.7	14.3	26.9	21.2	12.8
PM13Y	27.7	0	10	0	28.6	28	0
PM16Y	31	28	12	8	22.6	25.7	0
PM17Y	30.4	24.5	12.7	0	29.2	24.5	0
PM22B	28.2	0	11	12	26.5	27.7	11
PM24B	33	24.5	0	0	27.2	28.6	0
PM25B	23.6	17.6	0	16.44	27.8	28.4	0
PM26B	33.3	22	9.5	16.5	25.9	29.1	0
PM27B	27.8	24.5	0	0	28.4	29	0

Note. Zone diameters were interpreted according to BSAC/EUCAST criteria (see Table 2.7). Colour coding indicates resistance classification: Red = resistant; Blue = sensitive. Black values indicate cases where no definitive classification could be assigned, either because the BSAC guidelines do not define intermediate/sensitive breakpoints for that antibiotic (e.g. spectinomycin, streptomycin), or because non-standard disk concentrations

were used, preventing reliable differentiation between intermediate and sensitive categories. AMP, ampicillin; NA, nalidixic acid; SH, spectinomycin; S, streptomycin; TE, tetracycline; CTX, cefotaxime; PG, penicillin G.

3.4.5. Growth Curves of Selected *P. multocida* Strains

To facilitate reproducible phage experiments requiring specific bacterial concentrations (e.g., for determining Multiplicity of Infection (MOI) or standardising inoculum), the growth kinetics of the primary host strains, *P. multocida* PM13 and ATCC 43137, were characterised. The objective was to determine their growth rates under standard laboratory conditions and establish the correlation between optical density (OD_{600}) measurements and viable cell counts (CFU/mL).

A calibration curve was established to relate OD_{600} measurements to viable bacterial counts (CFU/mL). A linear correlation between OD_{600} and CFU was observed during the exponential growth phase. However, the relationship is not linear across the entire growth curve: at very low OD values (lag phase) and at high OD values (stationary phase), CFU counts no longer scale proportionally with OD. Therefore, CFU conversions from OD measurements in this study were restricted to the exponential growth range ($OD_{600} \approx 0.1–0.8$)

Strains PM13 and ATCC 43137 were chosen for comprehensive growth analysis based on their established susceptibility to the isolated phages and their reliable growth characteristics. Growth curves plotting OD_{600} over time, together with associated viable cell counts (CFU/mL), were produced for both strains (Figures 3.11 and 3.12). Analysis of these curves revealed distinct growth rates; strain PM13 grew faster, reaching the mid-exponential phase (defined here as approximately $OD_{600} = 0.5$) in about 150 min, whereas strain ATCC 43137 required approximately 240 minutes to reach a similar density. Crucially, the correlation between optical density and cell concentration was established; for strain PM13, an OD_{600} of 0.5 corresponded to approximately

10^9 CFU/mL (Figure 3.11, Graph B). A similar correlation was established for ATCC 43137 (Figure 3.12, Graph B).

The growth kinetics of the key host strains PM13 and ATCC 43137 were characterised, establishing the relationship between OD_{600} and CFU/mL. The data enable accurate estimation of bacterial cell concentrations from spectrophotometer readings in future experiments and demonstrate ~~the significantly~~ faster growth rate of PM13 relative to ATCC 43137 under the tested conditions.

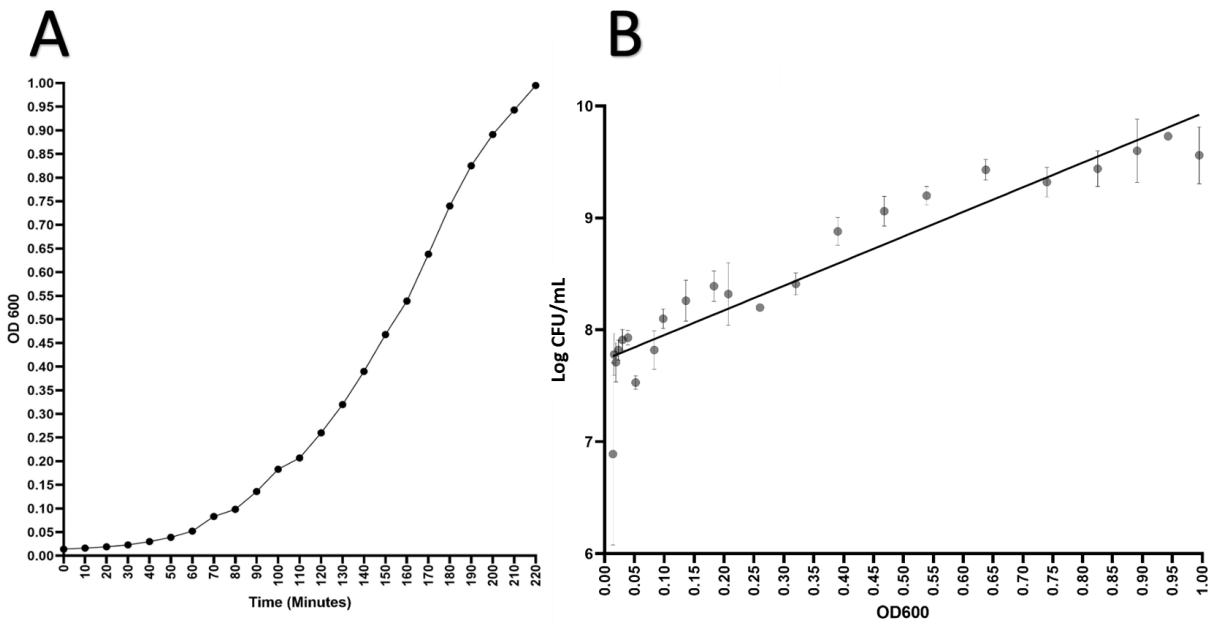

Figure 3.11. Growth Characteristics of *P. multocida* PM13 Strain in TSB Media at 37°C.
Graph A illustrates the growth curve of the *P. multocida* PM13 strain, derived from OD_{600} measurements taken at 10-min intervals during incubation in TSB media at 37°C. The growth curve illustrates the progression of the bacterial culture through the lag, exponential, and stationary growth phases.
Graph B illustrates the correlation between OD_{600} and bacterial counts (CFU/mL) for the PM13 strain at corresponding time points. Each data point signifies the mean of three replicates, while the error bars represent the standard deviation. The linear relationship indicates that OD_{600} serves as a reliable proxy for estimating bacterial concentration throughout growth.

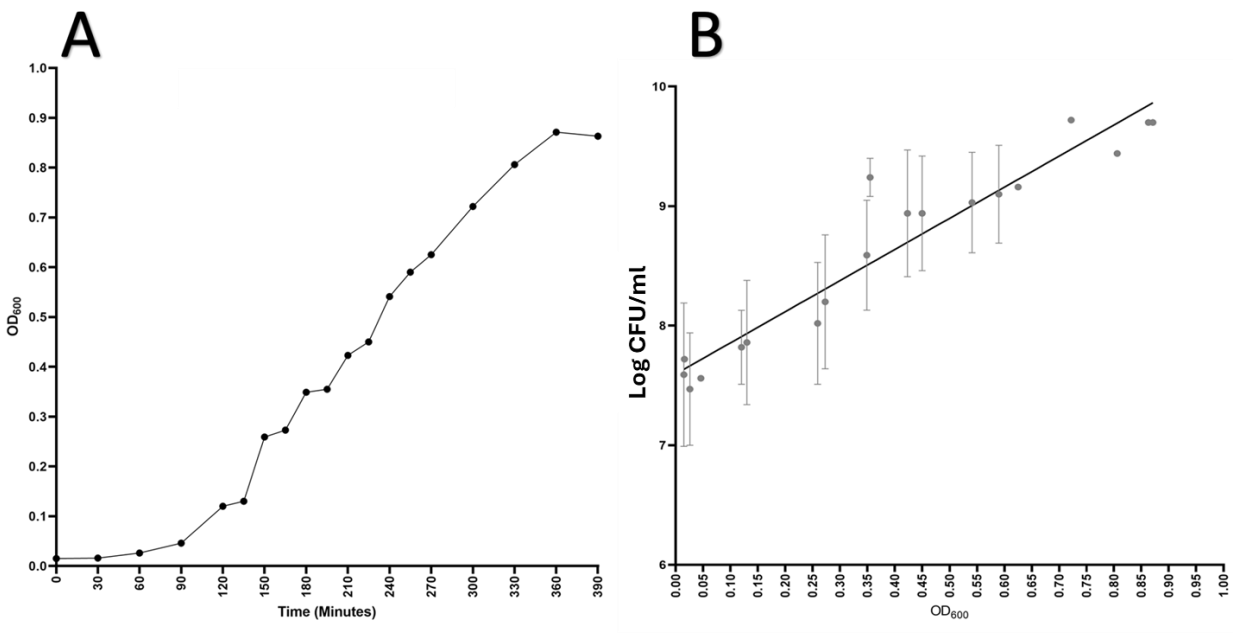

Figure 3.12. Growth Characteristics of *P. multocida* ATCC 43137 Strain in TSB Media at 37°C.
Graph A illustrates the growth curve of the *P. multocida* ATCC 43137 strain, derived from OD_{600} measurements recorded at 30-min intervals during incubation in TSB media at 37°C. The curve illustrates the progression of bacterial culture through the lag, exponential, and stationary growth phases.
Graph B illustrates the correlation between OD_{600} and total bacterial counts (log CFU/mL) for the ATCC 43137 strain. Each data point signifies the mean of three replicates, with error bars representing the standard deviation. A linear correlation is observed, confirming the validity of OD_{600} as a reliable measure for estimating bacterial concentration during growth.

3.4.6. Discussion

Challenges in Isolating *P. multocida* from Environmental Samples

This chapter initially aimed to isolate *P. multocida* for subsequent use in phage studies. However, this study encountered limitations in sample collection due to COVID-19 restrictions, which prevented access to farms, slaughterhouses, and sewage systems. To overcome these constraints, and in contrast to earlier studies on *P. multocida* that primarily obtained isolates from healthy or diseased animals and carcasses, we focused on environmental sources, particularly open water bodies adjacent to sewage plant outflows and areas frequently visited by wildfowl (Rigobelo et al., 2013; Tang et al., 2009; El Sayed et al., 2018; Eissa, 2019; Ugochukwu, 2009; Orynbayev et al., 2019). For the isolation of *P. multocida* and their phages, a range of accessible environmental samples were collected from across Nottinghamshire. These included water samples from lakes, rivers, ponds, and marinas, in addition to sewage from wastewater treatment centres, cattle faeces, and slurry from a dairy farm tank. These sites were selected due to their higher likelihood of contamination with *P. multocida*.

From 91 presumptive *Pasteurella* colonies isolated, 38 were able to grow on Pasteurella selective media but not on MacConkey agar, and all tested oxidase-negative and catalase-positive. Despite these characteristics, none of the isolates were confirmed as *P. multocida* following PCR analysis. Based on the current taxonomy of the Pasteurellaceae family provided by PubMLST, the most probable alternatives include members such as *Mannheimia haemolytica*, *Bibersteinia trehalosi*, *Gallibacterium anatis*, *Avibacterium* spp., *Actinobacillus* spp., and *Histophilus somni*, as well as non-*multocida Pasteurella* spp. (PubMLST, 2025). These outcomes align with the fastidious growth requirements of *P. multocida* and likely competition in the

sampled environments, which can favour hardier Pasteurellaceae taxa under nutrient-limited aquatic conditions.

Environmental Conditions Affecting Isolation

The ability to thrive of organisms in aquatic environments is reliant upon various factors, including temperature, pH, and the concentration of sodium chloride (NaCl), among others. *P. multocida* necessitates blood or specific serum types, as these provide essential proteins and growth factors that facilitate its growth. In environments lacking in these essential nutrients, the growth of *P. multocida* would be significantly diminished relative to other bacterial species competing for the available resources.

A study evaluating the impact of six environmental variables on *P. multocida* populations in water—namely, protein concentration, temperature, pH, and the presence of sodium chloride, clay, and sucrose—identified temperature as the predominant factor affecting the growth of *P. multocida* (Bredy and Botzler, 1989). *P. multocida* bacterial counts in water maintained at 18°C were significantly higher compared to counts in water maintained at 2°C over 14 days (Bredy and Botzler, 1989).

In our study, the source of water samples, local air temperature, and the date of sample collection ranged from 5 to 18 °C. However, the actual water temperature was not recorded, which represents a limitation of the work. Historical weather data for the United Kingdom indicate that the air temperature during the sampling period (March–May 2021) generally ranged from 6 to 11 °C, conditions described as very cold or cold for that season. While these values suggest that the sampled water bodies may have been at the lower end of the temperature spectrum, this cannot be confirmed without direct measurement. Previous research has

demonstrated that *P. multocida* survival in water is markedly reduced at lower temperatures (e.g., 2 °C) compared with higher temperatures (Bredy & Botzler, 1989). Therefore, although no definitive conclusion can be drawn, low water temperature remains a probable factor that may have influenced the difficulty of isolating *P. multocida* in this study

In habitats such as lakes, rivers or wetlands, where samples can be rapidly diluted, the chance of isolating fastidious bacteria is reduced, even when they are expected to be present, for example, during an outbreak. This is illustrated in a study on the presence of *P. multocida* in water and sediment from wetlands located at the Sacramento National Wildlife Refuge during an FC outbreak in local wildfowl (Lehr *et al.,* 2005). Their analysis of water and sediment samples from all wetlands proved negative for the recovery of *P. multocida*. This conclusion is in line with our findings regarding the inadequate isolation of *P. multocida* from water and environmental samples.

Alternative Isolation Approaches

Pre-screening environmental samples with *P. multocida*-specific PCR primers may enhance future isolation efforts prior to bacterial isolation attempts. The usage of selective media, such as Chromagar, facilitates the differentiation of *P. multocida*, *Histophilus somni*, and *Mannheimia haemolytica*, thereby enhancing isolation success. While these methods were not feasible in this study due to supply issues, they represent viable options for future research.

Construction Characterised Panel of *P. multocida*

In the absence of *P. multocida* isolates from this study's isolation efforts, a range of commercial and clinical strains were obtained for subsequent phage studies. These strains were characterised for potential phage-binding determinants (capsule type and LPS type) and their

relative replication characteristics. In addition, their toxin and AMR profiles were determined, as they would be useful for planned *Galleria* infection studies (described in Chapter 5).

Phage susceptibility is related to receptors on host strains, such as capsule or LPS, that facilitate attachment (Dowah and Clokie, 2018). The presence of a capsule has the potential to prevent phage adsorption by masking receptors located in the cell wall (Labrie *et al.*, 2010). Some bacteriophages commonly possess enzymes called depolymerases as integral components of their virion structure (Knecht *et al.,* 2020). Upon binding to the capsular polysaccharides of the host bacteria, the polysaccharide-repeating units are effectively cleaved. As the capsule is an important virulence factor, its thickness and structure (type) influence the virulence of the strain and are directly related to lethality (LD_{50}). LD_{50} is also a key factor in experiments investigating phage therapy in animal models; therefore, investigating the capsule type and thickness of the *P. multocida* isolates is important. Part of this project is to assess whether *G. mellonella* can be used as an infection model for phage therapy studies. It is known that *P. multocida* strains with certain capsule types are responsible for specific diseases and are more common in particular animal species (Harper *et al.,* 2006). Thus, understanding the capsule characteristics influencing phage susceptibility in these isolates may be important for understanding their infection properties in this model organism. Furthermore, if the *P. multocida* strains are able to synthesise PMT (Wilson and Ho, 2012), these capsule characteristics may also influence their virulence. Phage therapy has the potential to release toxins, which may affect treatment outcomes (Drulis-Kawa *et al.,* 2012). Any correlation between the phage susceptibility of the strains and their capsule types, capsule thickness and LPS types is important.

Differences in Capsule Size Between *P. multocida* Strains and Their Biological Significance

Microscopic analysis of the strains following India ink staining demonstrated that all *P. multocida* strains exhibited capsules, with noticeable variations in capsule thickness identified among the strains. ANOVA statistical analysis demonstrated that the differences in capsule size among strains within identical growth conditions (solid or liquid media) were statistically significant ($p < 0.05$). No significant differences in capsule size were observed between strains cultivated in solid and liquid media, as demonstrated by paired *t*-tests and Wilcoxon signed-rank tests ($p > 0.05$). The capsule size of *P. multocida* appears to be predominantly determined by the strain's genetic or phenotypic traits, rather than the culture medium used.

The size of the capsule significantly influences the virulence, immune evasion, and adaptability of bacteria to environmental stresses. These findings offer important insights into the biology of *P. multocida*. The variation in capsule size among different strains underscores the necessity of accounting for individual strain characteristics in the study of bacterial pathogenicity and the development of phage therapy strategies.

Capsular and LPS Typing of *P. multocida* Isolates

Capsular typing identified isolates of serogroups B, D, and F; however, the reference strain X73 (capsular type A) did not amplify under the PCR conditions used. This suggests a possible problem with the type A primer set and therefore results regarding the absence of type A among the study isolates must be interpreted with caution. While the detection of other capsular types provides confidence in the overall assay performance, the inability to confirm type A represents a limitation of the study. Future work will require optimisation or alternative approaches to validate the presence or absence of type A isolates.

Capsular typing is essential for understanding the pathogenicity and disease relationships of *P. multocida*. Serotypes A and F are frequently associated with FC, whereas serotypes B and E are related to HS in cattle. Serotype D strains that express PMT toxin are linked to AR in swine (Harper *et al*., 2006). While comprehensive clinical data regarding the sampled animals was lacking, it was observed that 15 of the isolates were derived from swine. Nine of these were untypable for capsule, whereas two were classified as capsular type D. These type D isolates were collected from nasal swabs, aligning with their established role in AR. The toxin positivity of these type D strains is consistent with existing literature, underscoring the importance of capsular typing in associating strains with particular disease symptoms.

PCR tests were employed to identify LPS genotypes in addition to capsule typing among the isolates. Seven strains were classified as L3, five as L4, three as L6, two each as L1 and L2, and one as L5. Four isolates could not be typed. Our collection included six of the eight identified LPS genotypes, with L7 and L8 being the only absent genotypes.

Antibiotic Susceptibility and Experimental Applications

Antibiotic resistance profiles were characterised for all strains. While AMR profiling may not directly relate to phage therapy, it is essential for designing selective media to isolate *P. multocida* in mixed bacterial populations during *in vivo* experiments. The resistance observed in commonly used antibiotics, including ampicillin, nalidixic acid, and tetracycline, underscores the necessity for customised strategies in selective bacterial enumeration.

Insights on Growth Curves

Growth curves for PM13 and ATCC 43137 were constructed to determine the correlation between OD_{600} and bacterial counts, consequently identifying the mid-exponential phase. This

information is essential for establishing the optimal timing of phage adsorption in isolation and experimental studies. The growth dynamics facilitate reproducibility and enhance the efficiency of phage-host interactions.

This study encountered considerable challenges in isolating *P. multocida* from environmental samples, attributed to the bacterium's fastidious nature, environmental conditions, and dilution effects in water sources. The findings corroborate earlier research indicating the challenges associated with isolating *P. multocida* from non-clinical samples. To address these challenges, it is advisable to employ alternative methods, including pre-screening with *P. multocida*-specific primers and utilising advanced selective media in future studies.

Capsular and LPS typing demonstrated a diverse array of types among the isolates, underscoring their potential implications for virulence and phage susceptibility. The identified strain-specific differences in capsule thickness and type highlight the significance of these traits in bacterial pathogenicity and their implications for phage therapy research. Although AMR profiling does not directly impact phage therapy, it offers important insights for the development of selective media and the differentiation of *P. multocida* in in vivo studies. The growth dynamics of PM13 and ATCC 43137 revealed the correlation between OD_{600} and bacterial counts, thereby establishing optimal conditions for phage isolation and experimental investigations. These findings establish a solid basis for the subsequent characterisation of *P. multocida* and their susceptibility to phage therapy, as discussed in the following chapters.

Together, these findings provide a strong foundation for the subsequent characterisation of *P. multocida* and their susceptibility to phage therapy, as explored in the following chapters.

Chapter 4. *Isolation, Host Range and Physicochemical Characterisation of P. multocida Phages*

Antibiotic resistance is increasingly widespread and perceived as a significant problem these days. Interest in alternative therapeutic approaches is increasing. Phage therapy is also included in these alternative approaches. *P. multocida* is one of the bacteria that has an increase in antibiotic resistance, so phage therapy to be developed against it is also important. In order to develop an effective phage therapy, it is essential to characterise the potential phages in detail. The characterisation steps that need to be performed after a successful phage isolation can be listed as determining the lytic properties of the phages, the morphological properties of their plaques and virions, host range, resistance to environmental factors and growth parameters.

In the literature, most of the *P. multocida* specific phages have been reported to be isolated from sewage. However, since access to new sewage samples was impossible due to Covid-19 restrictions, it was hypothesised that along with the previously collected sewage samples, wastewater from the nearest sewage facilities and environmental water samples that had contact with the faeces of animals where the target host could be colonised would be suitable for isolation.

Apart from the genomic characterisation that will be discussed in the next section, it is hypothesised that a detailed biological characterisation of phages can be performed by the methods listed below. For example, TEM imaging for morphological characterisation, host range experiments to determine the bacterial strain and species infected by phages, efficiency of

plating experiments to determine their lytic properties, variable pH, temperature and chloroform sensitivity experiments to partially measure their resistance to environmental factors, and one-step growth experiments to determine their growth parameters. It was also hypothesised that isolated phages would have different biological properties and that these properties could be determining factors in the selection for phage therapy.

4.1. Aims of Chapter

This chapter describes the procedures for isolating and biologically characterising *P. multocida* phages. Following isolation, the characterisation aimed to achieve the following objectives.

6. **Isolate Bacteriophages Specific to *P. multocida***:

Screen environmental samples from various sources, such as water, sewage and faeces, for the presence of bacteriophages that infect *P. multocida* strains. Establish a panel of phages targeting *P. multocida* for further study.

7. **Characterise the Isolated Bacteriophages**:

Assess the plaque morphology of the phages to understand their lytic activity. Examine the virion morphology of the phages using transmission electron microscopy and classify them taxonomically.

8. **Evaluate Host Range and Efficiency of Plating**:

Determine the host range of the isolated phages against a diverse panel of *P. multocida* strains. Measure the efficiency of plating (EOP) of the phages on susceptible strains to evaluate their infectivity and suitability for therapeutic applications.

9. **Assess the Stability of the Phages**:

Investigate the pH sensitivity, thermal stability and chloroform sensitivity of the phages to evaluate their robustness under different environmental conditions.

10. Determine the Growth Dynamics of Phages:

Generate one-step growth curves to determine latent periods, rise periods and burst sizes for each phage. Use these growth characteristics to identify phages with optimal replication and lytic activity for potential therapeutic applications.

11. Identify Promising Phages for Further Study:

Select bacteriophages with favourable host range, stability and growth dynamics for further investigation in later chapters, including efficacy studies in the *Galleria mellonella* infection model.

4.2. Isolation of Phage Specific to *P. multocida*

To develop effective phage-based strategies against *P. multocida*, a diverse collection of phages is desirable. This diversity is important both for understanding fundamental phage-host interactions, such as differences in virulence or host range determinants, and for practical applications like constructing phage cocktails. Cocktails containing multiple phages with different characteristics can potentially overcome the narrow host range often exhibited by individual phages and limit the emergence of phage-resistant bacteria, thus covering a wider spectrum of circulating *P. multocida* strains. Therefore, the objective of this work was to isolate and establish a panel of novel bacteriophages targeting *P. multocida* by screening various environmental samples, particularly those considered likely reservoirs for the host bacterium (such as sewage and faeces), using selected laboratory strains (*P. multocida* PM13 and ATCC 43137) as hosts in enrichment cultures.

In total, 15 phages were identified and isolated from mixed sewage. Phages —P1, P2, P3, P4, P5, P7 and P8—were isolated in one batch on the *Pasteurella* strain PM13; five phages—S1, S2, S3, S4 and S5—in a second batch also on the *Pasteurella* strain PM13 as the isolation; and three phages—N1, N2 and N4—on the *Pasteurella* strain ATCC 43137 as the isolation host.

This panel of 15 sewage-derived phages provided the foundation for subsequent biological and genomic characterisation aimed at understanding their diversity and therapeutic potential.

4.3. Plaque Morphology

To begin the phenotypic characterisation of the 15 newly isolated bacteriophages, their plaque morphology was examined on lawns of their respective isolation hosts (*P. multocida* PM13 or ATCC 43137). This analysis aimed to assess characteristics such as plaque clarity and size, providing initial insights into the phage's lytic activity and potential heterogeneity.

Upon plating on their host strains, all 15 phage isolates consistently generated clear plaques, indicative of efficient host cell lysis (Figure 4.1). While visual inspection suggested some variation in plaque diameters, quantitative measurement revealed no noticable difference in the *mean* plaque diameter between the different phage isolates. However, a notable observation was the variation in plaque size *within* each individual phage population; diameters typically ranged from 0.5 mm to 1.5 mm. This size heterogeneity persisted even after repeated rounds of single-plaque purification attempts; subsequent plating of phages derived from either small or large plaques consistently resulted in a similar range of plaque diameters.

The consistent formation of clear plaques by all 15 isolates suggests they possess lytic capabilities against their host strains under the tested conditions. The observed intra-isolate

variation in plaque size, which could not be resolved through standard purification, may reflect minor population heterogeneity or dynamic interactions between the phages and host lawn development affecting plaque expansion.

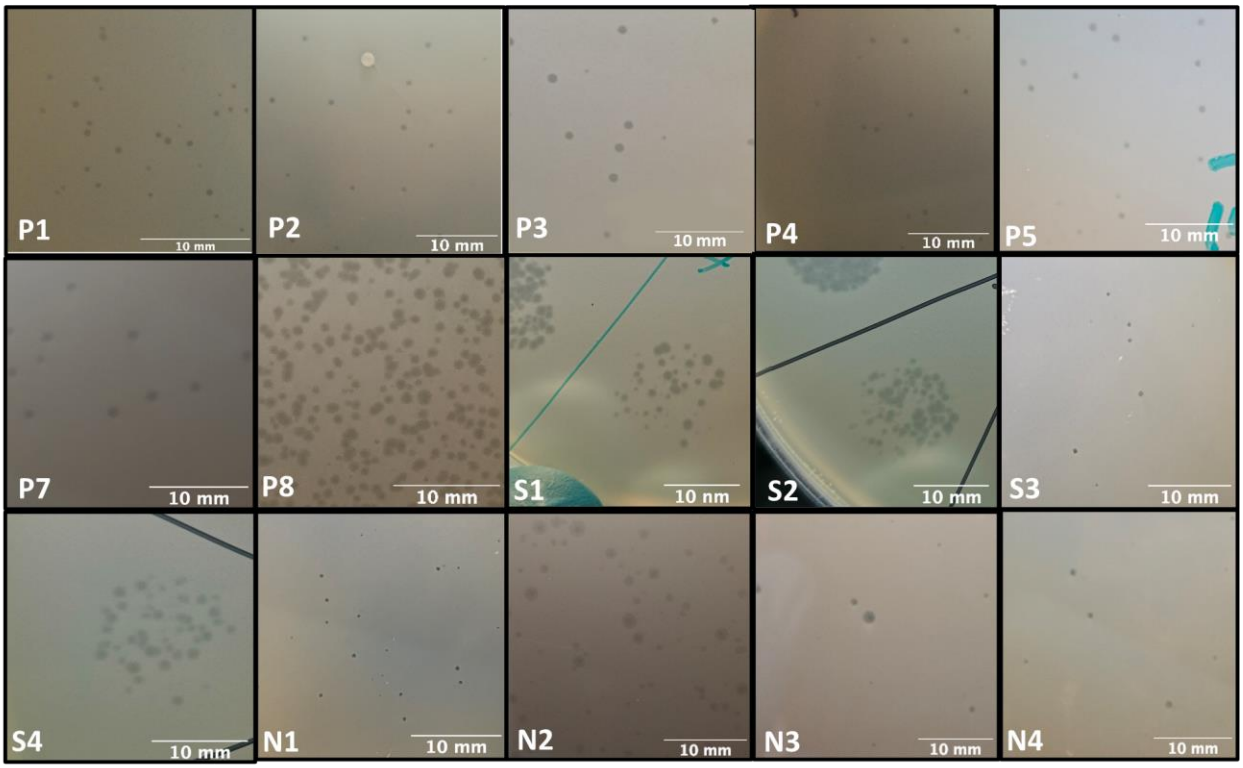

Figure 4.1. Plaque morphology of isolated bacteriophages infecting *P. multocida*.
Representative images of plaques formed by phages P1–P5, P7–P8, S1–S4, and N1–N4 on bacterial lawns. All phages produced clear plaques with diameters ranging from 0.5 mm to 1.5 mm. Photographs were captured under identical lighting and imaging conditions using a black background to ensure visual consistency. Measurements were standardized using ImageJ software (version IJ 1.46r) with a plate diameter of 100 mm as the reference scale. Despite repeated plaque purification, intra-isolate variability in plaque size remained, indicating heterogeneity within each phage population.

4.4. Virion Morphology

To determine the physical structure and taxonomic classification of the isolated bacteriophages, representative isolates were visualised using transmission electron microscopy (TEM). This analysis aimed to characterise the basic morphology (head shape, tail type) and

measure key dimensions (head diameter, tail length) to identify the viral family and assess morphological similarities or differences among the isolates.

The electron micrographs illustrate the precise structure of *P. multocida* phages, which are classified within the *Siphoviridae*-like morphotype due to their possession of an icosahedral capsid connected to a non-contractile tail. Measurements of the tail and head dimensions were taken for five *P. multocida* phages (N1, N3, N4, P1 and P8). The mean tail length of these phages ranged from 167.8 nm (N3) to 188.0 nm (N1), while the mean head size ranged from 52.8 nm (N3) to 60.4 nm (P8) (Table 4.1, Figure 4.1). Statistical analysis showed significant differences in both tail length (ANOVA: $F = 3.26$, $p = 0.0326$) and head size (ANOVA: $F = 6.72$, $p = 0.0013$) among the phages. Tukey's HSD post-hoc test revealed that the tail length of phage N3 was significantly shorter than that of phages N1 ($p < 0.05$) and P8 ($p < 0.05$). No statistically significant differences were observed among N1, N4, P1 and P8. Regarding head size, N3 exhibited significantly smaller heads than phages P1 ($p < 0.01$) and P8 ($p < 0.01$), while no significant differences were observed among N1, N4, P1 and P8.

TEM analysis confirmed that the isolated *P. multocida* phages belong to the *Siphoviridae*-like morphotype viruses, possessing typical icosahedral heads and long, non-contractile tails. While morphologically similar overall, quantitative analysis revealed statistically significant differences in virion dimensions, with phage N3 being smaller than some other isolates in the subset examined.

Table 4.1. Morphological Measurements of *P. multocida* Phage Virions Visualised by Transmission Electron Microscopy

Phage	***Tail length (nm, mean ± SEM)***	***Head size (nm, mean ± SEM)***	***n***
N1	*188 ± 1.5*	*57 ± 0.5*	*6*
N3	*167 ± 2*	*53 ± 1*	*6*
N4	*184 ± 3*	*59 ± 1*	*5*
P1	*183 ± 2.5*	*59 ± 1*	*5*
P8	*185 ± 2.5*	*60 ± 1*	*5*

Note. Tail and head dimensions were measured from individual phage particles (n = 5–6 per phage). Values are presented as mean ± SEM. Measurements were obtained from TEM images using ImageJ software. Tukey's HSD test indicated that N3 differed significantly in both tail and head dimensions compared with the other phages ($p < 0.05$), while no significant differences were observed among N1, N4, P1, and P8 in tail length. Significant head size differences were detected between N3 and P1/P8 ($p < 0.05$).

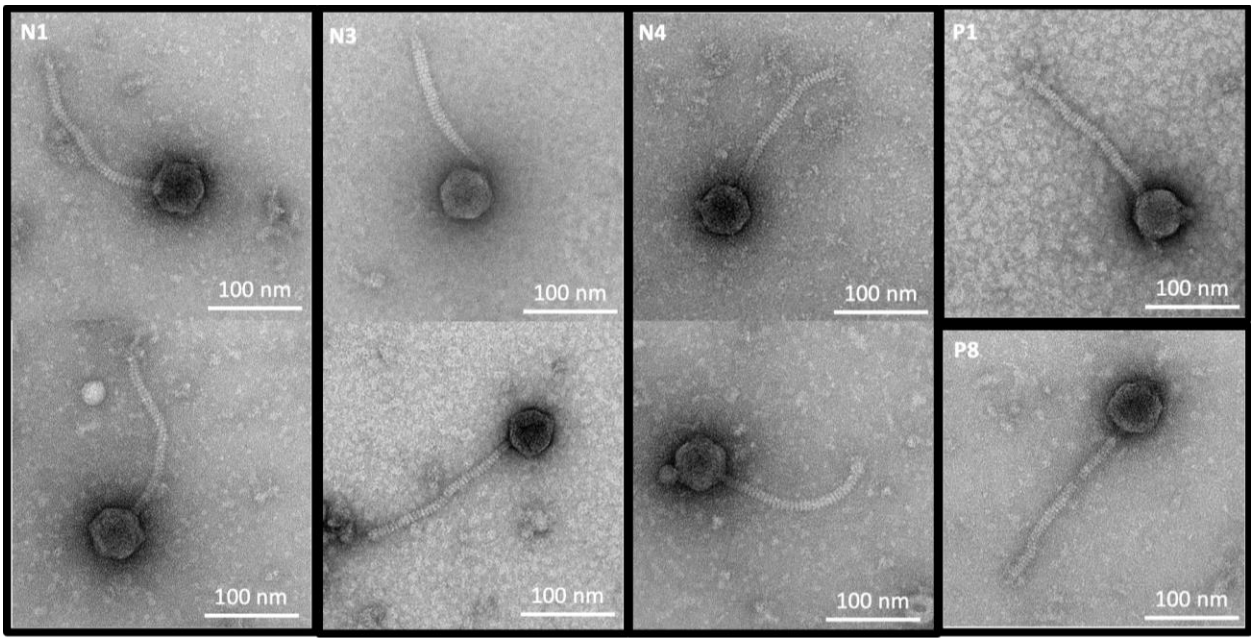

Figure 4.2. Transmission electron micrographs of *P. multocida* bacteriophages N1, N3, N4, P1, and P8.

Representative TEM images show the morphology of five phages infecting *P. multocida*, classified under the *Siphoviridae*-like morphotype viruses. Each phage displays an icosahedral capsid attached to a long, non-contractile tail. Samples were negatively stained with 1% uranyl acetate and visualized using a JEOL JEM-1400 TEM at 120 kV. Digital images were captured using an EMSIS Xarosa camera with Radius software. Tail and head dimensions were measured using ImageJ software. Mean tail lengths ranged from 167.8 nm (N3) to 188.0 nm (N1), while mean head diameters ranged from 52.8 nm (N3) to 60.4 nm (P8), as detailed in Table 4.1. Statistical analysis (one-way ANOVA with Tukey's HSD post-hoc test) revealed significant differences in both tail length ($p = 0.0326$) and head size ($p = 0.0013$), with N3 having significantly shorter tails and smaller heads compared to P1 and P8 ($p < 0.05$ and $p < 0.01$, respectively). The scale bar in each image represents 100 nm.

4.5. Host Range Profiling

The host range of a bacteriophage is determined by the bacterial genera, species and strains that it can successfully lyse. This characteristic is crucial in phage classification and has implications for phage therapy and bacterial resistance studies.

To assess host range, 15 phage isolates were tested against 29 *P. multocida* strains. The results were evaluated qualitatively based on plaque formation intensity, using the following scale: ++++ = Complete lysis; +++ = Semi-confluent lysis; ++ = Numerous plaques (too many to count); + = Few individual plaques; - = No plaques. A summary of phage lysis efficiency across

bacterial strains is presented in Table 4.2. Across all tested phages, the percentage of susceptible *P. multocida* isolates ranged from 24.1% to 27.5%. P and S phages exhibited the broadest host range, successfully lysing 8 of 29 isolates (27.5%). The N phage group infected 7 of 29 strains (24.1%), differing from P and S phages by failing to lyse PM13. Certain bacterial strains were highly susceptible, while others exhibited complete resistance to all tested phages. These findings confirm that P and S phages have identical lytic profiles, whereas N phages show a slightly narrower spectrum.

PM12Y, PM26B and PM18B exhibited the highest susceptibility, with lysis observed in multiple phages. In contrast, PM48, PM106 and PM222 were completely resistant, showing no plaque formation in any tested phages. The Host Susceptibility Index further supports these findings, highlighting bacteria most susceptible to phage attack. To determine whether phages differed significantly in lysis efficiency, a one-way ANOVA was conducted across all phage-host interactions ($F = 0.01$, $p = 0.9999$). The result indicates no statistically significant difference in lysis efficiency between the phage groups ($p > 0.05$). Despite some variations in host range, the lack of statistical significance suggests a largely uniform lytic pattern among the tested phages. This implies that no single phage was significantly more effective than others within the tested group. To assess host range similarities, a hierarchical clustering analysis was performed (Figure 4.4). P and S phages formed a single cluster, reinforcing their identical host range. N1, N2 and N4 phages clustered separately, confirming their slightly different lytic spectrum. This clustering suggests that certain phages may be functionally redundant, an important consideration for phage cocktail design**.**

Host range profiling demonstrated that the isolated phages possess narrow lytic spectra against the tested *P. multocida* panel. The P and S phage groups shared identical host ranges, while the N group exhibited a slightly narrower range, differing primarily in their activity against strain PM13. While specific bacterial strains showed high susceptibility or complete resistance, there was no statistically significant difference in the overall lysis efficiency among the phage groups tested despite minor spectrum variations.

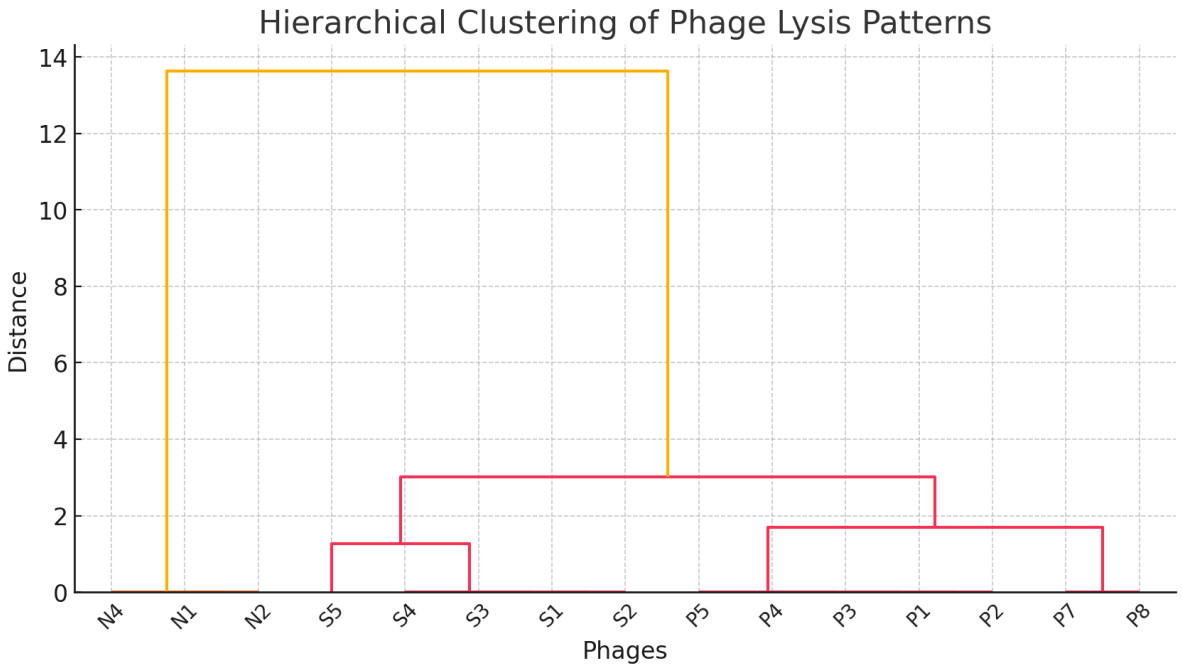

Figure 4.3. Hierarchical Clustering of Phage Lysis Profiles.
Dendrogram illustrating hierarchical clustering of phages based on host range similarity. The clustering was performed using Ward's method, grouping phages with similar lytic profiles across *P. multocida* strains. Closely clustered phages (e.g., P and S groups) share nearly identical host ranges, indicating functional redundancy. N1, N2 and N4 form a distinct cluster, suggesting a narrower or slightly different lytic spectrum. The distance between clusters represents the degree of similarity, with greater separation indicating more distinct host range profiles.

Correlation analysis of the phage lysis profiles revealed that P1–P8 and S1–S5 were highly correlated ($r > 0.98$), indicating strong similarities in host range. N1, N2, and N4 showed slightly lower correlation values ($r \approx 0.98–0.99$) compared to the other phages, consistent with their

reduced lytic profiles. Overall, the analysis confirmed a high degree of redundancy among most phages, with only a subset (N1, N2, N4) displaying more distinct host range characteristics.

4.6. Efficiency of Plating

Following the initial host range screening, Efficiency of Plating (EOP) assays were conducted to quantitatively assess the relative replication success of each phage on the different susceptible *P. multocida* strains. This study aimed to provide a more precise measure of virulence than qualitative lysis observations and to identify the most productive host strains for phage propagation and further experiments.

Phage titres achieved on each susceptible host (Table 4.3) were used to calculate the relative EOP (Table 4.4), indicating how efficiently each phage replicated on a given test strain compared to its optimal (reference) host. This quantitative analysis confirmed strains PM13 and PM12Y as highly productive hosts, where several phages plated with maximum efficiency (EOP ≈ 1); PM13 was the optimal host for P1, P3, P8 and S5, while PM12Y was optimal for P2, S1, S3, S4, N1 and N2. The variation in efficiency across different hosts was evident; for example, phage P1 plated with high relative efficiency on PM13 (EOP=1) and PM19B (EOP=0.65), moderate relative efficiency on PM18B (EOP=0.11) and PM12Y (EOP=0.059), but showed very low plating efficiency on strains PM26B (EOP=0.002) and ATCC 43137 (EOP ≈ 3.2×10^{-6}). Most other P- and S-series phages exhibited similar patterns of relative efficiency across the host panel. Phages S3 and S4 plated with moderate efficiency on strains PM18B and PM19B (EOP values 0.022–0.095). Significantly, strain PM52, despite showing some clearing in spot tests (Section 4.5), consistently exhibited an EOP of zero for all phages, confirming a lack of productive replication under these quantitative assay conditions.

An analysis exploring potential correlations between host characteristics and phage EOP suggested an inverse relationship between capsule thickness and plating efficiency; strains possessing thicker capsules generally exhibited lower EOP values (Figure 4.6). However, this correlation was not absolute, as exemplified by strain PM52, which, despite having a moderate capsule size (≈500 nm), yielded an EOP of zero. Furthermore, clustering analysis considering capsule size, LPS profiles and susceptibility suggested highly susceptible strains (high EOP; e.g., PM13, PM12Y, PM19B) were often associated with L3 or L4 LPS types and possessed moderate capsule thickness (≈400–700 nm), whereas highly resistant strains tended to have different LPS types (L5, L6 or untypable) and sometimes thicker capsules (>700 nm).

Hierarchical clustering analysis of capsular size, LPS profiles and phage susceptibility revealed three major groups. Highly susceptible strains (PM13, PM12Y, PM19B) were primarily associated with L3 and L4 LPS types and moderate capsule thickness (~400-700 nm). Moderately susceptible strains (PM18B, PM26B, ATCC 43137) exhibited more diverse capsular and LPS profiles, with greater variability in capsule size. Highly resistant strains (PM52, PM222, PM24B) were associated with LPS types L5, L6 and untypable capsular variants, with capsule sizes exceeding 700 nm in some cases.

Table 4.2. Susceptibility profiles of phage against field isolates (host range profile).

Phages ➔ Bacterial Strains ↓	P1	P2	P3	P4	P5	P7	P8	S1	S2	S3	S4	S5	N1	N2	N4	Host Susceptibility Index
PM13	++++	++++	++++	++++	++++	++++	++++	++++	++++	++++	++++	++++	-	-	-	48
ATCC 43137	++	++	++	++	++	++	++	++	++	++	++	++	++++	++++	++++	32
PM48	-	-	-	-	-	-	-	-	-	-	-	-	-	-	-	0
PM52	++	++	++	++	++	++	++	++	++	++	++	++	++	++	++	14
PM106	-	-	-	-	-	-	-	-	-	-	-	-	-	-	-	0
PM222	-	-	-	-	-	-	-	-	-	-	-	-	-	-	-	0
PM2Y	-	-	-	-	-	-	-	-	-	-	-	-	-	-	-	0
PM3Y	-	-	-	-	-	-	-	-	-	-	-	-	-	-	-	0
PM4Y	-	-	-	-	-	-	-	-	-	-	-	-	-	-	-	0
PM6Y	-	-	-	-	-	-	-	-	-	-	-	-	-	-	-	0
PM8Y	-	-	-	-	-	-	-	-	-	-	-	-	-	-	-	0
PM12Y	++++	++++	++++	++++	++++	++++	++++	++++	++++	++++	++++	++++	++++	++++	++++	60
PM13Y	-	-	-	-	-	-	-	-	-	-	-	-	-	-	-	0
PM16Y	-	-	-	-	-	-	-	-	-	-	-	-	-	-	-	0
PM17Y	-	-	-	-	-	-	-	-	-	-	-	-	-	-	-	0
PM18B	+++	+++	+++	+++	+++	+++	+++	++++	++++	++++	++++	++++	++++	++++	++++	53
PM19B	++++	++++	++++	++++	++++	+++	+++	+++	+++	+++	+++	+++	+++	+++	+++	50
PM22B	-	-	-	-	-	-	-	-	-	-	-	-	-	-	-	0
PM24B	-	-	-	-	-	-	-	-	-	-	-	-	-	-	-	0
PM25B	-	-	-	-	-	-	-	-	-	-	-	-	-	-	-	0
PM26B	++++	++++	++++	++++	++++	++++	++++	++++	++++	++++	++++	+++	+++	+++	+++	57
PM27B	-	-	-	-	-	-	-	-	-	-	-	-	-	-	-	0
PM28B	-	-	-	-	-	-	-	-	-	-	-	-	-	-	-	0
PM29B	-	-	-	-	-	-	-	-	-	-	-	-	-	-	-	0
	8/29	8/29	8/29	8/29	8/29	8/29	8/29	8/29	8/29	8/29	8/29	8/29	7/29	7/29	7/29	
	27.5%	27.5%	27.5%	27.5%	27.5%	27.5%	27.5%	27.5%	27.5%	27.5%	27.5%	27.5%	24.1%	24.1%	24.1%	

* The Host Susceptibility Index is a cumulative assessment of the qualitative scoring by the different phage on different host strains.
++++ for confluent lysis,
+++ semi-confluent lysis,
++ numerous plaques but too many to count,
+ a few individual plaques and
- if there were no plaques. In each experiment three biological and three technical replicates were performed.

Table 4.3. The titre of each phage obtained on each host strain.

	P1	P2	P3	P4	P5	P7	P8	S1	S2	S3	S4	S5	N1	N2	N4
PM13	**3.2×10^{10}**	3.3×10^{10}	**4.3×10^{10}**	2.1×10^{10}	8×10^{9}	**9×10^{9}**	**8×10^{9}**	7×10^{9}	**7×10^{9}**	4.1×10^{10}	2.1×10^{10}	**5.5×10^{10}**	0	0	0
ATCC 43137	1×10^{-5}	1×10^{-5}	1×10^{-5}	1×10^{-5}	1×10^{-5}	1×10^{-5}	1×10^{-5}	1×10^{-5}	1×10^{-5}	1×10^{-5}	1×10^{-5}	1×10^{-5}	1×10^{-5}	1×10^{-5}	1×10^{-5}
PM52	0	0	0	0	0	0	0	0	0	0	0	0	0	0	0
PM12Y.	$1.9\ 10^{10}$	**4.6×10^{10}**	1.2×10^{10}	1.4×10^{10}	5.8×10^{9}	5.6×10^{9}	5.6×10^{9}	**8.9×10^{9}**	3.8×10^{9}	**7.1×10^{10}**	**6.1×10^{10}**	2.3×10^{10}	**5.7×10^{9}**	**7.2×10^{9}**	2.4×10^{9}
PM18B.	3.6×10^{9}	1.1×10^{10}	4.8×10^{9}	6.7×10^{9}	5.1×10^{9}	7×10^{9}	1.5×10^{9}	4×10^{9}	2.2×10^{9}	3.3×10^{9}	1.4×10^{9}	7.7×10^{9}	1.4×10^{10}	2.73×10^{9}	**1×10^{10}**
PM19B.	2.1×10^{10}	1.2×10^{10}	1.1×10^{10}	**3.1×10^{10}**	**6×10^{9}**	1.2×10^{9}	3×10^{9}	3.1×10^{9}	4.2×10^{9}	3.9×10^{9}	4.3×10^{9}	7.7×10^{9}	1.5×10^{9}	1.8×10^{9}	1.2×10^{9}
PM26B.	9×10^{-7}	1.4×10^{-7}	1×10^{-7}	6 E+9	1×10^{-7}	1×10^{-7}	1×10^{-7}	1×10^{9}	1×10^{7}	4.2×10^{-7}	1×10^{-7}	1×10^{-7}	1×10^{-7}	1×10^{-7}	1×10^{-7}

*The Values are representing the titres of each phage in PFU/mL
**Green marked intersections are indicating the base strain of each phage where they yielded the highest titre.

Table 4.4. Efficiency of plating of each phage on each host strain.

	P1	P2	P3	P4	P5	P7	P8	S1	S2	S3	S4	S5	N1	N2	N4
PM13	1	0.71	1	0.67	0.88	1	1	0.78	1	0.57	0.34	1	0	0	0
ATCC 43137	3.2×10^{-6}	3×10^{-6}	2.3×10^{-6}	3.2×10^{-6}	1.6×10^{-5}	1.6×10^{-5}	1.2×10^{-5}	1.1×10^{-5}	1.4×10^{-6}	1.4×10^{-6}	1.6×10^{-6}	1.8×10^{-6}	1.7×10^{-6}	1.3×10^{-6}	1×10^{-7}
PM52	n/c	n/c	n/c	n/c	n/c	n/c	n/c	n/c	n/c	n/c	n/c	n/c	n/c	n/c	n/c
PM12Y.	0.059	1	0.27	0.45	0.96	0.62	0.7	1	0.54	1	1	0.41	1	1	0.41
PM18B.	0.11	0.36	0.11	0.21	0.85	0.77	0.18	0.34	0.31	0.08	0.06	0.14	0.4	0.31	1
PM19B.	0.65	0.36	0.25	1	1	0.13	0.37	0.44	0.6	0.095	0.022	0.14	0.16	0.25	0.12
PM26B.	0.002	3.4×10-4	2.3×10^{-4}	0.193	1.6×10^{-3}	1.6×10^{-3}	1.2×10^{-3}	0.89	1.4×10^{-4}	0.005	1.6×10^{-4}	1.8×10^{-4}	1.7×10^{-4}	1.3×10^{-4}	0.0007

= highly virulent (0.1 < EOP > 1.00)

= moderately virulent (0.001 < EOP < 0.099)

=Avirulent but active (EOP < 0.001),

=Avirulent

* n/c: not calculated

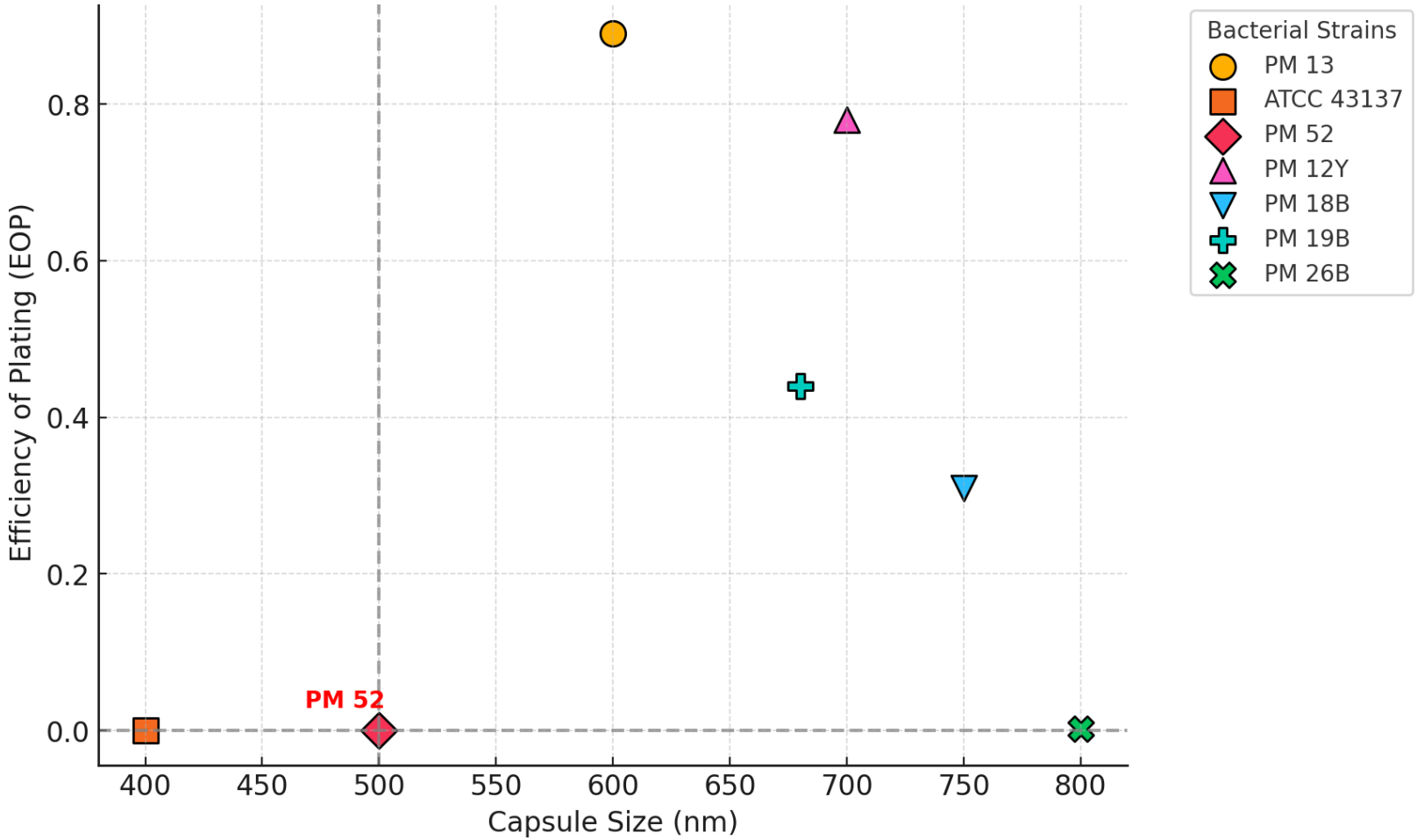

Figure 4.5. Relationship Between Capsule Size and Phage Efficiency of Plating (EOP).
This scatter plot illustrates the relationship between capsule size (nm) and phage Efficiency of Plating (EOP) across *P. multocida* strains. Each point represents a bacterial strain, with marker shape and colour distinguishing different strains. The EOP values plotted represent the average EOP across all tested phages for each strain, rather than individual phage-host interactions.

4.7. pH Sensitivity of *P. multocida* Phages

To assess the viability of the isolated phages under varying chemical conditions, their stability was evaluated across a broad pH spectrum (pH 2 to 12). This experiment aimed to determine the tolerance range of the phages to acidic and alkaline environments, providing crucial information relevant to potential storage conditions, formulation strategies and survival in different *in vivo* niches.

The stability assays demonstrated that all 15 phage isolates maintained high infectious titres when incubated for 60 minutes in buffers ranging from pH 4 to pH 10 (Figure 4.7). Within this range, minimal reduction in PFU/mL was observed, with peak stability noted around neutral pH (specifically pH 7.5, the standard SM buffer pH). However, exposure to extreme pH conditions resulted in rapid and complete inactivation; phage titres dropped below the limit of detection at both pH ≤ 2 and pH ≥ 12. Statistical analysis (ANOVA) revealed no significant differences ($p > 0.05$) in the pH sensitivity profiles among the different phage isolates, suggesting a highly conserved response to pH across this related group of phages. Post-hoc tests confirmed the significant decline in phage survival at the extreme pH values compared to neutral conditions ($p < 0.05$).

The isolated *P. multocida* phages exhibit substantial stability across a wide physiological pH range (4–10) but are susceptible to inactivation by strongly acidic (≤2) or alkaline (≥12) conditions. This consistent stability profile across all isolates suggests they are well-suited for environments near neutral pH but would likely require protective measures if exposed to extreme pH environments.

4.8. Thermal Stability of *P. multocida* Phages

To understand the resilience of the isolated phages to heat, their thermal stability was investigated across a range of elevated temperatures (40°C to 80°C) over a 60-minute period. This assessment is crucial for determining appropriate storage conditions, predicting viability during potential processing steps and evaluating suitability for application in environments with varying temperatures, including physiological conditions.

The thermal stability assays revealed temperature-dependent viability profiles for the 15 phages (Figure 4.8). All isolates demonstrated good stability at 40°C and 50°C, maintaining their initial infectious titres throughout the 60-min incubation period. However, exposure to higher temperatures significantly impacted viability. At 70°C and 80°C, phage titres rapidly decreased, falling below the limit of detection within the first 10 minutes of incubation for all isolates. At 60°C, a notable divergence in stability was observed: while the majority (12 out of 15) of the phages were inactivated or reduced below detectable levels by the end of the 60-minute incubation, three phages—P8, S1 and S2—exhibited enhanced thermal tolerance, retaining approximately 50% of their initial titre under these conditions.

The *P. multocida* phages are generally stable at temperatures up to 50°C, encompassing typical physiological temperatures, but are susceptible to inactivation at 60°C and rapidly lose viability at 70°C or higher. Importantly, isolates P8, S1 and S2 demonstrated significantly greater thermal tolerance at 60°C compared to the other phages in the panel, suggesting potentially advantageous characteristics for applications requiring enhanced heat stability.

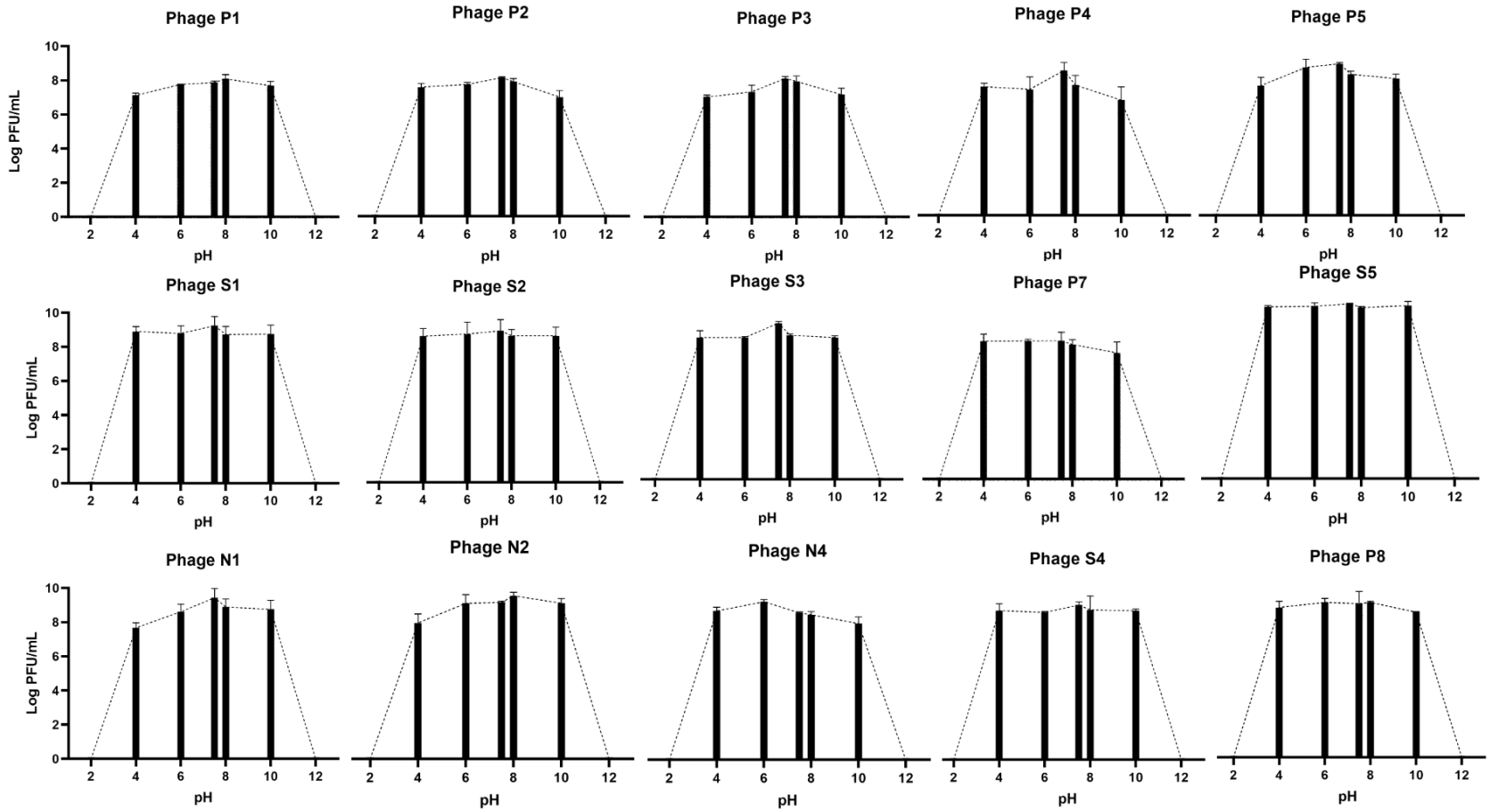

Figure 4.6. pH Sensitivity of 15 Phages.

Log-transformed plaque-forming units (PFU/mL) of phages P1–P8, S1–S5 and N1–N4 across different pH conditions (2–12). Each data point represents the mean PFU/mL from three biological and three technical replicates, with error bars indicating standard deviation. Phages exhibited stability between pH 4 and 10, with significant reductions ($p < 0.05$, ANOVA with Tukey's HSD test) in titres observed at extreme pH conditions (≤2 and ≥12). The highest titres were recorded at pH 7.5, corresponding to the pH of SM buffer, suggesting optimal preservation conditions.

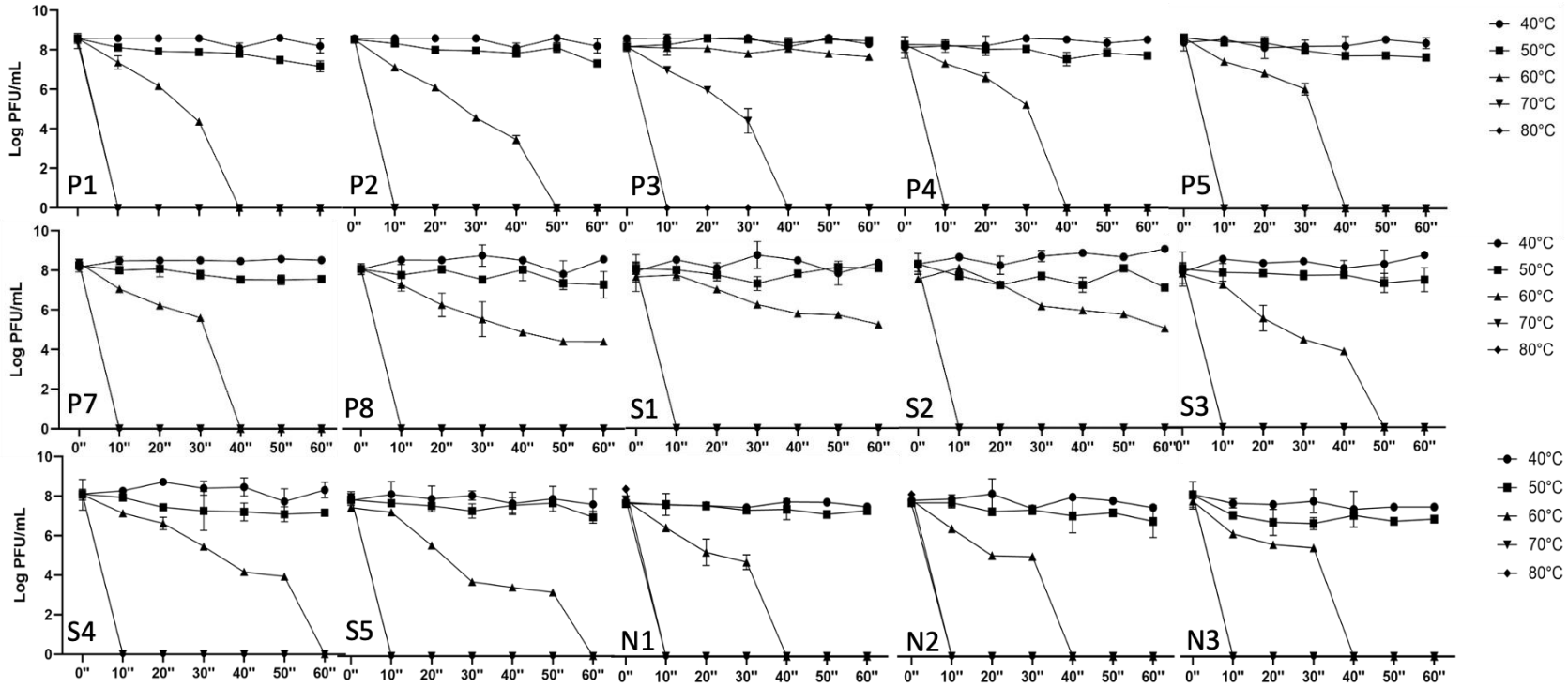

Figure 4.7. Thermal Stability of Phages.

Thermal stability of phages at temperatures ranging from 40°C to 80°C over 60 minutes. Log PFU/mL values are plotted against time for each phage, with different symbols representing temperature conditions (40°C ●, 50°C ■, 60°C ▲, 70°C ▼, 80°C♦). Error bars indicate standard deviations from three biological and three technical independent replicates. Phage stability decreased as temperature increased, with rapid inactivation observed at 70°C and 80°C for certain phages.

4.9. Chloroform Sensitivity. of *P. multocida* Phages

To evaluate the structural integrity of the phage virions, particularly concerning the presence of essential lipid components, their sensitivity to the organic solvent chloroform was assessed. This characteristic is also relevant, as chloroform is sometimes used during phage lysate purification.

Exposure to chloroform resulted in a statistically significant reduction in infectious titre for the phage isolates overall, as confirmed by both the paired *t*-test (t = -3.76, p = 0.0021) and the Wilcoxon signed-rank test (W = 10, p = 0.0026). However, the degree of sensitivity varied considerably among the different phage isolates (Figure 4.9). Some phages, P1 and P2, showed a pronounced reduction in titre following chloroform treatment, indicating higher sensitivity. In contrast, other phages, particularly N1 and N2, were relatively resistant, exhibiting only minor decreases in titre. This observed variability in chloroform sensitivity suggests potential differences in the structural composition or stability of the virions among the closely related isolates.

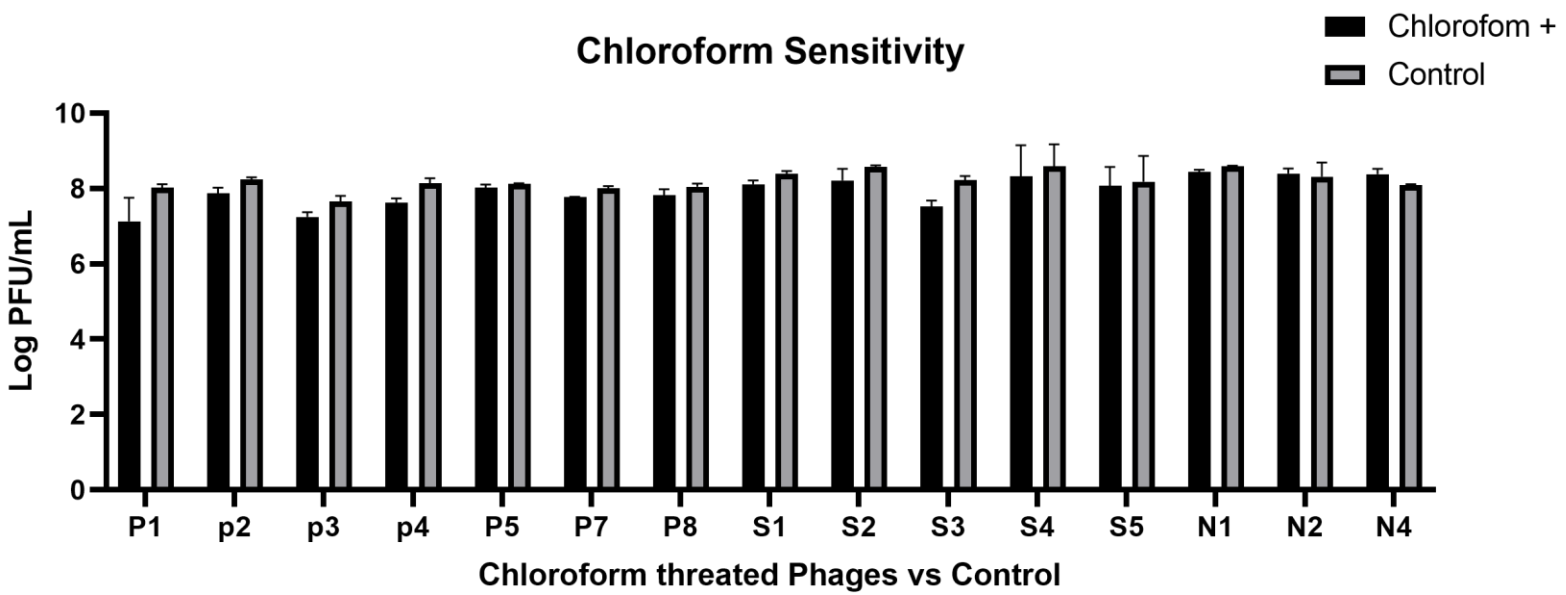

Figure 4.8. Chloroform Sensitivity of all Phages.

Comparison of log10 phage titres (PFU/mL) in chloroform-treated (black bars) and untreated (light grey bars) samples. Phages are ordered sequentially from P1 to N4. Error bars represent the standard deviation from independent biological replicates. Chloroform treatment significantly reduced phage titres (paired *t*-test: $p = 0.0021$, Wilcoxon signed-rank test: $p = 0.0026$), though sensitivity varied among phages**.**

4.10. Growth Dynamics and Selecting Phage for Phage Therapy

To accurately characterise and compare the fundamental infection kinetics of selected phage isolates under laboratory conditions, one-step growth experiments were performed. The objective was to determine key parameters defining their lytic cycle: the latent period (time from infection to lysis initiation), the rise period (duration of lysis) and the burst size (average number of progeny virions released per infected cell).

The infection cycle parameters were determined for ten representative phage isolates (growth curves shown in Figures 4.10, 4.11 and 4.12; summary data in Table 4.5). Analysis of the growth curves revealed variation in the timing and productivity of the lytic cycle among the phages. The latent period, representing the minimum time required before new virions are released, ranged from 35 minutes (observed for N2 and N4) to 45 minutes (observed for P5, S1 and N1). The subsequent rise period, during which the phage population increases exponentially as infected cells lyse, typically lasted between 30 and 45 minutes for most isolates. The burst size, indicating the average yield of phage progeny per lysed bacterium, also varied. Phages P1 and P8 exhibited the highest replication efficiency within this group, yielding approximately 52.5 and 52.1 PFU/cell, respectively. In contrast, phages P3, P5 and N2 displayed the lowest burst sizes, producing around 30 PFU/cell. All tested phages showed the characteristic logarithmic increase in titre during the rise period, generally occurring between 40- and 75-min post-infection.

The one-step growth experiments successfully quantified key lytic cycle parameters, revealing moderate but variable infection kinetics among the tested phage isolates. The determined latent periods (35–45 min) and burst sizes (approx. 30–53 PFU/cell) provide essential

comparative data on the temporal progression and efficiency of phage replication, identifying isolates such as P1 and P8 as having higher progeny yields under these conditions.

Table 4.5. Growth characteristic of phage isolates of this study.

Phage ID	Host strain	Latent period (min)	Rise period(min)	Burst size (PFU/cell)
P1	PM13	40	40	52.5
P2	PM13	35	40	35.5
P3	PM13	40	35	30.7
P4	PM13	40	35	42.3
P5	PM13	45	40	30.2
P8	PM13	40	45	52.1
S1	PM13	45	35	43.6
N1	ATCC43137	45	30	35.1
N2	ATCC43137	35	35	30.5
N4	ATCC43137	35	30	31.1

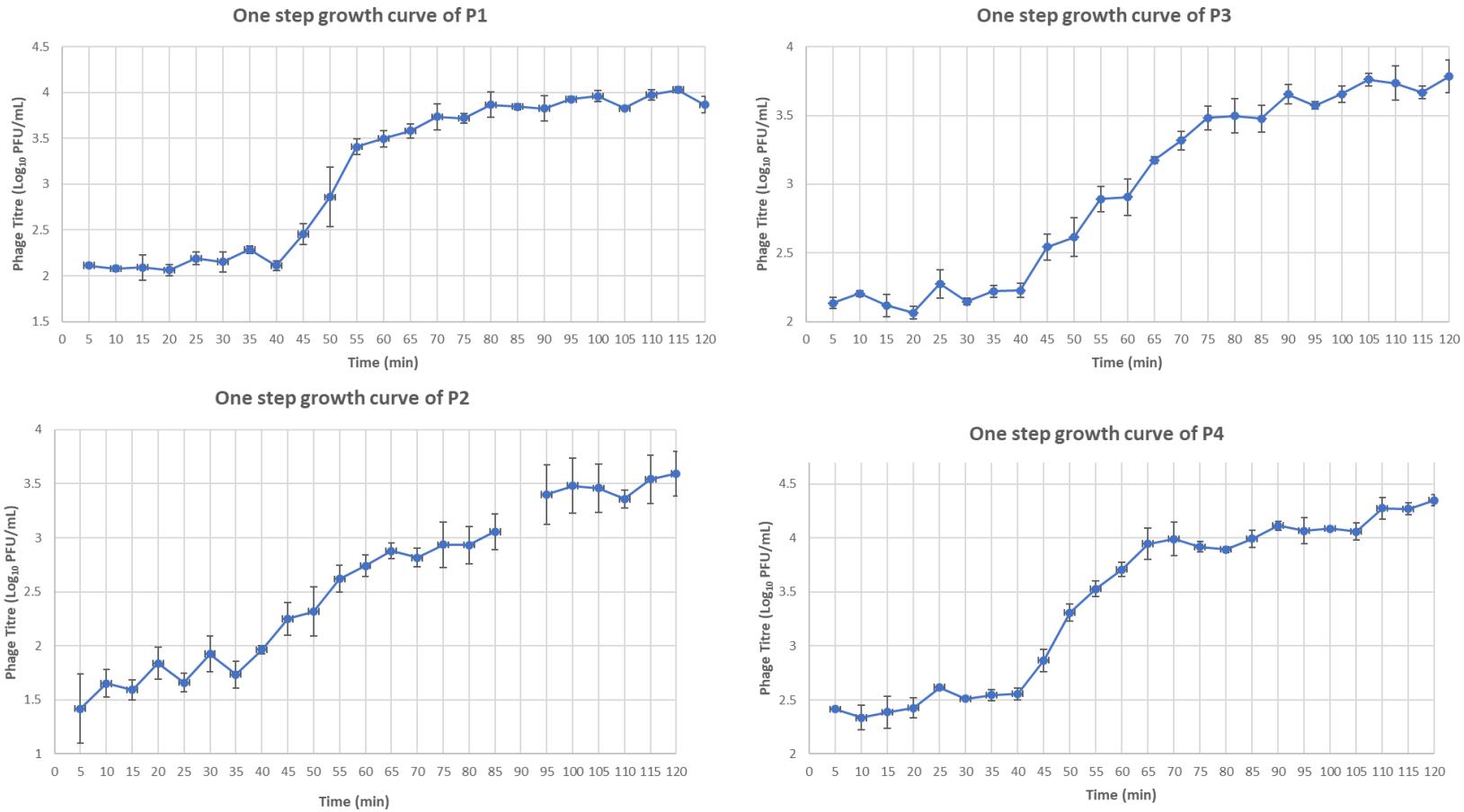

Figure 4.9. One Step Growth Curves of Phages P1, P2, P3 and P4.

The graphs depict the phage replication kinetics over a 120-minute period. Each curve represents the average phage titre (Log_{10} PFU/mL) measured at specified time intervals, based on three independent experiments (n = 3), with error bars representing the standard error of the mean (SEM). The growth curves exhibit distinct phases: A latent period (0–40 min), during which phage titres remained constant, a rise period, marked by a rapid increase in phage concentration, followed by a plateau phase, indicating completion of the lytic cycle. Burst size for each phage was calculated by dividing the average PFU/mL during the plateau by that of the latent period, yielding the following values: P1 = 52.5, P2 = 35.5, P3 = 30.7, and P4 = 42.3 PFU/infected cell.

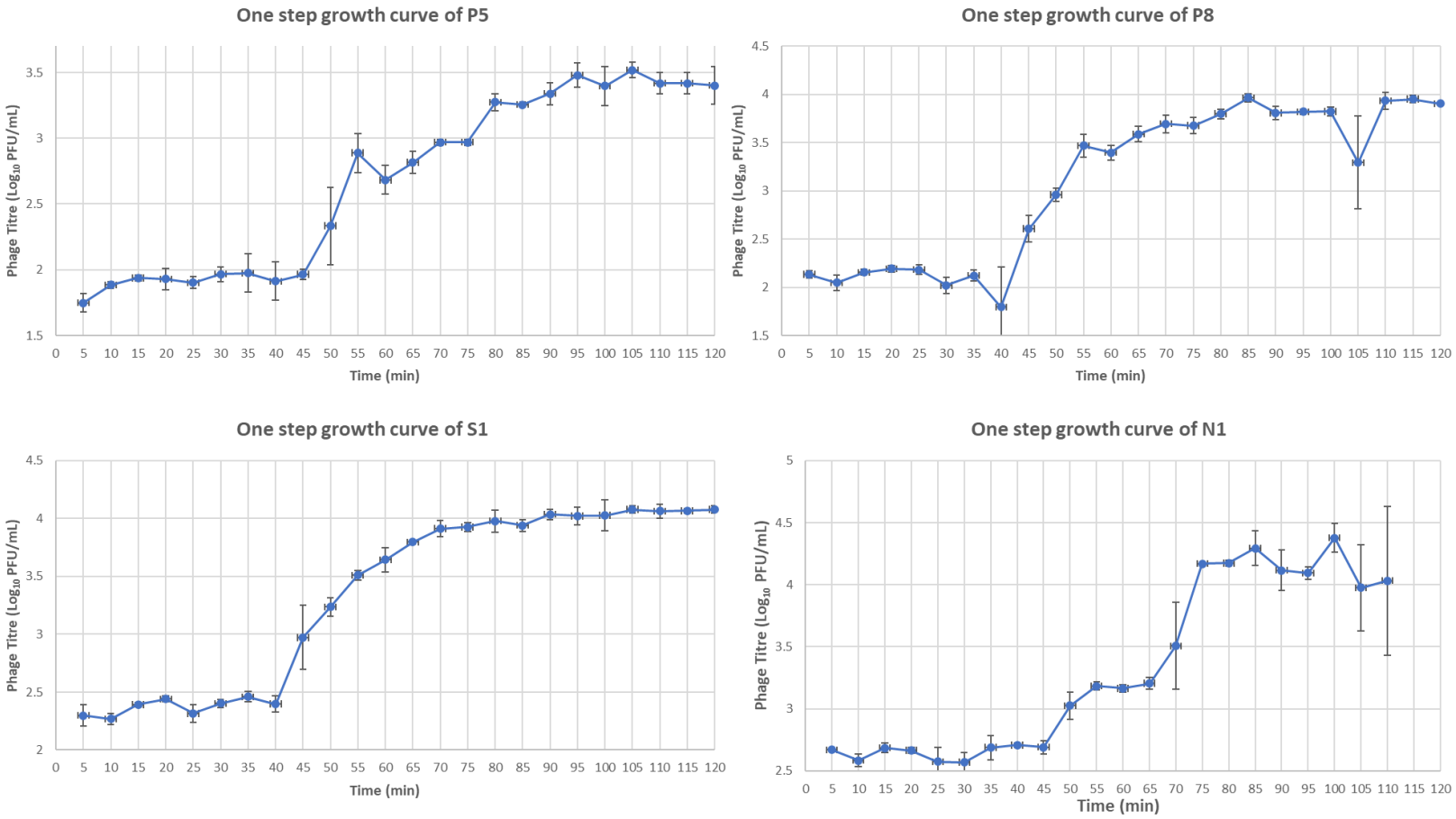

Figure 4.10. One Step Growth Curves of Phages P5, P8, S1 and N1.

The graphs depict the phage replication kinetics over a 120-minute period. Each curve represents the average phage titre (Log_{10} PFU/mL) measured at specified time intervals, based on three independent experiments (n = 3), with error bars representing the standard error of the mean (SEM). The growth curves exhibit distinct phases: A latent period (0–40 min), during which phage titres remained constant, a rise period, marked by a rapid increase in phage concentration, followed by a plateau phase, indicating completion of the lytic cycle. Burst size for each phage was calculated by dividing the average PFU/mL during the plateau by that of the latent period, yielding the following values: P5 = 30.2, P8 = 52.1, S1 = 43.6, and N1 = 35.2 PFU/infected cell.

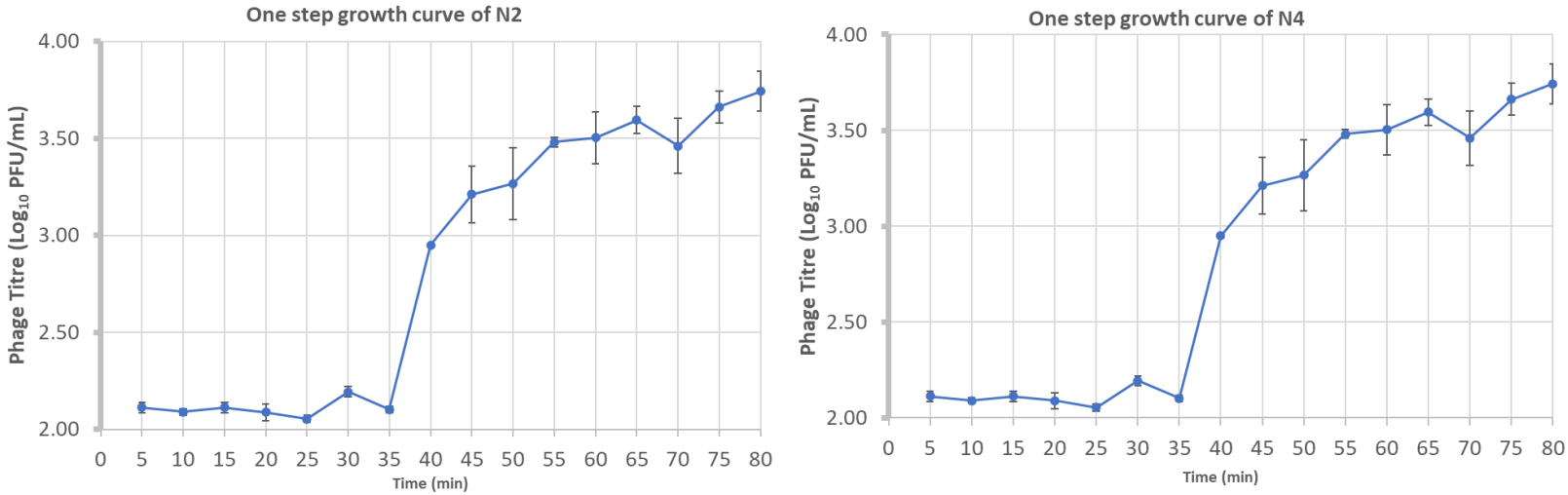

Figure 4.11. One Step Growth Curves of Phages N2 and N4.

The graphs depict the phage replication kinetics over a 120-minute period. Each curve represents the average phage titre (Log_{10} PFU/mL) measured at specified time intervals, based on three independent experiments (n = 3), with error bars representing the standard error of the mean (SEM). The growth curves exhibit distinct phases: A latent period (0–40 min), during which phage titres remained constant, a rise period, marked by a rapid increase in phage concentration, followed by a plateau phase, indicating completion of the lytic cycle. Burst size for each phage was calculated by dividing the average PFU/mL during the plateau by that of the latent period, yielding the following values: N2 = 30.5 and N4 = 31.1 PFU/infected cell.

4.11. Discussion

Phage Isolation

A total of 21 environmental samples were collected from 18 distinct locations and screened using six different *P. multocida* strains (PM13, PM48, PM52, PM106, PM222 and ATCC43137) across 27 isolation trials. However, no phages were successfully isolated from environmental water samples, likely because of the absence of host bacteria in these environments, as discussed in previous chapters. The fundamental principle of phage isolation states that bacteriophages are typically found where their host bacteria are present (can Charante *et al*., 2019). To date, no *P. multocida* phages have been recovered from environmental waters except sewage sources. The lack of access to sewage samples due to COVID-19 restrictions limited our sampling options. Nevertheless, phages were successfully isolated from previously collected sewage samples, providing a more suitable environment for host-phage interactions.

A total of 15 phages were isolated using previously collected sewage samples, seven of which were isolated in an experiment using *P. multocida* PM13 strain, while five were isolated from the same host but from a different algae sample. Three different phages were isolated in another setup using the *P. multocida* ATCC43137 strain and sewage sample. The fact that only three of the 27 isolation experiments, including other environmental samples, yielded positive results using a sewage sample supports the idea that sewage samples are the most suitable source for the isolation of such phages.

Plaque and Virion Morphology

After a successful isolation, the first variable that can be observed is the plaque morphology formed by the phages. Although it is not a definitive determinant on its own, plaque

morphology provides rough information about the lytic or temperate nature of the phage. Clear plaques are generally formed by lytic phages, while temperate phages tend to form turbid plaques (Ramesh *et al*., 2019). However, these statements may not always be true because, while some lytic phages can form opaque plaques, it has been observed that temperate phages that have lost their lysogeny form clear plaques. Therefore, this feature, which can be a guide in the initial phage selection, should be supported by genetic tests when it comes to characterisation (Science Education Alliance - Phages Hunters Advancing Genomics and Evolutionary Science [SEA-PHAGES]).

TEM imaging results proved that all phages isolated in this study belong to the *Siphoviridae*-like morphotype viruses. Phages characteristically have an icosahedral capsid with an average diameter of 57 nm and a non-contractile tail of approximately 181 nm in length. A single *P. multocida*-specific phage, PM-GAD-IND, belonging to this family has been reported previously (Qureshi *et al*., 2018). However, the size of this phage is significantly smaller than the phages in the present study, with a capsid of approximately 27 nm and a tail of 134 nm (Qureshi *et al*., 2018). This shows that the phages in this study have a capsule that is 111% larger and a tail that is 35% longer than their single counterparts.

There are other *P. multocida* phages isolated and investigated under TEM; results suggest that *P. multocida* pacific phages can be found under different phage families. For example, Chen *et al*. (2019) identified two phages, including PHB01 and PHB02, which infect *P. multocida* classified under the *Podoviridae* family, while Yoon (2015) isolated a lytic *P. multocida* phage, Pas-MUP-1, which similar to the *Myoviridae*-like *phages*. On the other hand, Campoy *et al*. (2006) report a temperate phage, F108, which is specific to *P. multocida* and similar to the *Myoviridae*

like phages. These findings suggest that *P. multocida* phages can be characterised with their varied morphologies, life cycles, and host ranges.

In the present study, another interesting finding observed in TEM imaging was that many phages were found in groups with their tails entangled with each other. In addition, many broken tails and deformed capsids were also observed. These results may be the reason why phage titres could not be increased above 10^{10} PFU/mL despite repeated attempts. Probably, phages with increased density were precipitated and subsequently entangled or damaged during the centrifugation stage applied in most concentration and purification techniques.

Host Range and LPS Typing

The importance of host range determination for phage therapy has been repeatedly reiterated in previous sections. In this study with the same purpose, host range determination was tested on a host panel consisting of 29 different *P. multocida* strains with different LPS and capsule types, and it was determined that the phages had a relatively narrow host range and that the phages could infect approximately 25% of the bacteria present. This finding aligns with the often-observed specificity of phages but underscores a key challenge for practical application: individual isolates are unlikely to cover the full diversity of circulating *P. multocida* strains, suggesting that phage cocktails would likely be necessary to achieve broader therapeutic coverage (Chung *et al.*, 2023; Fong *et al.*, 2021).

The susceptible strains predominantly belonged to the LPS L3 genotype (three of the six susceptible strains were L3, the others untypable), hinting that this specific LPS structure might serve as a key recognition or receptor site for this group of *Siphoviridae*-like phages. While this correlation is noteworthy, definitive confirmation would require further molecular studies, such

as the generation and testing of LPS mutant strains or direct phage-LPS binding assays. Identifying the receptor is crucial, as receptor availability and structure are primary determinants of host range (Holtappels *et al.*, 2023).

The host range profile of our isolates appears distinct from previously characterised *P. multocida* phages. For example, our phages did not lyse strains identified as capsular type D or F, unlike phage PHB01, which targets type D (Chen *et al.*, 2019). While we identified a capsular type B strain (PM19B) as susceptible, aligning partially with the activity reported for phage PMP-GAD-IND (Qureshi *et al.*, 2018), our phages differ significantly from others like PHB02, known to target capsular type A (Chen *et al.*, 2018). Although our ability to draw firm conclusions based on capsule type was limited by the high number of untypable strains (potentially due to limitations in the PCR assay for type A detection, as suggested by Harper *et al.*, 2006), the apparent preference for LPS L3 and the distinct overall host range suggest that these Mu-like temperate phages occupy a different biological niche compared to the lytic T7-like (PHB02) or other *P. multocida* phages previously studied. This distinction might imply different evolutionary pressures or receptor usage and potentially offers complementarity if used alongside other phage types in future cocktail formulations.

These host range findings indicate that while the isolated phages demonstrate clear lytic potential against certain strains (particularly those with L3 LPS), their narrow spectrum necessitates further investigation to determine their broader therapeutic relevance. The subsequent Efficiency of Plating (EOP) assays were therefore crucial to quantify the *degree* of replication efficiency within this limited host range and to select the most suitable host strains

(PM13 and ATCC43137) for reliable phage propagation, prioritising consistent lawn formation and plaque clarity essential for downstream experiments.

Physicochemical Stability of Phages

pH Sensitivity

All phages exhibited stability within pH 4–10, but titres significantly declined at pH < 2 and pH > 12. Similar trends were observed for PHB01 and PMP-GAD-IND, which remained stable from pH 5 to 9 but exhibited titre reductions at extreme pH values (Chen *et al.,* 2019; Qureshi *et al.,* 2018). Our pH testing range (pH 2, 4, 6, 8, 10, 12) differed from previous studies (pH 3, 5, 7, 9, 11), making direct comparisons challenging. These findings indicate that our phages could survive passage through most sections of the poultry digestive tract, except for the gizzard, where the pH ranges from 2.0 to 2.6. Given the 30–90 min transit time in the gizzard, most phages would likely lose viability in this highly acidic environment. This makes direct oral phage administration challenging, necessitating encapsulation technologies, polymer-based stabilisation or nano-assisted solutions to improve phage survival (Wdowiak *et al.,* 2022).

Thermal Stability

Thermal stability is a crucial factor in determining the potential for phage therapy, particularly in animal and human applications. Phages remained viable at 40°C and 50°C, temperatures that correspond to avian and mammalian body temperatures (poultry: ~41°C, mammals: ~37°C). However, rapid inactivation occurred at 70°C and 80°C, with titres dropping below detection limits within 10 min. At 60°C, most phages lost viability after 40 min, but P8, S1 and S2 retained ~50% of their initial titre at the end of 60 min, demonstrating enhanced thermal resistance. In contrast, PHB01 and PMP-GAD-IND lost viability at 60°C within 30 min (Chen *et al.,*

2019; Qureshi *et al.,* 2018). The higher temperature stability of phage P8, S2 and S2 compared to others suggests that they may be more suitable for use in phage therapy. Since the physiological body temperatures of the organisms to which the treatment is planned remain within the temperature range to which the phages are stable, it has been determined that they can be applied in vivo without a significant loss of titre.

Chloroform Sensitivity

The chloroform sensitivity test is generally used to determine whether phages can be used in environmental applications with various detergents, as well as to determine whether they are enveloped, because chloroform destroys lipid-containing structures. Although TEM imaging results showed that all isolated phages belonged to the *Siphoviridae*-like *phages* and as expected, did not contain any envelope, all phages showed unexpected sensitivity to chloroform. This unexpected loss of titre can be attributed to the structural proteins forming the capsid or tail being affected by chloroform. Another possibility is that receptor recognition proteins in the phage tail or enzymes that dissolve the bacterial cell wall, which play an important role in the adsorption stage, may have been damaged by chloroform. Chloroform is frequently used in many regular phage experiments, from phage isolation to concentration and even purification, it was frequently used in this study. This has caused limitations in practical applications. These limitations have tried to be eliminated by choosing techniques that do not involve chloroform as much as possible. The effect of chloroform on non-enveloped phages may be a possible future study. Phages exposed to chloroform can be observed again under TEM, and their damaged structures can be examined. Phages that have been mutated with single nucleotide polymorphs and have become resistant to chloroform can be compared with sensitive ones with both

genomic and physiological studies, and it can be determined which genes encode the structure that provides resistance. The results that can be obtained can be used to tailor existing phages for studies to be applied with chloroform.

Growth Dynamics of Phage Isolates

Determination of growth parameters such as rise period, latent period and burst size of a phage is of great importance for its use in phage therapy applications. In the present study, one step growth experiment was applied to determine these values of ten *P. multocida* phages. While the latent period of the phages was between 35 and 45 min, the rise period was observed between 30 and 45 min. Another parameter, burst size, was recorded as 30.2-52.5 PFU/cell.

Latent Period Comparison

The latent period of a bacteriophage represents the time between host infection and the first release of progeny phages. The latent periods of our phages ranged from 35 to 45 min, similar to *P. multocida* phage vB_PmuM_CFP3, which exhibited a latent period of 35 min (Chen *et al.,* 2024). Likewise, phage PHB02, isolated against *P. multocida* type A, had a latent period of 40 min, closely matching several of our isolates, particularly P3, P4 and P5 (Chen *et al.,* 2018). Another relevant study on PMP-GAD-IND, a *Siphoviridae*-like phage, reported a latent period of 35 min, consistent with our shortest latent periods (Qureshi *et al.,* 2018). In contrast, some phages used in phage therapy applications demonstrate shorter latent periods, potentially advantageous for rapid bacterial clearance. For instance, vB_PmuP_PHB01, a highly infectious *Podoviridae* phage, had a latent period of only 30 min (Chen *et al.,* 2019). Similarly, a phage therapy study against methicillin-resistant *Staphylococcus aureus* (MRSA) reported a latent period of 40 min, reinforcing that our values fall within the expected range for effective

therapeutic phages (Gharieb *et al.,* 2020). The shorter latent periods observed in PHB01 and therapy-focused phages suggest that phages with rapid infection cycles may be more suitable for therapeutic applications. However, our phages moderate latent periods (35–45 min) are comparable to those of most *P. multocida*-specific phages, indicating they still hold potential for targeted biocontrol and therapeutic applications.

Burst Size Comparison

The burst size represents the number of phage particles released per infected bacterial cell and is a crucial determinant of infection efficiency. Our highest burst sizes (P1 = 52.5 PFU/cell, P8 = 52.1 PFU/cell) are comparable to vB_PmuM_CFP3 (48 PFU/cell) (Chen *et al.,* 2024), indicating that our most productive phages fall within the expected range for *P. multocida* phages. Other *P. multocida* phages show slightly lower burst sizes; for example, PHB02 had a burst size of 40 PFU/cell, smaller than that of our most productive isolates but similar to that of our less productive ones (e.g., P3, P5 and N2, ranging from 30.2 to 30.7 PFU/cell) (Chen *et al.,* 2018). Similarly, PMP-GAD-IND exhibited a burst size of 37 PFU/cell, reinforcing that our phages fall within the expected burst size range for *Pasteurella* phages (Qureshi *et al.,* 2018). However, phages isolated for phage therapy applications typically demonstrate higher burst sizes, making them more efficient bacterial killers. For example, vB_PmuP_PHB01 had an exceptionally high burst size (165 PFU/cell), significantly exceeding those of our isolates (Chen *et al.,* 2019). Similarly, phages targeting MRSA reported burst sizes of approximately 120 PFU/cell, far greater than our phage's burst sizes (Gharieb *et al.,* 2020). This comparison suggests that while our phages perform well within the context of *P. multocida* infections, they may require higher MOI

or combination therapy to achieve equivalent effectiveness to high-burst phages used in clinical phage therapy.

Implications for Phage Therapy and Biocontrol Applications

When selecting phages for treatment, those with short latent periods and high burst sizes are preferred because they provide rapid and effective lysis and have a high probability of bacterial elimination without the development of phage resistance. The phages of the present study have a longer latent period and smaller burst sizes compared to other phages that have shown effective results in phage treatment. This supports the selection of the most effective phages among them in the case of therapeutic use and their application in higher doses than the others, if necessary, in the form of a cocktail formed by combining several phages.

Conclusion

In the present study, phage isolation studies were only successful in experiments carried out with sewage samples. This result is consistent with other isolation studies and supports the idea that sewage is the most suitable source for the isolation of *P. multocida* specific phages. On the other hand, the failure to provide successful isolation from environmental water samples despite repeated attempts is consistent with the failure to detect the presence of target bacteria in the same samples. This supports the hypothesis that phages should be isolated from environments where host bacteria are found and multiplied. Although all phages in this study belong to the *Siphoviridae*-like phages, when compared with previous studies, it was observed that *P. multocida* phages could also be from other phage families. Although host range determination resulted in a narrow host range, most of the phages were specific to strains with L3 LPS, which makes the phages of the present study different from those of other studies.

However, a detailed host range determination on a library of well characterised *P. multocida* strains was noted as a necessary future study. Sensitivity experiments show that phages were stable at physiological pH and temperatures and can be easily used in in vivo applications. Although there are viability losses in extreme conditions, they can be made more stable and applied with strategies such as phage encapsulation. In terms of growth parameters, phages are a bit behind compared to other phages that have been proven to be effective, but this limitation can be overcome to some extent with some adjustments in dosage and timing. The sensitivity of non-enveloped phages to chloroform was an interesting result, but it brings with it questions that can be studied in the future.

Final Remarks

Overall, our findings contribute to the growing understanding of *P. multocida* phages, providing insights into their isolation, morphology, stability and replication dynamics. While our phages hold potential for biocontrol and therapeutic applications, further research should focus on host range expansion and *in vivo* validation to fully assess their efficacy.

Chapter 5. *Genomic and Phylogenetic Analysis of P. multocida Phages*

Phage genome analysis is essential for understanding their biology, evolutionary development, and potential therapeutic applications. Fully assembled genomes provide detailed information on genome architecture, coding potential, and the presence or absence of genes associated with antimicrobial resistance or virulence (Chen et al., 2024). Genomic data also enable the distinction between lytic and temperate life cycles and clarify evolutionary relationships with other phages (Chen et al., 2024).

Despite substantial growth in interest in phage therapy, the genomic representation of Pasteurella multocida phages remains limited. Public databases now include an expanding catalogue of bacteriophage genomes. For example, as of October 2025, PhagesDB recorded 29,104 phage genomes. (PhagesDB, 2025) In comparison, only eleven P. multocida-specific phage genomes are available in the NCBI Virus database (ncbi.nlm.nih.gov/labs/virus). This limited genomic dataset restricts the scope of comparative analyses and constrains current understanding of P. multocida phage diversity.

The genomes of the P. multocida phages isolated in this study were sequenced, assembled, and annotated. Analyses addressed genome architecture, guanine-cytosine (G+C) content, gene content, and comparative phylogenetic placement with previously described phages. The investigation focused on genomic features indicative of phage lifestyle and the presence or absence of antimicrobial resistance and virulence genes to assess their safety and potential therapeutic relevance.

Aims of Chapter

This chapter aimed to characterise the genomes of 13 bacteriophages isolated on *P. multocida* strains PM13 and ATCC 43137 through comparative genomic analysis. By examining their genome structure, sequence similarity, and genetic composition, this study sought to determine their phylogenetic relationships, classification, and potential functions. Special attention was given to the presence of conserved and accessory genes, the identification of temperate or lytic characteristics, and the potential implications of gene content for phage biology, host interactions, and evolutionary significance. Additionally, this chapter explored the stability, mobility, and therapeutic potential of these phages by analysing antimicrobial resistance (AMR) genes, virulence factors, and genome modularity, providing insights into their role in bacterial evolution and phage therapy applications.

Chapter Objectives

1. Genomic Characterisation and Sequence Analysis

- To determine the genome size, organisation and G+C content of the isolated phages and compare them to previously characterised *P. multocida* phages.
- To generate high-quality genome assemblies suitable for downstream comparative analyses.

2. Comparative Genomics and Phylogenetic Analysis

- To evaluate genetic similarities and evolutionary relationships among the isolated phages through multiple sequence alignments and phylogenetic clustering.
- To compare these phages with previously characterised *P. multocida* phages and bacteriophages from other bacterial families, establishing their broader phylogenetic placement.

3. Functional Gene Annotation and Life Cycle Prediction

• To identify core and accessory genes, including those encoding structural proteins, replication-related enzymes and host interaction factors.

• To investigate the presence or absence of tRNA genes as an indicator of phage dependence on host translation machinery.

4. Potential for Horizontal Gene Transfer and Phage Therapy Safety

• To screen phage genomes for antimicrobial resistance (AMR) genes and virulence factors using bioinformatic prediction tools.

• To assess the potential for horizontal gene transfer by examining mobile genetic elements and integration-related genes.

5. Structural and Functional Variability Among Phage Isolates

• To characterise genomic variation among isolates and assess whether this corresponded to observed phenotypic traits (e.g., heat resistance, host range, burst size).

• To annotate hypothetical proteins and predict their potential biological roles through sequence homology and protein domain analyses.

6. Broader Evolutionary and Ecological Implications

• To investigate possible integration of these phages into *P. multocida* genomes and their role in bacterial evolution.

• To examine gene modularity and acquisition patterns, assessing how these phages may contribute to genetic exchange and adaptation within bacterial populations.

5.1. Quality and Quantity of Extracted Phage Genomes

Prior to genomic analysis, including restriction digestion and sequencing, it was essential to extract high-quality genomic DNA from the phage isolates. The aim of this step was to assess the purity, integrity and concentration of the extracted DNA to ensure its suitability for downstream molecular applications.

Genomic DNA was successfully extracted from the phage isolates. Spectrophotometric analysis (NanoDrop) was used to evaluate DNA purity and concentration (detailed results in Table 5.1). The assessment of purity via the A260/A280 ratio indicated potential protein contamination in some samples; specifically, the ratios for phages S2, S4, S5, N1 and N2 were below the generally accepted threshold of approximately 1.8 for pure DNA and fell below 1.70. However, analysis of the extracted DNA via agarose gel electrophoresis indicated good structural integrity for all samples (Figure 5.1).

Table 5.1 Nanodrop results of extracted Phage DNA

Phage	260/280 ratio	Concentration ng/µL
P1	1.73	414.7
P2	1.75	119.2
P3	1.74	222.0
P4	1.76	717.7
P5	1.78	398.1
P7	1.77	444.7
P8	1.70	362.8
S1	1.71	540.9
S2	1.51	259.9
S3	1.79	40
S4	1.69	860.8
S5	1.63	706.4
N1	1.65	476.5
N2	1.64	391
N4	1.72	316.7

The DNA migrated as high molecular weight bands, appearing concatenated, with no visible smearing indicative of degradation or multiple bands suggesting excessive contamination.

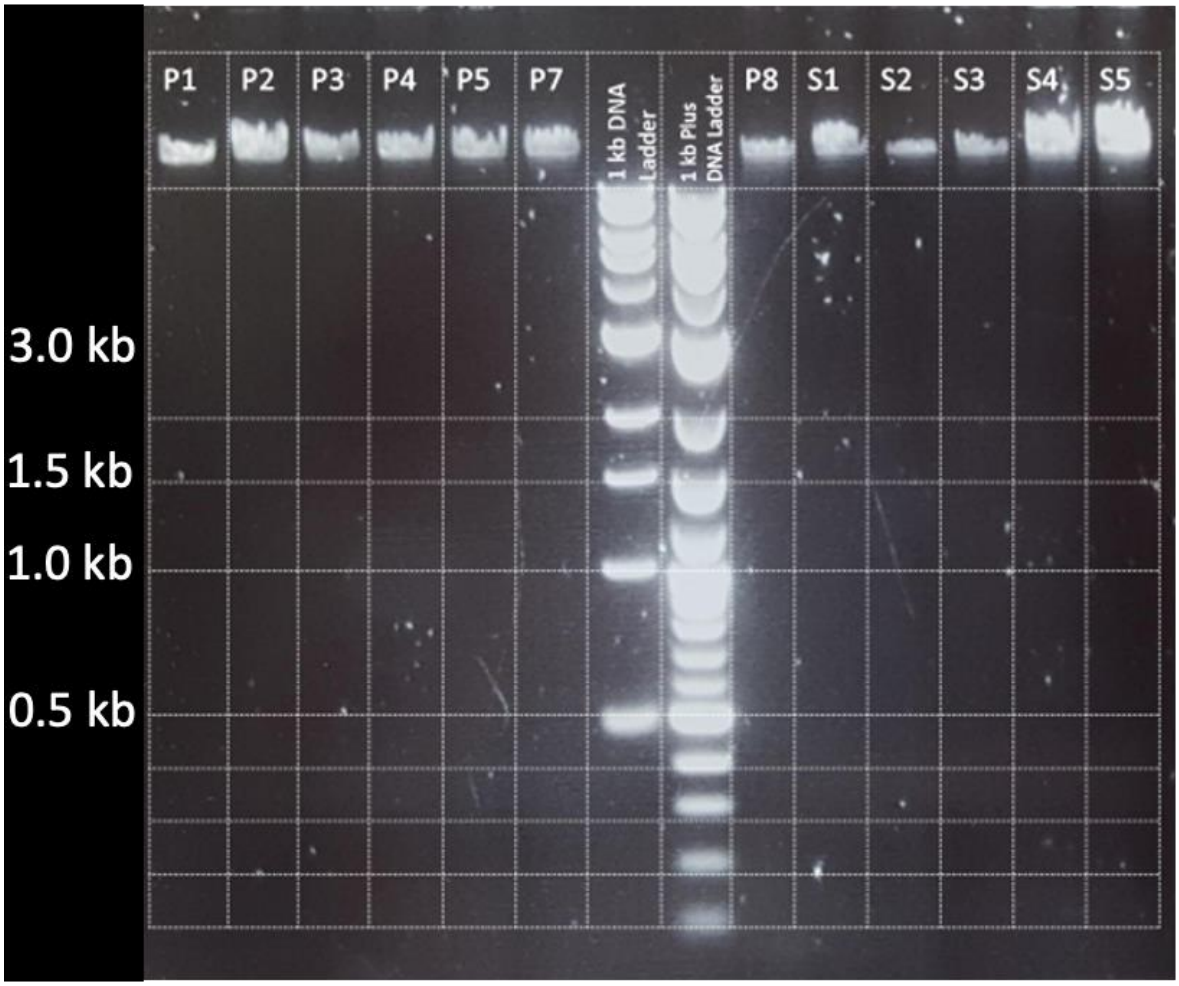

Figure 5.1. TAE Agarose Gel of DNA Preparations for Sequencing.
DNA isolated by phenol chloroform. 10 µL loaded per well. P1-P8 and S1-S5 are phage isolated from sewage sample on PM13 strain. DNA separated on 1% TAE agarose gel.

5.2. Restriction Digestion Analyses of Phage Genomes

To obtain a preliminary assessment of the genomic similarity and structural organisation among the newly isolated bacteriophages prior to full genome sequencing, Restriction Fragment Length Polymorphism (RFLP) analysis was conducted. This aimed to compare the pattern of restriction sites across the different phage genomes using a panel of restriction enzymes.

When the genomic DNA from the phage isolates was subjected to digestion with several different restriction enzymes (including BamHI, EcoRI and HindIII), subsequent analysis via agarose gel electrophoresis revealed identical banding patterns for all the tested phages (Figure 5.2). The complete congruence of these restriction patterns strongly indicated a high degree of sequence conservation and shared genomic organisation across these isolates. This initial observation of high similarity was subsequently confirmed by whole-genome sequencing and alignment, which showed approximately 99.6% sequence identity among the successfully assembled phage genomes (Section 5.4).

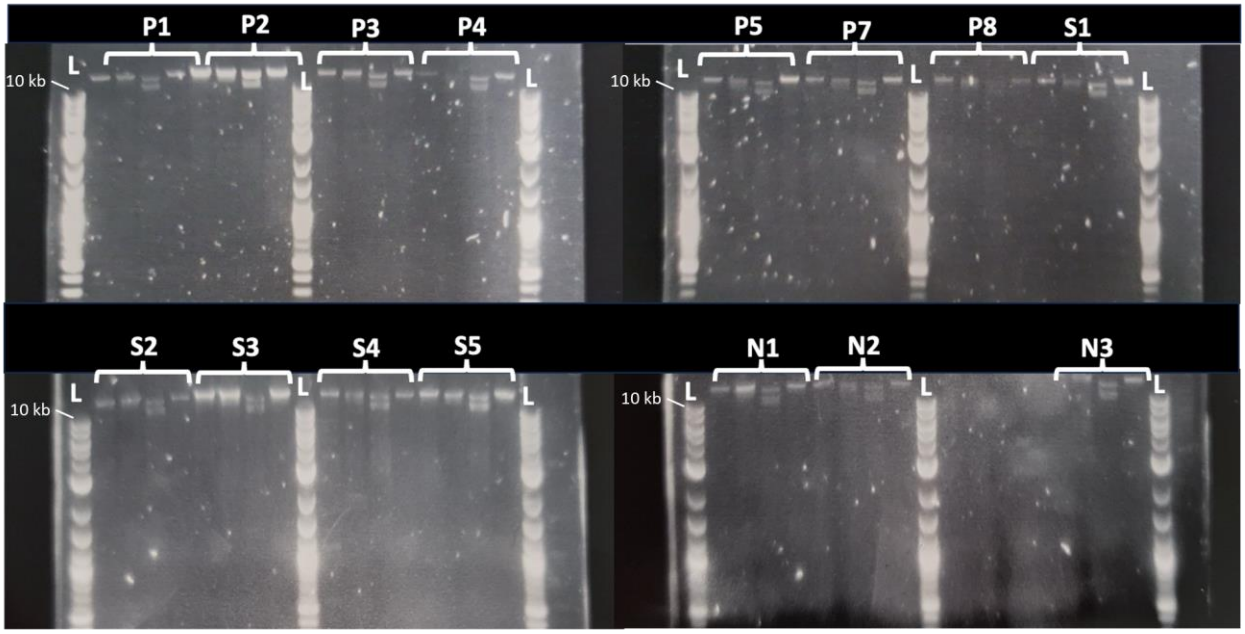

Figure 5.2. Agarose gel electrophoresis of restriction enzyme-digested phage DNA.

Agarose gel (1% w/v) prepared with 1× TAE buffer, stained with Nancy-520, and run for 1 hour in TAE buffer to visualise restriction digestion profiles of selected phages. The gel displays the restriction digestion patterns of Phages P1, P2, P3, P4, P5, P7, P8 and S1, treated with three restriction enzymes: HindIII, EcoRI and BamHI. Each phage DNA sample was loaded into four wells in the following order: uncut (control), HindIII-digested, EcoRI-digested and BamHI-digested DNA. A 1 kb Plus DNA ladder (L) was included for molecular weight reference. The observed banding patterns indicate high conservation of restriction sites among the phages, supporting their genomic similarity and shared evolutionary origin.

5.3. Genome analyses

Following DNA extraction, the primary objectives were to obtain high-quality whole-genome sequences for the phage isolates, assemble these sequences into complete genomes and determine fundamental genomic characteristics. This included defining the genome size, G+C content, and topology (linear or circular) and identifying basic features such as the presence or absence of phage-encoded tRNA genes, which can indicate reliance on host machinery.

Genome Sequencing and Assembly

The genomes of 15 phages were sequenced, of which 13 (P1, P2, P3, P4, P5, P7, P8, S1, S2, S3, N1, N2 and N4) were assembled into complete, single-contig sequences using SPAdes. The remaining two phages, S4 and S5, were not successfully assembled into single contigs (Table 5.2). Following *de novo* assembly, quality control filtering and trimming were performed using Trimmomatic to ensure high-confidence sequence data.

Table 5.2. Contig stats of genome sequences of phages after assembly.

Phage ID	Contigs	Length bp	GC %	Topology
P1	Contig 1	37474	41.4	Linear dsDNA
P2	Contig 1	37490	41.4	Linear dsDNA
P3	Contig 1	37351	41.4	Linear dsDNA
P4	Contig 1	37353	41.4	Linear dsDNA
P5	Contig 1	38606	41.4	Linear dsDNA
P7	Contig 1	37542	41.4	Linear dsDNA
P8	Contig 1	38121	41.4	Linear dsDNA
S1	Contig 1	37351	41.4	Linear dsDNA
S2	Contig 1	39037	41.4	Linear dsDNA
S3	Contig 1	37334	41.4	Linear dsDNA
N1	Contig 1	37496	41.4	Linear dsDNA
N2	Contig 1	37654	41.4	Linear dsDNA

N4	Contig 1	37624	41.4	Linear dsDNA

Genome Size and Alignment

The genome sizes of the 13 completely assembled phages ranged from 37,334 bp to 39,037 bp. Alignment of these genomes using Geneious Prime revealed 99.6% sequence similarity among them (Figure 5.6). The sequence comparison showed that the core genome size of the isolates was 37,321 bp, with minor variations at the terminal regions (Figure 5.5). Automatic ORF prediction identified coding sequences (CDS) within these terminal regions, which were extracted for further analysis.

Comparison with Known Sequences

BLAST analysis of phage P1 against the NCBI database revealed that the closest related organism was *P. multocida* strain P1702, with 93% coverage and 92.55% identity (E-value: 0.0). The first 100 BLAST hits contained no phage genomes. Alignment of phage P1 with *P. multocida* strains ATCC43137 and P1702 identified regions of similarity corresponding to location 1,429,000–1,472,800 bp in the *P. multocida* genome, suggesting a potential genomic relationship between the phages and these bacterial strains (Figure 5.4).

Taxonomic Classification and Genome Properties

Analysis of the phage genomes using PhageAI, a machine learning-based classification tool, identified all 13 phages as belonging to the *Vieuvirus* genus. The classification algorithm predicted a 98.04% probability that these phages exhibit a temperate lifecycle.

tRNA Content and Genetic Elements

No tRNA sequences were detected in any of the phage genomes by tRNAscan and ARAGORN. Screening for antimicrobial resistance and virulence genes using AMRFinderPlus and ABRicate did not identify any resistance or virulence-associated genes in the phage genomes.

Genomic Characterisation

A total of 53 genes were identified in phage P1 using PHASTEST, with a GC content of 41.53% (Table 5.3). Of these, 39 were annotated as phage-related genes, while 15 exhibited similarities to bacterial genes. Among the phage-related genes, 22 were classified as hypothetical proteins. Further characterisation of these hypothetical proteins was performed using BLASTp, InterProScan and UniProt, with results summarised in Tables 5.4 and 5.5.

Comparative Genomics and Phylogenetic Analysis

Comparative genomic analysis of phage P1 using PHASTEST identified the most closely related bacteriophage genomes as *Haemophilus* phage SuMu (22 shared genes) and *Mannheimia* phage vB_MhM_3927AP2 (20 shared genes). Additional related phages included *Pseudomonas* phage B3, *Pseudomonas* phage FHA0480, *Pseudomonas* phage JBD93, *Ralstonia* phage RS138 and *Pseudomonas* phage JBD18, each sharing between 5 and 7 genes with phage P1 (Figure 5.8).

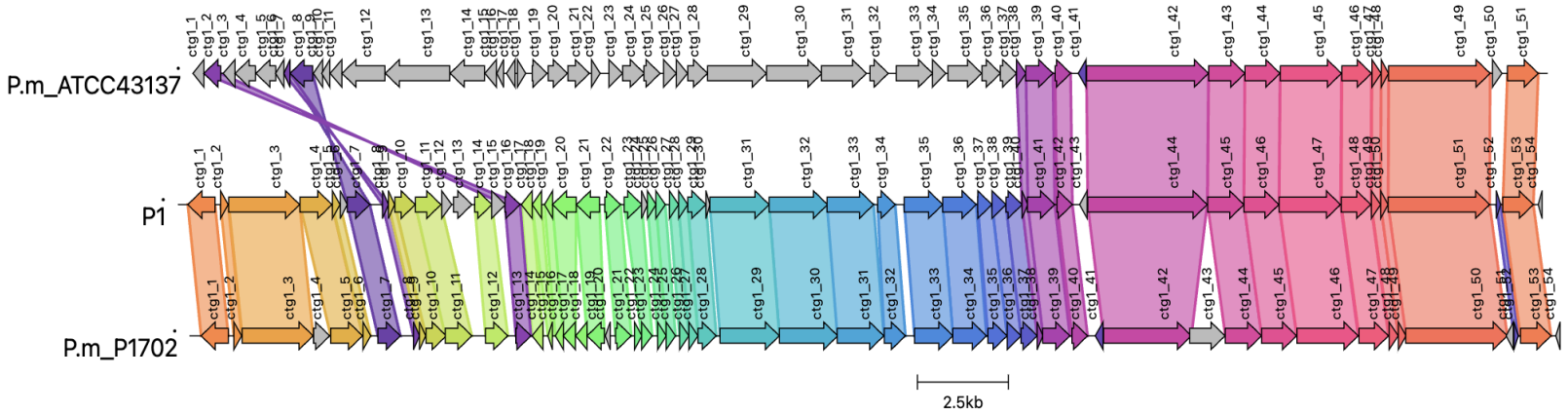

Figure 5.3. Comparative Genome Alignment of Phage P1 With *P. multocida* Strains ATCC 43137 And P1702.

Genome synteny analysis was performed using the Clinker tool (cagecat.bioinformatics.nl/) to compare the genomic organisation of phage P1 with its host strains, *P. multocida* ATCC 43137 (top row) and *P. multocida* P1702 (bottom row). Coloured arrows represent open reading frames (ORFs), with similar colours indicating homologous gene clusters across the genomes. Shaded regions connecting genes indicate high sequence similarity, with the intensity reflecting the degree of conservation. Phage P1 shares extensive sequence similarity with *P. multocida* P1702, particularly in the middle and right regions, suggesting possible integration into the bacterial chromosome. Less homology is observed between P1 and *P. multocida* ATCC 43137, indicating potential strain-specific integration or divergence in prophage regions. The first ~25% of P1's genome (orange/yellow regions) aligns strongly with P1702, while the remaining 75% shares homology with both host strains, suggesting modular genome architecture. Some non-homologous regions within P1 may represent phage-specific genes or recombination hotspots, potentially influencing host interactions or phage functionality. These findings support the hypothesis that phage P1 is a temperate phage capable of integrating into the *P. multocida* genome, playing a role in bacterial evolution and horizontal gene transfer. BLAST analysis of phage P1 against the NCBI database revealed that the closest related organism was *P. multocida* strain P1702, with 93% coverage and 92.55% identity (E-value: 0.0).

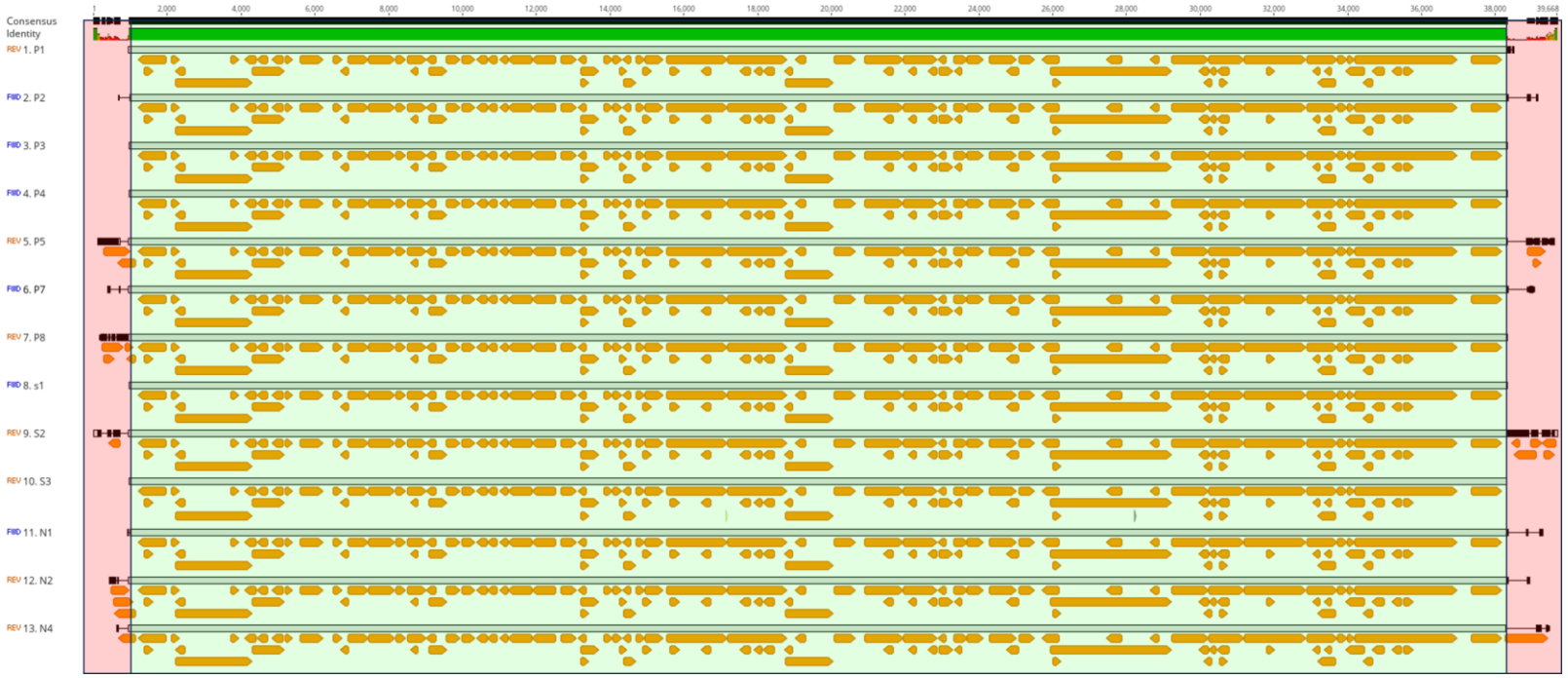

Figure 5.4. Open Reading Frame (ORF) Analysis of *P. multocida* Phages.

A total of 94 ORFs were identified across the phage genomes using a minimum threshold of 200 nucleotides and the standard bacterial start codons ATG, TTG and CTG. The genomic similarity between the phage isolates is depicted in green boxed regions, representing highly conserved gene blocks. Regions showing small sequence variations, particularly at the beginning and end of the genome sequences, are highlighted in red boxes, indicating minor structural or genetic differences. This image was generated using Geneious Prime 2024.0.4 to visualise genome-wide ORF distribution and comparative genomic conservation among the *P. multocida* phage isolates. The results suggest that these phages share a highly conserved core genome, with minor variations in terminal regions, possibly due to differences in genome packaging, integration sites or sequence assembly artifacts.

Figure 5.5. Linear representation of the phage P1 genome (37,474 bp).

The genome of phage P1 was visualized using PHASTEST in a linear format to annotate gene features, functional categories, and GC content distribution. This figure provides a comprehensive overview of the genomic architecture, highlighting key regions involved in replication, structural assembly, and host interaction. Outer Tracks – Annotated Genes: Phage-related genes are color-coded by function: Head, tail, and portal proteins (red, cyan, yellow): essential components for virion assembly. Terminase (green): involved in DNA packaging into the phage capsid. Phage-like regulatory proteins (blue): potential transcriptional regulators influencing host–phage interactions. Transposases (light blue): suggest mobile genetic elements or recombination hotspots. Bacterial genes (grey and orange): may represent horizontally transferred elements integrated into the phage genome. Inner Tracks – GC Content and Skew Analysis: The green track indicates GC content variation across the genome, offering insights into genomic composition and stability. The purple and pink tracks represent GC skew (+ and – strands, respectively), identifying asymmetries associated with replication origins or transcriptional directionality.

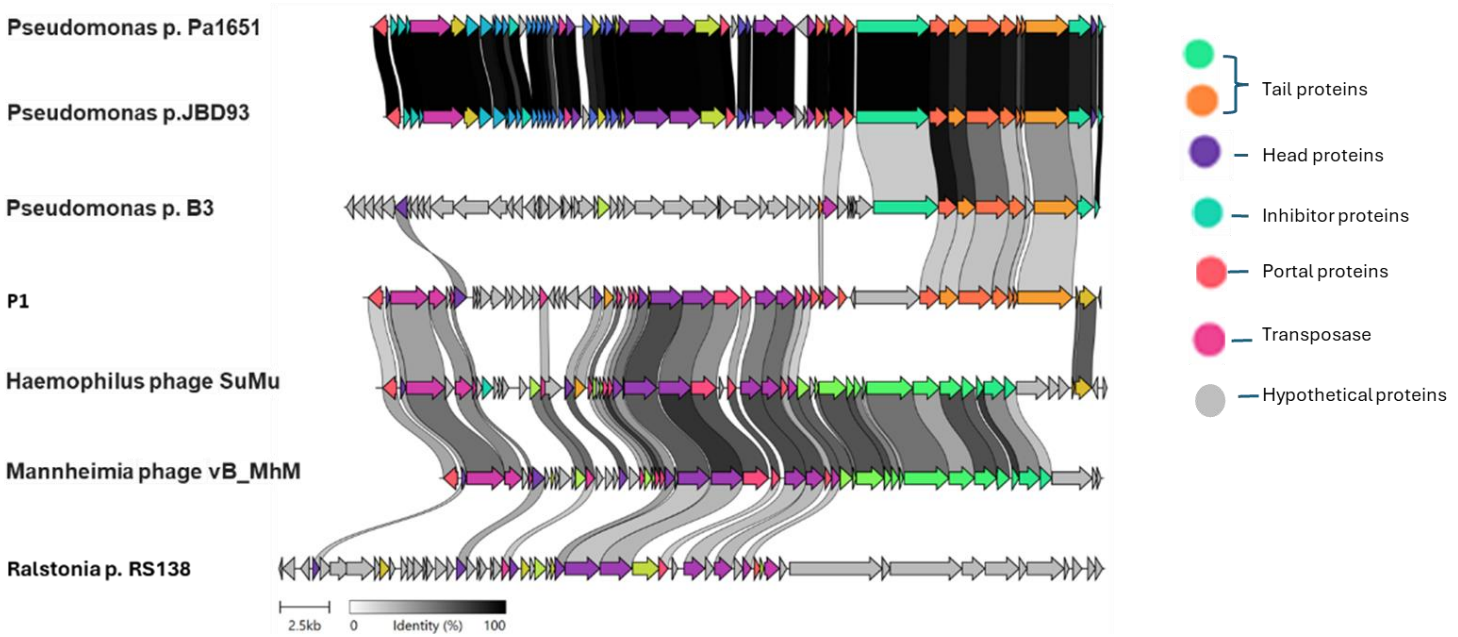

Figure 5.6. Comparative Genome Alignment of Phage P1 With Related Bacteriophages.

A whole-genome comparison was performed between phage P1 and closely related bacteriophages from different bacterial hosts, including *Pseudomonas, Haemophilus, Mannheimia* and *Ralstonia* phages. The analysis highlights gene conservation, structural similarities and evolutionary relationships. Coloured arrows represent different functional gene categories: Tail proteins (green) – Structural components for host recognition and infection. Head proteins (purple) – Capsid proteins involved in DNA packaging. Portal proteins (red) – Essential for genome entry and ejection. Transposases (pink) – Indicating mobile genetic elements and potential horizontal gene transfer. Inhibitor proteins (cyan) – Regulatory functions within the phage lifecycle. Hypothetical proteins (grey) – Genes with unknown function, requiring further characterisation. Shaded grey regions between genomes represent homologous sequences, with shading intensity reflecting sequence identity (scale 0–100%). The uppermost phages (Pseudomonas p. Pa1651 and JBD93) show high sequence conservation, while *Haemophilus* phage SuMu and *Mannheimia* phage vB_MhM exhibit moderate similarity with phage P1, suggesting shared ancestry. *Ralstonia* phage RS138 appears more distantly related, showing fewer conserved regions.

Alignment of P1 with these closely related phages revealed that the first 75% of the genome shared a high degree of similarity with *Haemophilus* phage SuMu and *Mannheimia* phage vB_MhM, while the remaining 25% of the genome was more similar to *Pseudomonas* phage B3 and *Pseudomonas* phage JBD93. A phylogenetic tree constructed from 80 phages (Figure 5.9) grouped the phages isolated in this study within the Mu-like phage cluster. The closest relative to the *P. multocida* phages was the *Pseudomonas* mu-like phage D3112, which was not among the top hits identified by PHASTEST. The next closest relatives were *Haemophilus* phage SuMu and *Mannheimia* phage vB_MhM. Other *P. multocida* phages from published studies were found in different phage families, including T7-like, lambda-like and other *Siphoviridae*-like phages.

Comparison with Published *P. multocida* Phage Genomes

To assess the genetic relationships between the newly isolated phages and previously characterised *P. multocida* phages, publicly available genomes were retrieved from NCBI and analysed using Clinker and VirClust (Figures 5.10 and 5.11). The comparative analysis revealed limited genetic similarity between the phages in this study and those reported in existing databases. Despite their classification within the same bacterial host, the genomes exhibited substantial variation in length and composition. Among the known *P. multocida* phages, Pm86 had the longest genome, measuring 56,048 bp, while F108 had the shortest, with a genome size of 30,505 bp. The GC content of these phages varied between 38.5% and 53.4%, yet no consistent pattern or correlation was observed between genome length and GC composition. While the newly isolated phages in this study shared a high degree of similarity among themselves, they exhibited only partial homology with previously published *P. multocida* phages.

Identification of Non-Core ORFs

Analysis of the non-core terminal ORFs from the 13 *P. multocida* phages revealed several unique genetic elements, with a mixture of hypothetical proteins and known functional genes (Table 5.6). Some ORFs exhibited strong homology to characterised proteins, suggesting potential roles in host interaction, metabolism or structural integrity. Among the notable findings, N2 ORF 43 shared 99.9% identity with a *P. multocida* metallo-beta-lactamase domain-containing protein, while N2 ORF 60 displayed 95.0% identity to a DctP family TRAP transporter solute-binding protein, a system involved in nutrient uptake. Similarly, N4 ORF 56 was identified as a C4-dicarboxylate transporter, a homologue of a protein found in *Haemophilus influenzae*, while S2 ORF 18 encoded a SIMPL domain-containing protein, known to participate in immune response regulation. Among the non-core ORFs, N2 ORF 60 (84 aa) showed homology to DctP family TRAP transporter solute-binding proteins from *P. multocida* and was also annotated as related to copper transport proteins based on UniProt analysis (Table 5.6).

Genome-Wide Protein Clustering Analysis

To further explore the evolutionary relationships and functional diversity of the phages, hierarchical clustering of viral protein families was performed using the VirClust tool (cagecat.bioinformatics.nl) (Figure 5.11). The analysis grouped phage proteins based on shared protein clusters (PSCs) and revealed a clear distinction between different *P. multocida* phage lineages. The newly isolated phages (P1–P8, S1–S3 and N1–N4) clustered together, reinforcing their common evolutionary origin and highly conserved core genome. In contrast, other *P. multocida* phages, such as PHB01, PHB02, PMP-GADVASU-IND and F108, formed distinct clusters, reflecting their genomic divergence from the phages in this study. The clustering analysis also

identified several unique proteins confined to specific viral genome clusters, which could indicate special host interactions or infection mechanisms. Additionally, a subset of proteins was found to be shared across multiple phage lineage.

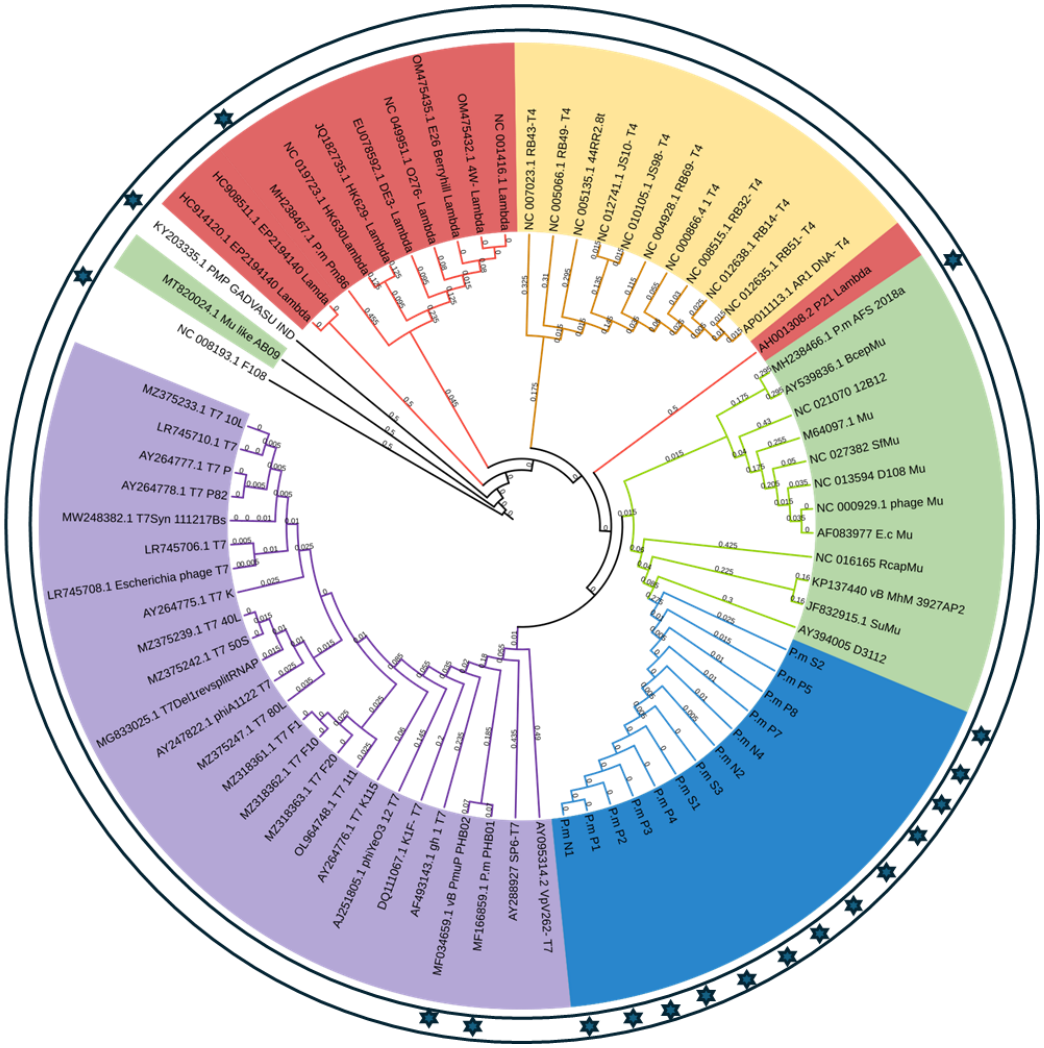

Figure 5.7. The phylogenetic tree includes 80 bacteriophages from various categories.

A maximum-likelihood phylogenetic tree was constructed to determine the evolutionary relationship of phage P1 with other known bacteriophages. The analysis was performed using the NGPhylogeny.fr web server, following a fully automated one-click workflow (Lemoine *et al.*, 2019), consisting of: Multiple Sequence Alignment (MAFFT) – Ensured accurate sequence alignment across all included phages. Alignment Curation (BMGE) – Removed poorly aligned regions to improve phylogenetic robustness. Tree Inference (PhyML) – Used maximum-likelihood estimation with automatic model selection to infer evolutionary relationships. Tree Rendering (Newick Display) – Produced a clear graphical representation of the evolutionary relationships among the phage isolates and reference genomes. Branches are colour-coded to represent distinct phage lineages, with bootstrap support values displayed on the nodes. The blue cluster represents the phages isolated in this study (P1, P2, P3, P4, P5, P7, P8, S1, S2, S3, N1, N2, N4), confirming their close evolutionary relationship. Green cluster includes Mu-like phages, such as *E. coli* Mu, Haemophilus phage SuMu and Mannheimia phage vB_MhM, suggesting that P1 and its relatives belong to the Mu-like phage family. Purple cluster includes T7-like phages, demonstrating clear divergence from the Mu-like lineage. Red and yellow clusters contain lambda-like and other temperate phages, showing distinct phylogenetic separation. Stars represents, *P. multocida*

specific phages. The positioning of PMP-GADVASU_IND (green cluster) and F108 (purple cluster) suggests their unique evolutionary history among *P. multocida* phages.

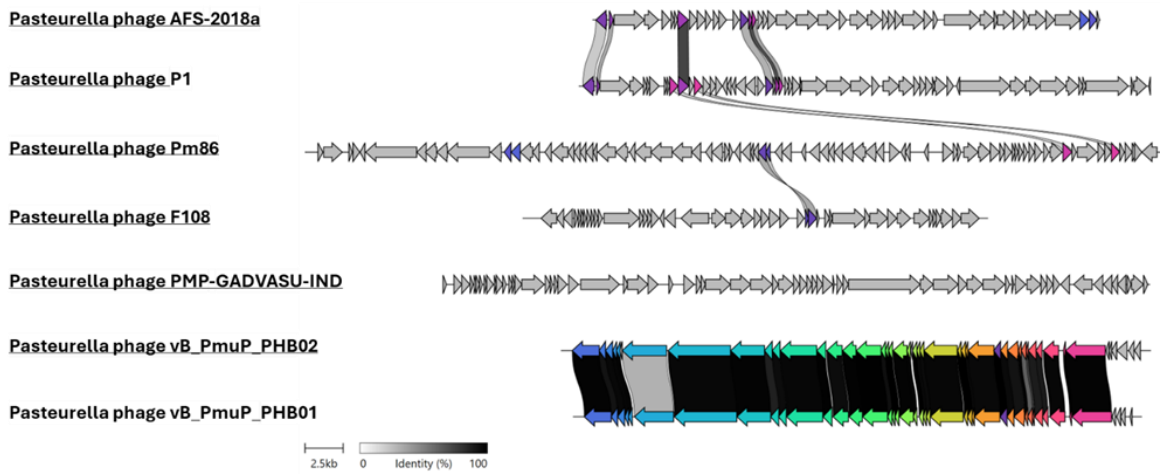

Figure 5.8. Comparative genome alignment of Pasteurella phage P1 with previously described *P. multocida* phages.

Except for phages PmuP_PHB01 and PmuP_PHB02, which were the isolates of the same study, none of the *P. multocida* phages share significant amounts of genes with each other. This explains why they clustered under different branches of phage families. The only phage which was also located under the Mu-like phages, AFS_2018a, shares 6 genes with phage P1; however, the identity of these genes is not significant.

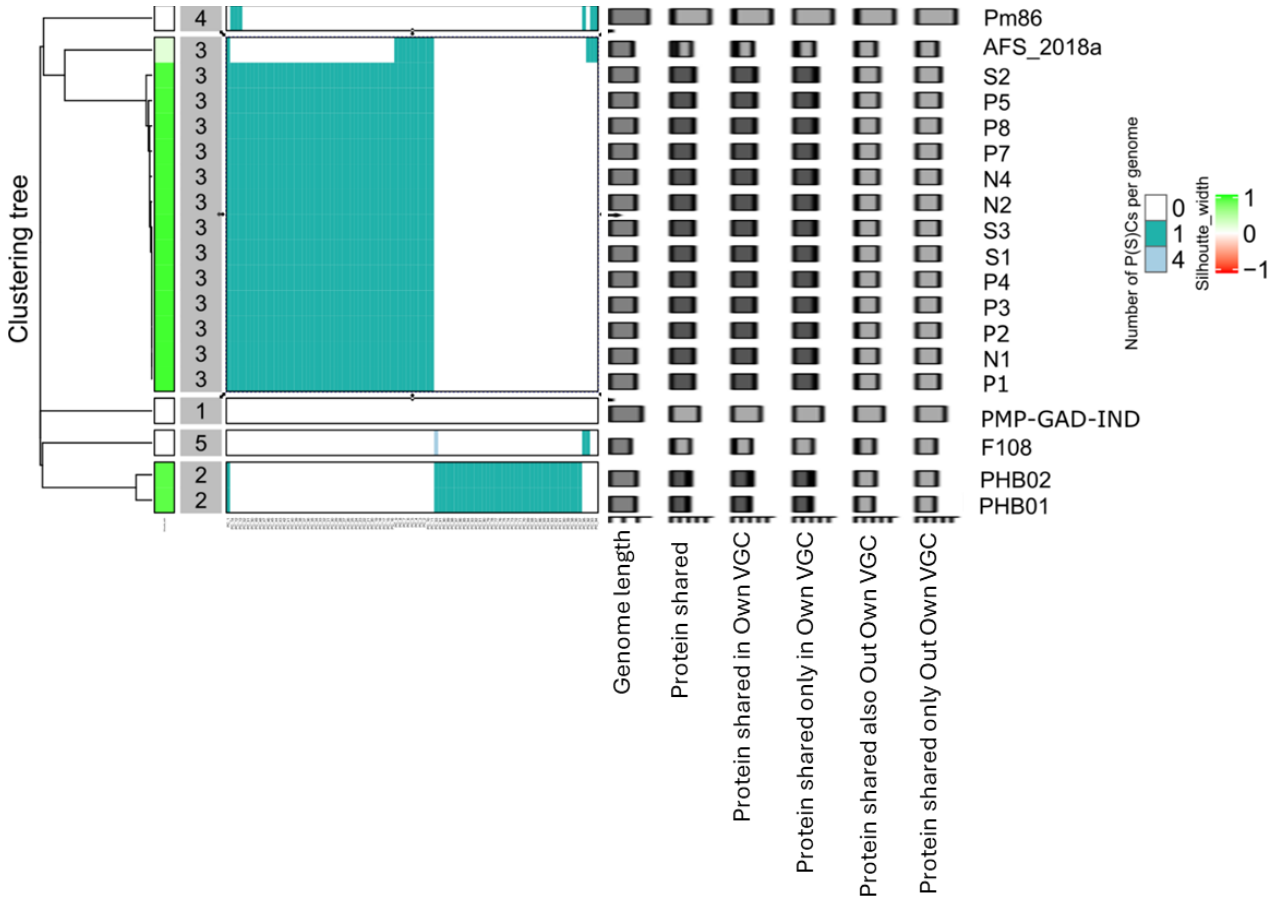

Figure 5.9. Grouping of Viral Proteins into Clusters of *P. multocida* Phages.

A hierarchical clustering analysis of viral protein families was performed using the VirClust tool (_cagecat.bioinformatics.nl), grouping phage proteins from *P. multocida* phages based on shared protein clusters (PSCs). The analysis provides insights into core and accessory proteins, as well as phage genome relationships. The clustering tree (left) groups phages based on their shared protein content, revealing distinct viral genome clusters (VGCs). Heatmap (centre) indicates the number of shared protein clusters per genome, with darker blue indicating higher values. Silhouette width (right scale) represents clustering confidence, with values ranging from -1 (poor clustering) to 1 (strong clustering). Black boxes (rightmost columns) summarise key protein-sharing statistics: Genome length – Total genome size for each phage. Protein shared – Number of proteins shared across genomes. Protein shared only in own VGC – Unique proteins confined to specific phage groups. Protein shared also out own VGC – Proteins present in multiple phage clusters. Protein shared only out own VGC – Proteins shared exclusively outside the cluster. The phages isolated in this study (P1–P8, S1–S3, N1–N4) cluster together, suggesting a common evolutionary origin and shared core genome. Phages PMP-GADVASU-IND, F108, PHB02 and PHB01 form distinct clusters, indicating significant genomic and functional divergence from other *P. multocida* phages. The presence of unique proteins within each VGC suggests that these phages may have evolved distinct host interactions or infection mechanisms. A subset of proteins is shared across multiple clusters, implying horizontal gene transfer or recombination between different *P. multocida* phages.

Table 5.3. Proteins Identified on Phage P1 Genome by PHASTEST.

CDS	Position	Top BLASTp Alignments	E-Value
1	270..1016	PP_00001;transcription regulator;phage;-;PHAGE_Haemop_SuMu_NC_019455	2.5e-32
2	1170..1379	PP_00002;Ner;phage;-;PHAGE_Escher_D108_NC_013594	6.06e-22
3	1396..3342	PP_00003;transposase;phage;-;PHAGE_Mannhe_vB_MhM_3927AP2_NC_028766	0.0
4	3353..4228	PP_00004;phage transposase;phage;-;PHAGE_Haemop_SuMu_NC_019455	1.09e-91
5	4460..4648	PP_00006;Gam;phage;-;PHAGE_Haemop_SuMu_NC_019455	5.12e-19
6	4651..5268	PP_00007;hypothetical protein;phage;-;PHAGE_Mannhe_vB_MhM_3927AP2_NC_028766	6.37e-96
7	5960..6517	PP_00010;hypothetical protein;phage;-;PHAGE_Entero_SfV_NC_003444	1.3e-24
8	6520..7221	PP_00011;hypothetical protein;phage;-;PHAGE_Aeromo_phiA8_29_NC_048660	4.38e-27
9	7567..8073	PP_00013;hypothetical protein;phage;-;PHAGE_Mannhe_vB_MhS_587AP2_NC_028743	1.2e-41
10	8150..8623	PP_00014;hypothetical protein;phage;-;PHAGE_Ralsto_RS138_NC_029107	4.95e-15
11	8983..9396	PP_00016;hypothetical protein;phage;-;PHAGE_Mannhe_vB_MhM_3927AP2_NC_028766	1.36e-30
12	11724..12155	PP_00022;hypothetical protein;phage;-;PHAGE_Haemop_SuMu_NC_019455	2.54e-36
13	12256..12741	PP_00023;c;-;PHAGE_Haemop_SuMu_NC_019455	1.97e-42
14	12895..13131	PP_00025;hypothetical protein;phage;-;PHAGE_Haemop_SuMu_NC_019455	3.74e-28
15	13499..13753	PP_00027;hypothetical protein;phage;-;PHAGE_Mannhe_vB_MhM_3927AP2_NC_028766	1.03e-11
16	13753..14001	PP_00028;hypothetical protein;phage;-;PHAGE_Mannhe_vB_MhM_3927AP2_NC_028766	9.48e-10
17	14005..14502	PP_00029;conserved possible DNA-binding protein;phage;-;PHAGE_Haemop_SuMu_NC_019455	2.78e-72
18	14609..16237	PP_00031;terminase;phage;-;PHAGE_Haemop_SuMu_NC_019455	0.0
19	16238..17842	PP_00032;portal protein gp29;phage;-;PHAGE_Haemop_SuMu_NC_019455	0.0
20	17829..19106	PP_00033;head morphogenesis protein;phage;-;PHAGE_Mannhe_vB_MhM_3927AP2_NC_028766	7.58e-142
21	19218..19700	PP_00034;putative capsid and scaffold protein;phage;-;PHAGE_Pseudo_vB_PaeS_PAO1_Ab30_NC_026601	1.54e-11
22	19949..21004	PP_00035;bacteriophage Mu I protein gp32;phage;-;PHAGE_Haemop_SuMu_NC_019455	1.53e-140
23	21004..21924	PP_00036;major head subunit T;phage;-;PHAGE_Mannhe_vB_MhM_3927AP2_NC_028766	4.75e-146
24	21967..22356	PP_00037;hypothetical protein;phage;-;PHAGE_Haemop_SuMu_NC_019455	1.61e-24
25	22360..22743	PP_00038;hypothetical protein;phage;-;PHAGE_Ralsto_RS138_NC_029107	7.76e-24
26	22740..23186	PP_00039;hypothetical protein;phage;-;PHAGE_Pseudo_D3112_NC_005178	1.07e-26
27	23183..23341	PP_00040;hypothetical protein;phage;-;PHAGE_Pseudo_B3_NC_006548	3.52e-07
28	23334..24080	PP_00041;hypothetical protein;phage;-;PHAGE_Pseudo_JBD24_NC_020203	1.86e-47
29	24141..24566	PP_00042;hypothetical protein;phage;-;PHAGE_Pseudo_JBD93_NC_030918	1.09e-23
30	24988..28269	PP_00044;tail length tape measure protein;phage;-;PHAGE_Mannhe_vB_MhS_1152AP2_NC_028956	1.08e-36
31	28282..29277	PP_00045;hypothetical protein;phage;-;PHAGE_Pseudo_B3_NC_006548	1.61e-40
32	29280..30239	PP_00046;hypothetical protein;phage;-;PHAGE_Pseudo_vB_PaeS_PM105_NC_028667	2.53e-31
33	30247..31929	PP_00047;hypothetical protein;phage;-;PHAGE_Pseudo_DMS3_NC_008717	5.16e-111
34	31954..32763	PP_00048;Uncharacterised+conserved+protein, phage+conserved+hypothetical+protein+BR0599, Phage+conserved+hypothetical+protein+BR0599;phage;-;PHAGE_Salmon_YSD1_NC_048666	1.25e-58
35	32780..33031	PP_00049;putative tail assembly protein 1;phage;-;PHAGE_Proteu_pPM_01_NC_028812	2.0e-17
36	33035..33238	PP_00050;tail assembly protein;phage;-;PHAGE_Vibrio_VpKK5_NC_026610	3.02e-13
37	33238..36027	PP_00051;conserved tail assembly protein;phage;-;PHAGE_Burkho_BcepNazgul_NC_005091	1.88e-143
38	36211..36330	PP_00052;Mu-like prophage protein Com;phage;-;PHAGE_Haemop_SuMu_NC_019455	1.62e-09
39	36389..37228	PP_00053;hypothetical protein;phage;-;PHAGE_Haemop_SuMu_NC_019455	1.15e-145

Table 5.4. Top Hists of Hypothetical Proteins on Phage P1 Genome After BLASTp Search (Phage Proteins).

Gene identifier	Length bps	LOCATION (bp)	BLASTp	Query Cover	E-value	Accession Number	Closest phage
PP_00007	618	4651..5268	DUF3164 family protein [*P. multocida*]	100%	2e-146	WP_324622965.1	Mannhe_vB_MhM_3927AP2_NC_028766
PP_00010	558	5960..6517	YfbR-like 5'-deoxynucleotidase [*P. multocida*]	100%	4e-134	WP_083004347.1	Entero_SfV_NC_003444
PP_00011	702	6520..7221	DUF2786 domain-containing protein [*P. multocida*]	100%	6e-172	WP_241951944.1	Aeromo_phiA8_29_NC_048660
PP_00013	507	7567..8073	TPA: DUF551 domain-containing protein [*P. multocida*]	100%	1e-121	HDR1847548.1	Mannhe_vB_MhS_587AP2_NC_028743
PP_00014	474	8150..8623	HP 1 [*P. multocida*]	100%	1e-112	WP_324622963.1	Ralsto_RS138_NC_029107
PP_00016	414	8983..9396	regulatory protein GemA [*P. multocida*]	99%	8e-91	WP_078801742.1	Mannhe_vB_MhM_3927AP2_NC_028766
PP_00022	432	11724..12155	TPA: mor transcription activator family protein [*P. multocida*]	100%	3e-101	HDR1236391.1	Haemop_SuMu_NC_019455

PP_00025	237	12895..13131	TPA: DUF2644 domain-containing protein [*P. multocida*]	100%	8e-49	HDR1278029.1	Haemop_SuMu_NC_019455
PP_00027	255	13499..13753	HP 2 [*P. multocida*]	100%	2e-52	WP_271343946.1	Mannhe_vB_MhM_3927AP2_NC_028766
PP_00028	249	13753..14001	HP 3 [*P. multocida*]	100%	1e-47	WP_271343947.1	Mannhe_vB_MhM_3927AP2_NC_028766
PP_00037	390	21967..22356	HP 4 [*P. multocida*]	100%	1e-79	WP_313904013.1	Haemop_SuMu_NC_019455
PP_00038	384	22360..22743	DUF1320 domain-containing protein [*P. multocida*]	100%	3e-88	WP_064972860.1	Ralsto_RS138_NC_029107
PP_00039	447	22740..23186	HP 5 [*P. multocida*]	100%	5e-103	HDR1365454.1	Pseudo_D3112_NC_005178
PP_00040	159	23183..23341	HP 6 [*P. multocida*]	100%	1e-27	HDR1365453.1	Pseudo_B3_NC_006548
PP_00041	747	23334..24080	HP 7 [*P. multocida*]				Pseudo_JBD24_NC_020203
PP_00042	426	24141..24566	DUF6631 family protein [*P. multocida*]	100%	7e-92	WP_250023819.1	Pseudo_JBD93_NC_030918
PP_00045	996	28282..29277	HP 8 [*P. multocida*]	100%	0.0	WP_064972863.1	Pseudo_B3_NC_006548
PP_00046	960	29280..30239	HP 9 [*P. multocida*]	100%	0.0	WP_250023822.1	Pseudo_vB_PaeS_PM105_NC_028667
PP_00047	1683	30247..31929	phage tail protein [*P. multocida*]	100%	0.0	WP_250037372.1	Pseudo_DMS3_NC_008717
PP_00048	810	31954..32763	phage BR0599 family protein [*P. multocida*]	100%	0.0	WP_005755567.1	Salmon_YSD1_NC_048666
PP_00053	840	36389..37228	HP 10 [*P. multocida*]	100%	0.0	WP_324622933.1	Haemop_SuMu_NC_019455

Table 5.5. BLASTp Results of Bacterial Hypothetical Proteins on Phage N1 Genome.

Gene identifier	LENGTH bps	LOCATION (bp)	BLASTp	Query Cover	E-value	Accession Number
PP-00005	210	4242..4451	HP 11 [*P. multocida*]	100%	7e-46	WP_005755565.1
PP-00008	168	5617..5784	HP 12 [*P. multocida*]	100%	3e-30	WP_324622964.1
PP_00009	171	5781..5951	HP 13 [*P. multocida*]	100%	1e-28	WP_005725244.1
PP_00012	276	7245..7520	HP 14 [*P. multocida*]	100%	6e-60	WP_241951943.1
PP_00015	381	8616..8996	HP 15 [*P. multocida*]	100%	3e-85	
PP_00017	297	9431..9727	HP 17 [*P. multocida*]	100%	7e-65	HDR1902459.1
PP_00018	258	9730..9987	HP 16 [*P. multocida*]	100%	2e-54	WP_064972844.1
PP_00019	222	10088..10309	**CopG family transcriptionalregulator**	100%	4e-45	HDR1236394.1
PP_00020	654	10286..10939	HP 17 [*P. multocida*]	100%	5e-158	HDR1236393.1
PP_00021	636	10942..11577	HP 18 [*P. multocida*]	100%	5e-148	HDR1845897.1
PP_00024	165	12734..12898	HP 19 [*P. multocida*]	100%	1e-30	HDR1278028.1
PP_00026	258	13128..13385	**DUF2681 domain-containing protein** [*P. multocida*]	100%	2e-53	HDR1278030.1
PP_00030	111	14502..14612	HP 20 [*P. multocida*]	100%	2e-14	ESQ72722.1
PP_00043	207	24765..24971	HP 21 [*P. multocida*]	100%	2e-39	HDX1164835.1
PP_00054	111	37362..37472	**chromosome partition protein MukB** [*P. multocida*]	97%	3e-14	WP_016532845.1

Table 5.6. Non-Core Terminal ORFs After Alignment of 13 *P. multocida* Phages of This Study.

		NCBI BLASTp Annotation				**InterProScan Annotation**	**UniProt BLAST Annotation**		
ORF ID	Length (aa)		Coverage (%)	E-value	Identity (%)			Identity (%)	E-value
N2 ORF 25	92	NSSF*	-	-	-	Cytoplasmic and transmembrane domain	HAT C-terminal dimerisation protein	33.3	2.9
N2 ORF 43	69	Metallo-hydrolase (*P. multocida*)	100	3e-3a9	99.9	MBL Glyoxalase II (IPR051453)	Metallo-beta-lactamase domain	95.7	8.3E-49
N2 ORF 60	84	DctP family TRAP transporter *(P. multocida*)	23	0.011	95.0	NSSF	Copper transport protein	34.5	0.5
N4 ORF 42	66	NSSF	-	-	-	Cytoplasmic and transmembrane domain	Fork head domain protein FD3	40.3	0.58
N4 ORF 56	76	C4-dicarboxylate transporter (*H. influenzae)*	-	-	-	C4-dicarboxylate transmembrane transporter	C4-dicarboxylate ABC transporter	-	-
P5 ORF 25	76	NSSF	-	-	-	NSSF*	Histone acetyltransferase	-	-
P5 ORF 43	136	YopT-type cysteine protease (*P. multocida)*	-	-	-	NSSF*	Large supernatant protein 1	-	-
P5 ORF 65	72	NSSF	-	-	-	NSSF*	NSSF	-	-
P5 ORF 82	158	Aminoacetone oxidase family FAD-binding enzyme (*P. multocida*)	-	-	-	3-Dehydro-bile acid delta(4,6)-reductase-like	NAD(P)/FAD-dependent oxidoreductase	-	-
P8 ORF 43	190	4'-phosphopantetheinyl transferase superfamily protein (*P. multocida*)	-	-	-	Phosphopantetheinyl Transferase Superfamily	Putative 4'-phosphopantetheinyl transferase PM0116	-	-
P8 ORF 60	90	NSSF*	-	-	-	TMhelix	NSSF	-	-

S2 ORF 18	120	SIMPL domain protein (*P. multocida*)	-	-	-	Interleukin-1 receptor-associated kinase 1-binding protein 1/DUF541	DUF541 domain-containing protein	-	-
S2 ORF 19	202	Peptidylprolyl isomerase (*P. multocida*)	-	-	-	Peptidyl-prolyl cis-trans isomerase activity	FKBP-type peptidyl-prolyl cis-trans isomerase SlyD	-	-
S2 ORF 37	76	NSSF*	-	-	-	TMHMM TMhelix	ABC transmembrane type-1 domain	-	-
S2 ORF 96	72	NSSF*	-	-	-	NSSF*	Probable nicotinate-nucleotide adenylyltransferase	-	-
S2 ORF 97	90	NSSF*	-	-	-	NSSF*	Raptor N-terminal CASPase-like domain	-	-

Note. This table presents the annotations and characteristics of selected non-core open reading frames (ORFs) located near the termini of the phage genomes. Annotations were derived using multiple platforms: NCBI BLASTp for protein homology, InterProScan for domain architecture and functional predictions, and UniProt BLAST for curated protein function information. ORFs marked as NSSF (*) indicate no significant similarity found in the corresponding database. ORF length is shown in amino acids (aa), and the most relevant hits include percentage identity, coverage, and E-value where available. Despite some ORFs lacking homology to known proteins, predicted features such as transmembrane domains or enzymatic functions were identified, indicating potential novel or poorly characterised gene functions at the phage genome termini.

Table 5.7. Summary of BLASTn Search Results Using Phage P1 Genome as Query Against the NCBI nr/nt Database (Top 30 Matches).

Organism	Scientific Name	Coverage	E—value	Per. Identity	Accession
P. multocida strain P1702 chromosome, complete genome	*P. multocida*	93%	0.0	92.55%	CP097616.1
Pasteurella canis strain HL_D3081 chromosome, complete genome	Pasteurella canis	91%	0.0	88.58%	CP085873.1
P. multocida strain 19BRD-057 chromosome, complete genome	*P. multocida*	61%	0.0	90.25%	CP123618.1
P. multocida strain 17BRD-035 chromosome, complete genome	*P. multocida*	61%	0.0	90.25%	CP082272.1
P. multocida strain RCAD0726 chromosome, complete genome	*P. multocida*	60%	0.0	90.01%	CP059703.1
P. multocida strain GS2020-X2 chromosome, complete genome	*P. multocida*	36%	0.0	95.13%	CP076113.1
P. multocida strain Ban-PM7 chromosome	*P. multocida*	30%	0.0	90.96%	CP052765.1
P. multocida strain Ban-PM4 chromosome	*P. multocida*	30%	0.0	90.96%	CP052764.1
P. multocida strain 33011 chromosome, complete genome	*P. multocida*	32%	0.0	89.34%	CP097612.1
P. multocida strain 32985 chromosome, complete genome	*P. multocida*	32%	0.0	89.34%	CP097610.1
P. multocida strain FDAARGOS_216 chromosome, complete genome	*P. multocida*	29%	0.0	89.32%	CP020403.2
P. multocida strain KVNON-213 chromosome, complete genome	*P. multocida*	28%	0.0	89.30%	CP049756.1
P. multocida strain 29792 chromosome, complete genome	*P. multocida*	29%	0.0	87.73%	CP097798.1
P. multocida strain BRMSA 1201	*P. multocida*	28%	0.0	87.73%	MG023086.1
P. multocida strain BRMSA 1199	*P. multocida*	28%	0.0	87.73%	MG023085.1
P. multocida strain NCTC10322 genome assembly, chromosome: 1	*P. multocida*	30%	0.0	87.73%	LT906458.1
P. multocida strain Pm6 chromosome, complete genome		29%	0.0	87.73%	CP154470.1
P. multocida strain 80176 chromosome, complete genome	*P. multocida*	29%	0.0	87.73%	CP135196.1
P. multocida strain LXSS001 chromosome, complete genome	*P. multocida*	61%	0.0	87.73%	CP119523.1

P. multocida strain 29135 chromosome, complete genome	*P. multocida*	29%	0.0	87.73%	CP097797.1
P. multocida strain ATCC 43137, complete genome	*P. multocida*	30%	0.0	87.73%	CP008918.1
P. multocida strain SD001 chromosome, complete genome	*P. multocida*	29%	0.0	87.73%	CP090428.1
P. multocida strain PM 8-6 chromosome, complete genome	*P. multocida*	30%	0.0	87.71%	CP040918.1
P. multocida strain EB104 chromosome, complete genome	*P. multocida*	30%	0.0	87.71%	CP040848.1
P. multocida strain BS168 chromosome, complete genome	*P. multocida*	30%	0.0	87.71%	CP031554.1
P. multocida strain EB168 chromosome, complete genome	*P. multocida*	30%	0.0	87.71%	CP031553.1
P. multocida strain TB168 chromosome, complete genome	*P. multocida*	30%	0.0	87.71%	CP031552.1
P. multocida strain PM8-1 chromosome, complete genome	*P. multocida*	30%	0.0	87.71%	CP031551.1
P. multocida subs*P. multocida* str. 3480, complete genome	*P. multocida* subs*P. multocida* str. 3480	29%	0.0	87.71%	CP001409.1
P. multocida subs*P. multocida* str. HB03, complete genome	*P. multocida* subs*P. multocida* str. HB03	30%	0.0	87.69%	CP003328.1

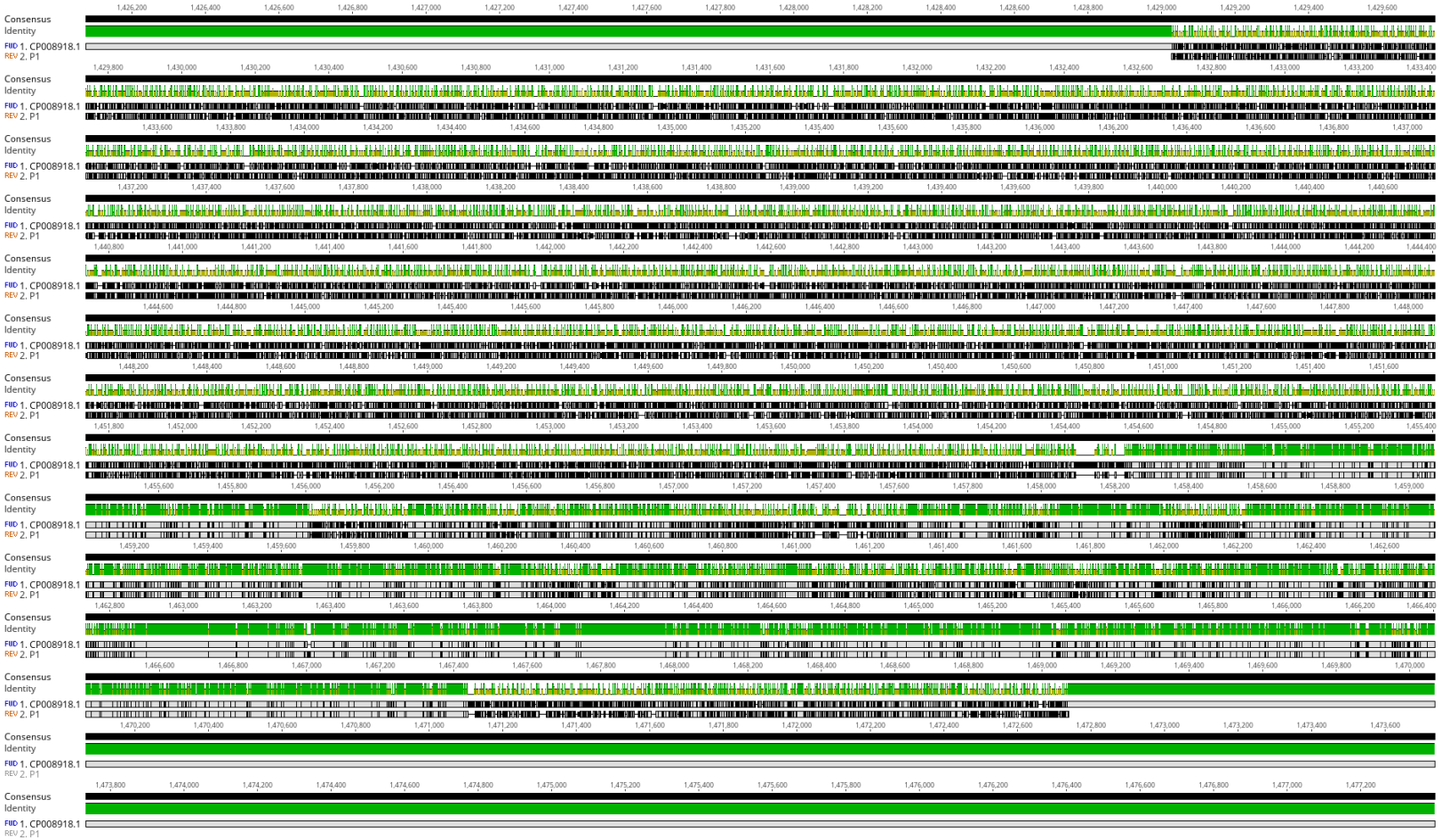

Figure 5.10. Alignments of Phage P1 Genome with *P. multocida* ATCC43137 genome.

The alignment compares the Phage P1 genome (Bottom track, labelled 2.P1) with a homologous region within the *P. multocida* ATCC 43137 chromosome (Top track, CP009681.1). The visualized bacterial region spans approximately base pairs 1,429,000 to 1,472,800. Blocks represent homologous regions connected by lines/shading, indicating sequence similarity. An average nucleotide identity of 60.69% was calculated for this aligned region. Alignment generated using Genius Prime software.

5.4. Discussion

This study presents a genomic analysis of 13 bacteriophages isolated on *P. multocida* PM13 and ATCC43137 strains. Multiple genome alignments revealed that the isolates were highly similar, with approximately 99.6% sequence identity. This high level of conservation is likely due to their shared origin from the same pooled sewage sample, was further supported by identical restriction enzyme digestion patterns observed prior to sequencing. In hindsight, using multiple independent environmental sources might have provided greater genomic diversity, but this was impossible due to site access restrictions during sample collection. Minor variations in DNA purity were observed, with 260/280 ratios slightly below optimal for five isolates; while most genomes assembled completely, potential contamination or other factors may have contributed to the incomplete assembly of phages S4 and S5.

Genome Size and Composition in Comparison to Published *P. multocida* Phages

The assembled phage genomes ranged in size from 37,334 to 39,037 bp, with a highly conserved core genome of 37,321 bp. This places them within the typical size range of *P. multocida* phages, which vary widely between approximately 30.5 kb (*Pasteurella* phage F108) and 56 kb (*Pasteurella* phage Pm86) (Campoy *et al.,* 2006; Fillol-Salom *et al.,* 2018). Our phages share a genome size similar to *Pasteurella* phage PHB01 (37,287 bp), a *Podoviridae* phage described by Chen *et al*. (2019). However, despite similarities in size and G+C content (41.4% in our phages vs. 40.8% in PHB01 and 40.7% in PHB02), comparative analysis revealed significant genetic differences between our isolates and PHB01/PHB02. The phylogenetic analysis confirmed that our isolates cluster separately, indicating they belong to a distinct lineage of *P. multocida* phages. In contrast to virulent *P. multocida* phages such as PHB01 and PHB02, which are strictly

lytic (Chen *et al.,* 2019), our isolates exhibit genomic features indicative of temperate phages, as will be discussed below. The G+C content of our phages closely matches that of their host genomes (*P. multocida* ATCC43137 and *P. multocida* P1702 at 41.1% and 40.4%, respectively), suggesting a long-term evolutionary association between these phages and their host strains (Qureshi *et al.,* 2018).

The comparison with previously published *P. multocida* phages underscores the genetic diversity of phages infecting this host. As visualised by VirClust analysis, our isolates form a distinct, tight cluster separate from other known *P. multocida* phages like F108, PHB01/02, and PMP-GADVASU-IND, which belong to different phylogenetic groups. This highlights that our study characterises a specific lineage of Mu-like temperate phages infecting *P. multocida*, which appears genetically distinct from most previously described phages for this bacterium.

Prophage Integration and Temperate Nature of the Isolates

The BLAST search results indicate that our phage genomes exhibit high similarity to *P. multocida* strain P1702, covering 93% of the genome with 92.55% sequence identity and align well with the ATCC43137 strain. This suggests that these phages may have integrated into the bacterial genome as prophages. Crucially, the top 100 BLASTn hits against the NCBI database were bacterial genomes, with no phage genomes appearing among the closest matches, strongly suggesting these sequences represent integrated prophages within *P. multocida* hosts like P1702 and that these phages are distinct from currently sequenced and deposited bacteriophages.

Alignment of our phage genomes with *P. multocida* P1702 identified a specific integration site between 1,429,000 and 1,472,800 bp, reinforcing the hypothesis that these are temperate phages capable of lysogeny. The presence of key genes involved in integration and recombination

supports this classification. Our isolates encode transposase genes, which facilitate site-specific integration, a hallmark of temperate phages (Harshey, 2014). Additionally, the absence of tRNA genes, detected using tRNAscan and ARAGORN, is another characteristic feature of temperate phages (Bailly-Bechet *et al.,* 2007). Temperate phages generally lack extensive tRNA repertoires, as they rely on the host translation machinery for protein synthesis. Further supporting their temperate nature, PhageAI, an artificial intelligence-based prediction tool, classified our isolates as temperate phages with a 98.04% confidence level. This aligns with previous studies where phage life cycle predictions using machine learning have accurately classified phages into virulent and temperate groups (Tynecki *et al.,* 2020).

Comparative Genomic and Phylogenetic Analysis

Comparative analyses using PHASTEST revealed that our phages share the highest similarity with *Haemophilus* phage SuMu, *Mannheimia* phage vB_MhM_3927AP2 and *Pseudomonas* phages B3 and FHA0480. While the first 75% of our phage genomes resemble *Haemophilus* and *Mannheimia* phages, the remaining 25% share similarity with *Pseudomonas* phages. This suggests that our phages may have undergone recombination events, incorporating genetic material from phages infecting different bacterial species. Horizontal gene transfer is a well-documented phenomenon among phages, allowing them to adapt to new hosts and environmental niches (Shackelton and Holmes, 2004).

Phylogenetic analysis further confirms that our phages belong to the Mu-like phage cluster, grouping closely with *P. multocida* phage ASF_2018a (Fillol-Salom *et al.,* 2018). Their placement within the Mu-like phage cluster is significant, as Mu-like phages are known for their replicative transposition mechanism and typically temperate lifecycles (Harshey, 2014),

consistent with our findings of transposase genes and predicted temperate nature. Unlike T7-like and lambda-like *P. multocida* phages, which fall into distinct evolutionary branches, Mu-like phages exhibit a modular genome structure, where gene modules are exchanged through recombination. This modularity may explain the observed genetic differences between our isolates and previously characterised *P. multocida* phages.

While comparative analysis based on shared gene content identified *Haemophilus* phage SuMu as having the most shared genes, whole-genome phylogenetic analysis placed *Pseudomonas* phage D3112 as the closest relative in the tree. This might reflect the different methodologies, with PHASTEST focusing on gene content similarity and phylogenetic inference capturing broader evolutionary signals across the entire genome, potentially influenced by the modular nature and recombination events common in Mu-like phages.

Hypothetical Proteins and Functional Predictions

A significant portion of the predicted ORFs in our phage isolates are annotated as hypothetical proteins. PHASTEST identified 53 genes in the P1 genome, of which 39 were classified as phage genes and 15 as bacterial genes. Among the phage genes, 22 were hypothetical proteins with no known function. Some hypothetical proteins showed weak similarity to those involved in DNA replication, transcriptional regulation or structural components. For instance, PP_00007 matched the DUF3164 family protein, which has been associated with metal ion insertases and stress responses (Reed *et al.,* 2021). Similarly, PP_00010, identified as YfbR-like 5'-deoxynucleotides, may play a role in nucleotide metabolism, a function known to be associated with phage-host interactions (Weiss, 2007). The non-core ORFs included genes that may be linked to host adaptation or lysogeny. For example, N2 ORF 60,

identified as a DctP family TRAP transporter solute-binding protein (SBP), suggests potential involvement in nutrient uptake or environmental sensing (Mulligan *et al.,* 2011). Tripartite ATP-independent periplasmic (TRAP) transporters are prevalent in prokaryotes, utilising high-affinity SBP (like the DctP family) to scavenge essential nutrients, primarily organic acids, relying on ion gradients for import rather than ATP (Mulligan *et al.,* 2011; Kelly and Thomas, 2001). The presence of a gene encoding just the SBP component in phage N2 is noteworthy. While potentially representing a horizontally transferred genetic remnant from a bacterial host rich in such transporters (Mulligan *et al.,* 2011), its retention could imply a functional role. If expressed, it might interact with or interfere with the host's own nutrient uptake systems, although its function without the corresponding membrane components remains unclear. The alternative annotation relating it to copper transport proteins is less directly associated with the canonical function of DctP family SBPs and requires further investigation. Regardless, the presence of N2 ORF 60 exemplifies the acquisition of bacterial-like genes by these phages, underscoring the need for functional studies to elucidate the actual roles and potential impacts of these non-core genes, particularly in the context of phage-host interactions and safety assessments.

Furthermore, the identification of S2 ORF 18, encoding a protein homologous to the mammalian interleukin-1 receptor-associated kinase 1-binding protein 1 (IRAK1BP1, containing a DUF541 domain), is noteworthy. While proteins containing this domain are implicated in immune modulation in mammalian systems (Vig *et al*., 2001), their function within a bacteriophage or its bacterial host is unclear, potentially suggesting an unusual interaction with host signalling or defence pathways that warrants further investigation. While its function in *P. multocida* phages remains unclear, it raises interesting questions about potential interactions

with bacterial host defence mechanisms. Other non-core genes like the predicted C4-dicarboxylate transporter (N4 ORF 56) could potentially modify host metabolism, while the peptidylprolyl isomerase (S2 ORF 19) might assist in the folding of phage or host proteins during infection or assembly.

Another notable finding among the non-core ORFs was N2 ORF 43, which encodes a protein with high identity (99.9%) to a *P. multocida* protein containing a metallo-beta-lactamase (MBL) domain, annotated by InterProScan and UniProt as related to MBL Glyoxalase II. The MBL superfamily fold is known for its functional diversity beyond antibiotic resistance; proteins with this fold are found across all life domains and participate in various cellular processes, including detoxification (like glyoxalase II, which degrades methylglyoxal), nucleic acid metabolism, and redox chemistry (PettinatiI *et al*., 2016). Glyoxalase II activity itself is crucial for bacterial survival and stress response (Scirè *et al.,* 2022; Haris *et al*., 2022).

While standard screening tools did not identify N2 ORF 43 as a canonical antibiotic resistance gene, the presence of an MBL domain warrants careful consideration. Genes encoding MBL-fold proteins have been identified in other bacteriophages (Joshi *et al.,* 2024). For instance, certain *Bacillus* phage MBL-fold proteins primarily function in anti-defence mechanisms (anti-Pycsar activity) but have been shown to possess promiscuous beta-lactamase activity *in vitro* (Joshi *et al.,* 2024). This suggests that even if the primary role of N2 ORF 43 is metabolic (e.g., related to glyoxalase II), the MBL fold itself represents a structural scaffold associated with β-lactam hydrolysis.

Therefore, although AMRFinderPlus and ABRicate screenings were negative, the identification of this MBL domain highlights a potential, albeit perhaps low, risk associated with

phage N2. It underscores the point that phages can acquire and potentially transfer genetic material (Muniesa *et al*., 2004) and that MBL-fold proteins might constitute an underexplored reservoir for resistance functions (Joshi *et al.,* 2024). This finding strongly supports the need for detailed functional characterisation of this specific protein (N2 ORF 43), as recommended in the future work, to experimentally determine its actual enzymatic activity (e.g., glyoxalase II activity versus potential β-lactamase activity) and fully assess its implications for therapeutic safety.

Further investigation into these hypothetical proteins is essential. For example, the presence of several predicted regulatory proteins (e.g., CopG family PP_00019, mor activator family PP_00022) may play roles in controlling the phage's lifecycle or responding to host conditions. The identification of 15 bacterial-like genes by PHASTEST also merits attention, reinforcing the potential for horizontal gene transfer.

Given the extremely high core genome identity (99.6%) among the 13 isolates, correlating the minor genomic variations observed, primarily in terminal regions and non-core ORFs, with specific phenotypic differences reported in Chapter 4 (e.g., host range, burst size) proved challenging / revealed subtle potential links / showed no clear correlation. This suggests the core conserved genome largely dictates the fundamental phenotype observed, although the variable terminal genes could play roles yet to be determined.

Potential for Phage Therapy and Future Research

Despite their temperate nature, standard bioinformatics screening using AMRFinderPlus and ABRicate did not detect currently recognised antimicrobial resistance (AMR) or virulence genes, which supports their further exploration for phage therapy potential. Nevertheless, the presence of non-core sequences derived from bacterial genomes, including those with homology

to potentially problematic domains like MBL (e.g., N2 ORF 43), suggests that these phages have the potential to act as gene transfer agents. This underscores the need for functional studies to assess their safety in therapeutic applications.

Future work should focus on:

Functional characterisation of hypothetical proteins. Proteomic studies and gene knockout experiments could provide insights into their roles.

Host range determination. Further screening against diverse *P. multocida* strains and other bacterial species could help determine the potential applications of these phages.

Assessing the switch between lysogeny and lysis. Transcriptomic studies could identify regulatory mechanisms that control the switch between these two life cycles.

Conclusion

This study provides a comprehensive genomic characterisation of *P. multocida* phages, revealing their close evolutionary relationship, temperate nature and potential for horizontal gene transfer. Comparative analyses show that while these phages are genetically distinct from previously described *P. multocida* phages, they share evolutionary links with *Haemophilus*, *Mannheimia* and *Pseudomonas* phages. Although our isolates do not carry AMR or virulence genes, further studies are necessary to assess their safety and potential for therapeutic applications.

6. Chapter 6. *In Vivo Assessment of Phage Therapy in a Galleria mellonella Model.*

Increasing antibiotic resistance among pathogens poses a global risk that threatens human and animal health and necessitates urgent alternative treatment methods (Kumar et al., 2021). International organizations such as the World Health Organization (WHO), The World Organisation for Animal Health (WOAH), and the Food and Agriculture Organization (FAO) suggests some approach to combating antibiotic resistance (Aslam et al., 2021, Ahmad et al., 2022). Among these approaches, bacteriophages are emerging as an attractive alternative due to their numerous advantages, including their ability to target and eliminate specific bacteria without disrupting the host microbiota (Helmy et al., 2023, Manohar et al., 2020). *P. multocida* is an important veterinary zoonotic pathogen that causes various diseases in many animals. Reported resistance to commonly used antibiotics in this pathogen also plays a significant role in the increasing global risk of AMR (Serna et al., 2025, Barta et al., 2025). Therefore, researching phage therapy against *P. multocida* is of great scientific and practical importance.

The selection of a relevant in vivo model is crucial for the evaluation of phage therapy against *P. multocida*. While mammalian models are the primary choice in this context, they present significant challenges when considering ethical, logistical, and cost considerations. *Galleria mellonella*, the greater wax moth larva, offers the advantages of possessing an innate immune system like mammals, being maintained at 37°C, being easy to administer, providing rapid response, and eliminating some of the challenges (Villani et al., 2025). It offers an important

alternative in vivo model. Additionally, *G. mellonella* has been previously used in numerous studies, including bacterial virulence, antibiotics, and phage therapy, and has been used in many successful methods, yielding significant results (Champion et al., 2018, Thomaz et al., 2020, Serrano et al., 2023, Gallorini et al., 2024). Importantly, this study is novel, as no previous study has reported *P. multocida* infection in *G. mellonella*.

Since the virulence of *P. multocida* strains in this model and the effects of *P. multocida* phages in this in vivo environment were previously unknown, establishing this model offers an opportunity to determine strain-specific virulence, the minimal lethal dose, and the efficacy of phage therapy.

6.1. Aims of Chapter

In previous chapters, a range of *P. multocida* strains were obtained, and phages that infect them were isolated and characterised. In this chapter, an infection model was developed to evaluate the effectiveness of the phages in reducing *P. multocida* in an invertebrate model. To do this, *G. mellonella* larvae were used. Based on the results of the characterisation of the phages, the hypothesis was that the phages would reduce the number of *P. multocida* in the *Galleria* model and potentially reduce mortality in *Galleria* larvae. To test this, a *P. multocida* infection was established in the *G. mellonella* model following these steps:

1. Determining the virulence of a panel of *P. multocida* strains to the *G. mellonella* larvae and identify suitable challenge strains for phage therapy assays.

2. Determining the LD_{50} doses of the selected *P. multocida* strains.

3. Assessing the effects of prophylactic and therapeutic applications of the previously characterised phages on the *P. multocida* infected larvae against lethal bacterial challenge.

It is hypothesised that different *P. multocida* strains will show varying levels of virulence when tested in the *G. mellonella* model, which will allow for the selection of highly pathogenic strains and the subsequent determination of their specific LD_{50} doses. It is further hypothesised that treating *G. mellonella* larvae with the previously characterised *P. multocida* phages (P1 and N1) will provide protection against a lethal challenge with *P. multocida*, leading to higher survival rates compared to larvae that do not receive phage treatment.

6.1. Pre-LD_{50} virulence test

To select appropriate challenge strains for establishing a *P. multocida* infection model in *Galleria mellonella* larvae suitable for subsequent LD_{50} determination and phage therapy evaluation, an initial virulence screening was conducted. The objective was to compare the relative pathogenicity of the available *P. multocida* strains in this invertebrate host system.

Twenty-five different *P. multocida* strains were assessed for their virulence by challenging *G. mellonella* larvae (details provided in Table 6.1). Significant variation in pathogenicity was observed among the strains. Based on larval mortality within the first 24 hours post-challenge, 16 strains were classified as highly virulent (>50% mortality), six exhibited moderate virulence (25–45% mortality) and three strains caused no significant mortality compared to controls. The difference in survival rates between the highly virulent and low-virulence strain groups was statistically significant ($p < 0.01$), confirming inherent strain-specific differences in virulence within this model. Further analysis revealed significant associations between virulence and bacterial surface structures; strains possessing capsular types A or B induced significantly higher mortality than untypable strains ($p = 0.003$), while the type F strain appeared non-virulent. Similarly, specific LPS types correlated with pathogenicity, with L3 and L4 genotypes associated

with increased larval mortality (p = 0.002), whereas L1 and L6 types were linked to reduced virulence. Based on these virulence assessments, combined with their previously determined high susceptibility to the isolated bacteriophages (Chapter 4), *P. multocida* strains PM13 and ATCC43137 (both demonstrating high virulence, causing near 100% mortality within 24 hours in this screen) were selected for detailed LD_{50} determination and subsequent phage therapy experiments.

The preliminary virulence screening demonstrated significant variation in the pathogenicity of different *P. multocida* strains in the *G. mellonella* model, with virulence correlating, at least partially, with capsular and LPS genotypes. This screen successfully identified strains PM13 and ATCC43137 as possessing both high virulence and phage susceptibility, making them suitable candidates for developing the *in vivo* phage therapy assessment model.

.

Table 6.1. Virulence Test for *P. multocida* in *G. mellonella* Larvae.

				Time in hour -post injection Alive /Dead			
CFU/mL	**Strain**	**Cap**	**LPS**	**0**	**24**	**36**	**48**
0	No injection control			10/0	10/0	10/0	10/0
0	Injection control			10/0	10/0	10/0	10/0
$2x10^8$	PM13*	U	L3	10/0	1/9	0/10	0/10
$1.3x10^8$	ATCC 43137*	A	L3	10/0	0/10	0/10	0/10
$5x10^8$	PM52	U	L3	10/0	10/0	10/0	10/0
$2.8x10^8$	PM106*	U	L3	10/0	4/6	3/7	1/9
$3.8x10^8$	PM222	U	L4	10/0	10/0	9/1	9/1
$3.5x10^8$	X 73*	A	L5	10/0	0/10	0/10	0/10
$3.6x10^8$	M 1404*	B	L2	10/0	3/7	2/8	2/8
$2.6x10^8$	P1235*	E	L2	10/0	3/7	3/7	3/7
$3..5x10^8$	P3881*	D	L6	10/0	0/10	0/10	0/10
$3.6x10^8$	P4679	F	L1	10/0	9/1	9/1	8/2
$3x10^8$	PM2Y	U	L6	10/0	9/1	9/1	9/1
$2.4x10^8$	PM3Y	U	L6	10/0	10/0	10/0	10/0
$2.6x10^8$	PM4Y*	U	L4	10/0	4/6	4/6	4/6
$5.8x10^8$	PM6Y*	U	L4	10/0	0/10	0/10	0/10
n/c	PM9Y *	n/a	n/a	10/0	3/7	2/8	2/8
$2.8x10^8$	PM12Y*	U	L3	10/0	0/10	0/10	0/10
$2.4x10^8$	PM13Y*	U	L4	10/0	0/10	0/10	0/10
$2.7x10^8$	PM16Y*	D	L4	10/0	0/10	0/10	0/10
$2.2x10^8$	PM17Y	D	L4	10/0	6/4	6/4	6/4
$5.7x10^8$	PM19B*	B	U	10/0	0/10	0/10	0/10
$2.3x10^8$	PM22B*	U	L1	10/0	3/7	0/10	0/10
$3.0x10^8$	PM24B	B	L3	10/0	8/2	8/2	8/2
$4.4x10^8$	PM25B*	U	U	10/0	0/10	0/10	0/10
$4.3x10^8$	PM26B*	U	U	10/0	0/10	0/10	0/10
$5.3x10^8$	PM27B*	U	U	10/0	0/10	0/10	0/10

Note. Larvae were injected with 10^6 CFU/larva with different *Pasteurella* strains and monitored over a period of 48 h to determine the number of larvae that died following injections. Strains with > 50% killing over 24 h. n/a = not available; n/c = not calculated; U = untypable

6.2. Determining the LD_{50} dose of *P. multocida* Strains in *G. mellonella* larvae

Following the selection of the highly virulent and phage-susceptible strains *P. multocida* PM13 and ATCC43137, it was necessary to precisely quantify their dose-dependent lethality in the *Galleria mellonella* model. The objective was to determine the 50% Lethal Dose (LD_{50}) for each strain, establishing a standardised bacterial challenge dose required to effectively assess the protective efficacy of phage therapy in subsequent *in vivo* experiments.

Dose-ranging experiments were conducted by challenging *G. mellonella* larvae with various concentrations of *P. multocida* strains PM13 and ATCC43137. Larval survival rates were monitored over 48 hours for each challenge dose (representative survival curves and dose-response plots are shown in Figures 6.1 and 6.2; replicate data in Appendix Figures 8.8–8.11). Based on the mortality data obtained across multiple independent trials (summarised in Table 6.2), the mean LD_{50} was calculated for each strain. The determined mean LD_{50} for *P. multocida* PM13 was 5.37×10^5 CFU/larva, and for *P. multocida* ATCC43137, it was 2.7×10^5 CFU/larva.

These determined LD_{50} doses provided the standardised challenge levels used in the subsequent phage therapy efficacy trials.

Table 6.2. The LD_{50} tests results of *P. multocida* strains PM13 and ATCC43137.

P. multocida strains	The number of LD_{50} tests			
	1st	2nd	3rd	Mean
PM13	1.9×10^5	1.3×10^6	1.2×10^5	**5.3×10^5**
ATCC43137	3.3×10^5	3.7×10^5	1.2×10^5	**2.7×10^5**

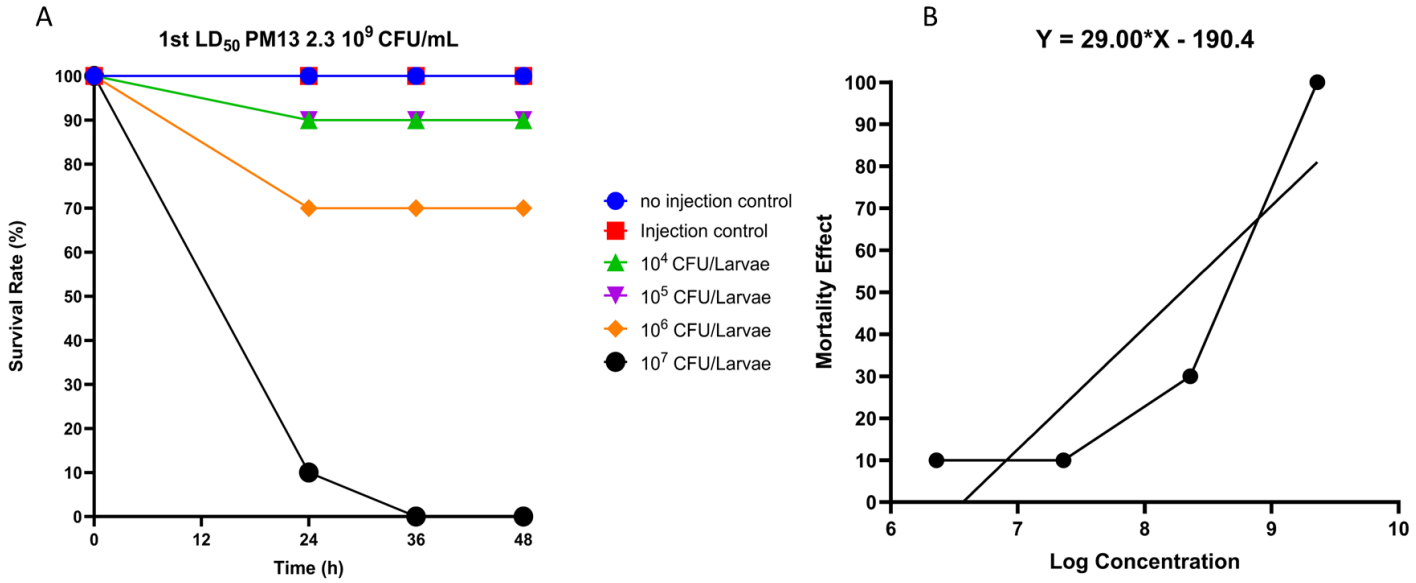

Figure 6.1. The Determination of LD_{50} for *P. multocida* PM13 Strain Infection of *G. mellonella* Larvae.

(A) The survival rate of *G. mellonella* larvae over 48 hours following infection with *P. multocida* PM13 at different concentrations. Each condition contained 10 larvae: a no-injection control, an injection control (10 µL of PBS) and four bacterial concentrations derived from a stock of 2.3×10^9 CFU/mL. (B) Log-transformed bacterial concentrations and their corresponding mortality effects. A linear regression model was fitted using GraphPad Prism (Version 10.2.0, Build 392) and the resulting equation (Y = 29.00X - 190.4) was used to determine the LD_{50} value for PM13.

.

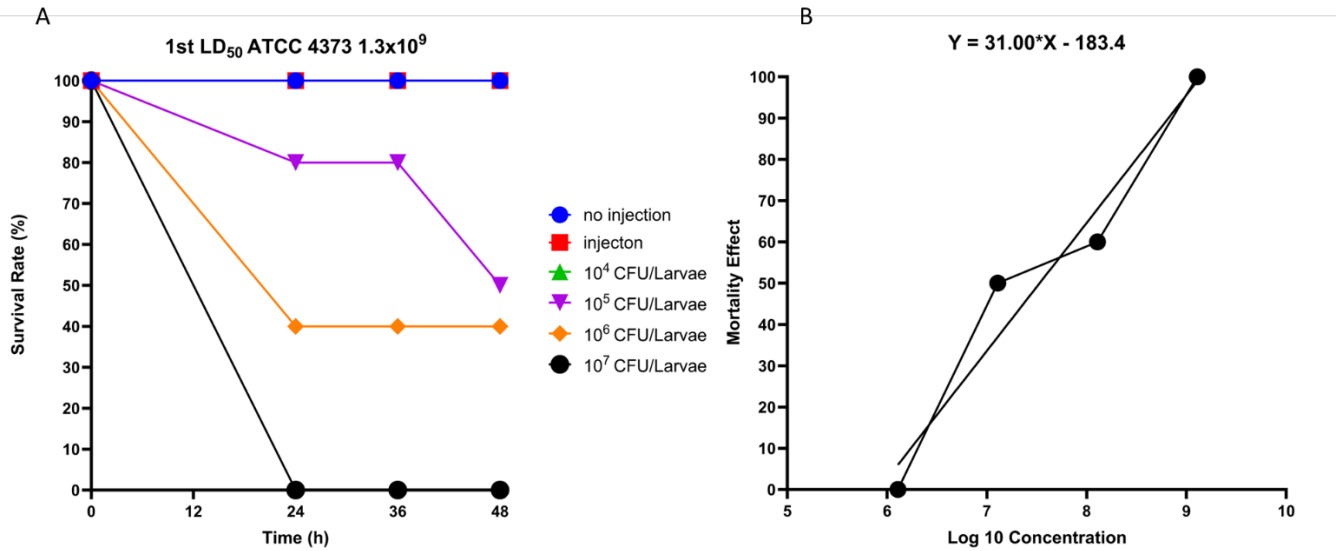

Figure 6.2. The Determination of LD_{50} For *P. multocida* ATCC43137 Strain Infection of *G. mellonella* Larvae.

(A) Survival data for 10 larvae per condition, including no injection control, PBS injection control (10 µL per larva) and four bacterial dilutions (ranging from 10^4 to 10^7 CFU/larva) of *P. multocida* ATCC43137. (B) Log-transformed bacterial concentrations plotted against the corresponding mortality effect (%), used to derive a linear regression model in GraphPad Prism (Version 10.2.0, Build 392). The regression equation was then used to calculate the LD_{50} for the ATCC43137 strain.

Figure 6.3. *P. multocida* PM13-infected *G. mellonella* larvae.
Left to right to healthy larvae, infected larvae and dead larvae.

6.4. Phage Therapy

To assess the potential therapeutic value of the isolated bacteriophages *in vivo*, the efficacy of selected phages (P1 and N1) was evaluated against lethal infections caused by their respective host strains (*P. multocida* PM13 and ATCC43137) in the established *Galleria mellonella* model. The study aimed to compare the protective effect of different treatment timings (prophylactic versus therapeutic administration) and phage doses (Multiplicity of Infection, MOI).

Control groups included no injection, PBS injection, phage-only, and bacterial supernatant challenges. After 48 hours, no mortality or symptoms of melanisation were observed in the no-injection and PBS injection control groups, confirming that the injection procedure itself did not cause significant harm. Mortality was detected in the phage-only control group in two out of six experiments, though this loss, accounting for approximately 10% of larvae, was not statistically significant. However, the bacterial supernatant controls had a notable impact on mortality, particularly in the case of PM13, where it led to a 20% reduction in survival when compared to the no-injection and PBS injection controls ($p < 0.005$). The ATCC43137 supernatant control had an even stronger effect, causing around 35% mortality, which was statistically significant at $p < 0.001$. Among the treatment groups, prophylactic administration of phages demonstrated superior protective effects compared to therapeutic applications. In the case of *P. multocida* PM13, bacteria-only infected larvae exhibited complete mortality within 24 hours. When phage P1 was administered prophylactically at an MOI of 100, 35% of larvae survived at 24 hours, though survival decreased slightly to 30% by 36 hours and remained stable until the end of the experiment ($p < 0.001$). Therapeutic administration of phage P1 at the same MOI resulted in

limited protection, with a survival rate of 6%, which was statistically significant when compared to the bacteria-only group ($p < 0.05$). However, lower MOI treatments (MOI 10 and MOI 1) in both prophylactic and therapeutic applications showed minimal efficacy, with survival rates dropping to around 2% by 48 hours. For *P. multocida* ATCC43137, the supernatant control had a much greater impact on mortality than that of PM13, causing a 35% reduction in survival ($p < 0.001$). Similar to PM13, the most effective treatment was the prophylactic application of phage N1 at MOI 100, which resulted in a survival rate of 25% at 48 hours ($p < 0.001$). Although this level of protection was lower than that observed with P1 against PM13, it remained significant ($p = 0.0052$). When comparing different MOI levels of prophylactic phage N1 treatments, MOI 100 showed the best survival rate, while MOI 10 provided initial protection of 15% at 24 hours but dropped to around 3% by 36 hours. Therapeutic application of phage N1 at MOI 100 also resulted in some protection, but the survival rate was approximately 20%, indicating that pre-infection phage treatment was more effective than post-infection treatment.

Table 6.3. Treatment regimens for the controls, prophylactic and therapeutic phage therapy used in this study.

Experimental Groups n=10*	Treatments	Time (h) 0	0.5
1	Control 1—No injection	-	-
2	Control 2—Injection	PBS	PBS
3	Control 3—Phage only	P	PBS
4	Control 4—CFS Control	S	PBS
5	*P. multocida*	P+B	BHI
6	Prophylactic regimen	P	B
7	Therapeutic regimen	B	P

PBS: Phosphate buffered saline, P: Phage, S: Supernatant, B Bacteria, CFS: Cell-free supernatant. **A total of ten larvae were utilized for each designated time point and treatment regimen. Each larva was subjected to treatment using a Hamilton syringe, with 10 µL of phage (P), bacteria (B), supernatant of bacteria (S) or PBS (as an injection control). The experiment was conducted independently on three separate occasions.

Table 6.4. Effect of Phage Therapy on *Galleria mellonella* Larvae Infected with *P. multocida* Strains PM13 and ATCC43137

Treatment	MOI	Dead 24h	Dead 36h	Dead 48h
PM13 + Phage P1 Therapy Results (Dead larvae, mean ± SEM)				
Injection control	–	0.3 ± 0.3	0.3 ± 0.3	0.3 ± 0.3
No injection control	–	0.0 ± 0.0	0.0 ± 0.0	0.0 ± 0.0
Pure phage P1 control	–	1.0 ± 0.6	1.3 ± 0.9	1.3 ± 0.9
Supernatant PM13	–	2.0 ± 0.6	2.3 ± 0.9	2.3 ± 0.9
Resuspended PM13	–	10.0 ± 0.0	10.0 ± 0.0	10.0 ± 0.0
Prophylactic P1	1	9.3 ± 0.3	10.0 ± 0.0	10.0 ± 0.0
Prophylactic P1	10	8.7 ± 0.3	9.7 ± 0.3	10.0 ± 0.0
Prophylactic P1	100	6.7 ± 0.9	7.3 ± 0.7	7.7 ± 0.9
Therapeutic P1	1	10.0 ± 0.0	10.0 ± 0.0	10.0 ± 0.0
Therapeutic P1	10	10.0 ± 0.0	10.0 ± 0.0	10.0 ± 0.0
Therapeutic P1	100	8.7 ± 0.3	9.7 ± 0.3	9.7 ± 0.3
ATCC43137 + Phage N1 Therapy Results (Dead larvae, mean ± SEM)				
Injection control	–	0.0 ± 0.0	0.0 ± 0.0	0.0 ± 0.0
No injection control	–	0.0 ± 0.0	0.0 ± 0.0	0.0 ± 0.0
Pure phage N1 control	–	0.7 ± 0.3	1.0 ± 0.6	1.0 ± 0.6
Supernatant ATCC	–	3.0 ± 1.5	3.7 ± 1.9	3.7 ± 1.9
Resuspended ATCC	–	10.0 ± 0.0	10.0 ± 0.0	10.0 ± 0.0
Prophylactic N1	1	8.7 ± 0.9	9.0 ± 1.0	9.0 ± 1.0
Prophylactic N1	10	9.3 ± 0.3	9.7 ± 0.3	10.0 ± 0.0
Prophylactic N1	100	7.7 ± 0.7	7.7 ± 0.7	8.0 ± 0.6
Therapeutic N1	1	10.0 ± 0.0	10.0 ± 0.0	10.0 ± 0.0
Therapeutic N1	10	9.3 ± 0.3	10.0 ± 0.0	10.0 ± 0.0
Therapeutic N1	100	8.7 ± 0.3	9.0 ± 0.6	9.0 ± 0.6

Larvae (n = 10 per group) were infected with resuspended *P. multocida* PM13 or ATCC43137 and treated prophylactically (30 min before infection) or therapeutically (30 min after infection) with purified phages P1 (PM13) or N1 (ATCC43137) at multiplicities of infection (MOI) 1, 10, or 100. Control groups included uninjected larvae, injection control (PBS), phage-only control, bacterial supernatant control, and resuspended bacteria without phage

treatment. Mortality was recorded at 24, 36, and 48 h. Data are presented as mean number of dead larvae ± SEM from three independent experiments.

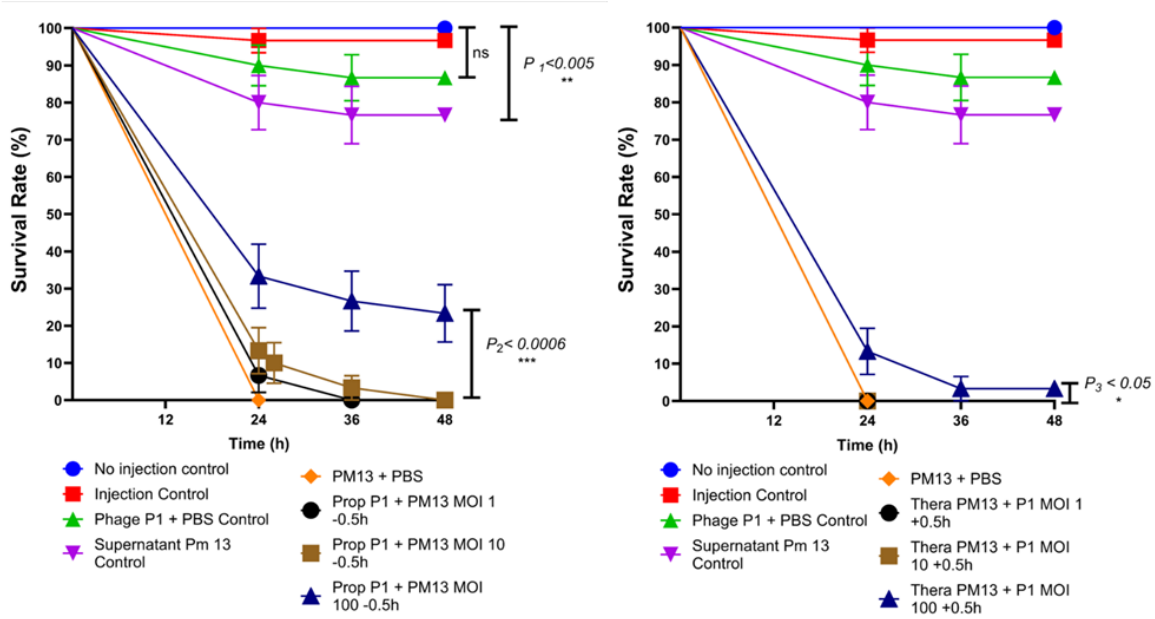

Figure 6.4. Kaplan-Meier Survival Curve of *G. Mellonella* Infected With *P. multocida* PM13 and Treated With Purified Phages in Two Therapy Regimens.

The larvae were treated prophylactically (left) or therapeutically (right) with phage P1. The treatment regimens were compared to four control groups: No injection control (received no injection); Injection Control (received two 10 µL injections of PBS at time 0 and time 0.5 h); Phage Control (received 10 µL of concentrated pure phage at time 0 and 10 µL of PBS at time 0.5 h); Cell-free supernatant (CFS) / Supernatant Control (received 10 µL of bacterial supernatant obtained at washing steps of bacteria at time 0 and 10 µL of PBS at time 0.5 h). Three rounds of individual experiments were conducted. GraphPad Prism Version 10.2.0 (392)'s Log Rank Mantel-Cox test was used to evaluate the data. Data represent mean ± SD. Significance level was set at $p<0.05$(*), $p<0.01$(**) or $p<0.001$(***).

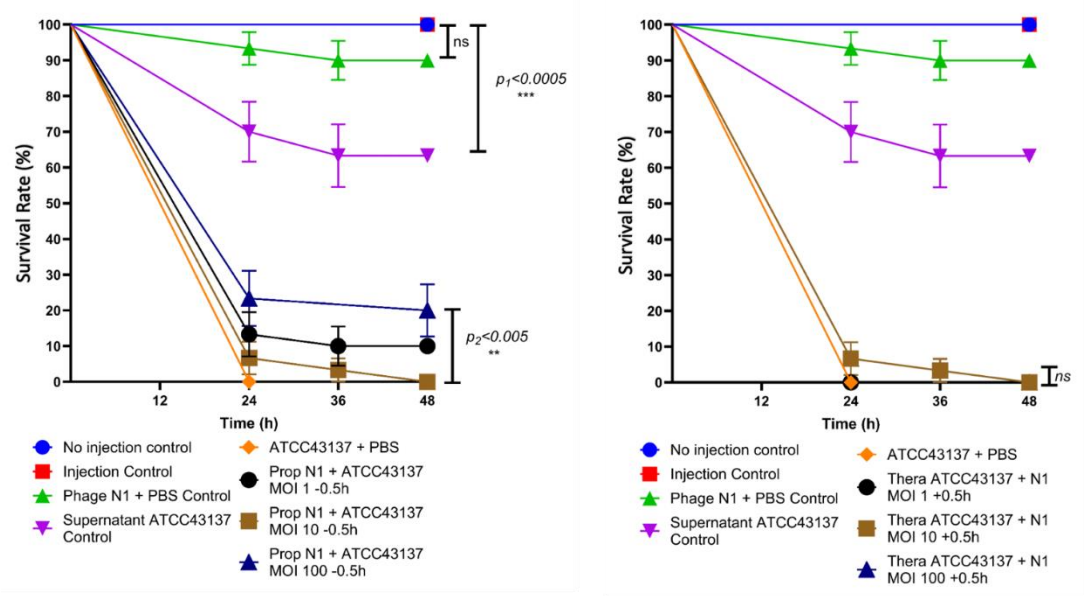

Figure 6.5. Kaplan-Meier Survival Curve of *G. mellonella* Infected With *P. multocida* ATCC43137 and Treated With Purified Phages in Two Therapy Regimens.

The larvae were treated prophylactically (left) or therapeutically (right) with phage N1. The treatment regimens were compared to four control groups: No injection control (received no injection); Injection Control (received two 10 µL injections of PBS at time 0 and time 0.5 h); Phage Control (received 10 µL of concentrated pure phage at time 0 and 10 µL of PBS at time 0.5 h); Cell-free supernatant (CFS) / Supernatant Control (received 10 µL of bacterial supernatant obtained at washing steps of bacteria at time 0 and 10 µL of PBS at time 0.5 h). Three rounds of individual experiments were conducted. GraphPad Prism Version 10.2.0 (392)'s Log Rank Mantel-Cox test was used to evaluate the data. Data represent mean ± SD. Significance level was set at $p<0.05$(*),$p<0.01$(**) or $p<0.001$(***).

6.5. Discussion

The aim of this chapter was first to determine the virulence of *P. multocida* strains in *Galleria mellonella* larvae, followed by determining the LD_{50} doses of selected strains for use in phage therapy assays. The primary objective was to assess whether the selected phages exhibited prophylactic or therapeutic effects on *P. multocida* infections in the larvae.

Variable Virulence of *P. multocida* Strains

The virulence screening of 25 *P. multocida* strains revealed considerable variation in their pathogenicity. Among the six LPS types and five capsule types tested, only CapF strains were found to be non-virulent. This observation is consistent with other research into *P. multocida* pathogenesis, which has demonstrated significant variability in strain virulence (Cheng *et al.,* 2020). A similar study reported mortality rates ranging from 0 to 70% in *Galleria* larvae infected with different *P. multocida* strains, which may be attributed to similarities in their capsular composition (Lv *et al.,* 2023). The three independent experimental trials produced slightly variable but statistically insignificant results (mean ± SD plotted on graphs). These minor variations may be attributed to differences in environmental factors, such as temperature and humidity, as well as variability in larval age and immune status. To mitigate these potential sources of variation, only healthy larvae were selected, and they were standardised based on weight and size prior to experimentation. Comparative analysis with previous studies using *G. mellonella* and murine models highlights similarities in LD_{50} values. A study on a wild-type *P. multocida* HuN001 capsular type A strain did not determine the LD_{50} but reported a 70% mortality rate following a single dose of 2.5×10^6 CFU/larva (Lv *et al.,* 2023). In our study, a comparable

mortality rate of 60% was observed when larvae were challenged with *P. multocida* ATCC43137 at a dose of 1.5×10^6 CFU/larva. These findings align with reports on other bacterial pathogens, where *Staphylococcus aureus* requires 10^5–10^6 CFU/larva for lethality, and *Helicobacter pylori* requires 10^6–10^7 CFU/larva for infection establishment. Conversely, highly virulent species such as *Acinetobacter baumannii* (10^4 CFU/larva) and *P. aeruginosa* (10 CFU/larva) have significantly lower LD_{50} values, making them extremely pathogenic in the *G. mellonella* model (Gibreel and Upton, 2013; Giannouli *et al.,* 2014; Peleg *et al.,* 2009; Beeton *et al.,* 2015).

Timing of Phage Administration

The effectiveness of phage therapy was evaluated by administering phages at different time points relative to bacterial infection. The results indicate that prophylactic administration was significantly more effective than therapeutic application. The group receiving phage 0.5 h before infection exhibited markedly higher survival rates than those treated post-infection. Even when applying tenfold higher phage concentrations for therapeutic treatment with phage N1 against ATCC43137-infected larvae, survival rates were lower than those observed in prophylactic treatment. The improved protection in prophylactic application is likely due to the phage dispersing throughout the haemolymph before bacterial colonisation, allowing for rapid bacterial suppression. Conversely, in the therapeutic model, *P. multocida* had time to establish infection and initiate virulence mechanisms before phage administration. Another factor limiting therapeutic efficacy may be the ability of *P. multocida* to invade epithelial cells, thereby shielding itself from phage attack (Lee *et al.,* 1994). Intracellular bacterial persistence has been recognised as a major challenge in phage therapy, as phages primarily target extracellular bacteria. Combined therapy incorporating antibiotics capable of penetrating host cells might improve

bacterial clearance. Although not directly investigated in this study, this intracellular survival strategy may explain the superior efficacy of the prophylactic model, where phages were administered before bacterial invasion into host cells. Additional limitations in therapeutic application may include the rate of phage replication within the larval environment and the rapid progression of *P. multocida* infection. The bacterial growth rate may exceed the phage replication rate, reducing phage-mediated bacterial suppression. At the time of therapeutic phage administration, the larvae exhibited symptoms of advanced morbidity, including dehydration and melanisation, which were indicative of systemic infection. These moribund larvae were likely more susceptible to secondary infections. Furthermore, the use of commercially sourced, non-sterile larvae introduces inherent variability. While efforts were made to mitigate this by standardising larvae based on health and physical parameters, this remains a potential limitation affecting result consistency. Other studies also conducted on *G. mellonella* larvae align with our results, suggesting that prophylactic application was more effective than therapeutic (Beeton *et al*. 2015, Nale *et al*. 2021). Beeton *et al*. (2015) conducted a similar experimental model to ours, where in the initial set of trials, *Galleria* were infected with the laboratory strain *P. aeruginosa* PAO1, and they were injected with different multiplicities of infection (MOI) of phages either 2 h post-infection (treatment) or 2 h pre-infection (prevention). All the larvae eventually died at the end of the experiment, but there were higher survival rates for infected larvae in the prevention vs therapy regimens at 24 h. On the other hand, the *Galleria* model conducted by Nale *et al*. (2021) used *Salmonella* for infection and a three-phage cocktail to test their efficacy in three different administration ways. *G. mellonella* larvae treated with phages 2 h before *Salmonella* exposure (prophylactic) survived, and bacteria were undetectable 24 h later and throughout the

experiment. Administering phages together with bacteria (co-infection) or 2 h after bacterial exposure (treatment) increased survival rates (73-100% and 15-88%, respectively) but was less effective than the prophylactic approach. The survival efficiency in the study by Nale *et al*. (2021) was most probably higher because the three-phage cocktail had different morphologies and could target different types of bacteria, leading to a broad-spectrum cocktail. If we compare these two experiments with this study, the extremely virulent *P. aeruginosa* (LD_{50} of 10 CFU/larva) might be the result of the total loss of the population, while *Salmonella* strains have very low LD_{50} ranging from 10^2 to 10^5, similar to our *P. multocida* strains PM13 and ATCC43137 (around 10^5), resulting in very high survival rates reaching 100%. The differences in the survival rates might be explained in three different ways: first, the lytic activity of the *Salmonella* phages might be higher; second, using a cocktail instead of one phage might overcome the phage resistance problem; and third, the administration method, as in the *Salmonella* study, they used an oral lavage method instead of injecting organisms with a syringe into prolegs, which might cause bleeding and disruption of physical barriers, making the larvae more vulnerable to secondary infections. Comparing these three models with varying virulence of the strains and the survival results suggests that using strictly lytic phages and phage cocktails administered by oral lavage would yield better results.

The effect of Cell Free Supernatant on Therapy

While the LD_{50} of both *P. multocida* PM13 and ATCC43137 ($5x10^7$ CFU/mL for PM13 and $3x10^7$ CFU/mL for ATCC43137) was quite similar, the supernatant of ATCC43137 had a higher mortality effect, killing almost 15% more of the population compared to the supernatant of PM13, which killed approximately 20% of the population. This might have resulted in a difference

in protection between the very similar phages P1 and N1. The same virulence effect of the bacterial supernatant could occur when the phage lyses the bacteria in the larvae and releases internal components, which might consist of some toxins or other virulence factors; that might be the reason why phage N1 protection is lower than P1. Similar results have been seen in a study where, in contrast to negative controls, a model of *G. mellonella* infection with *Clostridium perfringens* demonstrated the ability of cell-free supernatants to cause illness, suggesting that soluble components (toxins) have the potential to be pathogenic (Kay *et al*. 2019). That *Clostridium perfringens* strain has a similar LD_{50} to our *P. multocida* strains, and administration of its supernatant resulted in similar mortality rates, around 30% loss of population. Components of *P. multocida*'s LPS, Lipid A, are a potent virulence factors that trigger the innate and adaptive immune systems and cause endotoxic shock (Harper and Boyce 2017). LPS's potential to cause HS symptoms has been evaluated in a number of prior investigations. Buffalo calves were seldom fatally injected intravenously with a direct inoculation of semi-purified LPS. Purified LPS injection, therefore, mimics some of the symptoms of HS infection, such as widespread congestion, haemorrhage, oedema and necrosis, which were seen in the lungs, trachea, heart, liver, spleen, kidney and nerve tissues (Horadagoda *et al*. 2002, Chung *et al*. 2016, Marza *et al*. 2017). Similar effects of LPS residues in the supernatant might cause the negative effects on the survival of the larvae.

The Effect of Phage-only control group on Therapy

The effect of the phage-only control group was also significant, with approximately 10% loss of the larval population. This might reflect lysed bacterial molecules contaminating the lysate and impacting the larvae. The only purification method we used prior to this part of the study

was molecular weight cut-off, and these components, such as LPS, may come through. There are other methods that could be used to prepare purer phages, such as PEG precipitation, CsCl gradient centrifugation, purification using ultrafiltration or chromatography. In our study, except for using chromatography, other methods were tried but resulted in very low phage titres in the end. This fragility might also be the reason for the phage's fragile tail structure. This was interpreted from TEM results where there were many ruptured and clamped phage tails around with tail-free capsids. The methods mentioned above, which are commonly used for phage purification and resulted in low titres in the present study, could be investigated, and details could be compared to understand why they resulted in low titres with our phages in future work, as there might be various reasons, such as the several different chemicals or different degrees of g-force pressure by centrifugation used. Unfortunately, the limited time did not allow us to test them. The technique that enabled us to achieve the desired MOIs was only possible with the molecular weight cut-off method, so only it could be used. Phages P1 and N1 provided some protection, with approximately 30% higher survival compared to the bacteria-only injected larvae against *P. multocida* infections; however, this was quite low compared to other phage therapy studies where they reached almost 100% protection (Nale *et al*. 2021). This is most probably because of the differences between the phage's lytic cycle properties. Most phage therapy studies are conducted with strictly lytic phages, and their lysis capabilities are much higher than temperate phages (Beeton *et al*. 2015, Nale *et al*. 2016, Jeon *et al*. 2019). In this study, we only isolated lysogenic phages and had limited success in isolating lytic phages from a mix of sources. While not lytic, our phage isolates showed a broad host range and large burst size and so they were assessed for therapeutic properties. The application of temperate phages as therapeutics

against bacterial illnesses is now being explored thanks to developments in synthetic biology and sequencing technologies. These phages might be modified by removing the integrase and transposase genes and turned into lytic phages. There are many example studies aiming for this, such as: The lytic activity, productivity and host range were increased by genetic alterations to the temperate *Enterococcus faecalis* phage φEf11, which eliminates the lysogeny establishment and repressor sensitivity (Zhang *et al*. 2013). Two temperate *Listeria monocytogenes* phages were used to construct synthetic phages using *Listeria* L-forms to reboot the synthetic genomes; this was achieved with an endolysin gene, a synthetic virulent mutant of temperate phage PSA was able to attack phage-resistant bystander cells, and synthetic lytic versions of temperate phage B025 were more effective and caused less phage resistance in bacterial cells (Kilcher *et al*. 2018). Another study improved the lytic activity of temperate phages by using them as a combination; using a combination of four temperate phages, the *C. difficile* load in fermentation vessels was decreased by six times in a prophylactic regimen after five h and eradicated after 24 h of prophylactic or remedial regimens. The vessels were spiked with mixed faecal slurries from healthy volunteers (Nale *et al*. 2018). By doing these kinds of studies, we may significantly increase the arsenal we have against the growing danger posed by bacteria that are resistant to antibiotics. The genomic characterisation suggests that all phages we isolated were temperate phages, as they have transposase genes in their genomes. Using those phages for phage therapy was not suggested for a long time, but we thought our phage therapy study with temperate phages would fill some of the research gap in this area. For the objectives of phage treatment, strictly lytic phages have generally been selected. A described risk associated with the use of temperate phages is their potential ability to enable gene transfer between bacteria through

specialised transduction. This may pose an increased risk of transferring genes associated with bacterial pathogenicity, such as antibiotic resistance or toxin genes. Although there are several concerns about using temperate phages for medicinal purposes, these phages also have some very interesting positive traits. Since lysogens make up about half of all sequenced bacteria, temperate phages are highly prevalent in nature and are simple to discover and isolate (Touchon *et al*. 2016). For anaerobic and fastidious bacteria, where it has proven exceedingly difficult to isolate purely lytic phages, the ability to recognise temperate phages in bacterial genomes rather than the need to look for them in nature is especially helpful (Hargreaves, Clokie 2014). As was previously said, the integration of temperate phages into bacterial genomes is often considered a crucial issue, although it can also be investigated for beneficial purposes. For instance, temperate phages can be engineered to deliver synthetic gene networks that disrupt crucial bacterial intracellular processes to kill bacteria. The phage ĐSaBov was designed to transmit a CRISPR-Cas9 system that targets the *NUC* gene, which is found in all *S. aureus* cells; the phage mutant was able to eradicate all cells *in vitro* in 8 h, and no survivors showed up after 24 h. The phage mutant decreased the number of bacteria *in vivo* by a factor of more than two (Park *et al*. 2017). Additionally, temperate phage's genomes can be modified to remove genes linked to bacterial pathogenicity or the upkeep of a lysogenic life cycle (Zhang *et al*. 2013, Kilcher *et al*. 2018). Temperate phages become lytic as a result, and they can then be enhanced via synthetic biology techniques or used like any other naturally occurring, purely lytic phage. However, it should be mentioned that the majority of phage genes are unknown, and as such, they may be associated with unexpected harmful events, such as increasing the virulence of the bacteria or antibiotic resistance we might not know yet. This holds true for both temperate and lytic phages

and emphasises the necessity of learning more about fundamental gene function in order to strengthen phage engineering strategies. A few research studies have investigated the potential of temperate phages, even if strictly lytic phages are still the recommended choice for therapeutic purposes; for example, temperate *P. aeruginosa* phages have been used to reduce the swarming and twitching motility of the lysogenised bacteria, which significantly reduced mortality *in mice* as well as in flies (Chung *et al.,* 2012). While in another study, an *E. coli* lysogenised by phage λ mutant lost its resistance to nalidixic acid and streptomycin in terms of MIC values 2-fold and 133-fold, respectively (Edgar *et al.,* 2012). In both these cases, the lysogens have altered characteristics which could be beneficial in phage therapy.

To summarise, because of the urgent need to treat diseases that are resistant to multidrug, phage research is now being conducted as a possible antibiotic alternative. Data in this chapter indicate that *Galleria* can potentially be used as a model for the study of the virulence of several *P. multocida* strains by scoring for larval mortality, and this is consistent with other recent studies. In this study, phages were administered at various intervals, both before and after *P. multocida* infection, to see if they had any prophylactic or therapeutic effects. The prophylactic effects of phage therapy were much more significant, aligning with other studies. We observed that bacteria-free supernatants from the bacterial cultures had some toxic effects, which might be caused by intracellular toxins or other bacterial elements like lipid-A of the LPS, which might cause septic shock. The same impact on larvae observed in controls implies potential release due to phage lysis of the bacteria, with the purified phage preps showing some mortality effects on the larval population. That might reflect insufficient purification, as in this study we only applied one purification method because subsequent steps led to a significant and problematic titre drop.

In this study, *Pasteurella* Mu-like phage provided some protection but not as high as other phage therapy studies; this is probably because our phages might be temperate, not strictly lytic. We chose temperate phages for our study because we could not isolate strictly lytic phages for a long time. It has also been previously reported that isolation of lytic phages against fastidious bacteria is extremely hard (Hargreaves, Clokie 2014).

Chapter 7. General Discussion

This work set out to isolate and characterise *P. multocida* phages and assess their efficacy against *Pasteurella* infection in a *G. mellonella* infection model.

The first aim was to isolate *P. multocida* from environmental samples and use these isolates for phage studies. The initial aim was to isolate the bacteria from raw sewage samples and animal-related samples. However, due to UK pandemic restrictions, the gathering of samples was limited to open water sources. Sources located near sewage outputs or sites often visited by wild birds were chosen to compensate for this. After isolating samples from various water sources, a total of 91 putative *Pasteurella* colonies were obtained. Although these colonies showed growth on expected *Pasteurella* sp. selective conditions and had positive oxidase and catalase responses, they could not be confirmed as *multocida* by PCR. The findings indicate that the isolates might potentially be classified as additional species of *Pasteurella* or closely related taxa within the *Pasteurellaceae* family, such as *Haemophilus*, *Mannheimia* or *Actinobacillus*. This emphasises a notable difficulty separating *P. multocida* from samples taken from the environment, most likely because the bacterium has specific and demanding growth conditions and environmental limitations. This may be compounded by dilution effects in the water sources, which in turn affected the effectiveness of isolating the bacteria. In addition, the diluting effect in vast water bodies such as lakes and rivers probably further hindered isolation attempts. Lehr *et al*. (2005) discovered that *P. multocida* was not present in water and sediment samples during an FC outbreak. This finding supports the idea that it is difficult to identify this bacterium in these types of conditions. We therefore used strains sourced from different collections. If further strains

were required, then more defined sampling at the originally proposed sites may increase chances of isolation. The use of *Pasteurella* Chromagar could streamline the isolation process.

In the absence of newly isolated *P. multocida* strains, 22 commercial and clinical strains were employed for phage studies. These strains were characterised for capsule type, LPS type, toxin production and antibiotic resistance, all critical factors for understanding phage-host interactions and virulence. Capsule typing revealed a predominance of capsule types D and B. While this is a bias, it reflects strains described in infections, where type D is associated with AR in swine and type B with HS in cattle. LPS typing identified six of the eight potential LPS genotypes, indicating a good coverage for studying phage binding specificities.

For phage isolation, 21 field samples were screened on six different *P. multocida* strains, but no phages were isolated from environmental waters. This may reflect the limited or very dilute presence of *P. multocida* and the principle that bacteriophages are best isolated from environments where their host bacteria are abundant. Phages were successfully isolated from our pooled raw sewage sample, highlighting the critical role of sample source in phage isolation. Electron microscopy revealed all phages had an icosahedral capsid and a non-contractile tail, with dimensions larger than previously published *P. multocida* phages. Phage susceptibility was primarily observed in strains with LPS type L3, indicating a possible correlation between LPS type and phage susceptibility.

The physicochemical characterisation demonstrated that the isolated phages were stable within a pH range of 4 to 10, but their concentration significantly dropped under highly acidic or alkaline conditions. This suggests that while phages can survive most parts of the digestive tract, they may lose viability in highly acidic environments like the gizzard of birds, unless stabilised

through various methods such as encapsulation or polymer-based stabilisation (Loh *et al.,* 2021; Malik *et al.,* 2017). Thermal stability tests indicated that while phages remained viable up to 50°C, three (P8, S1 and S2) exhibited higher thermal stability; they maintained approximately half of their initial titre at 60°C, which makes these phages suitable for therapeutic applications, as this is within the typical body temperature range.

Genomic analysis of the phages isolated in this study revealed a core genome with a high degree of similarity, with sequence identities of approximately 99.6%. This homogeneity is likely due to their origin from the same pooled sewage sample. The variability we did observe came from flanking regions, and analysis showed that all had the same Mu phage core genome and sequences picked up on excision from the bacterial genome. Phylogenetic analysis clustered the isolates with other Mu phages, although the structure was a hybrid: one region resembled *Mannheimia* and *Haemophilus* Mu phages in gene structure, while the other resembled *Pseudomonas* Mu phages, interspersed with regions containing several predicted *Pasteurella* Mu phage coding sequences. Subsequent analysis with PhageAI indicated that these phages belong to and *Vieuvirus* genus, with a 98.04% confidence level for being temperate. Alignment of phage genomes within published *P. multocida* genomes revealed equivalent integrated Mu phages with ca. 92.55% identity were present in at least two of the published sequences assessed. This suggests that these phages are common in the wider *P. multocida* population. The first 30 organisms matching the phages of this study from a BLAST search on the NCBI database were *P. multocida* with very high similarity rates and low e-values, suggesting the presence of Mu prophages in the *P. multocida* population is significantly high. While we isolated phages from filter samples, we indicated their presence as free phages; however, their genetic characteristics

clearly indicate temperate integration. No tRNAs were detected in the phage genomes, suggesting reliance on the host's translation machinery. This lack of tRNAs, along with other indicators, supports the classification of these phages as temperate, as virulent phages typically have more tRNAs to enhance their fitness (Bailly-Bechet, Vergassola and Rocha, 2007).

Concerns regarding the use of temperate phages in therapy relate to their potential to carry virulence and AMR genes between bacteria and into the genome. No evidence of these genes was found in these isolates, but the flanking regions are a concern due to their non-specificity and potential for gene transfer. Further, these phages are very closely related, with only variation in the flanks, suggesting that this is more variable given the narrow sample source. Irrespective of the broader risk if used in a wider setting, it was interesting to assess how temperate phages perform in larval therapy trials using a model. This area is not widely explored in phage therapy, which focuses on lytic phages.

To this end, we developed a mortality model of *P. multocida* strains in *G. mellonella* larvae and evaluated selected strains. We observed variations in virulence among different *P. multocida* strains, with differences observed even among strains of the same capsular type. These observations align with previous research indicating variability in the pathogenicity of *P. multocida* strains. How these variations relate to virulence in real-world infections remains to be seen, and it would be good in the future to compare strain infectivity in *Galleria* with strains assessed in animal infections or from clinical cases to help understand how the larval model performs in relation to mammalian and avian infections.

We investigated the prophylactic and therapeutic effects of selected phages against *P. multocida* infections in larvae. The timing of phage administration was found to be critical, with

prophylactic application showing greater efficacy compared to therapeutic application. The interpretation of this data is limited by a lack of understanding of the exact cellular location of *Pasteurella* in the larvae. Several possible reasons for poor efficacy should be considered. It is possible that the larval environment is not suitable for phage attachment and replication. The bacteria are known to have invasive potential, so they could potentially be invading cells in the larvae and therefore avoiding phage attack. To assess this, a better understanding of bacterial location and phage replication dynamics *in vivo* would be required. Furthermore, we used temperate phages, and so it would be good to control our work and directly compare lytic and temperate phages. When compared to other *Salmonella* and *P. aeruginosa* research using *G. mellonella* larvae infection models, they also observed that prophylactic phage application was generally more effective than therapeutic application, even though these phages were lytic, consistent with other studies. Differences in survival rates were noted, which could be attributed to variations in bacterial virulence and phage properties across different studies. The impact of bacterial culture supernatant and 'impure' phage highlights the importance of selecting appropriate purification methods to obtain pure phage samples. This could be an issue in the commercial application of these phages. Despite limitations in phage purification, the study demonstrated some level of protection against *P. multocida* infections with the prophylactically administered phages, although lower than observed in studies using strictly lytic phages.

While strictly lytic phages are generally preferred for therapeutic use, temperate phages offer advantages such as prevalence in nature and ease of isolation. Moreover, temperate phages can be engineered to deliver synthetic gene networks or modified to remove genes associated

with bacterial pathogenicity or those associated with regulating lysogeny, such as integrase and transposase, thereby enhancing their therapeutic potential.

Overall, we show the limited presence of *Pasteurella* in water sources, even near sewage outflows. That the phage present in some bacterial genomes is lytic in sewage, as shown by our isolation. While our phages were highly similar, they had picked up different flanking DNA reflecting their random insertion points and excision. Although no related structural genes were found in the flanking (different) region, the proteins which are still unknown might play a role in the difference in the host range. In addition, there was no correlation between the capsular or LPS group with the host range. Therefore, it is more likely that lytic phages may have potential in therapy, but further understanding of the *Pasteurella Galleria* model would be required to fully interpret the reasons for poor efficacy.

Appendix

Chapter 2 supplementary materials

Reagents, Buffers and Medias

All commercial media were prepared according to manufacturer's instructions unless stated otherwise. All media and solutions were sterilised by autoclaving at 121°C and 15 psi for 20 min unless stated otherwise.

Tris-HCl (Tris(hydroxymethyl)aminomethane-Hydrochloric acid), 1 M pH 7.6 (100 mL)

Solutions were prepared as described in Cold Spring Harbour Protocols (2006. Briefly, 12.11 g Tris base was added into 80 mL deionized water (H_2O) (diH_2O) and dissolved using a magnetic stirrer Heidolp, MR3001. The pH was adjusted to 7.6 by adding 1 M HCl.

Sulphate Of Magnesium (SM) buffer

SM buffer was prepared based on a previously published method of Cold Spring Harbour Protocols (2006). Briefly, 5.8 g NaCl and 2 g $MgSO_4{\cdot}_7H_2O$ were dissolved in 800 mL reverse osmosis (RO) H_2O. Then, 50 mL of 1 M Tris-HCl was added to achieve a final concentration of 50 mM. The volume was adjusted to 1 litre with RO H_2O before sterilisation.

Phosphate-buffered saline (PBS)

PBS was made following the manufacturer's instructions using pre weighed tablets of PBS (Gibco, UK). Each 5 g tablet was dissolved in 500 mL RO H_2O water to a final concentration of 140 mM NaCl, 2.68 mM KCl, 10 mM Na_3HPO_4 and sterilised.

Appendix Figure 0.1. Environmental sample collection locations. Pointed on the map.

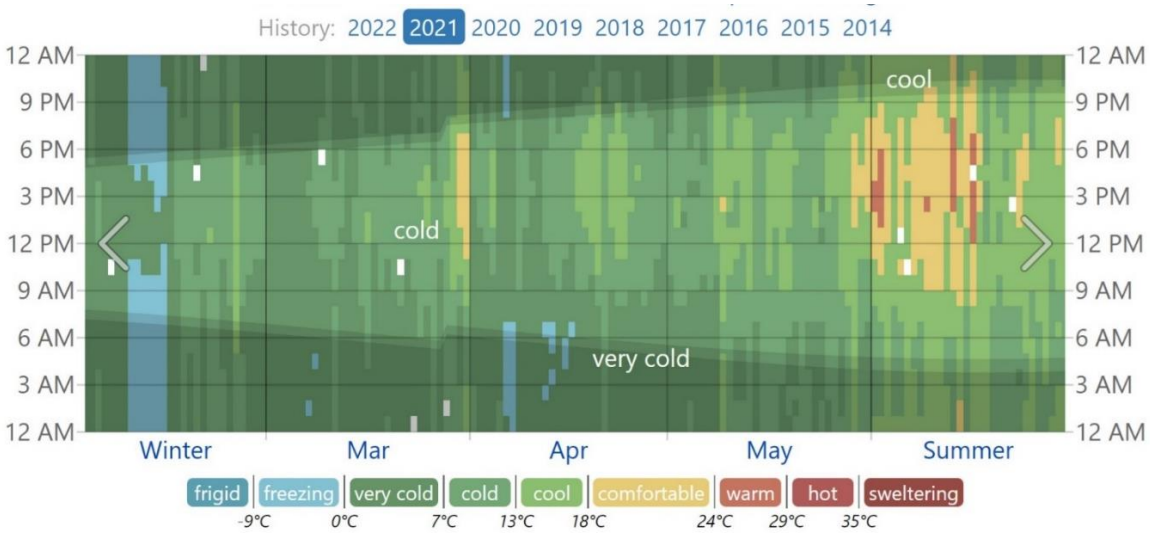

The hourly reported temperature, color coded into bands. The shaded overlays indicate night and civil twilight.

Appendix Figure 0.2. Hourly temperature in the spring of 2021 in Nottingham ("Nottingham Spring 2021 Historical Weather Data (United Kingdom) - Weather Spark," n.d.)

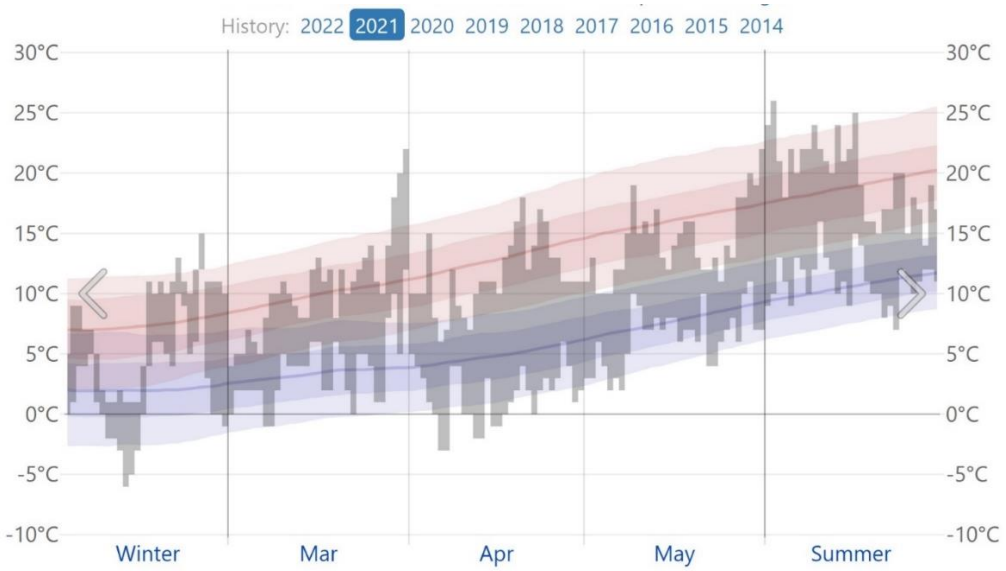

Appendix Figure 0.3. Nottingham temperature history in the Spring of 2021 ("Nottingham Spring 2021 Historical Weather Data (United Kingdom) - Weather Spark," n.d.)

Appendix Table 0.1. The summary of the steps of *P. multocida* isolation trials

Isolate	Name	Source	Growth on PSM	Growth on MC agar	Catalase	Oxidase	*PCR confirmation*
-	ATCC 43137	control	+	-	+	+	+
-	PM13	control	+	-	+	+	+
-	PM48	control	+	-	+	+	+
-	PM52	control	+	-	+	+	+
-	PM106	control	+	-	+	+	+
-	PM222	control	+	-	+	+	+
7.	Colwick 1-2	Lake	+	+			
8.	Stoke Bardolph 1	River	+	+			
9.	Stoke Bardolph 2	River	+	+			
10.	Stoke Bardolph 3	River	+	+			
11.	Stoke Bardolph 4	River	+	-	+	+	-
12.	Black Pool 1	Pond	+	-	-		
13.	Black Pool 7	Pond	+	-	-		
14.	Black Pool 8	Pond	+	+			
15.	Black Pool 10	Pond	+	+			
16.	Attenborough 1-1	Lake	+	-	-		
17.	Attenborough 1-2	Lake	+	+			
18.	Attenborough 1-3	Lake	+	+			
19.	Attenborough 2-1	Lake	+	-	+	+	-
20.	Attenborough 2-2	Lake	+	-	+	+	-
21.	Attenborough 2-3	Lake	+	-	+	+	-
22.	Attenborough 2-4	Lake	+	-	+	+	-

23.	Attenborough 2-5	Lake	+	-	+	+	-
24.	Attenborough 2-6	Lake	+	-	+	+	-
25.	Attenborough 2-7	Lake	+	-	+	+	-
26.	Attenborough 3-1	Lake	+	-	+	+	-
27.	Attenborough 3-2	Lake	+	-	-		
28.	Attenborough 3-3	Lake	+	-	+	+	-
29.	Attenborough 3-4	Lake	+	-	+	+	-
30.	Toton Bridge 1-1	River	+	+			
31.	Toton Bridge 1-2	River	+	-	+	+	-
32.	Toton Bridge 1-3	River	+	+			
33.	Toton Bridge 1-4	River	+	-	+	+	-
34.	Toton Bridge 1-5	River	+	+			
35.	Toton Bridge 1-6	River	+	+			
36.	Toton Bridge 1-7	River	+	+			
37.	Arboretum 1-1	Pond	+	-	+	+	-
38.	Arboretum 1-2	Pond	+	-	+	+	-
39.	Arboretum 1-3	Pond	+	+			
40.	Arboretum 1-4	Pond	+	-	+	+	-
41.	Arboretum 2-1	Pond	+	-	+	+	-
42.	Arboretum 2-2	Pond	+	+			
43.	Arboretum 2-3	Pond	+	-	+	+	-
44.	Arboretum 2-4	Pond	+	+			
45.	Arboretum 2-5	Pond	+	-	+	+	-
46.	Arboretum 2-6	Pond	+	-	+	+	-
47.	Arboretum 2-7	Pond	+	-	+	+	-
48.	Jubilee 1-1	Lake	+	-	+	+	-
49.	Jubilee 1-2	Lake	+	-	+	+	-
50.	Jubilee 1-3	Lake	+	-	+	+	-
51.	Jubilee 1-4	Lake	+	-	+	+	-
52.	Jubilee 1-5	Lake	+	-	+	+	-
53.	Jubilee 1-6	Lake	+	-	+	+	-
54.	Derby S. Derwent 1	River	+	+			
55.	Derby S. Derwent 2	River	+	+			
56.	Derby S. Derwent 3	River	+	-	+	+	-
57.	Derby S. Derwent 4	River	+	+			
58.	Derby S. Derwent 5	River	+	+			
59.	Derby S. Derwent 6	River	+	-	+	-	-
60.	Derby S. Derwent 7	River	+	+			
61	Derby S. Derwent 8	River	+	-	+	+	-
62	Derby S. Derwent 9	River	+	+			
63.	Derby S. Derwent 10	River	+	+			
64.	Derby S. Derwent 11	River	+	-	+	+	-
65.	Chapel Farm 1	Marina	+	+			
66.	Chapel Farm 2	Marina	+	-	-		
67.	Chapel Farm 3	Marina	+	-	+	+	-
68.	Chapel Farm 6	Marina	+	+			
69.	Chapel Farm 5	Marina	+	-	-		
70.	Chapel Farm 6	Marina	+	-	+	+	-
71	Chapel Farm 7	Marina	+	+			
72	Chapel Farm 8	Marina	+	+			
73	Milker 6-1	Faces	+	-	-		

74	Milker 6-2	Faces	+	-	-	
75	Milker 6-3	Faces	+	-	-	
76	Milker 6-4	Faces	+	-	+	-
77	Milker 6-5	Faces	+	+		
78	Milker 7-1	Faces	+	+		
79	Milker 7-2	Faces	+	+		
80	Milker 7-3	Faces	+	-	-	
81	Milker 7-4	Faces	+	+		
82	Milker 7-5	Faces	+	+		
83	Milker 8-1	Faces	+	+		
84	Milker 8-2	Faces	+	+		
85	Milker 8-3	Faces	+	+		
86	Milker 8-4	Faces	+	-	-	
87	Milker 8-5	Faces	+	-	-	
88	Milker 9-1	Faces	+	+		
89	Milker 9-2	Faces	+	-	-	
90	Milker 9-3	Faces	+	-	-	
91	Milker 9-4	Faces	+	-	-	
92	Milker 9-5	Faces	+	-	-	
93	Milker 10-1	Faces	+	+		
94	Milker 10-2	Faces	+	+		
95	Milker 10-3	Faces	+	+		
96	Milker 10-4	Faces	+	+		
97	Milker 10-5	Faces	+	+		

Chapter 3 supplementary materials

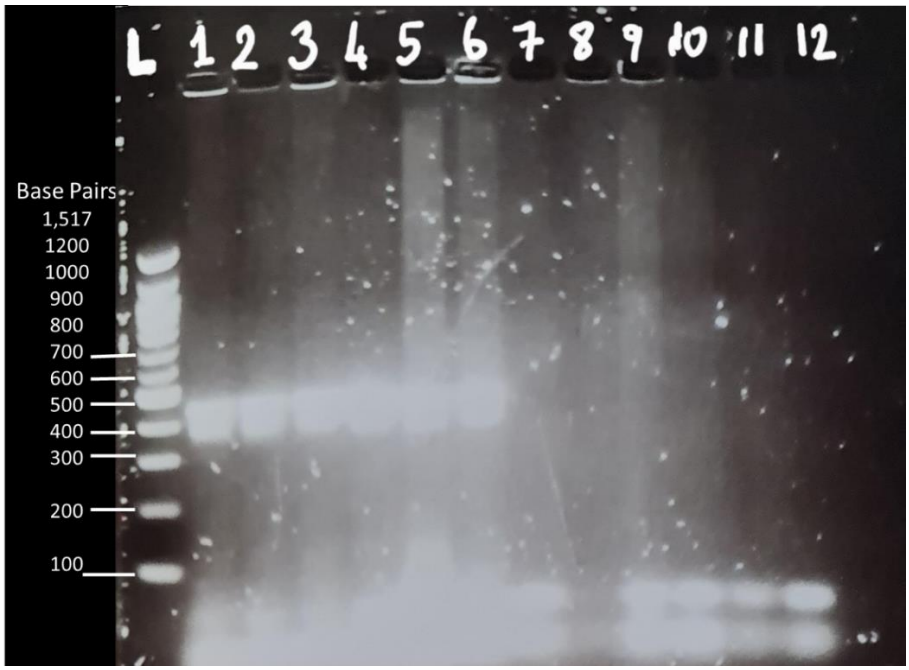

Appendix Figure 0.1. *P. multocida*-specific PCR assay 1.
This figure illustrates fragments specifically amplified by PCR in all *P. multocida* subspecies and serotypes by means of the primers KMT1-R and KMT1-F. The panel shows the following: lane M, 100-bp DNA marker (Biolabs, Quick Load); lane 1, PM13; lane 2, ATCC 43137; lane 3, PM48; lane 4, PM52; lane 5, PM106; lane 6, PM222; lane 7, Isolates of Stoke Bardolph 4; lane 8, Negative control, water; lane 9, Isolates of Attenborough 2-1; lane 10, , Isolates of Toton Bridge 1-4; lane 11, , Isolates of Arboretum 2-1; lane 12, , Isolates of Jubilee 1-1; lane 12, , Isolates of Jubilee 1-6. Samples were electrophoresed at 100 v for 1 h in a 1% agarose gel (1x TAE), stained with Nancy-520, visualized by UV illumination, photographed and printed.

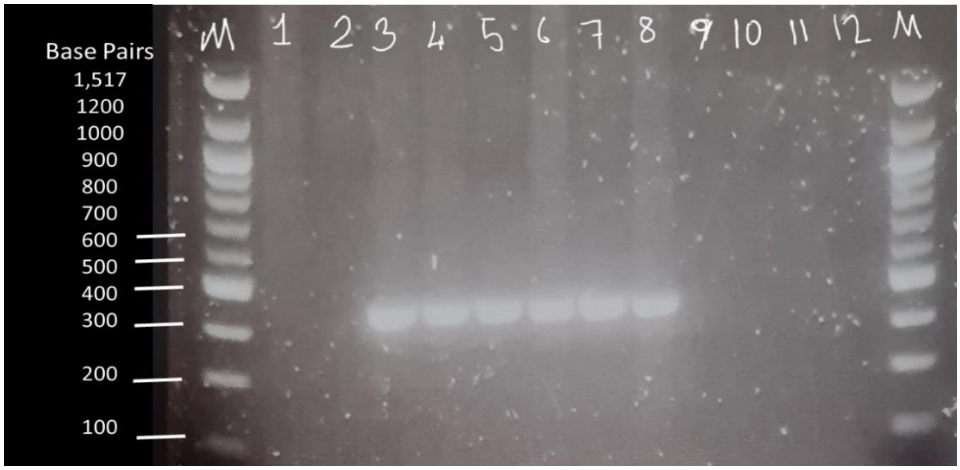

Appendix Figure 0.2. *P. multocida*-specific PCR assay 2

Lane M, 100-bp DNA marker (Biolabs, Quick Load); lane 1, Attenborough 2-2; lane 2 Negative control, water; lane 3, PM222; lane 4, PM106; lane 5, PM52; lane 6, PM48; lane 7, PM43; lane 8, PM13; lane 9, Arb 1-2; lane10; Jubile 1-2; lane 11, Jubile 1-3; lane 12, Jubile 1-4, lane 13, Jubilee 1-5. Samples were electrophoresed at 100 v for 1 h in a 1% agarose gel (1x TAE), stained with Nancy-520, visualized by UV illumination, photographed and printed.

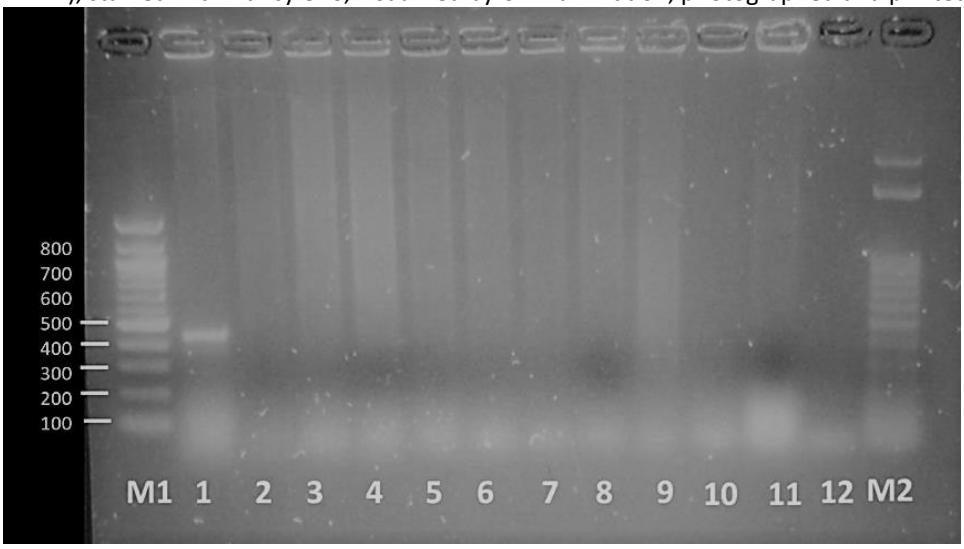

Appendix Figure 0.3. *P. multocida*-specific PCR assay 3.

Lane M 1, 100-bp DNA marker (Biolabs, Quick Load); lane 1, PM43137; lane 2, Att2-3; lane 3, Att2-4; lane 4, Att2-5; lane 5, Att2-6; lane 6, Att2-7; lane 7, Att3-1; lane 8, Att3-3; lane 9, Att3-4; lane10, Arb1-4; lane 11, Arb2-3; lane 12, Negative control, water; lane M2, 50-bp DNA marker. Samples were electrophoresed at 100 v for 2 h in a 1,35% agarose gel (1x TAE), stained with Nancy-520, visualized by UV illumination, photographed and printed.

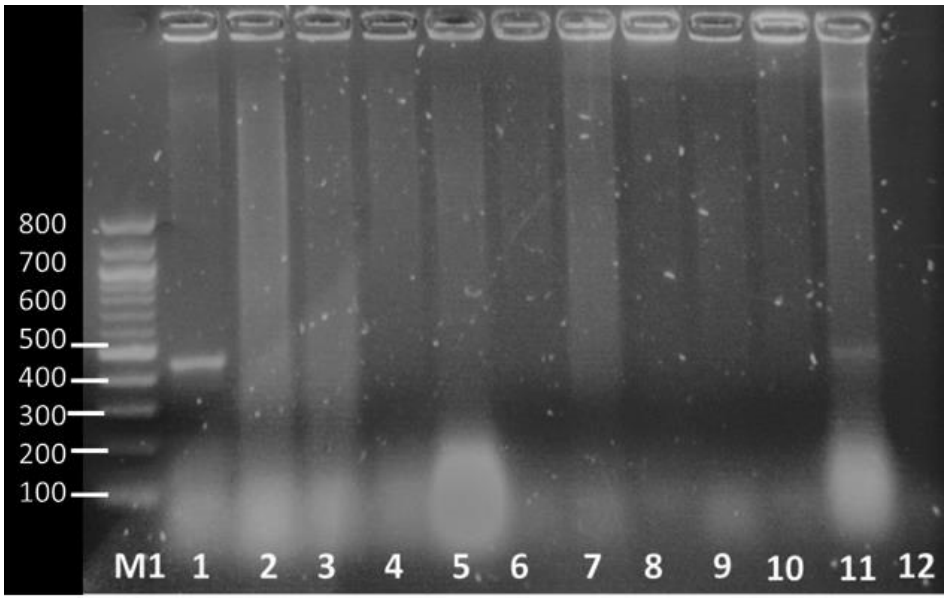

Appendix Figure 0.4. *P. multocida*-specific PCR assay 4.
Lane M 1, 100-bp DNA marker (Biolabs, Quick Load); lane 1, PM43137; lane2, Arb2-6; lane 3, Arb2-7; lane 4, Jubile 1-6; lane 5, DSD3; lane 6, DSD8; lane 7, DSD11; lane 8, Chap F1; lane 9, Chap F4; lane 10, Chap F6, lane 11, PM13; lane 12, Negative control, water; lane M2, 50-bp DNA marker. Samples were electrophoresed at 100 v for 2 h in a 1,44% agarose gel (1x TAE), stained with Nancy-520, visualized by UV illumination, photographed and printed.

Appendix Table 0.1. Water samples and the host strains used isolation trials.

Isolation source	PM13	ATCC 43137	PM48	PM52	PM106	PM222
Old Sewage Mix	+	+	-	-	-	-
Hyde Park	-	-	-	-	-	-
Highfield Park	-	-	-	-	-	-
Attenborough	-	-	-	-	-	-
Black Pool, SB	-	-	-	-	-	-
Stoke Bardolph	-	-	-	-	-	-
Colwick Park 1	-	-	-	-	-	-
Colwick Park 2	-	-	-	-	-	-
Colwick Park 3	-	-	-	-	-	-
Martin's Pond	-	-	-	-	-	-
Harrison's Plantation	-	-	-	-	-	-
Wollaton Park 1	-	-	-	-	-	-
Wollaton Park 2	-	-	-	-	-	-

Wollaton Park 3	-	-	-	-	-	-
Attenborough 1	-	-	-	-	-	-
Attenborough 2	-	-	-	-	-	-
Attenborough 3	-	-	-	-	-	-
Jubilee Campus 1	-	-	-	-	-	-
Jubilee Campus 2	-	-	-	-	-	-
Arboretum 1	-	-	-	-	-	-
Arboretum 2	-	-	-	-	-	-
Arboretum 3	-	-	-	-	-	-
Toton Bridge	-	-	-	-	-	-
Derby Sewage Derwent	-	-	-	-	-	-
Chapel Farm	-	-	-	-	-	-
Shardlow Marina	-	-	-	-	-	-
UoN Dairy Farm Slurry	-	-	-	-	-	-

Chapter 6 supplementary materials

2^{nd} LD_{50} for PM 13 $2.3x10^9$	24-h post injection	36-h post injection	48-h post injection
No injection Control	10/0	10/0	10/0
Injection Control	10/0	10/0	10/0
10^{-3} dilution	10/0	10/0	**10/0**
10^{-2} dilution	9/1	9/1	**9/1**
10^{-1} dilution	5/5	5/5	**5/5**
10^{0} dilution	1/9	0/10	**0/10**

Actual concentration	Log 10 Concentration	Effect
$2.3*10^9$	9.36	100.00
$2.3*10^8$	8.36	50.00
$2.3*10^7$	7.36	10.00
$2.3*10^6$	6.36	0

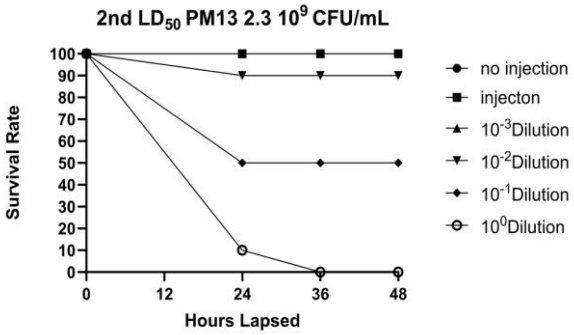

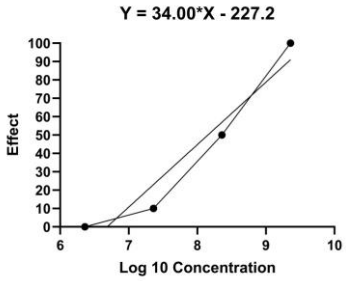

Log LD_{50}=Y = 34.00*X - 227.2
Log LD_{50}=8.15
LD_{50} =1.3*10^8

Appendix Figure 0.1. 2nd *LD_{50}* PM13

3rd LD_{50} for PM 13 2.8x10^8	24-h post injection	36-h post injection	48-h post injection
No injection Control	10/0	10/0	10/0
Injection Control	10/0	10/0	10/0
10^{-3} dilution	10/0	9/1	**9/1**
10^{-2} dilution	9/1	8/2	**8/2**
10^{-1} dilution	7/3	5/5	**5/5**
10^{0} dilution	1/9	0/10	**0/10**

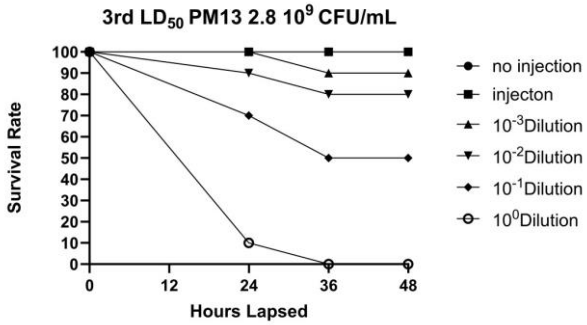

Actual concentration	Log 10 Concentration	Effect
$2.8*10^9$	8.45	100.00
$2.8*10^8$	7.45	50.00
$2.8*10^7$	6.45	20.00
$2.8*10^6$	5.45	10.00

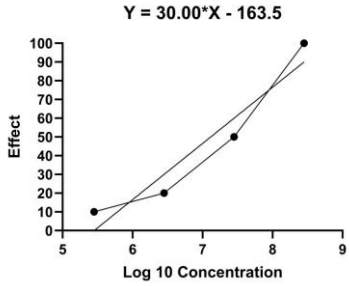

Log LD_{50}=Y = 30.00*X - 163.5
Log LD_{50}=7.11
LD_{50} =1.2*10^7

Appendix Figure 0.2. 3rd *LD_{50}* PM13

2nd LD50 ATCC 4373 1x10^9	24-h post injection	36-h post injection	48-h post injection
No injection Control	10/0	10/0	10/0
Injection Control	10/0	10/0	10/0
10^{-3} dilution	10/0	10/0	10/0
10^{-2} dilution	10/0	10/0	9/1
10^{-1} dilution	2/8	2/8	2/8
10^{0} dilution	0/10	0/10	0/10

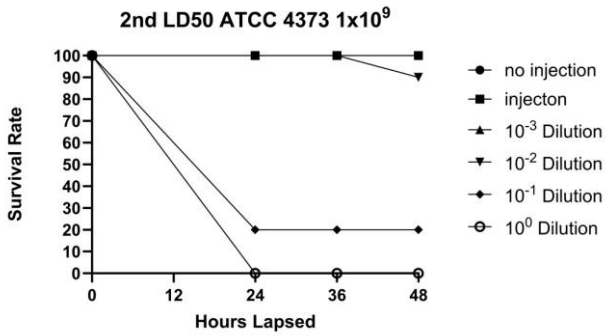

Actual concentration	Log 10 Concentration	Effect
$1*10^9$	9.00	100
$1*10^8$	8.00	80
$1*10^7$	7.00	10
$1*10^6$	6.00	0

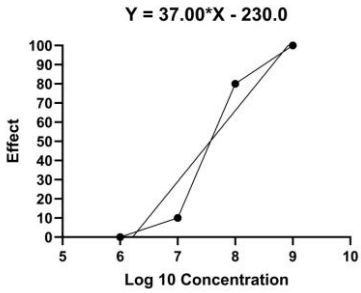

Log LD_{50}=Y = 37.00*X - 230.0
Log LD_{50}=7.57
LD_{50} =3.7*10^7

Appendix Figure 0.3. 2nd *LD_{50}* ATCC43137

3rd LD_{50} ATCC 4373 1,3x10^8	24-h post injection	36-h post injection	48-h post injection
No injection Control	10/0	10/0	10/0
Injection Control	10/0	10/0	10/0
10^{-3}	10/0	10/0	10/0
10^{-2}	8/2	8/2	7/3
10^{-1}	6/4	6/4	6/4
10^{0}	2/8	2/8	2/8

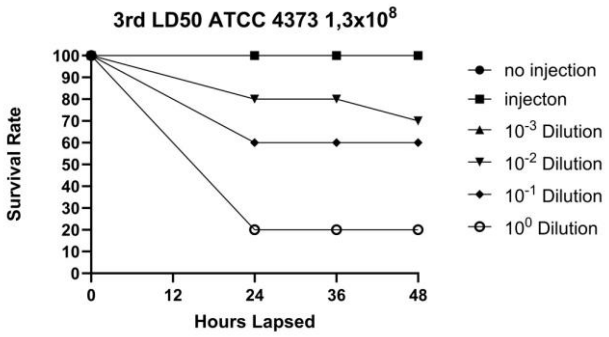

Actual concentration	Log 10 Concentration	Effect
$1.3*10^9$	8.11	80.00
$1.3*10^8$	7.11	40.00
$1.3*10^7$	6.11	30.00
$1.3*10^6$	5.11	0.00

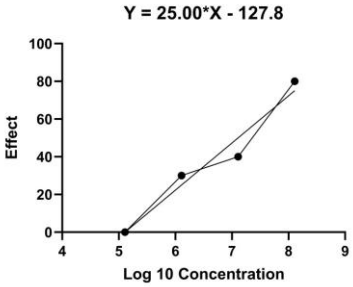

Log LD_{50}=Y = 25.00*X - 127.8
Log LD_{50}=7.11
LD_{50} =1.2*10^7

Appendix Figure 0.4. 3rd *LD_{50}* ATCC43137

Bibliography

Abbasifar, R., Kropinski, A. M., Sabour, P. M., Chambers, J. R., MacKinnon, J., Malig, T., & Griffiths, M. W. (2014). Efficiency of bacteriophage therapy against *Cronobacter sakazakii* in *Galleria mellonella* (greater wax moth) larvae. *Archives of Virology, 159*(9), 2253–2261. https://doi.org/10.1007/s00705-014-2055-x

Abdelsattar, A., Dawooud, A., Rezk, N., Makky, S., Safwat, A., Richards, P., & El-Shibiny, A. (2021a). How to train your phage: The recent efforts in phage training. *Biologics, 1*(2), 70–88. https://doi.org/10.3390/biologics1020005

Abdelsattar, A. S., Safwat, A., Nofal, R., Elsayed, A., Makky, S., & El-Shibiny, A. (2021b). Isolation and characterisation of bacteriophage ZCSE6 against *Salmonella* spp.: Phage application in milk. *Biologics, 1*(2), 164–176. https://doi.org/10.3390/biologics1020010

Abdulrahman, R. F., & Davies, R. L. (2021). Diversity and characterisation of temperate bacteriophages induced in *P. multocida* from different host species. *BMC Microbiology, 21,* Article 97. https://doi.org/10.1186/s12866-021-02155-9

Abedon, S. T., García, P., Mullany, P., & Aminov, R. (2017). Editorial: Phage therapy: Past, present and future. *Frontiers in Microbiology, 8,* 981. https://doi.org/10.3389/fmicb.2017.00981

Abedon, S. T., Kuhl, S. J., Blasdel, B. G., & Kutter, E. M. (2011). Phage treatment of human infections. *Bacteriophage*, *1*(2), 66–85. https://doi.org/10.4161/bact.1.2.15845

Ackermann H. W. (2009). Phage classification and characterization. *Methods in molecular biology (Clifton, N.J.)*, *501*, 127–140. https://doi.org/10.1007/978-1-60327-164-6_13.

Ackermann, H.-W. (2001). Frequency of morphological phage descriptions in the year 2000. *Archives of Virology, 146*(5), 843–857. https://doi.org/10.1007/s007050170120

Ackermann, H.-W. (2003). Bacteriophage observations and evolution. *Research in Microbiology, 154*(4), 245–251. https://doi.org/10.1016/S0923-2508(03)00067-6

Ackermann, H.-W., & Karaivanov, L. (1984). Morphology of *P. multocida* bacteriophages. *Canadian Journal of Microbiology, 30*(9), 1141–1148. https://doi.org/10.1139/m84-179

Ackermann H. W. (2007). 5500 Phages examined in the electron microscope. *Archives of virology*, *152*(2), 227–243. https://doi.org/10.1007/s00705-006-0849-1.

Ackermann, H. W. (2011). Bacteriophage taxonomy. *Microbiology Australia, 32*(2), 90. https://doi.org/10.1071/MA11090

Adams, P. E. (1959). Bacteriophages. Mark H. Adams. *The Quarterly Review of Biology, 34*(2), 179–180. https://doi.org/10.1086/402714

Adhikary, S., Bisgaard, M., Foster, G., Kiessling, N., Fahlén, A. R., Olsen, J. E., & Christensen, H. (2013). Comparative study of PCR methods to detect Pasteurella multocida. *Berliner und Munchener tierarztliche Wochenschrift*, *126*(9-10), 415–422.

Adler, B., Bulach, D., Chung, J., Doughty, S., Hunt, M., Rajakumar, K., Serrano, M., van Zanden, A., Zhang, Y., & Ruffolo, C. (1999). Candidate vaccine antigens and genes in *P. multocida*. *Journal of Biotechnology, 73*(2–3), 83–90. https://doi.org/10.1016/S0168-1656(99)00111-X

Adler, R., & Adler, B. (1991). Opsonic monoclonal antibodies against lipopolysaccharide (LPS) antigens of *P. multocida* and the role of LPS in immunity. *Veterinary Microbiology, 26*(4), 335–347. https://doi.org/10.1016/0378-1135(91)90027-D

Ahmad, N., Joji, R. M., & Shahid, M. (2023). Evolution and implementation of One Health to control the dissemination of antibiotic-resistant bacteria and resistance genes: A review. *Frontiers in cellular and infection microbiology*, *12*, 1065796. https://doi.org/10.3389/fcimb.2022.1065796.

Akhtar, M., Viazis, S., & Diez-Gonzalez, F. (2014). Isolation, identification and characterisation of lytic, wide host range bacteriophages from waste effluents against *Salmonella enterica* serovars. *Food Control, 38,* 67–74. https://doi.org/10.1016/j.foodcont.2013.09.064

Akmal, M., Rahimi-Midani, A., Hafeez-Ur-Rehman, M., Hussain, A., & Choi, T. J. (2020). Isolation, Characterization, and Application of a Bacteriophage Infecting the Fish Pathogen *Aeromonas hydrophila*. *Pathogens (Basel, Switzerland)*, *9*(3), 215. https://doi.org/10.3390/pathogens9030215.

Aksyuk, A. A., & Rossmann, M. G. (2011). Bacteriophage assembly. *Viruses, 3*(3), 172–203. https://doi.org/10.3390/v3030172

Al-Zubidi, M., Widziolek, M., Court, E. K., Gains, A. F., Smith, R. E., Ansbro, K., Alrafaie, A., Evans, C., Murdoch, C., Mesnage, S., Douglas, C. W. I., Rawlinson, A., & Stafford, G. P. (2019). Identification of novel bacteriophages with therapeutic potential that target *Enterococcus faecalis*. *Infection and Immunity, 87*(11), e00512-19. https://doi.org/10.1128/IAI.00512-19

Almoheer, R., Abd Wahid, M. E., Zakaria, H. A., Jonet, M. A. B., Al-Shaibani, M. M., Al-Gheethi, A., & Addis, S. Nor K. (2022). Spatial, temporal and demographic patterns in the prevalence of hemorrhagic septicaemia in 41 countries in 2005–2019: A systematic analysis with special focus on the potential development of a new-generation vaccine. *Vaccines, 10*(2), 315. https://doi.org/10.3390/vaccines10020315

Altschul, S. F., Gish, W., Miller, W., Myers, E. W., & Lipman, D. J. (1990). Basic local alignment search tool. *Journal of Molecular Biology, 215*(3), 403–410. https://doi.org/10.1016/S0022-2836(05)80360-2

Anandasekaran, G., Bardhan, D., Kumar, S., Karthiga, S., & Kumar, P. S. (2020). Estimation of economic losses due to haemorrhagic septicaemia in livestock of southern part of India. *Journal of Entomology and Zoology Studies, 8*(3), 32–35.

Andres, D., Gohlke, U., Broeker, N. K., Schulze, S., Rabsch, W., Heinemann, U., Barbirz, S., & Seckler, R. (2013). An essential serotype recognition pocket on phage P22 tailspike protein forces *Salmonella enterica* serovar Paratyphi A O-antigen fragments to bind as nonsolution conformers. *Glycobiology, 23*(4), 486–494. https://doi.org/10.1093/glycob/cws224

Andrews, S. (2023). *FastQC* (Version 0.12.0) [Computer software]. Babraham Bioinformatics. https://www.bioinformatics.babraham.ac.uk/projects/fastqc/ bioinformatics.babraham.ac.uk

Weather Spark (2021). https://weatherspark.com/h/s/41783/2021/0/Historical-Weather-Spring-2021-in-Nottingham-United-Kingdom

Antoine, C., Laforêt, F., Blasdel, B., Fall, A., Duprez, J.-N., Mainil, J., Delcenserie, V., & Thiry, D. (2021). In vitro characterisation and in vivo efficacy assessment in *Galleria mellonella* larvae of newly isolated bacteriophages against *Escherichia coli* K1. *Viruses, 13*(10), 2005. https://doi.org/10.3390/v13102005

Arias, C. F., Acosta, F. J., Bertocchini, F., Herrero, M. A., & Fernández-Arias, C. (2022). The coordination of anti-phage immunity mechanisms in bacterial cells. *Nature Communications, 13*(1). https://doi.org/10.1038/s41467-022-35203-7

Arndt, D., Grant, J. R., Marcu, A., Sajed, T., Pon, A., Liang, Y., & Wishart, D. S. (2016). PHASTER: A better, faster version of the PHAST phage search tool. *Nucleic Acids Research, 44*(W1), W16–W21. https://doi.org/10.1093/nar/gkw387

Aslam, B., Khurshid, M., Arshad, M. I., Muzammil, S., Rasool, M., Yasmeen, N., Shah, T., Chaudhry, T. H., Rasool, M. H., Shahid, A., Xueshan, X., & Baloch, Z. (2021). Antibiotic resistance: One health one world outlook. *Frontiers in Cellular and Infection Microbiology, 11,* 771510. https://doi.org/10.3389/fcimb.2021.771510

Aslam, S., Courtwright, A. M., Koval, C., Lehman, S. M., Morales, S., Furr, C. L. L., Rosas, F., Brownstein, M. J., Fackler, J. R., Sisson, B. M., Biswas, B., Henry, M., Luu, T., Bivens, B. N., Hamilton, T., Duplessis, C., Logan, C., Law, N., Yung, G., Turowski, J., Anesi, J., Strathdee, S. A., & Schooley, R. T. (2019). Early clinical experience of bacteriophage therapy in 3 lung transplant recipients. *American Journal of Transplantation, 19*(9), 2631–2639. https://doi.org/10.1111/ajt.15503

Ataei Kachooei, S., Ranjbar, M. M., & Ataei Kachooei, S. (2017). Evaluation of *P. multocida* serotype B:2 resistance to immune serum and complement system. *Veterinary Research Forum, 8*(3), 179–184.

Atterbury, R. J., Van Bergen, M. A. P., Ortiz, F., Lovell, M. A., Harris, J. A., De Boer, A., Wagenaar, J. A., Allen, V. M., & Barrow, P. A. (2007). Bacteriophage therapy to reduce *Salmonella* colonization of broiler chickens. *Applied and Environmental Microbiology, 73*(14), 4543–4549. https://doi.org/10.1128/AEM.00049-07

Augustine, J., Gopalakrishnan, M. V., & Bhat, S. G. (2014). Application of ΦSP-1 and ΦSP-3 as a therapeutic strategy against *Salmonella Enteritidis* infection using *Caenorhabditis*

elegans as model organism. *FEMS Microbiology Letters, 356*(1), 113–117. https://doi.org/10.1111/1574-6968.12493

Avril, J. L., Donnio, P. Y., & Pouedras, P. (1990). Selective medium for *P. multocida* and its use to detect oropharyngeal carriage in pig breeders. *Journal of Clinical Microbiology, 28*(6), 1438–1440. https://doi.org/10.1128/JCM.28.6.1438-1440.1990

Ayaz, M. (2017). Cellular efflux transporters and the potential role of natural products in combating efflux-mediated drug resistance. *Frontiers in Bioscience, 22*(4), 732–756. https://doi.org/10.2741/4513

Ayaz, M., Ullah, F., Sadiq, A., Ullah, F., Ovais, M., Ahmed, J., & Devkota, H. P. (2019). Synergistic interactions of phytochemicals with antimicrobial agents: Potential strategy to counteract drug resistance. *Chemico-Biological Interactions, 308,* 294–303. https://doi.org/10.1016/j.cbi.2019.05.050

Azabo, R., Dulle, F., Mshana, S. E., Matee, M. I., & Kimera, S. I. (2022). Antimicrobial use in cattle and poultry production on occurrence of multidrug-resistant *Escherichia coli*: A systematic review with focus on sub-Saharan Africa. *Frontiers in Veterinary Science, 9.*

Azizian, R., Mousavi Nasab, S. D., & Ahmadi, N. A. (2013). Bacteriophage as a novel antibacterial agent in industry and medicine. *Journal of Paramedical Sciences, 4*(4), 92–100.

Baalsrud, K. J. (1987). The effect of atrophic rhinitis on growth rate. *Acta Veterinaria Scandinavica, 28*(3–4), 299–304.

Backstrand, J. M., & Botzler, R. G. (1986). Survival of *P. multocida* in soil and water in an area where avian cholera is enzootic. *Journal of Wildlife Diseases, 22*(2), 257–259. https://doi.org/10.7589/0090-3558-22.2.257

Bailly-Bechet, M., Vergassola, M., & Rocha, E. (2007). Causes for the intriguing presence of tRNAs in phages. *Genome Research, 17*(10), 1486–1495. https://doi.org/10.1101/gr.6649807

Bamford, D., & Mindich, L. (1982). Structure of the lipid-containing bacteriophage PRD1: Disruption of wild-type and nonsense mutant phage particles with guanidine hydrochloride. *Journal of Virology, 44*(3), 1031–1038. https://doi.org/10.1128/JVI.44.3.1031-1038.1982

Bankevich, A., Nurk, S., Antipov, D., Gurevich, A. A., Dvorkin, M., Kulikov, A. S., Lesin, V. M., Nikolenko, S. I., Pham, S., Prjibelski, A. D., Pyshkin, A. V., Sirotkin, A. V., Vyahhi, N., Tesler, G., Alekseyev, M. A., & Pevzner, P. A. (2012). SPAdes: A new genome assembly algorithm and its applications to single-cell sequencing. *Journal of Computational Biology, 19*(5), 455–477. https://doi.org/10.1089/cmb.2012.0021

Bardhan, D., Kumar, S., & Kumar, A. (2020). Economic losses due to hemorrhagic septicaemia in India. *The Indian Journal of Animal Sciences, 90*(3), 341–346. https://doi.org/10.56093/ijans.v90i3.102320

Barrow, P., Lovell, M., & Berchieri, A. (1998). Use of lytic bacteriophage for control of experimental *Escherichia coli* septicaemia and meningitis in chickens and calves. *Clinical and Diagnostic Laboratory Immunology, 5*(3), 294–298. https://doi.org/10.1128/CDLI.5.3.294-298.1998

Barrow, P. A. (2001). The use of bacteriophages for treatment and prevention of bacterial disease in animals and animal models of human infection. *Journal of Chemical Technology and Biotechnology, 76*(7), 677–682. https://doi.org/10.1002/jctb.436

Barrow, P. A., & Soothill, J. S. (1997). Bacteriophage therapy and prophylaxis: Rediscovery and renewed assessment of potential. *Trends in Microbiology, 5*(7), 268–271. https://doi.org/10.1016/S0966-842X(97)01054-8

Barta, L., Stöger, A., Polzer, D., Ruppitsch, W., Schmoll, F., & Sattler, T. (2025). Phenotypical and genotypical resistance testing of *Pasteurella multocida* isolated from different animal species in Austria. *Frontiers in Veterinary Science, 12.*

Bayat, F., Hilal, A., Thirugnanasampanthar, M., Tremblay, D., Filipe, C. D. M., Moineau, S., Didar, T. F., & Hosseinidoust, Z. (2024). High throughput platform technology for rapid target identification in personalized phage therapy. *Nature Communications, 15*(1), 5626. https://doi.org/10.1038/s41467-024-49710-2

Beeton, M. L., Alves, D. R., Enright, M. C., & Jenkins, A. T. A. (2015). Assessing phage therapy against *Pseudomonas aeruginosa* using a *Galleria mellonella* infection model. *International Journal of Antimicrobial Agents, 46*(2), 196–200. https://doi.org/10.1016/j.ijantimicag.2015.04.005

Benkirane, A., & De Alwis, M. C. L. (2002). Haemorrhagic septicaemia, its significance, prevention and control in Asia. *Veterinární Medicína, 47*(8), 234–240. https://doi.org/10.17221/5830-VETMED

Bernheim, A., & Sorek, R. (2020). The pan-immune system of bacteria: Antiviral defence as a community resource. *Nature Reviews Microbiology, 18*(2), 113–119. https://doi.org/10.1038/s41579-019-0278-2

Bertani, B., & Ruiz, N. (2018). Function and biogenesis of lipopolysaccharides. In J. M. Slauch (Ed.), *EcoSal Plus, 8*(1). https://doi.org/10.1128/ecosalplus.ESP-0001-2018

Bertozzi Silva, J., Storms, Z., & Sauvageau, D. (2016). Host receptors for bacteriophage adsorption. *FEMS Microbiology Letters, 363*(4), fnw002. https://doi.org/10.1093/femsle/fnw002

Birge, E. A. (2000). *Bacterial and bacteriophage genetics.* https://doi.org/10.1007/978-1-4757-3258-0

Blackall, P. J., & Miflin, J. K. (2000). Identification and typing of *Pasteurella multocida*: A review. *Avian Pathology, 29*(4), 271–287. https://doi.org/10.1080/03079450050118395

Blakebrough-Hall, C., McMeniman, J. P., & González, L. A. (2020). An evaluation of the economic effects of bovine respiratory disease on animal performance, carcass traits, and economic outcomes in feedlot cattle defined using four BRD diagnosis methods. *Journal of Animal Science, 98*(2), skaa005. https://doi.org/10.1093/jas/skaa005

Blasco, L., & Tomás, M. (2023). Use of *Galleria mellonella* as an animal model for studying the antimicrobial activity of bacteriophages with potential use in phage therapy. *Methods in Molecular Biology,* 171–180. https://doi.org/10.1007/978-1-0716-3523-0_11

Bogovazova, G. G., Voroshilova, N. N., & Bondarenko, V. M. (1991). Effektivnost' bakteriofaga *Klebsiella pneumoniae* pri terapii éksperimental'noĭ klebsielleznoĭ infektsii [The efficacy of *Klebsiella pneumoniae* bacteriophage in the therapy of experimental *Klebsiella* infection]. *Zhurnal Mikrobiologii, Epidemiologii i Immunobiologii, (4),* 5–8.

Bohannan, B. J. M., & Lenski, R. E. (1997). Effect of resource enrichment on a chemostat community of bacteria and bacteriophage. *Ecology, 78*(8), 2303. https://doi.org/10.2307/2265893

Bolger, A. M., Lohse, M., & Usadel, B. (2014a). Trimmomatic: A flexible trimmer for Illumina sequence data. *Bioinformatics, 30*(15), 2114–2120. https://doi.org/10.1093/bioinformatics/btu170

Bonilla, N., Rojas, M. I., Netto Flores Cruz, G., Hung, S. H., Rohwer, F., & Barr, J. J. (2016). Phage on tap—A quick and efficient protocol for the preparation of bacteriophage laboratory stocks. *PeerJ, 4,* e2261. https://doi.org/10.7717/peerj.2261

Borges, A. L., Zhang, J. Y., Rollins, M. F., Osuna, B. A., Wiedenheft, B., & Bondy-Denomy, J. (2018). Bacteriophage cooperation suppresses CRISPR-Cas3 and Cas9 immunity. *Cell, 174*(4), 917–925.e10. https://doi.org/10.1016/j.cell.2018.06.013

Borrathybay, E., Sawada, T., Kataoka, Y., Ohtsu, N., Takagi, M., Nakamura, S., & Kawamoto, E. (2003). A 39 kDa protein mediates adhesion of avian *P. multocida* to chicken embryo fibroblast cells. *Veterinary Microbiology, 97*(3–4), 229–243. https://doi.org/10.1016/j.vetmic.2003.09.010

Botka, T., Pantůček, R., Mašlaňová, I., Benešík, M., Petráš, P., Růžičková, V., Havlíčková, P., Varga, M., Žemličková, H., Koláčková, I., Florianová, M., Jakubů, V., Karpíšková, R., & Doškař, J. (2019). Lytic and genomic properties of spontaneous host-range Kayvirus mutants prove their suitability for upgrading phage therapeutics against staphylococci. *Scientific Reports, 9*, 5475. https://doi.org/10.1038/s41598-019-41868-w

Botzler, R. G. (1991). Epizootiology of avian cholera in wildfowl. *Journal of Wildlife Diseases, 27*(3), 367–395. https://doi.org/10.7589/0090-3558-27.3.367

Bourgeois, J., Lazinski, D. W., & Camilli, A. (2020). Identification of spacer and protospacer sequence requirements in the *Vibrio cholerae* type I-E CRISPR/Cas system. *mSphere, 5*(6). https://doi.org/10.1128/mSphere.00813-20

Bourély, C., Cazeau, G., Jouy, É., Haenni, M., Madec, J., Jarrige, N., Leblond, A., & Gay, E. (2019). Antimicrobial resistance of *Pasteurella multocida* isolated from diseased food-producing animals and pets. *Veterinary Microbiology, 235,* 280–284.

Boyce, J. D., & Adler, B. (2000). The capsule is a virulence determinant in the pathogenesis of *P. multocida* M1404 (B:2). *Infection and Immunity, 68*(6), 3463–3468. https://doi.org/10.1128/IAI.68.6.3463-3468.2000

Boyce, J. D., Harper, M., Wilkie, I. W., & Adler, B. (2010). Pasteurella. In *Pathogenesis of bacterial infections in animals* (pp. 325–346). https://doi.org/10.1002/9780470958209.ch17

Braunstein, R., Hubanic, G., Yerushalmy, O., Oren-Alkalay, S., Rimon, A., Coppenhagen-Glazer, S., Niv, O., Marom, H., Barsheshet, A., & Hazan, R. (2024). Successful phage-antibiotic therapy of *P. aeruginosa* implant-associated infection in a Siamese cat. *The Veterinary Quarterly, 44,* 1–9.

Bredy, J. P., & Botzler, R. G. (1989a). The effects of six environmental variables on *P. multocida* populations in water. *Journal of Wildlife Diseases, 25*(2), 232–239. https://doi.org/10.7589/0090-3558-25.2.232

Breitbart, M. (2012). Marine viruses: Truth or dare. *Annual Review of Marine Science, 4*(1), 425–448. https://doi.org/10.1146/annurev-marine-120709-142805

Brix, A., Cafora, M., Aureli, M., & Pistocchi, A. (2020a). Animal models to translate phage therapy to human medicine. *International Journal of Molecular Sciences, 21*(10), 3715. https://doi.org/10.3390/ijms21103715

Brooks, K. R., Raper, K. C., Ward, C. E., Holland, B. P., Krehbiel, C. R., & Step, D. L. (2011). Economic effects of bovine respiratory disease on feedlot cattle during backgrounding and finishing phases. *The Professional Animal Scientist, 27,* 195–203.

Brunel, J.-S., & Guery, B. (2017). Multidrug resistant (or antimicrobial-resistant) pathogens—Alternatives to new antibiotics? *Swiss Medical Weekly, 147*(4748), w14553. https://doi.org/10.4414/smw.2017.14553

Brüssow, H., Canchaya, C., & Hardt, W. D. (2004). Phages and the evolution of bacterial pathogens: From genomic rearrangements to lysogenic conversion. *Microbiology and Molecular Biology Reviews, 68*(3), 560–602. https://doi.org/10.1128/MMBR.68.3.560-602.2004

Bucher, M. J., & Czyż, D. M. (2024). Phage against the machine: The SIE-ence of superinfection exclusion. *Viruses, 16*(9), 1348. https://doi.org/10.3390/v16091348

Buchon, N., Silverman, N., & Cherry, S. (2014). Immunity in *Drosophila melanogaster*—From microbial recognition to whole-organism physiology. *Nature Reviews Immunology, 14*(12), 796–810. https://doi.org/10.1038/nri3763

Burnet, F. M. (1933). The classification of dysentery-coli bacteriophages. III. A correlation of the serological classification with certain biochemical tests. *This Journal, 36,* 179–184.

Cafora, M., Deflorian, G., Forti, F., Ferrari, L., Binelli, G., Briani, F., Ghisotti, D., & Pistocchi, A. (2019). Phage therapy against *Pseudomonas aeruginosa* infections in a cystic fibrosis zebrafish model. *Scientific Reports, 9*(1). https://doi.org/10.1038/s41598-018-37636-x

Campoy, S., Aranda, J., Àlvarez, G., Barbé, J., & Llagostera, M. (2006a). Isolation and sequencing of a temperate transducing phage for *P. multocida*. *Applied and Environmental Microbiology, 72*(5), 3154–3160. https://doi.org/10.1128/AEM.72.5.3154-3160.2006

Capitini, C. M., Herrero, I. A., Patel, R., Ishitani, M. B., & Boyce, T. G. (2002). Wound infection with *Neisseria weaveri* and a novel subspecies of *P. multocida* in a child who sustained a tiger bite. *Clinical Infectious Diseases, 34*(12), e74–e76. https://doi.org/10.1086/340712

Capra, M. L., Quiberoni, A., & Reinheimer, J. (2006). Phages of *Lactobacillus casei/paracasei*: Response to environmental factors and interaction with collection and commercial strains. *Journal of Applied Microbiology, 100*(2), 334–342. https://doi.org/10.1111/j.1365-2672.2005.02767.x

Carlson, K. (2005). Appendix: Working with bacteriophages: Common techniques and methodological approaches. In E. Kutter & A. Sulakvelidze (Eds.), *Bacteriophages: Biology and applications* (pp. 437–494). CRC Press.

Carter, G. R. (1984). Serotyping of *P. multocida*. *Methods in Microbiology,* 247–258. https://doi.org/10.1016/S0580-9517(08)70394-5

Catry, B., Chiers, K., Schwarz, S., Kehrenberg, C., Decostere, A., & de Kruif, A. (2005). Fatal peritonitis caused by *P. multocida* capsular type F in calves. *Journal of Clinical Microbiology, 43*(3), 1480–1483.

Cesta, N., Pini, M., Mulas, T., Materazzi, A., Ippolito, E., Wagemans, J., Kutateladze, M., Fontana, C., Sarmati, L., Tavanti, A., Lavigne, R., Andreoni, M., & Di Luca, M. (2023). Application of phage therapy in a case of a chronic hip-prosthetic joint infection due to *Pseudomonas aeruginosa*: An Italian real-life experience and in vitro analysis. *Open Forum Infectious Diseases, 10*(2), ofad051. https://doi.org/10.1093/ofid/ofad051

Champion, O. L., Titball, R. W., & Bates, S. (2018). Standardization of *G. mellonella* larvae to provide reliable and reproducible results in the study of fungal pathogens. *Journal of Fungi, 4.*

Chan, B. K., Abedon, S. T., & Loc-Carrillo, C. (2013). Phage cocktails and the future of phage therapy. *Future Microbiology, 8*(6), 769–783. https://doi.org/10.2217/fmb.13.47

Chan, B. K., Sistrom, M., Wertz, J. E., Kortright, K. E., Narayan, D., & Turner, P. E. (2016). Phage selection restores antibiotic sensitivity in MDR *Pseudomonas aeruginosa*. *Scientific Reports, 6*(1). https://doi.org/10.1038/srep26717

Chan, P. P., & Lowe, T. M. (2019). tRNAscan-SE: Searching for tRNA genes in genomic sequences. *Methods in Molecular Biology,* 1–14. https://doi.org/10.1007/978-1-4939-9173-0_1

Chanter, N., Goodwin, R. F., & Rutter, J. M. (1989). Comparison of methods for the sampling and isolation of toxigenic *P. multocida* from the nasal cavity of pigs. *Research in Veterinary Science, 47*(3), 355–358.

Chen, H., Jiang, N., Fu, G., Fu, Q., Wan, C., Huang, Y., Liu, Y., Liu, R., Liang, Q., & Cheng, L. (2024). Characterisation and potential application of phage vB_PmuM_CFP3 for phage therapy against avian *P. multocida*. *Animals, 14*(22), 3268. https://doi.org/10.3390/ani14223268

Chen, W., Xiao, H., Wang, X., Song, S., Han, Z., Li, X., Yang, F., Wang, L., Song, J., Liu, H., & Cheng, L. (2020). Structural changes of a bacteriophage upon DNA packaging and maturation. *Protein & Cell, 11*(5), 374–379. https://doi.org/10.1007/s13238-020-00715-9

Chen, Y., Batra, H., Dong, J., Chen, C., Rao, V. B., & Tao, P. (2019). Genetic engineering of bacteriophages against infectious diseases. *Frontiers in Microbiology, 10,* 954. https://doi.org/10.3389/fmicb.2019.00954

Chen, Y., Guo, G., Sun, E., Song, J., Yang, L., Zhu, L., Liang, W., Hua, L., Peng, Z., Tang, X., Chen, H., & Wu, B. (2019). Isolation of a T7-like lytic *Pasteurella* bacteriophage vB_PmuP_PHB01 and its potential use in therapy against *P. multocida* infections. *Viruses, 11*(1), 86. https://doi.org/10.3390/v11010086

Chen, Y., Sun, E., Song, J., Yang, L., & Wu, B. (2018a). Complete genome sequence of a novel T7-like bacteriophage from a *P. multocida* capsular type A isolate. *Current Microbiology, 75*(5), 574–579. https://doi.org/10.1007/s00284-017-1419-3

Chen, Y., Sun, E., Yang, L., Song, J., & Wu, B. (2018c). Therapeutic application of bacteriophage PHB02 and its putative depolymerase against *P. multocida* capsular type A in mice. *Frontiers in Microbiology, 9,* 1678. https://doi.org/10.3389/fmicb.2018.01678

Cheng, J.-H., Yang, H., Liu, M.-L., Su, W., Feng, P.-M., Ding, H., Chen, W., & Lin, H. (2018). Prediction of bacteriophage proteins located in the host cell using hybrid features. *Chemometrics and Intelligent Laboratory Systems, 180,* 64–69. https://doi.org/10.1016/j.chemolab.2018.07.006

Cheng, Y., Wang, K., Lin, L., Zhao, X., Pan, Z., & Zhou, Z. (2020). Differences in pathogenicity and virulence-associated gene expression among *P. multocida* strains with high and low virulence in a lung tissue model. *Microbial Pathogenesis, 140,* 103911. https://doi.org/10.1016/j.micpath.2019.103911

Chirase, N. K., & Greene, L. W. (2001). Dietary zinc and manganese sources administered from the fetal stage onwards affect immune response of transit stressed and virus-infected offspring steer calves. *Animal Feed Science and Technology, 93*(3–4), 217–228. https://doi.org/10.1016/S0377-8401(01)00277-2

Cho, J.-H., Lee, G. M., Ko, S., Kim, Y., & Kim, D. (2025). Characterization and therapeutic potential of newly isolated bacteriophages against *Staphylococcus* species in bovine mastitis. *Journal of Virology, 99*(3), e0190124. https://doi.org/10.1128/JVI.01901-24

Christensen, H., & Bisgaard, M. (2006a). The genus *Pasteurella*. In *The Prokaryotes* (pp. 1062–1090). https://doi.org/10.1007/0-387-30746-X_41

Chromagar. (2021, December 22). New product: CHROMagar™ *Pasteurella*. Chromagar. https://www.chromagar.com/en/new-product-chromagar-pasteurella/ (Accessed 5 February 2024)

Chung, E. L. T., Abdullah, F. F. J., Ibrahim, H. H., Marza, A. D., Zamri-Saad, M., Haron, A. W., Lila, M. A. M., & Norsidin, M. J. (2016). Clinico-pathology, hematology and biochemistry responses in buffaloes towards *P. multocida* type B:2 immunogen lipopolysaccharide via oral and intravenous routes of infection. *Microbial Pathogenesis, 91,* 141–154. https://doi.org/10.1016/j.micpath.2015.12.003

Chung, I. Y., Jang, H. J., Bae, H. W., & Cho, Y. H. (2014). A phage protein that inhibits the bacterial ATPase required for type IV pilus assembly. *Proceedings of the National Academy*

of Sciences of the United States of America, 111(31), 11503–11508. https://doi.org/10.1073/pnas.1403537111

Chung, I.-Y., Sim, N., & Cho, Y.-H. (2012). Antibacterial efficacy of temperate phage-mediated inhibition of bacterial group motilities. *Antimicrobial Agents and Chemotherapy, 56*(11), 5612–5617. https://doi.org/10.1128/AAC.00504-12

Chung, J. Y., Wilkie, I., Boyce, J. D., & Adler, B. (2005). Vaccination against fowl cholera with acapsular *P. multocida* A:1. *Vaccine, 23*(21), 2751–2755. https://doi.org/10.1016/j.vaccine.2004.11.036

Chung, J. Y., Wilkie, I., Boyce, J. D., Townsend, K. M., Frost, A. J., Ghoddusi, M., & Adler, B. (2001). Role of capsule in the pathogenesis of fowl cholera caused by *P. multocida* serogroup A. *Infection and Immunity, 69*(4), 2487–2492. https://doi.org/10.1128/IAI.69.4.2487-2492.2001

Chung, K. M., Liau, X. L., & Tang, S. S. (2023). Bacteriophages and their host range in multidrug-resistant bacterial disease treatment. *Pharmaceuticals, 16*(10), 1467. https://doi.org/10.3390/ph16101467

Cieślik, M., Bagińska, N., Jończyk-Matysiak, E., Węgrzyn, A., Węgrzyn, G., & Górski, A. (2021). Temperate bacteriophages—The powerful indirect modulators of eukaryotic cells and immune functions. *Viruses, 13*(6), 1013. https://doi.org/10.3390/v13061013

Clark, J. R., & March, J. B. (2006). Bacteriophages and biotechnology: Vaccines, gene therapy and antibacterials. *Trends in Biotechnology, 24*(5), 212–218. https://doi.org/10.1016/j.tibtech.2006.03.003

Clokie, M. R. J., Kropinski, A. M., & Lavigne, R. (2017). *Bacteriophages.* Humana Press.

Clokie, M. R. J., Millard, A. D., Letarov, A. V., & Heaphy, S. (2011). Phages in nature. *Bacteriophage, 1*(1), 31–45. https://doi.org/10.4161/bact.1.1.14942

Comeau, A. M., Short, S., & Suttle, C. A. (2004). The use of degenerate-primed random amplification of polymorphic DNA (DP-RAPD) for strain-typing and inferring the genetic similarity among closely related viruses. *Journal of Virological Methods, 118*(2), 95–100. https://doi.org/10.1016/j.jviromet.2004.01.020

Cook, R., Hooton, S., Trivedi, U., King, L., Dodd, C. E. R., Hobman, J. L., Stekel, D. J., Jones, M. A., & Millard, A. D. (2021a). Hybrid assembly of an agricultural slurry virome reveals a diverse and stable community with the potential to alter the metabolism and virulence of veterinary pathogens. *Microbiome, 9*(1). https://doi.org/10.1186/s40168-021-01010-3

Corbett, D., & Roberts, I. S. (2008). Capsular polysaccharides in *Escherichia coli*. *Advances in Applied Microbiology,* 1–26. https://doi.org/10.1016/S0065-2164(08)00601-1

Crawford, J. T., & Goldberg, E. B. (1977). The effect of baseplate mutations on the requirement for tail-fiber binding for irreversible adsorption of bacteriophage T4. *Journal of Molecular Biology, 111*(3), 305–313. https://doi.org/10.1016/S0022-2836(77)80053-3

Crawford, R. L., Blyde, D., Blackall, P. J., Forde, B. M., Beatson, S. A., Harris, L. M., Turni, C., & Omaleki, L. (2019). Novel insights into pasteurellosis in captive pinnipeds. *Veterinary Microbiology, 231,* 232–237. https://doi.org/10.1016/j.vetmic.2019.03.017.

Dabo, S. M., Confer, A., Montelongo, M., York, P., & Wyckoff, J. H. (2008). Vaccination with *P. multocida* recombinant OmpA induces strong but non-protective and deleterious Th2-type immune response in mice. *Vaccine, 26*(34), 4345–4351. https://doi.org/10.1016/j.vaccine.2008.06.029

Dabo, S. M., Confer, A. W., & Quijano-Blas, R. A. (2003). Molecular and immunological characterisation of *P. multocida* serotype A:3 OmpA: Evidence of its role in *P. multocida* interaction with extracellular matrix molecules. *Microbial Pathogenesis, 35*(4), 147–157. https://doi.org/10.1016/S0882-4010(03)00098-6

Dabo, S. M., Taylor, J. D., & Confer, A. W. (2007a). *P. multocida* and bovine respiratory disease. *Animal Health Research Reviews, 8*(2), 129–150. https://doi.org/10.1017/S1466252307001399

Dale, J. W., & Park, S. F. (2010). *Molecular genetics of bacteria.* Wiley.

Davies, R. L. (2004). Genetic diversity among *P. multocida* strains of avian, bovine, ovine and porcine origin from England and Wales by comparative sequence analysis of the 16S rRNA gene. *Microbiology, 150*(12), 4199–4210. https://doi.org/10.1099/mic.0.27409-0

Davies, R. L., Caffrey, B., & Watson, P. J. (2003). Comparative analyses of *P. multocida* strains associated with the ovine respiratory and vaginal tracts. *Veterinary Record, 152*(1), 7–10. https://doi.org/10.1136/vr.152.1.7

Davies, R. L., MacCorquodale, R., Baillie, S., & Caffrey, B. (2003). Characterisation and comparison of *P. multocida* strains associated with porcine pneumonia and atrophic rhinitis. *Journal of Medical Microbiology, 52*(1), 59–67. https://doi.org/10.1099/jmm.0.05019-0

De Alwis, & Carter. (1989). Haemorrhagic septicaemia. In Rutter & Adlam (Eds.), *Pasteurella and pasteurellosis* (pp. 131–160). Academic Press.

De Alwis, M. C. L. (1992). Haemorrhagic septicaemia—A general review. *British Veterinary Journal, 148*(2), 99–112. https://doi.org/10.1016/0007-1935(92)90101-6

DeAngelis, P. L., & Padgett-McCue, A. J. (2000). Identification and molecular cloning of a chondroitin synthase from *P. multocida* type F. *Journal of Biological Chemistry, 275*(31), 24124–24129. https://doi.org/10.1074/jbc.M003385200

DeAngelis, P. L., & White, C. L. (2004). Identification of a distinct, cryptic heparosan synthase from *P. multocida* types A, D and F. *Journal of Bacteriology, 186*(24), 8529–8532. https://doi.org/10.1128/JB.186.24.8529-8532.2004

Donkó, T., Kovács, M., & Magyar, T. (2005). Association of growth performance with atrophic rhinitis and pneumonia detected at slaughter in a conventional pig herd in Hungary. *Acta Veterinaria Hungarica, 53*(3), 287–298. https://doi.org/10.1556/AVet.53.2005.3.2

Dowah, A. S. A., & Clokie, M. R. J. (2018). Review of the nature, diversity and structure of bacteriophage receptor binding proteins that target Gram-positive bacteria. *Biophysical Reviews, 10*(2), 535–542. https://doi.org/10.1007/s12551-017-0382-3

Drulis-Kawa, Z., Majkowska-Skrobek, G., Maciejewska, B., Delattre, A.-S., & Lavigne, R. (2012). Learning from bacteriophages—Advantages and limitations of phage and phage-encoded protein applications. *Current Protein and Peptide Science, 13*(8), 699–722. https://doi.org/10.2174/138920312804871193

Duckworth, D. H., & Gulig, P. A. (2002). Bacteriophages. *BioDrugs, 16*(1), 57–62. https://doi.org/10.2165/00063030-200216010-00006

Dy, R. L., Richter, C., Salmond, G. P., & Fineran, P. C. (2014). Remarkable mechanisms in microbes to resist phage infections. *Annual Review of Virology, 1*(1), 307–331. https://doi.org/10.1146/annurev-virology-031413-085500

Dziva, F., Muhairwa, A. P., Bisgaard, M., & Christensen, H. (2008a). Diagnostic and typing options for investigating diseases associated with *P. multocida*. *Veterinary Microbiology, 128*(1–2), 1–22. https://doi.org/10.1016/j.vetmic.2007.10.018

Džunková, M., Moraru, C., & Anantharaman, K. (2023). Editorial: Advances in viromics: New tools, challenges, and data towards characterizing human and environmental viromes. *Frontiers in Microbiology, 14,* 1290062. https://doi.org/10.3389/fmicb.2023.1290062

d'Herelle, F. D. (1917). Sur un microbe invisible antagoniste des bacilles dysentériques. *Comptes Rendus de l'Académie des Sciences, 165,* 373–375.

Edgar, R., Friedman, N., Molshanski-Mor, S., & Qimron, U. (2012a). Reversing bacterial resistance to antibiotics by phage-mediated delivery of dominant sensitive genes. *Applied and Environmental Microbiology, 78*(3), 744–751. https://doi.org/10.1128/AEM.05741-11

Eissa, N., Hussin, K., & El-Mabrok, A. (2019). Isolation, identification and antibiogram of *P. multocida* isolated from apparently healthy rabbits in Al-Bayda, Libya. *Benha Veterinary Medical Journal, 36*(1), 393–398. https://doi.org/10.21608/bvmj.2019.114265

El Sayed, M., El-Mowalid, G., Ali, A., Arnaout, M., & Abd El Hamid, M. (2018). Isolation, identification and antimicrobial susceptibility patterns of *P. multocida* isolated from diseased rabbits. *Suez Canal Veterinary Medicine Journal (SCVMJ), 23*(1), 13–26. https://doi.org/10.21608/scvmj.2018.60744

El-Demerdash, A. S., Mowafy, R. E., Fahmy, H. A., Matter, A. A., & Samir, M. (2023). Pathognomonic features of *P. multocida* isolates among various avian species in Sharkia Governorate, Egypt. *World Journal of Microbiology and Biotechnology, 39*(12). https://doi.org/10.1007/s11274-023-03774-2

Endale, H., Mathewos, M., & Abdeta, D. (2023). Potential causes of spread of antimicrobial resistance and preventive measures in One Health perspective—A review. *Infection and Drug Resistance, 16,* 7515–7545.

Eriksson, H., Maciejewska, B., Latka, A., Majkowska-Skrobek, G., Hellstrand, M., Melefors, Ö., Wang, J.-T., Kropinski, A. M., Drulis-Kawa, Z., & Nilsson, A. S. (2015). A suggested new bacteriophage genus, "Kp34likevirus," within the *Autographivirinae* subfamily of *Podoviridae*. *Viruses, 7*(4), 1804–1822. https://doi.org/10.3390/v7041804

Evrard, B., Balestrino, D., Dosgilbert, A., Bouya-Gachancard, J.-L. J., Charbonnel, N., Forestier, C., & Tridon, A. (2010). Roles of capsule and lipopolysaccharide O antigen in interactions of human monocyte-derived dendritic cells and *Klebsiella pneumoniae*. *Infection and Immunity, 78*(1), 210–219. https://doi.org/10.1128/IAI.00864-09

Ewers, C., Lubkebecker, A., Bethe, A., Kiesling, S., Filter, M., & Wieler, L. (2006). Virulence genotype of *P. multocida* strains isolated from different hosts with various disease status. *Veterinary Microbiology, 114*(3–4), 304–317. https://doi.org/10.1016/j.vetmic.2005.12.012

Fatma, S., Chakravarti, A., Zeng, X., & Huang, R. H. (2021). Molecular mechanisms of the CdnG-Cap5 antiphage defense system employing 3',2'-cGAMP as the second messenger. *Nature Communications, 12*(1), 6381. https://doi.org/10.1038/s41467-021-26738-2

Feiss, M., & Rao, V. B. (2012). The bacteriophage DNA packaging machine. *Advances in Experimental Medicine and Biology, 726,* 489–509. https://doi.org/10.1007/978-1-4614-0980-9_22

Fillol-Salom, A., Martínez-Rubio, R., Abdulrahman, R. F., Chen, J., Davies, R., & Penadés, J. R. (2018). Phage-inducible chromosomal islands are ubiquitous within the bacterial universe. *The ISME Journal, 12*(9), 2114–2128. https://doi.org/10.1038/s41396-018-0156-3

Filée, J., Tétart, F., Suttle, C. A., & Krisch, H. M. (2005). Marine T4-type bacteriophages, a ubiquitous component of the dark matter of the biosphere. *Proceedings of the National Academy of Sciences, 102*(35), 12471–12476. https://doi.org/10.1073/pnas.0503404102

Fokine, A., & Rossmann, M. G. (2014). Molecular architecture of tailed double-stranded DNA phages. *Bacteriophage, 4*(1), e28281. https://doi.org/10.4161/bact.28281

Fong, K., Wong, C. W. Y., Wang, S., & Delaquis, P. (2021). How broad is enough: The host range of bacteriophages and its impact on the agri-food sector. *PHAGE: Therapy, Applications, and Research, 2*(2), 83–89. https://doi.org/10.1089/phage.2020.0036

Foysal, M., Imam, T., Das, S. B., Gibson, J. S., Mahmud, R., Gupta, S. D., Fournié, G., Hoque, M. A., & Henning, J. (2024). Association between antimicrobial usage and resistance on commercial broiler and layer farms in Bangladesh. *Frontiers in Veterinary Science, 11.*

Friend, M., & Franson, J. C. (1999). *Field manual of wildlife diseases: General field procedures and diseases of birds* (Information and Technology Report 1999-001). U.S. Department of the Interior, U.S. Geological Survey, Biological Resources Division.

Fuller, T. E., Kennedy, M. J., & Lowery, D. E. (2000). Identification of *P. multocida* virulence genes in a septicemic mouse model using signature-tagged mutagenesis. *Microbial Pathogenesis, 29*(1), 25–38. https://doi.org/10.1006/mpat.2000.0365

Gadberry, J. L., & Miller, N. G. (1978). Characterisation of a *P. multocida* bacteriophage. *American Journal of Veterinary Research, 39*(9), 1565–1566.

Gallorini, M., Marinacci, B., Pellegrini, B., Cataldi, A., Dindo, M. L., Carradori, S., & Grande, R. (2024). Immunophenotyping of hemocytes from infected *Galleria mellonella* larvae as an innovative tool for immune profiling, infection studies and drug screening. *Scientific Reports, 14.*

Galyean, M. L., Perino, L. J., & Duff, G. C. (1999). Interaction of cattle health/immunity and nutrition. *Journal of Animal Science, 77*(5), 1120–1134. https://doi.org/10.2527/1999.7751120x

García-Alvarez, A., Vela, A. I., San Martín, E., Chaves, F., Fernández-Garayzábal, J. F., Lucas, D., & Cid, D. (2017). Characterisation of *P. multocida* associated with ovine pneumonia using multi-locus sequence typing (MLST) and virulence-associated gene profile analysis and comparison with porcine isolates. *Veterinary Microbiology, 204,* 180–187. https://doi.org/10.1016/j.vetmic.2017.04.015

Garrido, M. E., Bosch, M., Bigas, A., Badiola, I., Barbé, J., & Llagostera, M. (2008). Heterologous protective immunization elicited in mice by *P. multocida* fur ompH. *International Microbiology, 11*(1), 17–24. https://doi.org/10.2436/20.1501.01.40

Ge, X., & Wang, J. (2024). Structural mechanism of bacteriophage lambda tail's interaction with the bacterial receptor. *Nature Communications, 15*(1), 4185. https://doi.org/10.1038/s41467-024-48686-3

Geda, A. M. (2024). Fowl cholera in chickens: Current trends in diagnosis and phenotypic drug resistance in Gondar City, Ethiopia. *Veterinary Medicine International, 2024,* 6613019. https://doi.org/10.1155/VMI/6613019

Gharieb, R. M. A., Saad, M. F., Mohamed, A. S., & Tartor, Y. H. (2020). Characterisation of two novel lytic bacteriophages for reducing biofilms of zoonotic multidrug-resistant

Staphylococcus aureus and controlling their growth in milk. *LWT, 124,* 109145. https://doi.org/10.1016/j.lwt.2020.109145

Giannouli, M., Palatucci, A. T., Rubino, V., Ruggiero, G., Romano, M., Triassi, M., Ricci, V., & Zarrilli, R. (2014). Use of larvae of the wax moth *Galleria mellonella* as an in vivo model to study the virulence of *Helicobacter pylori*. *BMC Microbiology, 14*(1). https://doi.org/10.1186/s12866-014-0228-0

Gibreel, T. M., & Upton, M. (2013). Synthetic epidermicin NI01 can protect *Galleria mellonella* larvae from infection with *Staphylococcus aureus*. *Journal of Antimicrobial Chemotherapy.* https://doi.org/10.1093/jac/dkt195

Gilchrist, C. L. M., & Chooi, Y. H. (2021). clinker & clustermap.js: Automatic generation of gene cluster comparison figures. *Bioinformatics, 37*(16), 2473–2475. https://doi.org/10.1093/bioinformatics/btab007

Gill, J., & Hyman, P. (2010). Phage choice, isolation and preparation for phage therapy. *Current Pharmaceutical Biotechnology, 11*(1), 2–14. https://doi.org/10.2174/138920110790725311

Gluecks, I. V., Bethe, A., Younan, M., & Ewers, C. (2017). Molecular study on *P. multocida* and *Mannheimia granulomatis* from Kenyan camels (*Camelus dromedarius*). *BMC Veterinary Research, 13*(1). https://doi.org/10.1186/s12917-017-1189-y

Goodridge, L. (2010). Designing phage therapeutics. *Current Pharmaceutical Biotechnology, 11*(1), 15–27. https://doi.org/10.2174/138920110790725348

Gordillo Altamirano, F., Forsyth, J. H., Patwa, R., Kostoulias, X., Trim, M., Subedi, D., Archer, S. K., Morris, F. C., Oliveira, C., Kielty, L., Korneev, D., O'Bryan, M. K., Lithgow, T. J., Peleg, A. Y., & Barr, J. J. (2021). Bacteriophage-resistant *Acinetobacter baumannii* are

resensitized to antimicrobials. *Nature Microbiology, 6*(2), 157–161. https://doi.org/10.1038/s41564-020-00830-7

Gorre, V., Sriram, V. K., Ramasamy, K., Putty, K., Jemmigumpula, S. J., & Manchikatla, S. (2025). Molecular identification and characterization of *Pasteurella multocida* isolates from pneumonic sheep and goats. *Veterinaria Italiana, 61*(1). https://doi.org/10.12834/VetIt.3000.22207.2

Govande, A. A., Duncan-Lowey, B., Eaglesham, J. B., Whiteley, A. T., & Kranzusch, P. J. (2021). Molecular basis of CD-NTase nucleotide selection in CBASS anti-phage defense. *Cell Reports, 35*(9), 109206. https://doi.org/10.1016/j.celrep.2021.109206

Grath, S. M., & Van Sinderen, D. (2007). *Bacteriophage.* Caister Academic Press.

Green, M. R., & Sambrook, J. (2012). *Molecular cloning: A laboratory manual* (4th ed.). Cold Spring Harbor Laboratory Press.

Guegler, C. K., & Laub, M. T. (2021). Shutoff of host transcription triggers a toxin-antitoxin system to cleave phage RNA and abort infection. *Molecular Cell, 81*(11), 2361–2373.e9. https://doi.org/10.1016/j.molcel.2021.03.027

Gummalla, V. S., Zhang, Y., Liao, Y. T., & Wu, V. C. H. (2023). The role of temperate phages in bacterial pathogenicity. *Microorganisms, 11*(3), 541. https://doi.org/10.3390/microorganisms11030541

Guo, J., Gao, S.-H., Lu, J., Bond, P. L., Verstraete, W., & Yuan, Z. (2017a). Copper oxide nanoparticles induce lysogenic bacteriophage and metal-resistance genes in *Pseudomonas aeruginosa* PAO1. *ACS Applied Materials & Interfaces, 9*(27), 22298–22307. https://doi.org/10.1021/acsami.7b06433

Guo, Z., Xie, C., Zhang, P., Zhang, J., Wang, G., He, X., Ma, Y., Zhao, B., & Zhang, Z. (2017b). Toxicity and transformation of graphene oxide and reduced graphene oxide in bacteria biofilm. *Science of the Total Environment, 580,* 1300–1308. https://doi.org/10.1016/j.scitotenv.2016.12.093

Gutiérrez, D., Vandenheuvel, D., Martínez, B., Rodríguez, A., Lavigne, R., & García, P. (2015). Two phages, phiIPLA-RODI and phiIPLA-C1C, lyse mono- and dual-species staphylococcal biofilms. *Applied and Environmental Microbiology, 81*(10), 3336–3348. https://doi.org/10.1128/AEM.03560-14

Guttman, B. (2013). Virus. In *Brenner's Encyclopedia of Genetics* (pp. 291–294). https://doi.org/10.1016/B978-0-12-374984-0.01626-0

Głowacka-Rutkowska, A., Gozdek, A., Empel, J., Gawor, J., Żuchniewicz, K., Kozińska, A., Dębski, J., Gromadka, R., & Łobocka, M. (2019). The ability of lytic staphylococcal podovirus vB_SauP_phiAGO1.3 to coexist in equilibrium with its host facilitates the selection of host mutants of attenuated virulence but does not preclude the phage antistaphylococcal activity in a nematode infection model. *Frontiers in Microbiology, 9.* https://doi.org/10.3389/fmicb.2018.03227

Ha, E., Son, B., & Ryu, S. (2018). *Clostridium perfringens* virulent bacteriophage CPS2 and its thermostable endolysin LysCPS2. *Viruses, 10*(5), 251. https://doi.org/10.3390/v10050251

Hambly, E., & Suttle, C. A. (2005). The viriosphere: Diversity and genetic exchange within phage communities. *Current Opinion in Microbiology, 8*(4), 444–450. https://doi.org/10.1016/j.mib.2005.06.005

Hampton, H. G., Watson, B. N. J., & Fineran, P. C. (2020). The arms race between bacteria and their phage foes. *Nature, 577*(7790), 327–336. https://doi.org/10.1038/s41586-019-1894-8

Hansen, L. M., & Hirsh, D. C. (1989). Serum resistance is correlated with encapsulation of avian strains of *P. multocida*. *Veterinary Microbiology, 21*(2), 177–184. https://doi.org/10.1016/0378-1135(89)90030-8

Harada, L. K., Silva, E. C., Campos, W. F., Del Fiol, F. S., Vila, M., Dąbrowska, K., Krylov, V. N., & Balcão, V. M. (2018). Biotechnological applications of bacteriophages: State of the art. *Microbiological Research, 212–213,* 38–58. https://doi.org/10.1016/j.micres.2018.04.007

Hargreaves, K. R., & Clokie, M. R. J. (2014). *Clostridium difficile* phages: Still difficult? *Frontiers in Microbiology, 5,* 184. https://doi.org/10.3389/fmicb.2014.00184

Haris, M., Chen, C., & Wu, J. (2022). Inducible knockdown of *Mycobacterium smegmatis* MSMEG_2975 (glyoxalase II) affected bacterial growth, antibiotic susceptibility, biofilm, and transcriptome. *Archives of Microbiology, 204,* Article 97. https://doi.org/10.1007/s00203-021-02652-5

Harmon, B. G., Glisson, J. R., Latimer, K. S., Steffens, W. L., & Nunnally, J. C. (1991). Resistance of *P. multocida* A:3,4 to phagocytosis by turkey macrophages and heterophils. *American Journal of Veterinary Research, 52*(9), 1507–1511. https://doi.org/10.2460/ajvr.1991.52.09.1507

Harper, M., & Boyce, J. (2017). The myriad properties of *P. multocida* lipopolysaccharide. *Toxins, 9*(8), 254. https://doi.org/10.3390/toxins9080254

Harper, M., Boyce, J. D., & Adler, B. (2006a). *P. multocida* pathogenesis: 125 years after Pasteur. *FEMS Microbiology Letters, 265*(1), 1–10. https://doi.org/10.1111/j.1574-6968.2006.00442.x

Harper, M., Boyce, J. D., & Adler, B. (2012). The key surface components of *P. multocida*: Capsule and lipopolysaccharide. In *Current Topics in Microbiology and Immunology* (pp. 39–51). https://doi.org/10.1007/82_2012_202

Harper, M., Boyce, J. D., Cox, A. D., St. Michael, F., Wilkie, I. W., Blackall, P. J., & Adler, B. (2007). *P. multocida* expresses two lipopolysaccharide glycoforms simultaneously, but only a single form is required for virulence: Identification of two acceptor-specific heptosyl I transferases. *Infection and Immunity, 75*(8), 3885–3893. https://doi.org/10.1128/IAI.00212-07

Harper, M., Cox, A. D., St. Michael, F., Wilkie, I. W., Boyce, J. D., & Adler, B. (2004). A heptosyltransferase mutant of *P. multocida* produces a truncated lipopolysaccharide structure and is attenuated in virulence. *Infection and Immunity, 72*(6), 3436–3443. https://doi.org/10.1128/IAI.72.6.3436-3443.2004

Harper, M., John, M., Turni, C., Edmunds, M., St. Michael, F., Adler, B., Blackall, P. J., Cox, A. D., & Boyce, J. D. (2015). Development of a rapid multiplex PCR assay to genotype *P. multocida* strains by use of the lipopolysaccharide outer core biosynthesis locus. *Journal of Clinical Microbiology, 53*(2), 477–485. https://doi.org/10.1128/JCM.02824-14

Harper, M., St. Michael, F., Vinogradov, E., John, M., Steen, J. A., Van Dorsten, L., Boyce, J. D., Adler, B., & Cox, A. D. (2012). Structure and biosynthetic locus of the lipopolysaccharide outer core produced by *P. multocida* serovars 8 and 13 and the identification of a novel phospho-glycero moiety. *Glycobiology, 23*(3), 286–294. https://doi.org/10.1093/glycob/cws154

Harper, M., St. Michael, F., John, M., Vinogradov, E., Adler, B., Boyce, J. D., & Cox, A. D. (2014). Structural analysis of lipopolysaccharide produced by Heddleston serovars 10, 11, 12 and 15 and the identification of a new *P. multocida* lipopolysaccharide outer core biosynthesis locus, L6. *Glycobiology, 24*(7), 649–659. https://doi.org/10.1093/glycob/cwu030

Harper, M., St. Michael, F., John, M., Vinogradov, E., Adler, B., Boyce, J. D., & Cox, A. D. (2011a). *P. multocida* Heddleston serovars 1 and 14 express different lipopolysaccharide structures but share the same lipopolysaccharide biosynthesis outer core locus. *Veterinary Microbiology, 150*(3–4), 289–296. https://doi.org/10.1016/j.vetmic.2011.01.028

Harper, M., St. Michael, F., John, M., Steen, J., van Dorsten, L., Parnas, H., Vinogradov, E., Adler, B., Cox, A. D., & Boyce, J. D. (2013). *P. multocida* Heddleston serovar 3 and 4 strains share a common lipopolysaccharide biosynthesis locus but display both inter- and intrastrain lipopolysaccharide heterogeneity. *Journal of Bacteriology, 195*(21), 4854–4864. https://doi.org/10.1128/JB.00779-13

Harper, M., St. Michael, F., John, M., Vinogradov, E., Boyce, J. D., Adler, B., & Cox, A. D. (2011c). Characterisation of the lipopolysaccharide from *P. multocida* Heddleston serovar 9: Identification of a proposed bi-functional dTDP-3-acetamido-3,6-dideoxy-*D*-glucose biosynthesis enzyme. *Glycobiology, 22*(3), 332–344. https://doi.org/10.1093/glycob/cwr147

Harrington, L. B., Doxzen, K. W., Ma, E., Liu, S. Y., Knott, G. J., Edraki, A., ... & Doudna, J. A. (2017). A broad-spectrum inhibitor of CRISPR-Cas9. *Cell, 170*(6), 1224–1233.e15. https://doi.org/10.1016/j.cell.2017.07.037

Harshey, R. M. (2014). Transposable phage Mu. *Microbiology Spectrum, 2*(5). https://doi.org/10.1128/microbiolspec.MDNA3-0007-2014

Hatfaludi, T., Al-Hasani, K., Boyce, J. D., & Adler, B. (2010). Outer membrane proteins of *P. multocida*. *Veterinary Microbiology, 144*(1–2), 1–17. https://doi.org/10.1016/j.vetmic.2010.01.027

Hatfull, G. F., & Hendrix, R. W. (2011). Bacteriophages and their genomes. *Current Opinion in Virology, 1*(4), 298–303. https://doi.org/10.1016/j.coviro.2011.06.009

Hayes, S., Mahony, J., Nauta, A., & van Sinderen, D. (2017). Metagenomic approaches to assess bacteriophages in various environmental niches. *Viruses, 9*(6), 127. https://doi.org/10.3390/v9060127

He, S. L., & Green, R. (2013). Northern blotting. In *Laboratory methods in enzymology: RNA* (pp. 75–87). https://doi.org/10.1016/B978-0-12-420037-1.00003-8

Heddleston, K. L., Gallagher, J. E., & Rebers, P. A. (1972). Fowl cholera: Gel diffusion precipitin test for serotyping *P. multocida* from avian species. *Avian Diseases, 16*(4), 925. https://doi.org/10.2307/1588773

Heddleston, K. L., Watko, L. P., & Rebers, P. A. (1964). Dissociation of a fowl cholera strain of *P. multocida*. *Avian Diseases, 8*(4), 649. https://doi.org/10.2307/1587953

Heinrichs, M. E., De Corte, D., Engelen, B., & Pan, D. (2021). An advanced protocol for the quantification of marine sediment viruses via flow cytometry. *Viruses, 13*(1), 102. https://doi.org/10.3390/v13010102

Held, N. L., Herrera, A., Cadillo-Quiroz, H., & Whitaker, R. J. (2010). CRISPR-associated diversity within a population of *Sulfolobus islandicus*. *PLoS ONE, 5*(9), e12988. https://doi.org/10.1371/journal.pone.0012988

Helmy, Y. A., Taha-Abdelaziz, K., Hawwas, H. A., Ghosh, S., Alkafaas, S. S., Moawad, M. M., Saied, E. M., Kassem, I. I., & Mawad, A. M. (2023). Antimicrobial resistance and recent alternatives to antibiotics for the control of bacterial pathogens with an emphasis on foodborne pathogens. *Antibiotics, 12.*

Hendrix, R. W. (2002). Bacteriophages: Evolution of the majority. *Theoretical and Applied Genetics, 104*(1–2), 1–8.

Holtappels, D., Alfenas-Zerbini, P., & Koskella, B. (2023). Drivers and consequences of bacteriophage host range. *FEMS Microbiology Reviews, 47*(4), fuad038. https://doi.org/10.1093/femsre/fuad038

Horadagoda, N. U., Hodgson, J. C., Moon, G. M., Wijewardana, T. G., & Eckersall, P. D. (2002a). Development of a clinical syndrome resembling haemorrhagic septicaemia in the buffalo following intravenous inoculation of *P. multocida* serotype B:2 endotoxin and the role of tumour necrosis factor-α. *Research in Veterinary Science, 72*(3), 194–200. https://doi.org/10.1053/rvsc.2001.0538

Horiguchi, Y. (2012). Swine atrophic rhinitis caused by *P. multocida* toxin and *Bordetella* dermonecrotic toxin. In *Current Topics in Microbiology and Immunology* (pp. 113–129). https://doi.org/10.1007/82_2012_206

Hsieh, P.-F., Lin, H.-H., Lin, T.-L., Chen, Y.-Y., & Wang, J.-T. (2017). Two T7-like bacteriophages, K5-2 and K5-4, each encodes two capsule depolymerases: Isolation and functional characterisation. *Scientific Reports, 7*(1). https://doi.org/10.1038/s41598-017-04644-2

Hsuan, S.-L., Liao, C.-C., Huang, C., Yen, M.-H., Chen, Y.-C., Wu, C.-M., Tsai, M.-S., Chen, T.-H., & Cheng, I.-H. (2009). Efficacy of a novel *P. multocida* vaccine against progressive atrophic rhinitis of swine. *Vaccine, 27,* 2923–2929. https://doi.org/10.1016/j.vaccine.2009.03.049

Hu, B., Margolin, W., Molineux, I. J., & Liu, J. (2013). The bacteriophage T7 virion undergoes extensive structural remodeling during infection. *Science, 339*(6119), 576–579. https://doi.org/10.1126/science.1231887

Hu, M., Zhang, H., Gu, D., Ma, Y., & Zhou, X. (2020). Identification of a novel bacterial receptor that binds tail tubular proteins and mediates phage infection of *Vibrio parahaemolyticus*. *Emerging Microbes & Infections, 9*(1), 855–867. https://doi.org/10.1080/22221751.2020.1754134

Huang, C., Virk, S. M., Shi, J., Zhou, Y., Willias, S. P., Morsy, M. K., Abdelnabby, H. E., Liu, J., Wang, X., & Li, J. (2018). Isolation, characterisation, and application of bacteriophage LPSE1 against *Salmonella enterica* in ready-to-eat foods. *Frontiers in Microbiology, 9,* 1046. https://doi.org/10.3389/fmicb.2018.01046

Huang, L., & Xiang, Y. (2020). Structures of the tailed bacteriophages that infect Gram-positive bacteria. *Current Opinion in Virology, 45,* 65–74. https://doi.org/10.1016/j.coviro.2020.09.002

Hudzicki, J. (2009). Kirby–Bauer disk diffusion susceptibility test protocol. American Society for Microbiology.

Hyman, P. (2019). Phages for phage therapy: Isolation, characterisation, and host range breadth. *Pharmaceuticals, 12*(1), 35. https://doi.org/10.3390/ph12010035

Hör, J., Wolf, S. G., & Sorek, R. (2024). Bacteria conjugate ubiquitin-like proteins to interfere with phage assembly. *Nature, 631*(8022), 850–856. https://doi.org/10.1038/s41586-024-07616-5

ICTV. (2020). Virus taxonomy: The ICTV report on virus classification and taxon nomenclature. https://ictv.global/report/about (Accessed 24 April 2024)

Ives, S. E., & Richeson, J. T. (2015). Use of antimicrobial metaphylaxis for the control of bovine respiratory disease in high-risk cattle. *Veterinary Clinics of North America: Food Animal Practice, 31*(3), 341–v. https://doi.org/10.1016/j.cvfa.2015.05.008

Jaglic, Z., Jeklova, E., Leva, L., Kummer, V., Kucerova, Z., Faldyna, M., Maskova, J., Nedbalcova, K., & Alexa, P. (2008). Experimental study of pathogenicity of *P. multocida* serogroup F in rabbits. *Veterinary Microbiology, 126*(1–3), 168–177. https://doi.org/10.1016/j.vetmic.2007.06.008

Jaglic, Z., Kucerova, Z., Nedbalcova, K., Hlozek, P., & Bartos, M. (2004). Identification of *P. multocida* serogroup F isolates in rabbits. *Journal of Veterinary Medicine, Series B, 51*(10), 467–469. https://doi.org/10.1111/j.1439-0450.2004.00807.x

Jakhetia, R., & Verma, N. K. (2015). Identification and molecular characterisation of a novel Mu-like bacteriophage, SfMu, of *Shigella flexneri*. *PLOS ONE, 10*(4), e0124053. https://doi.org/10.1371/journal.pone.0124053

Jennes, S., Merabishvili, M., Soentjens, P., Pang, K. W., Rose, T., Keersebilck, E., Pirnay, J.-P., & De Vos, D. (2017). Use of bacteriophages in the treatment of colistin-only-sensitive *Pseudomonas aeruginosa* septicaemia in a patient with acute kidney injury—A case report. *Critical Care, 21*(1), 129. https://doi.org/10.1186/s13054-017-1709-y

Jeon, J., Park, J.-H., & Yong, D. (2019). Efficacy of bacteriophage treatment against carbapenem-resistant *Acinetobacter baumannii* in *Galleria mellonella* larvae and a mouse model of acute pneumonia. *BMC Microbiology, 19*(1). https://doi.org/10.1186/s12866-019-1443-5

Jerab, J. G., Chantziaras, I., Van Limbergen, T., Van Erum, J., Boel, F., Hoeven, E., & Dewulf, J. (2023). Antimicrobial use in on-farm hatching systems vs. traditional hatching systems: A case study. *Animals, 13.*

Jolley, K. A., Bray, J. E., & Maiden, M. C. J. (2018). Open-access bacterial population genomics: BIGSdb software, the PubMLST.org website and their applications. *Wellcome Open Research, 3,* 124. https://doi.org/10.12688/wellcomeopenres.14826.1

Joshi, P., Krco, S., Davis, S. J., Asser, L., Brück, T., Soo, R. M., Bodén, M., Hugenholtz, P., Wilson, L. A., Schenk, G., & Morris, M. T. (2024). Phage anti-Pycsar proteins efficiently degrade β-lactam antibiotics. *Applied Biosciences, 3*(4), 438–449. https://doi.org/10.3390/applbiosci3040028

Jończyk-Matysiak, E., Weber-Dąbrowska, B., Owczarek, B., Międzybrodzki, R., Łusiak-Szelachowska, M., Łodej, N., & Górski, A. (2017). Phage–phagocyte interactions and their implications for phage application as therapeutics. *Viruses, 9*(6), 150. https://doi.org/10.3390/v9060150

Jurczak-Kurek, A., Gąsior, T., Nejman-Faleńczyk, B., Dydecka, A., Przybylska-Gornowicz, M., Wolińska, K., ... Korzeniowska-Kowal, A. (2016). Biodiversity of bacteriophages: Morphological and biological properties of a large group of phages isolated from urban sewage. *Scientific Reports, 6,* 34338. https://doi.org/10.1038/srep34338

Kahler, C. M., & Stephens, D. S. (1998). Genetic basis for biosynthesis, structure, and function of meningococcal lipooligosaccharide (endotoxin). *Critical Reviews in Microbiology, 24*(4), 281–334. https://doi.org/10.1080/10408419891294216

Kasten, R. W., Carpenter, T. E., Snipes, K. P., & Hirsh, D. C. (1997). Detection of *Pasteurella multocida*-specific DNA in turkey flocks by use of the polymerase chain reaction. *Avian Diseases, 41*(3), 676–682.

Kasten, R. W., Hansen, L. M., Hinojoza, J., Bieber, D., Ruehl, W. W., & Hirsh, D. C. (1995). *Pasteurella multocida* produces a protein with homology to the P6 outer membrane protein of *Haemophilus influenzae*. *Infection and Immunity, 63*(3), 989–993. https://doi.org/10.1128/IAI.63.3.989-993.1995

Kawasaki, M., Young, J. R., Suon, S., Bush, R. D., & Windsor, P. A. (2014). The socioeconomic impacts of clinically diagnosed haemorrhagic septicaemia on smallholder large ruminant farmers in Cambodia. *Transboundary and Emerging Diseases, 61*(6), 491–504. https://doi.org/10.1111/tbed.12174

Kay, S., Edwards, J., Brown, J., & Dixon, R. (2019). *Galleria mellonella* infection model identifies both high and low lethality of *Clostridium perfringens* toxigenic strains and their response to antimicrobials. *Frontiers in Microbiology, 10,* 1281. https://doi.org/10.3389/fmicb.2019.01281

Keen, E. C., & Adhya, S. L. (2015). Phage therapy: Current research and applications. *Clinical Infectious Diseases, 61*(1), 141–142. https://doi.org/10.1093/cid/civ257

Kelly, D. J., & Thomas, G. H. (2001). The tripartite ATP-independent periplasmic (TRAP) transporters of bacteria and archaea. *FEMS Microbiology Reviews, 25*(4), 405–424. https://doi.org/10.1111/j.1574-6976.2001.tb00584.x

Kemp, P., Gupta, M., & Molineux, I. J. (2004). Bacteriophage T7 DNA ejection into cells is initiated by an enzyme-like mechanism. *Molecular Microbiology, 53*(4), 1251–1265. https://doi.org/10.1111/j.1365-2958.2004.04204.x

Kerek, Á., Szabó, Á., & Jerzsele, Á. (2024). Antimicrobial susceptibility profiles of *Pasteurella multocida* isolates from clinical cases of waterfowl in Hungary between 2022 and 2023. *Veterinary Sciences, 11.*

Khamesipour, F., Momtaz, H., & Azhdary Mamoreh, M. (2014). Occurrence of virulence factors and antimicrobial resistance in *P. multocida* strains isolated from slaughter cattle in Iran. *Frontiers in Microbiology, 5,* 536. https://doi.org/10.3389/fmicb.2014.00536

Khan, M. S., Pande, T., & van de Ven, T. G. (2015). Qualitative and quantitative detection of T7 bacteriophages using paper-based sandwich ELISA. *Colloids and Surfaces B: Biointerfaces, 132,* 264–270. https://doi.org/10.1016/j.colsurfb.2015.05.028

Kifelew, L. G., Warner, M. S., Morales, S., Vaughan, L., Woodman, R., Fitridge, R., Mitchell, J. G., & Speck, P. (2020). Efficacy of phage cocktail AB-SA01 therapy in diabetic mouse

wound infections caused by multidrug-resistant *Staphylococcus aureus*. *BMC Microbiology, 20*(1), 204. https://doi.org/10.1186/s12866-020-01891-8

Kilcher, S., Studer, P., Muessner, C., Klumpp, J., & Loessner, M. J. (2018a). Cross-genus rebooting of custom-made, synthetic bacteriophage genomes in L-form bacteria. *Proceedings of the National Academy of Sciences, 115*(3), 567–572. https://doi.org/10.1073/pnas.1714658115

Kim, K. P., Cha, J. D., Jang, E. H., Klumpp, J., Hagens, S., Hardt, W. D., Lee, K. Y., & Loessner, M. J. (2008). PEGylation of bacteriophages increases blood circulation time and reduces T-helper type 1 immune response. *Microbial Biotechnology, 1*(3), 247–257. https://doi.org/10.1111/j.1751-7915.2008.00028.x

Kirchner, C., & Eisenstark, A. (1956). Lysogeny in *P. multocida*. ← (Kaynak/jurnal bilgisi yoktu; istersen ekleyebilirim.)

Klima, C. L., Holman, D. B., Cook, S. R., Conrad, C. C., Ralston, B. J., Allan, N., Anholt, R. M., Niu, Y. D., Stanford, K., Hannon, S. J., Booker, C. W., & McAllister, T. A. (2020). Multidrug resistance in Pasteurellaceae associated with bovine respiratory disease mortalities in North America from 2011 to 2016. *Frontiers in Microbiology, 11,* 606438. https://doi.org/10.3389/fmicb.2020.606438

Kloos, B., Chakraborty, S., Lindner, S. G., Noack, K., Harre, U., Schett, G., Krämer, O. H., & Kubatzky, K. F. (2015). *P. multocida* toxin-induced osteoclastogenesis requires mTOR activation. *Cell Communication and Signaling, 13*(1). https://doi.org/10.1186/s12964-015-0117-7

Knecht, L. E., Veljkovic, M., & Fieseler, L. (2020). Diversity and function of phage encoded depolymerases. *Frontiers in Microbiology, 10.* https://doi.org/10.3389/fmicb.2019.02949

Knight, D. P., Paine, J. E., & Speller, D. C. (1983). A selective medium for *P. multocida* and its use with animal and human specimens. *Journal of Clinical Pathology, 36*(5), 591–594. https://doi.org/10.1136/jcp.36.5.591

Koonin, E. V., Krupovic, M., & Agol, V. I. (2021). The Baltimore classification of viruses 50 years later: How does it stand in the light of virus evolution? *Microbiology and Molecular Biology Reviews, 85*(3). https://doi.org/10.1128/MMBR.00053-21

Kostyuchenko, V. A., Chipman, P. R., Leiman, P. G., Arisaka, F., Mesyanzhinov, V. V., & Rossmann, M. G. (2005). The tail structure of bacteriophage T4 and its mechanism of contraction. *Nature Structural & Molecular Biology, 12*(9), 810–813. https://doi.org/10.1038/nsmb975

Kosznik-Kwaśnicka, K., Stasiłojć, M., Grabowski, Ł., Zdrojewska, K., Węgrzyn, G., & Węgrzyn, A. (2022). Efficacy and safety of phage therapy against *Salmonella enterica* serovars Typhimurium and Enteritidis estimated by using a battery of in vitro tests and the *Galleria mellonella* animal model. *Microbiological Research, 261,* 127052. https://doi.org/10.1016/j.micres.2022.127052

Kropinski, A. M., Mazzocco, A., Waddell, T. E., Lingohr, E., & Johnson, R. P. (2009). Enumeration of bacteriophages by double agar overlay plaque assay. In M. R. Clokie & A. M. Kropinski (Eds.), *Bacteriophages* (Methods in Molecular Biology, Vol. 501, pp. 69–76). Humana Press. https://doi.org/10.1007/978-1-60327-164-6_7

Kumar, A. A., Shivachandra, S. B., Biswas, A., Singh, V. P., Singh, V. P., & Srivastava, S. K. (2004). Prevalent serotypes of *P. multocida* isolated from different animal and avian species in India. *Veterinary Research Communications, 28*(8), 657–667. https://doi.org/10.1023/B:VERC.0000045959.36513.e9

Kumar, M., Sarma, D. K., Shubham, S., Kumawat, M., Verma, V., Nina, P. B., Jp, D. O., Kumar, S., Singh, B., & Tiwari, R. R. (2021). Futuristic non-antibiotic therapies to combat antibiotic resistance: A review. *Frontiers in Microbiology, 12.*

Kurzepa, A., Dabrowska, K., Skaradziński, G., & Górski, A. (2009). Bacteriophage interactions with phagocytes and their potential significance in experimental therapy. *Clinical and Experimental Medicine, 9*(2), 93–100. https://doi.org/10.1007/s10238-008-0027-8

Kutter, E. (2009). Phage host range and efficiency of plating. *Methods in Molecular Biology, 501,* 141–149. https://doi.org/10.1007/978-1-60327-164-6_14

Kutter, E., De Vos, D., Gvasalia, G., Alavidze, Z., Gogokhia, L., Kuhl, S., & Abedon, S. T. (2010). Phage therapy in clinical practice: Treatment of human infections. *Current Pharmaceutical Biotechnology, 11*(1), 69–86. https://doi.org/10.2174/138920110790725401

Labrie, S. J., Samson, J. E., & Moineau, S. (2010). Bacteriophage resistance mechanisms. *Nature Reviews Microbiology, 8*(5), 317–327. https://doi.org/10.1038/nrmicro2315

Laslett, D. (2004). ARAGORN, a program to detect tRNA genes and tmRNA genes in nucleotide sequences. *Nucleic Acids Research, 32*(1), 11–16. https://doi.org/10.1093/nar/gkh152

Latka, A., Maciejewska, B., Majkowska-Skrobek, G., Briers, Y., & Drulis-Kawa, Z. (2017). Bacteriophage-encoded virion-associated enzymes to overcome the carbohydrate barriers during the infection process. *Applied Microbiology and Biotechnology, 101*(8), 3103–3119. https://doi.org/10.1007/s00253-017-8224-6

LaVergne, S., Hamilton, T., Biswas, B., Kumaraswamy, M., Schooley, R. T., & Wooten, D. (2018). Phage therapy for a multidrug-resistant *Acinetobacter baumannii* craniectomy site infection. *Open Forum Infectious Diseases, 5*(4), ofy064. https://doi.org/10.1093/ofid/ofy064

Lee, C. W., Wilkie, I. W., Townsend, K. M., & Frost, A. J. (2000). The demonstration of *Pasteurella multocida* in the alimentary tract of chickens after experimental oral infection. *Veterinary Microbiology, 72*(1–2), 47–55. https://doi.org/10.1016/S0378-1135(99)00186-8

Lee, M. D., Wooley, R. E., & Glisson, J. R. (1994). Invasion of epithelial cell monolayers by turkey strains of *P. multocida*. *Avian Diseases, 38*(1), 72. https://doi.org/10.2307/1591839

Lee, S., Lewis, D. E. A., & Adhya, S. (2018). The developmental switch in bacteriophage λ: A critical role of the Cro protein. *Journal of Molecular Biology, 430*(1), 58–68. https://doi.org/10.1016/j.jmb.2017.11.005

Lefkowitz, E. J., Dempsey, D. M., Hendrickson, R. C., Orton, R. J., Siddell, S. G., & Smith, D. B. (2018). Virus taxonomy: The database of the International Committee on Taxonomy of Viruses (ICTV). *Nucleic Acids Research, 46*(D1), D708–D717. https://doi.org/10.1093/nar/gkx932

Lehr, M. A., Botzler, R. G., Samuel, M. D., & Shadduck, D. J. (2005a). Associations between water quality, *P. multocida* and avian cholera at Sacramento National Wildlife Refuge. *Journal of Wildlife Diseases, 41*(2), 291–297. https://doi.org/10.7589/0090-3558-41.2.291

Le Guellec, S., Pardessus, J., Bodier-Montagutelli, E., L'Hostis, G., Dalloneau, E., Piel, D., Samaï, H. C., Guillon, A., Mujic, E., Guillot-Combe, E., Ehrmann, S., Morello, E., Gabard, J., Heuzé-Vourc'h, N., Fèvre, C., & Vecellio, L. (2023). Administration of bacteriophages via nebulization during mechanical ventilation: *In vitro* study and lung deposition in macaques. *Viruses, 15*(3), 602. https://doi.org/10.3390/v15030602

Leiman, P. G., & Shneider, M. M. (2011). Contractile tail machines of bacteriophages. In *Viral molecular machines* (pp. 93–114). https://doi.org/10.1007/978-1-4614-0980-9_5

Lemoine, F., Correia, D., Lefort, V., Doppelt-Azeroual, O., Mareuil, F., Cohen-Boulakia, S., & Gascuel, O. (2019). NGPhylogeny.fr: New generation phylogenetic services for non-specialists. *Nucleic Acids Research, 47*(W1), W260–W265. https://doi.org/10.1093/nar/gkz303

Lemon, S. M., Maniloff, J., Mayo, M. A., McGeoch, D. J., Pringle, C. R., & Wickner, R. B. (2001). *[Review of the book] Virology Division, International Union of Microbiological Societies. Virus Research, 83*(1–2), 221–222. https://doi.org/10.1016/S0168-1702(01)00352-5

Lenski, R. E. (1988). Experimental studies of pleiotropy and epistasis in *Escherichia coli*. I. Variation in competitive fitness among mutants resistant to virus T4. *Evolution, 42*(3), 425. https://doi.org/10.2307/2409028

Letarov, A. V. (2020). History of early bacteriophage research and emergence of key concepts in virology. *Biochemistry (Moscow), 85*(9), 1093–1010. https://doi.org/10.1134/S0006297920090096

Letarov, A. V., Golomidova, A. K., & Tarasyan, K. K. (2010). Ecological basis for rational phage therapy. *Acta Naturae, 2*(1), 60–71. https://doi.org/10.32607/actanaturae.10756

Levin, B. R., & Bull, J. J. (2004). Population and evolutionary dynamics of phage therapy. *Nature Reviews Microbiology, 2*(2), 166–173. https://doi.org/10.1038/nrmicro822

Li, G., Shen, M., Yang, Y., Le, S., Li, M., Wang, J., Zhao, Y., Tan, Y., Hu, F., & Lu, S. (2018). Adaptation of *Pseudomonas aeruginosa* to phage PaP1 predation via O-antigen polymerase mutation. *Frontiers in Microbiology, 9,* 1170. https://doi.org/10.3389/fmicb.2018.01170

Li, X., Chen, Y., Wang, S., Duan, X., Zhang, F., Guo, A., Tao, P., Chen, H., Li, X., & Qian, P. (2022). Exploring the benefits of metal ions in phage cocktail for the treatment of

methicillin-resistant *Staphylococcus aureus* (MRSA) infection. *Infection and Drug Resistance, 15,* 2689–2702. https://doi.org/10.2147/IDR.S362743

Li, Z., Cheng, F., Lan, S., Guo, J., Liu, W., Li, X., Luo, Z., Zhang, M., Wu, J., & Shi, Y. (2018). Investigation of genetic diversity and epidemiological characteristics of *P. multocida* isolates from poultry in southwest China by population structure, multi-locus sequence typing and virulence-associated gene profile analysis. *Journal of Veterinary Medical Science, 80*(6), 921–929. https://doi.org/10.1292/jvms.18-0049

Lin, D. M., Koskella, B., & Lin, H. C. (2017). Phage therapy: An alternative to antibiotics in the age of multi-drug resistance. *World Journal of Gastrointestinal Pharmacology and Therapeutics, 8*(3), 162–173. https://doi.org/10.4292/wjgpt.v8.i3.162

Lindberg, A. A. (1973). Bacteriophage receptors. *Annual Review of Microbiology, 27*(1), 205–241. https://doi.org/10.1146/annurev.mi.27.100173.001225

Lindberg, H. M., McKean, K. A., & Wang, I.-N. (2014). Phage fitness may help predict phage therapy efficacy. *Bacteriophage, 4*(4), e964081. https://doi.org/10.4161/21597073.2014.964081

Loc-Carrillo, C., & Abedon, S. T. (2011). Pros and cons of phage therapy. *Bacteriophage, 1*(2), 111–114. https://doi.org/10.4161/bact.1.2.14590

Loh, B., Gondil, V. S., Manohar, P., Khan, F. M., Yang, H., & Leptihn, S. (2021). Encapsulation and delivery of therapeutic phages. *Applied and Environmental Microbiology, 87*(5). https://doi.org/10.1128/AEM.01979-20

Loneragan, G. H., Dargatz, D. A., Morley, P. S., & Smith, M. A. (2001). Trends in mortality ratios among cattle in US feedlots. *Journal of the American Veterinary Medical Association, 219*(8), 1122–1127. https://doi.org/10.2460/javma.2001.219.1122

Looijesteijn, P. J., Trapet, L., de Vries, E., Abee, T., & Hugenholtz, J. (2001). Physiological function of exopolysaccharides produced by *Lactococcus lactis*. *International Journal of Food Microbiology, 64*(1–2), 71–80. https://doi.org/10.1016/S0168-1605(00)00437-2

Lopatina, A., Tal, N., & Sorek, R. (2020). Abortive infection: Bacterial suicide as an antiviral immune strategy. *Annual Review of Virology, 7*(1), 371–384. https://doi.org/10.1146/annurev-virology-011620-040628

Louten, J. (2016). Virus structure and classification. In *Essential human virology* (pp. 19–29). https://doi.org/10.1016/B978-0-12-800947-5.00002-8

Lowe, T. M., & Eddy, S. R. (1997). tRNAscan-SE: A program for improved detection of transfer RNA genes in genomic sequence. *Nucleic Acids Research, 25*(5), 955–964. https://doi.org/10.1093/nar/25.5.955

Lu, T. K., & Collins, J. J. (2007). Dispersing biofilms with engineered enzymatic bacteriophage. *Proceedings of the National Academy of Sciences, 104*(27), 11197–11202. https://doi.org/10.1073/pnas.0704624104

Luria, S. E., Delbrück, M., & Anderson, T. F. (1943). Electron microscope studies of bacterial viruses. *Journal of Bacteriology, 46*(1), 57–77. https://doi.org/10.1128/jb.46.1.57-77.1943

Lv, Q., Shang, Y., Bi, H., Yang, J., Lin, L., Shi, C., Wang, M., Xie, R., Zhu, Z., Wang, F., Hua, L., Chen, H., Wu, B., & Peng, Z. (2025). Identification of two-component system ArcAB and the universal stress protein E in *P. multocida* and their effects on bacterial fitness and pathogenesis. *Microbes and Infection, 27*(1), 105235. https://doi.org/10.1016/j.micinf.2023.105235

Lwoff, A. (1953). Lysogeny. *Bacteriological Reviews, 17*(4), 269–337. https://doi.org/10.1128/br.17.4.269-337.1953

Lwoff, A., & Tournier, P. (1966). The classification of viruses. *Annual Review of Microbiology, 20*(1), 45–74. https://doi.org/10.1146/annurev.mi.20.100166.000401

Lyra, C., Savilahti, H., & Bamford, D. H. (1991). High-frequency transfer of linear DNA containing 5′-covalently linked terminal proteins: Electroporation of bacteriophage PRD1 genome into *Escherichia coli*. *Molecular & General Genetics, 228*(1–2), 65–69. https://doi.org/10.1007/BF00282449

Lüthje, P., & Brauner, A. (2014). Virulence factors of uropathogenic *E. coli* and their interaction with the host. *Advances in Microbial Physiology, 65,* 337–372. https://doi.org/10.1016/bs.ampbs.2014.08.006

Maginnis, M. S. (2018). Virus–receptor interactions: The key to cellular invasion. *Journal of Molecular Biology, 430*(17), 2590–2611. https://doi.org/10.1016/j.jmb.2018.06.024

Magiorakos, A.-P., Srinivasan, A., Carey, R. B., Carmeli, Y., Falagas, M. E., Giske, C. G., Harbarth, S., Hindler, J. F., Kahlmeter, G., Olsson-Liljequist, B., Paterson, D. L., Rice, L. B., Stelling, J., Struelens, M. J., Vatopoulos, A., Weber, J. T., & Monnet, D. L. (2012). Multidrug-resistant, extensively drug-resistant and pandrug-resistant bacteria: An international expert proposal for interim standard definitions for acquired resistance. *Clinical Microbiology and Infection, 18*(3), 268–281. https://doi.org/10.1111/j.1469-0691.2011.03570.x

Majkowska-Skrobek, G., Łątka, A., Berisio, R., Maciejewska, B., Squeglia, F., Romano, M., Lavigne, R., Struve, C., & Drulis-Kawa, Z. (2016). Capsule-targeting depolymerase, derived from *Klebsiella* KP36 phage, as a tool for the development of anti-virulent strategy. *Viruses, 8*(12), 324. https://doi.org/10.3390/v8120324

Malik, D. J., Sokolov, I. J., Vinner, G. K., Mancuso, F., Cinquerrui, S., Vladisavljevic, G. T., Clokie, M. R. J., Garton, N. J., Stapley, A. G. F., & Kirpichnikova, A. (2017). Formulation, stabilisation and encapsulation of bacteriophage for phage therapy. *Advances in Colloid and Interface Science, 249,* 100–133. https://doi.org/10.1016/j.cis.2017.05.014

Manikandan, P., Sandhya, S., Nadig, K., Paul, S., Srinivasan, N., Rothweiler, U., & Singh, M. (2022). Identification, functional characterisation, assembly and structure of ToxIN type III toxin–antitoxin complex from *E. coli*. *Nucleic Acids Research, 50*(3), 1687–1700. https://doi.org/10.1093/nar/gkab1264

Manohar, P., Loh, B., Athira, S., Nachimuthu, R., Hua, X., Welburn, S. C., & Leptihn, S. (2020). Secondary bacterial infections during pulmonary viral disease: Phage therapeutics as alternatives to antibiotics? *Frontiers in Microbiology, 11.*

Marston, M. F., & Sallee, J. L. (2003). Genetic diversity and temporal variation in the cyanophage community infecting marine *Synechococcus* species in Rhode Island's coastal waters. *Applied and Environmental Microbiology, 69*(8), 4639–4647. https://doi.org/10.1128/AEM.69.8.4639-4647.2003

Marza, A. D., Abdullah, F. F. J., Ahmed, I. M., Chung, E. L. T., Ibrahim, H. H., Zamri-Saad, M., Omar, A. R., Abu Bakar, M. Z., Saharee, A. A., Haron, A. W., Alwan, M. J., & Mohd Lila, M. A. (2017). The ability of lipopolysaccharide (LPS) of *P. multocida* B:2 to induce clinical and pathological lesions in the nervous system of buffalo calves following experimental inoculation. *Microbial Pathogenesis, 104,* 340–347. https://doi.org/10.1016/j.micpath.2017.01.031

Massacci, F. R., Magistrali, C. F., Cucco, L., Curcio, L., Bano, L., Mangili, P., Scoccia, E., Bisgaard, M., Aalbæk, B., & Christensen, H. (2018). Characterisation of *P. multocida* involved in

rabbit infections. *Veterinary Microbiology, 213,* 66–72. https://doi.org/10.1016/j.vetmic.2017.11.023

Maynou, G., Bach, A., & Terré, M. (2017). Feeding of waste milk to Holstein calves affects antimicrobial resistance of *Escherichia coli* and *P. multocida* isolated from fecal and nasal swabs. *Journal of Dairy Science, 100*(4), 2682–2694. https://doi.org/10.3168/jds.2016-11891

Mazzocco, A., Waddell, T. E., Lingohr, E., & Johnson, R. P. (2009). Enumeration of bacteriophages using the small drop plaque assay system. In *Methods in molecular biology* (pp. 81–85). https://doi.org/10.1007/978-1-60327-164-6_9

McNair, K., Bailey, B. A., & Edwards, R. A. (2012). PHACTS, a computational approach to classifying the lifestyle of phages. *Bioinformatics, 28*(5), 614–618. https://doi.org/10.1093/bioinformatics/bts014

Merabishvili, M., Pirnay, J. P., Verbeken, G., Chanishvili, N., Tediashvili, M., Lashkhi, N., Glonti, T., Krylov, V., Mast, J., Van Parys, L., Lavigne, R., Volckaert, G., Mattheus, W., Verween, G., De Corte, P., Rose, T., Jennes, S., Zizi, M., De Vos, D., & Vaneechoutte, M. (2009). Quality-controlled small-scale production of a well-defined bacteriophage cocktail for use in human clinical trials. *PLoS ONE, 4*(3), e4944. https://doi.org/10.1371/journal.pone.0004944

Middelboe, M., Holmfeldt, K., Riemann, L., Nybroe, O., & Haaber, J. (2009). Bacteriophages drive strain diversification in a marine *Flavobacterium*: Implications for phage resistance and physiological properties. *Environmental Microbiology, 11*(8), 1971–1982. https://doi.org/10.1111/j.1462-2920.2009.01920.x

Miller, R. W., Skinner, J., Sulakvelidze, A., Mathis, G. F., & Hofacre, C. L. (2010). Bacteriophage therapy for control of necrotic enteritis of broiler chickens experimentally infected

with *Clostridium perfringens*. *Avian Diseases, 54*(1), 33–40. https://doi.org/10.1637/8953-060509-REG.1

Mitchison, M., Wei, L., Kwang, J., Wilkie, I., & Adler, B. (2000). Overexpression and immunogenicity of the Oma87 outer membrane protein of *P. multocida*. *Veterinary Microbiology, 72*(1–2), 91–96. https://doi.org/10.1016/S0378-1135(99)00190-X

Miyazawa, M., Kitadokoro, K., Kamitani, S., Shime, H., & Horiguchi, Y. (2006). Crystallization and preliminary crystallographic studies of the *P. multocida* toxin catalytic domain. *Acta Crystallographica Section F: Structural Biology and Crystallization Communications, 62*(9), 906–908. https://doi.org/10.1107/S1744309106030375

Mogensen, T. H. (2009). Pathogen recognition and inflammatory signaling in innate immune defenses. *Clinical Microbiology Reviews, 22*(2), 240–273. https://doi.org/10.1128/CMR.00046-08

Mohamed, M.-W. A., & Mageed, M. A. A. M. A. (2014). Molecular analysis of *P. multocida* strains isolated from fowl cholera infection in backyard chickens. *Asian Pacific Journal of Tropical Biomedicine, 4*(1), 8–12. https://doi.org/10.1016/S2221-1691(14)60200-8

Mohd Yasin, I. S., Mohd Yusoff, S., Mohd, Z. S., & Abd Wahid Mohd, E. (2011). Efficacy of an inactivated recombinant vaccine encoding a fimbrial protein of *P. multocida* B:2 against hemorrhagic septicemia in goats. *Tropical Animal Health and Production, 43*(1), 179–187. https://doi.org/10.1007/s11250-010-9672-5

Molineux, I. J. (2001). No syringes please, ejection of phage T7 DNA from the virion is enzyme driven. *Molecular Microbiology, 40*(1), 1–8. https://doi.org/10.1046/j.1365-2958.2001.02357.x

Montag, D., Riede, I., Eschbach, M. L., Degen, M., & Henning, U. (1987). Receptor-recognising proteins of T-even type bacteriophages: Constant and hypervariable regions and an unusual case of evolution. *Journal of Molecular Biology, 196*(1), 165–174. https://doi.org/10.1016/0022-2836(87)90519-5

Monteiro, R., Pires, D. P., Costa, A. R., & Azeredo, J. (2019). Phage therapy: Going temperate? *Trends in Microbiology, 27*(4), 368–378. https://doi.org/10.1016/j.tim.2018.10.008

Moraru, C. (2023). VirClust—A tool for hierarchical clustering, core protein detection and annotation of (prokaryotic) viruses. *Viruses, 15*(4), 1007. https://doi.org/10.3390/v15041007

Morella, N. M., Yang, S. C., Hernandez, C. A., & Koskella, B. (2018). Rapid quantification of bacteriophages and their bacterial hosts in vitro and in vivo using droplet digital PCR. *Journal of Virological Methods, 259,* 18–24. https://doi.org/10.1016/j.jviromet.2018.05.007

Morozova, V. V., Kozlova, Y. N., & Tikunova, N. V. (2024). Successful use of phage and antibiotics therapy for the eradication of two bacterial pathogens from the respiratory tract of an infant. *Methods in Molecular Biology, 2734,* 237–243. https://doi.org/10.1007/978-1-0716-3523-0_15

Morris, E. J. (1958). Selective media for some *Pasteurella* species. *Journal of General Microbiology, 19*(2), 305–311. https://doi.org/10.1099/00221287-19-2-305

Morris, J. L., Letson, H. L., Elliott, L., Grant, A. L., Wilkinson, M., Hazratwala, K., & McEwen, P. (2019). Evaluation of bacteriophage as an adjunct therapy for treatment of peri-prosthetic joint infection caused by *Staphylococcus aureus*. *PLoS ONE, 14*(12), e0226574. https://doi.org/10.1371/journal.pone.0226574

Morris, M. P., & Fletcher, O. J. (1988). Estimate of economic impact of fowl cholera in turkeys in Georgia in 1986. *Avian Diseases, 32*(2), 369–372. PMID: 3202770

Mulligan, C., Fischer, M., & Thomas, G. H. (2011). Tripartite ATP-independent periplasmic (TRAP) transporters in bacteria and archaea. *FEMS Microbiology Reviews, 35*(1), 68–86. https://doi.org/10.1111/j.1574-6976.2010.00236.x

Muniesa, M., García, A., Miró, E., Mirelis, B., Prats, G., Jofre, J., & Navarro, F. (2004). Bacteriophages and diffusion of beta-lactamase genes. *Emerging Infectious Diseases, 10*(6), 1134–1137. https://doi.org/10.3201/eid1006.030472

Muniesa, M., Lucena, F., & Jofre, J. (1999). Study of the potential relationship between the morphology of infectious somatic coliphages and their persistence in the environment. *Journal of Applied Microbiology, 87*(3), 402–409. https://doi.org/10.1046/j.1365-2672.1999.00833.x

Mutters, R., Ihm, P., Pohl, S., Frederiksen, W., & Mannheim, W. (1985). Reclassification of the genus *Pasteurella* Trevisan 1887 on the basis of deoxyribonucleic acid homology, with proposals for the new species *Pasteurella dagmatis*, *Pasteurella canis*, *Pasteurella stomatis*, *Pasteurella anatis* and *Pasteurella langaa*. *International Journal of Systematic Bacteriology, 35*(3), 309–322. https://doi.org/10.1099/00207713-35-3-309

Myrenås, M., Pringle, M., Harbom, B., & Bengtsson, B. (2024). *Pasteurella multocida* from deep nasal swabs and tracheobronchial lavage in bovine calves from Sweden. *Acta Veterinaria Scandinavica, 66*(1), 58. https://doi.org/10.1186/s13028-024-00781-7

Mäntynen, S., Sundberg, L.-R., Oksanen, H., & Poranen, M. (2019). Half a century of research on membrane-containing bacteriophages: Bringing new concepts to modern virology. *Viruses, 11*(1), 76. https://doi.org/10.3390/v11010076

Nale, J. Y., Vinner, G. K., Lopez, V. C., Thanki, A. M., Phothaworn, P., Thiennimitr, P., Garcia, A., AbuOun, M., Anjum, M. F., Korbsrisate, S., Galyov, E. E., Malik, D. J., & Clokie, M. R. J. (2021). An optimized bacteriophage cocktail can effectively control *Salmonella in vitro* and

in *Galleria mellonella*. *Frontiers in Microbiology, 11*, 609955. https://doi.org/10.3389/fmicb.2020.609955

Nale, J., Redgwell, T., Millard, A., & Clokie, M. (2018a). Efficacy of an optimised bacteriophage cocktail to clear *Clostridium difficile* in a batch fermentation model. *Antibiotics, 7*(1), 13. https://doi.org/10.3390/antibiotics7010013

Nale, J. Y., Chutia, M., Carr, P., Hickenbotham, P. T., & Clokie, M. R. J. (2016a). "Get in early": Biofilm and wax moth (*Galleria mellonella*) models reveal new insights into the therapeutic potential of *Clostridium difficile* bacteriophages. *Frontiers in Microbiology, 7*, 1383. https://doi.org/10.3389/fmicb.2016.01383

Nale, J. Y., Spencer, J., Hargreaves, K. R., Buckley, A. M., Trzepiński, P., Douce, G. R., & Clokie, M. R. J. (2016b). Bacteriophage combinations significantly reduce *Clostridium difficile* growth *in vitro* and proliferation *in vivo*. *Antimicrobial Agents and Chemotherapy, 60*(2), 968–981. https://doi.org/10.1128/AAC.01774-15

Namioka, S., & Murata, M. (1961). Serological studies on *Pasteurella multocida* I: A simplified method for capsule typing of the organism. *The Cornell Veterinarian, 51*, 498–521.

Neely, M. N., Pfeifer, J. D., & Caparon, M. (2002). *Streptococcus*-zebrafish model of bacterial pathogenesis. *Infection and Immunity, 70*(7), 3904–3914. https://doi.org/10.1128/IAI.70.7.3904-3914.2002

Nguyen, A. T., & McFall-Ngai, M. J. (2020). The zebrafish as a model for gastrointestinal tract–microbe interactions. *Cellular Microbiology, 22*(1), e13152. https://doi.org/10.1111/cmi.13152

Niki, H., Imamura, R., Kitaoka, M., Yamanaka, K., Ogura, T., & Hiraga, S. (1992). *E. coli* MukB protein involved in chromosome partition forms a homodimer with a rod-and-hinge

structure having DNA-binding and ATP/GTP-binding activities. *The EMBO Journal, 11*(13), 5101–5109. https://doi.org/10.1002/j.1460-2075.1992.tb05617.x

Nir-Paz, R., Gelman, D., Khouri, A., Sisson, B. M., Fackler, J., Alkalay-Oren, S., Khalifa, L., Rimon, A., Yerushalmy, O., Bader, R., Amit, S., Coppenhagen-Glazer, S., Henry, M., Quinones, J., Malagon, F., Biswas, B., Moses, A. E., Merril, G., Schooley, R. T., Brownstein, M. J., … Hazan, R. (2019). Successful treatment of antibiotic-resistant, polymicrobial bone infection with bacteriophages and antibiotics combination. *Clinical Infectious Diseases, 69*(11), 2015–2018. https://doi.org/10.1093/cid/ciz222

Oechslin, F. (2018). Resistance development to bacteriophages occurring during bacteriophage therapy. *Viruses, 10*(7), 351. https://doi.org/10.3390/v10070351

Oh, H. K., Cha, K., Hwang, Y. J., Cho, J., Jo, Y., & Myung, H. (2018). Complete genome sequence of a novel bacteriophage, PBKP05, infecting *Klebsiella pneumoniae*. *Archives of Virology, 164*(3), 885–888. https://doi.org/10.1007/s00705-018-04121-9

Oliveira, A., Sereno, R., Nicolau, A., & Azeredo, J. (2009). The influence of the mode of administration in the dissemination of three coliphages in chickens. *Poultry Science, 88*(4), 728–733. https://doi.org/10.3382/ps.2008-00378

Olsen, R. H., Siak, J. S., & Gray, R. H. (1974). Characteristics of PRD1, a plasmid-dependent broad host range DNA bacteriophage. *Journal of Virology, 14*(3), 689–699. https://doi.org/10.1128/JVI.14.3.689-699.1974

Olszak, T., Danis-Wlodarczyk, K., Arabski, M., Gula, G., Maciejewska, B., Wasik, S., Lood, C., Higgins, G., Harvey, B. J., Lavigne, R., & Drulis-Kawa, Z. (2019). *Pseudomonas aeruginosa* PA5oct jumbo phage impacts planktonic and biofilm population and reduces its host virulence. *Viruses, 11*(12), 1089. https://doi.org/10.3390/v11121089

Orth, J. H. C., & Aktories, K. (2010). *P. multocida* toxin activates various heterotrimeric G proteins by deamidation. *Toxins, 2*(2), 205–214. https://doi.org/10.3390/toxins2020205

Orynbayev, M. B., Sultankulova, K. T., Sansyzbay, A. R., Rystayeva, R. A., Kopeyev, S. K., Kiyan, V. S., Kassenov, M. M., Kerimbayev, A. A., Barakbayev, B. B., Yespembetov, B. A., Nurabayev, S. S., Burabayev, A. S., Myrzakhmetova, B. S., Nakhanov, A. K., Kuznetsov, A. N., Khairullin, B. M., Mamadaliyev, S. M., Abduraimov, Y. O., Chervyakova, O. V., ... Zakarya, K. D. (2019). Biological characterisation of *P. multocida* present in the Saiga population. *BMC Microbiology, 19*, 37. https://doi.org/10.1186/s12866-019-1407-9

Oślizło, A., Miernikiewicz, P., Piotrowicz, A., Owczarek, B., Kopciuch, A., Figura, G., & Dąbrowska, K. (2011). Purification of phage display-modified bacteriophage T4 by affinity chromatography. *BMC Biotechnology, 11*, 59. https://doi.org/10.1186/1472-6750-11-59

O'Flynn, G., Coffey, A., Fitzgerald, G. F., & Ross, R. P. (2006a). The newly isolated lytic bacteriophages st104a and st104b are highly virulent against *Salmonella enterica*. *Journal of Applied Microbiology, 101*(1), 251–259. https://doi.org/10.1111/j.1365-2672.2005.02792.x

Pandit, K. K., & Smith, J. E. (1993). Capsular hyaluronic acid in *P. multocida* type A and its counterpart in type D. *Research in Veterinary Science, 54*(1), 20–24. https://doi.org/10.1016/0034-5288(93)90005-z

Parija, S. C. (2016). *Textbook of microbiology and immunology – E-book.* Elsevier Health Sciences.

Park, G. Y., Yu, H. J., Son, J. S., Park, S. J., Cha, H.-J., & Song, K. S. (2020). *P. multocida*-specific bacteriophage suppresses *P. multocida*-induced inflammation: Identification of genes related to bacteriophage signaling by *P. multocida*-infected swine nasal turbinate cells. *Genes & Genomics, 42*(2), 235–243. https://doi.org/10.1007/s13258-019-00898-4

Park, J. Y., Moon, B. Y., Park, J. W., Thornton, J. A., Park, Y. H., & Seo, K. S. (2017). Genetic engineering of a temperate phage-based delivery system for CRISPR/Cas9 antimicrobials against *Staphylococcus aureus*. *Scientific Reports, 7*(1), 44929. https://doi.org/10.1038/srep44929

Patel, A., Noble, R. T., Steele, J. A., Schwalbach, M. S., Hewson, I., & Fuhrman, J. A. (2007). Virus and prokaryote enumeration from planktonic aquatic environments by epifluorescence microscopy with SYBR Green I. *Nature Protocols, 2*(2), 269–276. https://doi.org/10.1038/nprot.2007.6

Pawluk, A., Davidson, A. R., & Maxwell, K. L. (2017). Anti-CRISPR: Discovery, mechanism and function. *Nature Reviews Microbiology, 16*(1), 12–17. https://doi.org/10.1038/nrmicro.2017.120

Payne, R. J. H., & Jansen, V. A. A. (2001). Understanding bacteriophage therapy as a density-dependent kinetic process. *Journal of Theoretical Biology, 208*(1), 37–48. https://doi.org/10.1006/jtbi.2000.2198

Peankuch, E., & Kausche, G. A. (1940). Isolierung und übermikroskopische Abbildung eines Bakteriophagen. *Die Naturwissenschaften, 28*(3), 46. https://doi.org/10.1007/bf01486932

Pearce, M. E., Alikhan, N. F., Dallman, T. J., Zhou, Z., Grant, K., & Maiden, M. C. J. (2018). Comparative analysis of core genome MLST and SNP typing within a European *Salmonella* serovar Enteritidis outbreak. *International Journal of Food Microbiology, 274*, 1–11. https://doi.org/10.1016/j.ijfoodmicro.2018.02.023

Pedersen, K. B., & Elling, F. (1984). The pathogenesis of atrophic rhinitis in pigs induced by toxigenic *P. multocida*. *Journal of Comparative Pathology, 94*(2), 203–214. https://doi.org/10.1016/0021-9975(84)90041-0

Peleg, A. Y., Jara, S., Monga, D., Eliopoulos, G. M., Moellering, R. C., & Mylonakis, E. (2009). *Galleria mellonella* as a model system to study *Acinetobacter baumannii* pathogenesis and therapeutics. *Antimicrobial Agents and Chemotherapy, 53*(6), 2605–2609. https://doi.org/10.1128/aac.01533-08

Peng, Z., Liang, W., Wang, F., Xu, Z., Xie, Z., Lian, Z., Hua, L., Zhou, R., Chen, H., & Wu, B. (2018). Genetic and phylogenetic characteristics of *P. multocida* isolates from different host species. *Frontiers in Microbiology, 9*, 1408. https://doi.org/10.3389/fmicb.2018.01408

Peng, Z., Liang, W., Wang, Y., Liu, W., Zhang, H., Yu, T., Zhang, A., Chen, H., & Wu, B. (2017a). Experimental pathogenicity and complete genome characterisation of a pig-origin *P. multocida* serogroup F isolate HN07. *Veterinary Microbiology, 198*, 23–33. https://doi.org/10.1016/j.vetmic.2016.11.028

Peng, Z., Wang, H., Liang, W., Chen, Y., Tang, X., Chen, H., & Wu, B. (2017b). A capsule/lipopolysaccharide/MLST genotype D/L6/ST11 of *P. multocida* is likely to be strongly associated with swine respiratory disease in China. *Archives of Microbiology, 200*(1), 107–118. https://doi.org/10.1007/s00203-017-1421-y

Peng, Z., Wang, X., Zhou, R., Chen, H., Wilson, B. A., & Wu, B. (2019). *P. multocida*: Genotypes and genomics. *Microbiology and Molecular Biology Reviews, 83*(4), e00014-19. https://doi.org/10.1128/mmbr.00014-19

Periasamy, S., Praveena, P. E., & Singh, N. (2018). Effects of *P. multocida* lipopolysaccharides on bovine leukocytes. *Microbial Pathogenesis, 119*, 225–232. https://doi.org/10.1016/j.micpath.2018.04.030

Pertics, B. Z., Cox, A., Nyúl, A., Szamek, N., Kovács, T., & Schneider, G. (2021). Isolation and characterisation of a novel lytic bacteriophage against the K2 capsule-expressing hypervirulent

Klebsiella pneumoniae strain 52145 and identification of its functional depolymerase. *Microorganisms, 9*(3), 650. https://doi.org/10.3390/microorganisms9030650

Petersen, S. K., Foged, N. T., Bording, A., Nielsen, J. P., Riemann, H. K., & Frandsen, P. L. (1991). Recombinant derivatives of *P. multocida* toxin: Candidates for a vaccine against progressive atrophic rhinitis. *Infection and Immunity, 59*(4), 1387–1393. https://doi.org/10.1128/iai.59.4.1387-1393.1991

Pettinati, I., Brem, J., Lee, S. Y., McHugh, P. J., & Schofield, C. J. (2016). The chemical biology of human metallo-β-lactamase fold proteins. *Trends in Biochemical Sciences, 41*(4), 338–355. https://doi.org/10.1016/j.tibs.2015.12.007

Pires, D. P., Melo, L., Vilas Boas, D., Sillankorva, S., & Azeredo, J. (2017). Phage therapy as an alternative or complementary strategy to prevent and control biofilm-related infections. *Current Opinion in Microbiology, 39*, 48–56. https://doi.org/10.1016/j.mib.2017.09.004

Pirnay, J. P., De Vos, D., Verbeken, G., Merabishvili, M., Chanishvili, N., Vaneechoutte, M., Zizi, M., Laire, G., Lavigne, R., Huys, I., Van den Mooter, G., Buckling, A., Debarbieux, L., Pouillot, F., Azeredo, J., Kutter, E., Dublanchet, A., Górski, A., & Adamia, R. (2011). The phage therapy paradigm: Prêt-à-porter or sur-mesure? *Pharmaceutical Research, 28*(4), 934–937. https://doi.org/10.1007/s11095-010-0313-5

Pirnay, J. P., Merabishvili, M., Van Raemdonck, H., De Vos, D., & Verbeken, G. (2018). Bacteriophage production in compliance with regulatory requirements. In J. Azeredo & S. Sillankorva (Eds.), *Bacteriophage therapy: From lab to clinical practice* (pp. 233–252). Humana Press.

Plattner, M., Shneider, M. M., Arbatsky, N. P., Shashkov, A. S., Chizhov, A. O., Nazarov, S., Prokhorov, N. S., Taylor, N. M. I., Buth, S. A., Gambino, M., Gencay, Y. E., Brøndsted, L.,

Kutter, E. M., Knirel, Y. A., & Leiman, P. G. (2019). Structure and Function of the Branched Receptor-Binding Complex of Bacteriophage CBA120. *Journal of molecular biology*, *431*(19), 3718–3739. https://doi.org/10.1016/j.jmb.2019.07.022

Pont, S., & Blanc-Potard, A. B. (2021). Zebrafish embryo infection model to investigate *Pseudomonas aeruginosa* interaction with innate immunity and validate new therapeutics. *Frontiers in Cellular and Infection Microbiology, 11*, 745851. https://doi.org/10.3389/fcimb.2021.745851

Preuß, I., Kurig, B., Nürnberg, B., Orth, J. H. C., & Aktories, K. (2009). *P. multocida* toxin activates Gβγ dimers of heterotrimeric G proteins. *Cellular Signalling, 21*(4), 551–558. https://doi.org/10.1016/j.cellsig.2008.12.007

Preview. (2020). Economic effects of bovine respiratory disease. *Journal of Animal Science, 98*(2), skaa042. https://doi.org/10.1093/jas/skaa042

Price, J. I., & Brand, C. J. (1984). Persistence of *P. multocida* in Nebraska wetlands under epizootic conditions. *Journal of Wildlife Diseases, 20*(2), 90–94. https://doi.org/10.7589/0090-3558-20.2.90

Principi, N., Silvestri, E., & Esposito, S. (2019). Advantages and limitations of bacteriophages for the treatment of bacterial infections. *Frontiers in Pharmacology, 10*, 513. https://doi.org/10.3389/fphar.2019.00513

Prjibelski, A., Antipov, D., Meleshko, D., Lapidus, A., & Korobeynikov, A. (2020). Using SPAdes de novo assembler. *Current Protocols in Bioinformatics, 70*(1), e102. https://doi.org/10.1002/cpbi.102

Pruimboom, I. M., Rimler, R. B., Ackermann, M. R., & Brogden, K. A. (1996). Capsular hyaluronic acid-mediated adhesion of *P. multocida* to turkey air sac macrophages. *Avian Diseases, 40*(4), 887. https://doi.org/10.2307/1592313

Publications Service. (2007). On an invisible microbe antagonistic toward dysenteric bacilli: Brief note by Mr. F. D'Herelle, presented by Mr. Roux. *Research in Microbiology, 158*(7), 553–554. https://doi.org/10.1016/j.resmic.2007.07.005

PubMLST. (n.d.). *rMLST species taxonomy.* Retrieved September 30, 2025, from https://pubmlst.org/static/rmlst/taxonomy.shtml

Pullinger, G. D., & Lax, A. J. (2007). Histidine residues at the active site of the *P. multocida* toxin. *The Open Biochemistry Journal, 1*, 7–11. https://doi.org/10.2174/1874091X00701010007

Pullinger, G. D., Bevir, T., & Lax, A. J. (2003a). The *P. multocida* toxin is encoded within a lysogenic bacteriophage. *Molecular Microbiology, 51*(1), 255–269. https://doi.org/10.1046/j.1365-2958.2003.03829.x

Qureshi, S., Saxena, H. M., Imam, N., Kashoo, Z., Banday, M. S., Alam, A., Malik, M. Z., Ishrat, R., & Bhat, B. (2018). Isolation and genome analysis of a lytic *P. multocida* bacteriophage PMP-GAD-IND. *Letters in Applied Microbiology, 67*(3), 244–253. https://doi.org/10.1111/lam.13010

Rakhuba, D. V., Kolomiets, E. I., Dey, E. S., & Novik, G. I. (2010a). Bacteriophage receptors, mechanisms of phage adsorption and penetration into host cell. *Polish Journal of Microbiology, 59*(3), 145–155. https://doi.org/10.33073/pjm-2010-023

Ramesh, N., Archana, L., Royam, M. M., Manohar, P., & Eniyan, K. (2019). Effect of various bacteriological media on the plaque morphology of *Staphylococcus* and *Vibrio* phages. *Access Microbiology, 1*(4), 36. https://doi.org/10.1099/acmi.0.000036

Ranade, K., & Poteete, A. R. (1993). Superinfection exclusion (*sieB*) genes of bacteriophages P22 and lambda. *Journal of Bacteriology, 175*(15), 4712–4718. https://doi.org/10.1128/jb.175.15.4712-4718.1993

Randhawa, M. A. (2009). Calculation of LD50 values from the method of Miller and Tainter, 1944. *Journal of Ayub Medical College, Abbottabad, 21*(3), 184–185.

Reed, C. J., Hutinet, G., & De Crécy-Lagard, V. (2021). Comparative genomic analysis of the DUF34 protein family suggests role as a metal ion chaperone or insertase. *Biomolecules, 11*(9), 1282. https://doi.org/10.3390/biom11091282

Reindel, R., & Fiore, C. R. (2017). Phage therapy: Considerations and challenges for development. *Clinical Infectious Diseases, 64*(11), 1589–1590. https://doi.org/10.1093/cid/cix188

Reuben, R. C., Sarkar, S. L., Ibnat, H., Setu, M. A. A., Roy, P. C., & Jahid, I. K. (2021). Novel multi-strain probiotics reduce *P. multocida*-induced fowl cholera mortality in broilers. *Scientific Reports, 11*(1), 8885. https://doi.org/10.1038/s41598-021-88299-0

Rhoades, K. R., & Rimler, R. B. (1987). Capsular groups of *P. multocida* isolated from avian hosts. *Avian Diseases, 31*(4), 895. https://doi.org/10.2307/1591048

Riede, I., & Eschbach, M. L. (1986). Evidence that TraT interacts with OmpA of *Escherichia coli*. *FEBS Letters, 205*(2), 241–245. https://doi.org/10.1016/0014-5793(86)80905-X

Rigobelo, E. C., Blackall, P. J., Maluta, R. P., & de Ávila, F. A. (2013). Identification and antimicrobial susceptibility patterns of *P. multocida* isolated from chickens and Japanese quails in Brazil. *Brazilian Journal of Microbiology, 44*(1), 161–164. https://doi.org/10.1590/S1517-83822013000100023

Rimler, R., & Rhoades, K. R. (1989). *P. multocida.* In *Pasteurella and pasteurellosis* (pp. 37–73). Academic Press Limited.

Rimler, R. (1994). Presumptive identification of *P. multocida* serogroups A, D, and F by capsule depolymerisation with mucopolysaccharidases. *Veterinary Record, 134*(8), 191–192. https://doi.org/10.1136/vr.134.8.191

Rodriguez-Brito, B., Li, L., Wegley, L., Furlan, M., Angly, F., Breitbart, M., Buchanan, J., Desnues, C., Dinsdale, E., Edwards, R., Felts, B., Haynes, M., Liu, H., Lipson, D., Mahaffy, J., Martin-Cuadrado, A. B., Mira, A., Nulton, J., Pašić, L., ... Rohwer, F. (2010). Viral and microbial community dynamics in four aquatic environments. *The ISME Journal, 4*(6), 739–751. https://doi.org/10.1038/ismej.2010.1

Rohde, C., Wittmann, J., & Kutter, E. (2018). Bacteriophages: A therapy concept against multi-drug-resistant bacteria. *Surgical Infections, 19*(8), 737–744. https://doi.org/10.1089/sur.2018.184

Rossmann, M. G., Morais, M. C., Leiman, P. G., & Zhang, W. (2005). Combining X-ray crystallography and electron microscopy. *Structure, 13*(3), 355–362. https://doi.org/10.1016/j.str.2005.01.005

Rostøl, J. T., & Marraffini, L. (2019). (Ph)ighting phages: How bacteria resist their parasites. *Cell Host and Microbe, 25*(2), 184–194. https://doi.org/10.1016/j.chom.2019.01.009

Ruffolo, C. G., Tennent, J. M., Michalski, W. P., & Adler, B. (1997). Identification, purification, and characterisation of the type 4 fimbriae of *P. multocida*. *Infection and Immunity, 65*(1), 339–343. https://doi.org/10.1128/iai.65.1.339-343.1997

Ruska, H. (1940). Die Sichtbarmachung der bakteriophagen Lyse im übermikroskop. *Die Naturwissenschaften, 28*(3), 45–46. https://doi.org/10.1007/bf01486931

Ruska, H. (1943). Versuch zu einer Ordnung der Virusarten. *Archives of Virology, 2*(5), 480–498. https://doi.org/10.1007/bf01244584

Ryan, E. M., Gorman, S. P., Donnelly, R. F., & Gilmore, B. F. (2011). Recent advances in bacteriophage therapy: How delivery routes, formulation, concentration, and timing influence the success of phage therapy. *Journal of Pharmacy and Pharmacology, 63*(10), 1253–1264. https://doi.org/10.1111/j.2042-7158.2011.01324.x

Rydman, P. S., & Bamford, D. H. (2000). Bacteriophage PRD1 DNA entry uses a viral membrane-associated transglycosylase activity. *Molecular Microbiology, 37*(2), 356–363. https://doi.org/10.1046/j.1365-2958.2000.01996.x

Salmond, G. P. C., & Fineran, P. C. (2015). A century of the phage: Past, present and future. *Nature Reviews Microbiology, 13*(12), 777–786. https://doi.org/10.1038/nrmicro3564

Samson, J. E., Magadán, A. H., Sabri, M., & Moineau, S. (2013). Revenge of the phages: Defeating bacterial defences. *Nature Reviews Microbiology, 11*(10), 675–687. https://doi.org/10.1038/nrmicro3096

Santos, S. B., Carvalho, C., Azeredo, J., & Ferreira, E. C. (2014). Population dynamics of a *Salmonella* lytic phage and its host: Implications of the host bacterial growth rate in modelling. In J. Vera (Ed.), *PLoS ONE, 9*(7), e102507. https://doi.org/10.1371/journal.pone.0102507

Sarangi, L. N., Priyadarshini, A., Kumar, S., Thomas, P., Gupta, S. K., Nagaleekar, V. K., & Singh, V. P. (2014). Virulence genotyping of *Pasteurella multocida* isolated from multiple hosts from India. *The Scientific World Journal, 2014*, 814109. https://doi.org/10.1155/2014/814109

Sarangi, L. N., Thomas, P., Gupta, S. K., Priyadarshini, A., Kumar, S., Nagaleekar, V. K., Kumar, A., & Singh, V. P. (2015). Virulence gene profiling and antibiotic resistance pattern of Indian isolates of *Pasteurella multocida* of small ruminant origin. *Comparative Immunology, Microbiology and Infectious Diseases, 38*, 33–39. https://doi.org/10.1016/j.cimid.2014.11.003

Satam, H., Joshi, K., Mangrolia, U., Waghoo, S., Zaidi, G., Rawool, S., Thakare, R. P., Banday, S., Mishra, A. K., & Das, G. (2023). Next-generation sequencing technology: Current trends and advancements. *Biology, 12*(7), 997. https://doi.org/10.3390/biology12070997

Scholl, D., Adhya, S., & Merril, C. (2005). *Escherichia coli* K1's capsule is a barrier to bacteriophage T7. *Applied and Environmental Microbiology, 71*(8), 4872–4874. https://doi.org/10.1128/AEM.71.8.4872-4874.2005

Schooley, R. T., Biswas, B., Gill, J. J., Hernandez-Morales, A., Lancaster, J., Lessor, L., Barr, J. J., Reed, S. L., Rohwer, F., Benler, S., Segall, A. M., Taplitz, R., Smith, D. M., Kerr, K., Kumaraswamy, M., Nizet, V., Lin, L., McCauley, M. D., Strathdee, S. A., Benson, C. A., … Hamilton, T. (2017). Development and use of personalized bacteriophage-based therapeutic cocktails to treat a patient with a disseminated resistant *Acinetobacter baumannii* infection. *Antimicrobial Agents and Chemotherapy, 61*(10), e00954-17. https://doi.org/10.1128/AAC.00954-17

Science Education Alliance – Phage Hunters Advancing Genomics and Evolutionary Science (SEA-PHAGES). (n.d.). *3.0 Overview. SEA-PHAGES Phage Discovery Guide.* Retrieved from https://seaphagesphagediscoveryguide.helpdocsonline.com/3-0-overview

Scirè, A., Cianfruglia, L., Minnelli, C., Romaldi, B., Laudadio, E., Galeazzi, R., Antognelli, C., & Armeni, T. (2022). Glyoxalase 2: Towards a broader view of the second player of the glyoxalase system. *Antioxidants, 11*(11), 2131. https://doi.org/10.3390/antiox11112131

Seed, K. D., & Dennis, J. J. (2009). Experimental bacteriophage therapy increases survival of *Galleria mellonella* larvae infected with clinically relevant strains of the *Burkholderia cepacia* complex. *Antimicrobial Agents and Chemotherapy, 53*(5), 2205–2208. https://doi.org/10.1128/AAC.01166-08

Seed, K. D. (2015). Battling phages: How bacteria defend against viral attack. In V. L. Miller (Ed.), *PLOS Pathogens, 11*(6), e1004847. https://doi.org/10.1371/journal.ppat.1004847

Selander, R. K., Caugant, D. A., Ochman, H., Musser, J. M., Gilmour, M. N., & Whittam, T. S. (1986). Methods of multilocus enzyme electrophoresis for bacterial population genetics and systematics. *Applied and Environmental Microbiology, 51*(5), 873–884. https://doi.org/10.1128/AEM.51.5.873-884.1986

Serna, C., Calderón Bernal, J. M., Torre-Fuentes, L., García Muñoz, Á., Díez Guerrier, A., Hernández, M., Fernández-Garayzábal, J. F., Vela, A. I., Cid, D., & Álvarez, J. (2025). Integrative and conjugative elements associated with antimicrobial resistance in multidrug-resistant *Pasteurella multocida* isolates from bovine respiratory disease (BRD)-affected animals in Spanish feedlots. *The Veterinary Quarterly, 45*, 1–15.

Serrano, I., Verdial, C., Tavares, L., & Oliveira, M. (2023). The virtuous *Galleria mellonella* model for scientific experimentation. *Antibiotics, 12*.

Shackelton, L. A., & Holmes, E. C. (2004). The evolution of large DNA viruses: Combining genomic information of viruses and their hosts. *Trends in Microbiology, 12*(10), 458–465. https://doi.org/10.1016/j.tim.2004.08.005

Shao, Y., & Wang, I.-N. (2008a). Bacteriophage adsorption rate and optimal lysis time. *Genetics, 180*(1), 471–482. https://doi.org/10.1534/genetics.108.090100

Sharma, S., Chatterjee, S., Datta, S., Prasad, R., Dubey, D., Prasad, R. K., & Vairale, M. G. (2016). Bacteriophages and its applications: An overview. *Folia Microbiologica, 62*(1), 17–55. https://doi.org/10.1007/s12223-016-0471-x

Shen, X., Li, M., Zeng, Y., Hu, X., Tan, Y., Rao, X., Jin, X., Li, S., Zhu, J., & Zhang, K. (2012). Functional identification of the DNA packaging terminase from *Pseudomonas aeruginosa*

phage PaP3. *Archives of Virology, 157*(11), 2133–2141. https://doi.org/10.1007/s00705-012-1409-5

Shen, A., & Millard, A. (2021). Phage genome annotation: Where to begin and end. *PHAGE, 2*(4), 183–193. https://doi.org/10.1089/phage.2021.0015

Shi, K., Oakland, J. T., Kurniawan, F., Moeller, N. H., Banerjee, S., & Aihara, H. (2020). Structural basis of superinfection exclusion by bacteriophage T4 Spackle. *Communications Biology, 3*(1), 691. https://doi.org/10.1038/s42003-020-01412-3

Shivachandra, S. B., Kumar, A. A., Biswas, A., Ramakrishnan, M. A., Singh, V. P., & Srivastava, S. K. (2004). Antibiotic sensitivity patterns among Indian strains of avian *Pasteurella multocida*. *Tropical Animal Health and Production, 36*(8), 743–750. https://doi.org/10.1023/B:TROP.0000045950.35070.7f

Sidi Mabrouk, A., Ongenae, V., Claessen, D., Brenzinger, S., & Briegel, A. (2023). A flexible and efficient microfluidics platform for the characterisation and isolation of novel bacteriophages. *Applied and Environmental Microbiology, 89*(1), e0159622. https://doi.org/10.1128/aem.01596-22

Sillankorva, S., Oliveira, R., Vieira, M. J., Sutherland, I. W., & Azeredo, J. (2004). Bacteriophage phi S1 infection of *Pseudomonas fluorescens* planktonic cells versus biofilms. *Biofouling, 20*(3), 133–138. https://doi.org/10.1080/08927010410001723834

Simmonds, P., Adriaenssens, E. M., Zerbini, F. M., Abrescia, N. G. A., Aiewsakun, P., Alfenas-Zerbini, P., Bao, Y., Barylski, J., Drosten, C., Duffy, S., Duprex, W. P., Dutilh, B. E., Elena, S. F., García, M. L., Junglen, S., Katzourakis, A., Koonin, E. V., Krupovic, M., Kuhn, J. H., Lambert, A. J., … Vasilakis, N. (2023). Four principles to establish a universal virus taxonomy. *PLOS Biology, 21*(2), e3001922. https://doi.org/10.1371/journal.pbio.3001922

Singh, B., Prasad, S., Verma, M. R., & Sinha, D. K. (2014). Estimation of economic losses due to haemorrhagic septicaemia in cattle and buffaloes in India. *Agricultural Economics Research Review, 27*(2), 271. https://doi.org/10.5958/0974-0279.2014.00030.5

Sitaraman, R. (2016). The role of DNA restriction-modification systems in the biology of *Bacillus anthracis*. *Frontiers in Microbiology, 7*, 11. https://doi.org/10.3389/fmicb.2016.00011

Smith, E., Miller, E., Aguayo, J. M., Figueroa, C. F., Nezworski, J., Studniski, M., Wileman, B., & Johnson, T. (2021). Genomic diversity and molecular epidemiology of *Pasteurella multocida*. *PLOS ONE, 16*(4), e0249138. https://doi.org/10.1371/journal.pone.0249138

Smith, H. W., & Huggins, M. B. (1982). Successful treatment of experimental *Escherichia coli* infections in mice using phage: Its general superiority over antibiotics. *Journal of General Microbiology, 128*(2), 307–318. https://doi.org/10.1099/00221287-128-2-307

Snipes, K. P., & Hirsh, D. C. (1986). Association of complement sensitivity with virulence of *Pasteurella multocida* isolated from turkeys. *Avian Diseases, 30*(3), 500. https://doi.org/10.2307/1590413

Snipes, K. P., Ghazikhanian, G. Y., & Hirsh, D. C. (1987). Fate of *Pasteurella multocida* in the blood vascular system of turkeys following intravenous inoculation: Comparison of an encapsulated, virulent strain with its avirulent, acapsular variant. *Avian Diseases, 31*(2), 254. https://doi.org/10.2307/1590869

Speck, P., & Smithyman, A. (2016). Safety and efficacy of phage therapy via the intravenous route. *FEMS Microbiology Letters, 363*(3), fnv242. https://doi.org/10.1093/femsle/fnv242

Srujana, A., Sonalika, J., Akhila, D. S., Juliet, M., & Sheela, P. A. (2021). Isolation of phages and study of their *in vitro* efficacy on *Staphylococcus aureus* isolates originating from bovine subclinical mastitis. *Indian Journal of Animal Research.*

Stanley, S. Y., & Maxwell, K. L. (2018). Phage-encoded anti-CRISPR defenses. *Annual Review of Genetics, 52*, 445–464. https://doi.org/10.1146/annurev-genet-120417-031321

Steinbacher, S., Miller, S., Baxa, U., Budisa, N., Weintraub, A., Seckler, R., & Huber, R. (1997). Phage P22 tailspike protein: Crystal structure of the head-binding domain at 2.3 Å, fully refined structure of the endorhamnosidase at 1.56 Å resolution, and the molecular basis of O-antigen recognition and cleavage. *Journal of Molecular Biology, 267*(4), 865–880. https://doi.org/10.1006/jmbi.1997.0922

Stone, E., Campbell, K., Grant, I., & McAuliffe, O. (2019). Understanding and exploiting phage–host interactions. *Viruses, 11*(6), 567. https://doi.org/10.3390/v11060567

Storms, Z. J., Teel, M. R., Mercurio, K., & Sauvageau, D. (2020). The virulence index: A metric for quantitative analysis of phage virulence. *PHAGE, 1*(1), 27–36. https://doi.org/10.1089/phage.2019.0001

Strotskaya, A., Savitskaya, E., Metlitskaya, A., Morozova, N., Datsenko, K. A., Semenova, E., & Severinov, K. (2017). The action of *Escherichia coli* CRISPR-Cas system on lytic bacteriophages with different lifestyles and development strategies. *Nucleic Acids Research, 45*(4), 1946–1957. https://doi.org/10.1093/nar/gkx042

Sturino, J. M., & Klaenhammer, T. R. (2006). Engineered bacteriophage-defence systems in bioprocessing. *Nature Reviews Microbiology, 4*(5), 395–404. https://doi.org/10.1038/nrmicro1393

Subaaharan, S., Blackall, L. L., & Blackall, P. J. (2010). Development of a multi-locus sequence typing scheme for avian isolates of *Pasteurella multocida*. *Veterinary Microbiology, 141*(3–4), 354–361. https://doi.org/10.1016/j.vetmic.2010.01.017

Sullivan, M. B., Coleman, M. L., Quinlivan, V., Rosenkrantz, J. E., DeFrancesco, A. S., Tan, G., Fu, R., Lee, J. A., Waterbury, J. B., Bielawski, J. P., & Chisholm, S. W. (2008). Portal protein diversity and phage ecology. *Environmental Microbiology, 10*(10), 2810–2823. https://doi.org/10.1111/j.1462-2920.2008.01702.x

Summers, W. C. (2001). Bacteriophage therapy. *Annual Review of Microbiology, 55*(1), 437–451. https://doi.org/10.1146/annurev.micro.55.1.437

Summers, W. C. (2012). The strange history of phage therapy. *Bacteriophage, 2*(2), 130–133. https://doi.org/10.4161/bact.20757

Summers, W. C. (2016). Félix Hubert d'Herelle (1873–1949): History of a scientific mind. *Bacteriophage, 6*(4), e1270090. https://doi.org/10.1080/21597081.2016.1270090

Sumrall, E. T., Shen, Y., Keller, A. P., Rismondo, J., Pavlou, M., Eugster, M. R., Boulos, S., Disson, O., Thouvenot, P., Kilcher, S., Wollscheid, B., Cabanes, D., Lecuit, M., Gründling, A., & Loessner, M. J. (2019). Phage resistance at the cost of virulence: *Listeria monocytogenes* serovar 4b requires galactosylated teichoic acids for InlB-mediated invasion. *PLOS Pathogens, 15*(10), e1008032. https://doi.org/10.1371/journal.ppat.1008032

Suttle, C. A. (2005). Viruses in the sea. *Nature, 437*(7057), 356–361. https://doi.org/10.1038/nature04160

Sutton, T. D. S., & Hill, C. (2019). Gut bacteriophage: Current understanding and challenges. *Frontiers in Endocrinology, 10*, 784. https://doi.org/10.3389/fendo.2019.00784

Swanstrom, M., & Adams, M. H. (1951). Agar layer method for production of high titer phage stocks. *Experimental Biology and Medicine, 78*(2), 372–375. https://doi.org/10.3181/00379727-78-19076

Swayne, D. E. (2013). Pasteurellosis and other respiratory bacterial infections. In *Diseases of poultry* (13th ed.). Wiley. https://doi.org/10.1002/9781119421481.ch19

Tang, X., Zhao, Z., Hu, J., Wu, B., Cai, X., He, Q., & Chen, H. (2009a). Isolation, antimicrobial resistance and virulence genes of *Pasteurella multocida* strains from swine in China. *Journal of Clinical Microbiology, 47*(4), 951–958. https://doi.org/10.1128/JCM.02029-08

Teney, C., Poupelin, J. C., Briot, T., Le Bouar, M., Fèvre, C., Brosset, S., Martin, O., Valour, F., Roussel-Gaillard, T., Leboucher, G., Ader, F., Lukaszewicz, A. C., Ferry, T., & PHAGEinLYON Clinic Study Group. (2024). Phage therapy in a burn patient colonized with extensively drug-resistant *Pseudomonas aeruginosa* responsible for relapsing ventilator-associated pneumonia and bacteremia. *Viruses, 16*(7), 1080. https://doi.org/10.3390/v16071080

Thanki, A. M., Mignard, G., Atterbury, R. J., Barrow, P., Millard, A. D., & Clokie, M. R. J. (2022). Prophylactic delivery of a bacteriophage cocktail in feed significantly reduces *Salmonella* colonization in pigs. *Microbiology Spectrum, 10*(3), e0042222. https://doi.org/10.1128/spectrum.00422-22

Thomaz, L., de Almeida, L. G., Silva, F. R., Cortez, M., Taborda, C. P., & Spira, B. (2020). *In vivo* activity of silver nanoparticles against *Pseudomonas aeruginosa* infection in *Galleria mellonella*. *Frontiers in Microbiology, 11*, 577. https://doi.org/10.3389/fmicb.2020.00577

Tock, M. R., & Dryden, D. T. (2005). The biology of restriction and anti-restriction. *Current Opinion in Microbiology, 8*(4), 466–472. https://doi.org/10.1016/j.mib.2005.06.003

Touchon, M., Bernheim, A., & Rocha, E. P. C. (2016). Genetic and life-history traits associated with the distribution of prophages in bacteria. *The ISME Journal, 10*(11), 2744–2754. https://doi.org/10.1038/ismej.2016.47

Townsend, K. M., Frost, A. J., Lee, C. W., Papadimitriou, J. M., & Dawkins, H. J. (1998). Development of PCR assays for species- and type-specific identification of *Pasteurella multocida* isolates. *Journal of Clinical Microbiology, 36*(4), 1096–1100. https://doi.org/10.1128/JCM.36.4.1096-1100.1998

Townsend, K. M., Boyce, J. D., Chung, J. Y., Frost, A. J., & Adler, B. (2001a). Genetic organization of *Pasteurella multocida* cap loci and development of a multiplex capsular PCR typing system. *Journal of Clinical Microbiology, 39*(3), 924–929. https://doi.org/10.1128/JCM.39.3.924-929.2001

Tsai, C. J.-Y., Loh, J. M. S., & Proft, T. (2016). *Galleria mellonella* infection models for the study of bacterial diseases and for antimicrobial drug testing. *Virulence, 7*(3), 214–229. https://doi.org/10.1080/21505594.2015.1135289

Tsehay, M. T., Zeru, A. G., & Mengist, G. K. (2024). Review on fowl cholera. *Journal of Life Sciences Research and Reviews, 3*(1), 1–4. https://doi.org/10.47363/JLSRR/2025(3)131

Tsuji, M., & Matsumoto, M. (1989). Pathogenesis of fowl cholera: Influence of encapsulation on the fate of *Pasteurella multocida* after intravenous inoculation into turkeys. *Avian Diseases, 33*(2), 238. https://doi.org/10.2307/1590838

Turner, D., Shkoporov, A. N., Lood, C., Millard, A. D., Dutilh, B. E., Alfenas-Zerbini, P., van Zyl, L. J., Aziz, R. K., Oksanen, H. M., Poranen, M. M., Kropinski, A. M., Barylski, J., Brister, J. R., Chanishvili, N., Edwards, R. A., Enault, F., Gillis, A., Knezevic, P., Krupovic, M., Kurtböke, I., … Adriaenssens, E. M. (2023). Abolishment of morphology-based taxa and change to binomial

species names: 2022 taxonomy update of the ICTV bacterial viruses subcommittee. *Archives of Virology, 168*(2), 74. https://doi.org/10.1007/s00705-022-05694-2

Turni, C., Singh, R., & Blackall, P. (2018). Genotypic diversity of *Pasteurella multocida* isolates from pigs and poultry in Australia. *Australian Veterinary Journal, 96*(10), 390–394. https://doi.org/10.1111/avj.12748

Tynecki, P., Guziński, A., Kazimierczak, J., Jadczuk, M., Dastych, J., & Onisko, A. (2020). PhageAI – Bacteriophage life cycle recognition with machine learning and natural language processing. *bioRxiv.* https://doi.org/10.1101/2020.07.11.198606

Ugochukwu, E. (2009). Isolation and characterisation of *Pasteurella multocida* from caprine pneumonic lungs. *Animal Research International, 5*(2). https://doi.org/10.4314/ari.v5i2.48751

Ujvári, B., Makrai, L., & Magyar, T. (2018). Characterisation of a multiresistant *Pasteurella multocida* strain isolated from cattle. *Acta Veterinaria Hungarica, 66*(1), 12–19. https://doi.org/10.1556/004.2018.002

Vale, P. F., & Little, T. J. (2010). CRISPR-mediated phage resistance and the ghost of coevolution past. *Proceedings of the Royal Society B: Biological Sciences, 277*(1691), 2097–2103. https://doi.org/10.1098/rspb.2010.0055

van Charante, F., Holtappels, D., Blasdel, B., & Burrowes, B. (2019). Isolation of bacteriophages. In D. Harper, S. Abedon, B. Burrowes, & M. McConville (Eds.), *Bacteriophages* (pp. 1–15). Springer. https://doi.org/10.1007/978-3-319-40598-8_14-1

Van Twest, R., & Kropinski, A. M. (2009). Bacteriophage enrichment from water and soil. *Methods in Molecular Biology, 501*, 15–21. https://doi.org/10.1007/978-1-60327-164-6_2

Vandenheuvel, D., Rombouts, S., & Adriaenssens, E. M. (2018). Purification of bacteriophages using anion-exchange chromatography. *Methods in Molecular Biology, 1681*, 59–69. https://doi.org/10.1007/978-1-4939-7343-9_5

Verbeken, G., Huys, I., Pirnay, J. P., Jennes, S., Chanishvili, N., Scheres, J., Górski, A., De Vos, D., & Ceulemans, C. (2014). Taking bacteriophage therapy seriously: A moral argument. *BioMed Research International, 2014*, 621316. https://doi.org/10.1155/2014/621316

Verma, S., Sharma, M., Katoch, S., Verma, L., Kumar, S., Dogra, V., Chahota, R., Dhar, P., & Singh, G. (2012). Profiling of virulence-associated genes of *Pasteurella multocida* isolated from cattle. *Veterinary Research Communications, 37*(1), 83–89. https://doi.org/10.1007/s11259-012-9539-5

Vig, E., Green, M., Liu, Y., Yu, K.-Y., Kwon, H.-J., Tian, J., Goebl, M. G., & Harrington, M. A. (2001). SIMPL is a tumor necrosis factor-specific regulator of nuclear factor-κB activity. *Journal of Biological Chemistry, 276*(11), 7859–7866. https://doi.org/10.1074/jbc.M010399200

Villani, S., Calcagnile, M., Demitri, C., & Alifano, P. (2025). *Galleria mellonella* (greater wax moth) as a reliable animal model to study the efficacy of nanomaterials in fighting pathogens. *Nanomaterials, 15*(1), 67. https://doi.org/10.3390/nano15010067

Virgo, M., Mostowy, S., & Ho, B. T. (2024). Use of zebrafish to identify host responses specific to type VI secretion system–mediated interbacterial antagonism. *PLOS Pathogens, 20*(7), e1012384. https://doi.org/10.1371/journal.ppat.1012384

Voorhees, P. J., Ponek, R. M., Liu, J. D., & Lai, S. K. (2024). A droplet digital PCR assay for quantification of bacteriophage viral vector titer and purity. *bioRxiv.* https://doi.org/10.1101/2024.11.20.624577

Vu-Khac, H., Trinh, T. T. H., Nguyen, T. T. G., Nguyen, X. T., & Nguyen, T. T. (2020). Prevalence of virulence factor, antibiotic resistance, and serotype genes of *Pasteurella multocida* strains isolated from pigs in Vietnam. *Veterinary World, 13*(5), 896–904. https://doi.org/10.14202/vetworld.2020.896-904

Waldor, M. K., & Mekalanos, J. J. (1996). Lysogenic conversion by a filamentous phage encoding cholera toxin. *Science, 272*(5270), 1910–1914. https://doi.org/10.1126/science.272.5270.1910

Wanasawaeng, W., Thomrongsuwannakij, T., & Chansiripornchai, N. (2025). Isolation, characterization, and application of bacteriophage for *Salmonella* control in broiler chickens. *Veterinary Medicine International, 2025*, Article ID 987654.

Wang, X., Loh, B., Gordillo Altamirano, F., Yu, Y., Hua, X., & Leptihn, S. (2021). Colistin–phage combinations decrease antibiotic resistance in *Acinetobacter baumannii* via changes in envelope architecture. *Emerging Microbes & Infections, 10*(1), 2205–2219. https://doi.org/10.1080/22221751.2021.2002671

Wang, X., Xie, Z., Zhao, J., Zhu, Z., Yang, C., & Liu, Y. (2021). Prospects of inhaled phage therapy for combatting pulmonary infections. *Frontiers in Cellular and Infection Microbiology, 11*, 758392. https://doi.org/10.3389/fcimb.2021.758392

Wang, Y., Fan, H., & Tong, Y. (2023). Unveil the secret of the bacteria and phage arms race. *International Journal of Molecular Sciences, 24*(5), 4363. https://doi.org/10.3390/ijms24054363

Watson, B. N. J., Vercoe, R. B., Salmond, G. P. C., Westra, E. R., Staals, R. H. J., & Fineran, P. C. (2019). Type I-F CRISPR-Cas resistance against virulent phages results in abortive

infection and provides population-level immunity. *Nature Communications, 10*(1), 5526. https://doi.org/10.1038/s41467-019-13445-2

Watts, J. L., & Sweeney, M. T. (2010). Antimicrobial resistance in bovine respiratory disease pathogens: Measures, trends, and impact on efficacy. *Veterinary Clinics of North America: Food Animal Practice, 26*(1), 79–88. https://doi.org/10.1016/j.cvfa.2009.10.009

Wdowiak, M., Paczesny, J., & Raza, S. (2022). Enhancing the stability of bacteriophages using physical, chemical, and nano-based approaches: A review. *Pharmaceutics, 14*(9), 1936. https://doi.org/10.3390/pharmaceutics14091936

Wei, Y., Li, Z., Lao, J., Huang, J., Chen, H., Li, J., Deng, Y., Mao, X., Ma, R., Wu, Y., Tan, Y., Li, X., Lu, Y., Jiang, S., & Wang, X. (2025). Isolation and characterization of *Pseudomonas* phage HJ01 and its therapeutic efficacy in canine pyoderma. *BMC Veterinary Research, 21*(1), 443. https://doi.org/10.1186/s12917-025-04877-8

Weinbauer, M. G. (2004). Ecology of prokaryotic viruses. *FEMS Microbiology Reviews, 28*(2), 127–181. https://doi.org/10.1016/j.femsre.2003.08.001

Weiss, B. (2007). The deoxycytidine pathway for thymidylate synthesis in *Escherichia coli*. *Journal of Bacteriology, 189*(21), 7922–7926. https://doi.org/10.1128/JB.00461-07

Weitz, J. S., Hartman, H., & Levin, S. A. (2005). Coevolutionary arms races between bacteria and bacteriophage. *Proceedings of the National Academy of Sciences, 102*(27), 9535–9540. https://doi.org/10.1073/pnas.0504062102

Wen, Y., Behiels, E., & Devreese, B. (2014). Toxin–antitoxin systems: Their role in persistence, biofilm formation, and pathogenicity. *Pathogens and Disease, 70*(3), 240–249. https://doi.org/10.1111/2049-632X.12145

Wibisono, C., Wijayanti, A. D., Muzaki, A. Y., Widiasih, D. A., & Noviatri, A. (2024). Validation of the method for determining lincomycin levels and calculating lincomycin levels in broiler chicken plasma using high-performance liquid chromatography. *Open Veterinary Journal, 14*, 1453–1459.

Wickramasinghe, S. R., Kalbfuss, B., Zimmermann, A., Thom, V., & Reichl, U. (2005). Tangential flow microfiltration and ultrafiltration for human influenza A virus concentration and purification. *Biotechnology and Bioengineering, 92*(2), 199–208. https://doi.org/10.1002/bit.20599

Wilcox, S. A., Toder, R., & Foster, J. W. (1996). Rapid isolation of recombinant lambda phage DNA for use in fluorescence *in situ* hybridization. *Chromosome Research, 4*(5), 397–404. https://doi.org/10.1007/BF02257276

Wilkie, I. W., Harper, M., Boyce, J. D., & Adler, B. (2012a). *Pasteurella multocida*: Diseases and pathogenesis. *Current Topics in Microbiology and Immunology,* 1–22. https://doi.org/10.1007/82_2012_216

Williamson, K. E., Radosevich, M., & Wommack, K. E. (2005). Abundance and diversity of viruses in six Delaware soils. *Applied and Environmental Microbiology, 71*(6), 3119–3125. https://doi.org/10.1128/AEM.71.6.3119-3125.2005

Williamson, K. E., Wommack, K. E., & Radosevich, M. (2003). Sampling natural viral communities from soil for culture-independent analyses. *Applied and Environmental Microbiology, 69*(11), 6628–6633. https://doi.org/10.1128/AEM.69.11.6628-6633.2003

Wilson, B. A., & Ho, M. (2012). *Pasteurella multocida* toxin interaction with host cells: Entry and cellular effects. *Current Topics in Microbiology and Immunology,* 93–111. https://doi.org/10.1007/82_2012_219

Wilson, B. A., & Ho, M. (2013). *Pasteurella multocida*: From zoonosis to cellular microbiology. *Clinical Microbiology Reviews, 26*(3), 631–655. https://doi.org/10.1128/CMR.00024-13

Wishart, D. S., Han, S., Saha, S., Oler, E., Peters, H., Grant, J., Stothard, P., & Gautam, V. (2023). PHASTEST: Faster than PHASTER, better than PHAST. *Nucleic Acids Research, 51*(W1), W74–W81. https://doi.org/10.1093/nar/gkad382

Wittebole, X., De Roock, S., & Opal, S. M. (2014). A historical overview of bacteriophage therapy as an alternative to antibiotics for the treatment of bacterial pathogens. *Virulence, 5*(1), 226–235. https://doi.org/10.4161/viru.25991

Wongtavatchai, J., McLean, L., Ramos, F., & Arnold, D. (2004). Chloramphenicol. In *World Health Organization: Joint FAO/WHO Expert Committee on Food Additives (JECFA), WHO Food Additives Series* (Vol. 53, pp. 7–85). International Programme on Chemical Safety (IPCS). Retrieved from http://www.inchem.org/documents/jecfa/jecmono/v53je02.htm

Wu, M.-C., Yang, C.-Y., Lin, T.-L., Wang, J.-T., Yang, F.-C., Wu, S.-H., Hu, B., Chou, T.-F., Tsai, M.-H., Lin, C.-Y., & Hsieh, S.-L. (2009). Humoral immunity against capsule polysaccharide protects the host from *magA+ Klebsiella pneumoniae*-induced lethal disease by evading Toll-like receptor 4 signaling. *Infection and Immunity, 77*(2), 670–677. https://doi.org/10.1128/IAI.00931-08

Yoon, S. J. (2015). *P. multocida* bacteriophage Pas-MUP-1 and use thereof for inhibiting proliferation of *P. multocida* (U.S. Patent No. US10568917B2). *Google Patents.* https://patents.google.com/patent/US10568917B2

Yoshida, M., Yoshida, T., Yoshida-Takashima, Y., Kashima, A., & Hiroishi, S. (2010). Real-time PCR detection of host-mediated cyanophage gene transcripts during infection of a

natural *Microcystis aeruginosa* population. *Microbes and Environments, 25*(3), 211–215. https://doi.org/10.1264/jsme2.me10117

Zahid, M. S. H., Udden, S. M. N., Faruque, A. S. G., Calderwood, S. B., Mekalanos, J. J., & Faruque, S. M. (2008). Effect of phage on the infectivity of *Vibrio cholerae* and emergence of genetic variants. *Infection and Immunity, 76*(11), 5266–5273. https://doi.org/10.1128/IAI.00578-08

Zaki, B. M., Fahmy, N. A., Aziz, R. K., Samir, R., & El-Shibiny, A. (2023). Characterisation and comprehensive genome analysis of novel bacteriophage vB_Kpn_ZCKp20p with lytic and anti-biofilm potential against clinical multidrug-resistant *Klebsiella pneumoniae*. *Frontiers in Cellular and Infection Microbiology, 13*, 1077995. https://doi.org/10.3389/fcimb.2023.1077995

Zehr, E. S., Tabatabai, L. B., & Bayles, D. O. (2012). Genomic and proteomic characterisation of SuMu, a Mu-like bacteriophage infecting *Haemophilus parasuis*. *BMC Genomics, 13*(1), 331. https://doi.org/10.1186/1471-2164-13-331

Zhang, H., Fouts, D. E., DePew, J., & Stevens, R. H. (2013a). Genetic modifications to temperate *Enterococcus faecalis* phage φEf11 that abolish the establishment of lysogeny and sensitivity to repressor and increase host range and productivity of lytic infection. *Microbiology, 159*(Pt_6), 1023–1035. https://doi.org/10.1099/mic.0.067116-0

Zhang, J., Cao, Z., Li, Z., Wang, L., Li, H., Wu, F., Jin, L., Li, X., Li, S., & Xu, Y. (2015). Effect of bacteriophages on *Vibrio alginolyticus* infection in the sea cucumber *Apostichopus japonicus* (*Selenka*). *Journal of the World Aquaculture Society, 46*(1), 149–158. https://doi.org/10.1111/jwas.12177

Zhou, S., Liu, Z., Song, J., & Chen, Y. (2023). Disarm the bacteria: What temperate phages can do. *Current Issues in Molecular Biology, 45*(2), 1149–1167. https://doi.org/10.3390/cimb45020110

Zhu, D., Yuan, D., Wang, M., Jia, R., Chen, S., Liu, M., Zhao, X., Yang, Q., Wu, Y., Zhang, S., Huang, J., Liu, Y., Zhang, L., Yu, Y., Pan, L., Chen, X., & Cheng, A. (2020). Emergence of a multidrug-resistant hypervirulent *Pasteurella multocida* ST342 strain with a *floR*-carrying plasmid. *Journal of Global Antimicrobial Resistance, 20*, 348–350. https://doi.org/10.1016/j.jgar.2019.09.012

Zhukov-Verezhnikov, N. N., Peremitina, L. D., Berillo, E. A., Komissarov, V. P., & Bardymov, V. M. (1978). Therapeutic effect of bacteriophage preparations in the complex treatment of suppurative surgical diseases. *Sovetskaia Meditsina, 12*, 64–66.

Ziagham, A., Gharibi, D., Mosallanejad, B., & Avizeh, R. (2024). Molecular characterization of *Pasteurella multocida* from cats and antibiotic sensitivity of the isolates. *Veterinary Medicine and Science, 10*(3), e1424. https://doi.org/10.1002/vms3.1424

Zimmerman, M. D., Proudfoot, M., Yakunin, A., & Minor, W. (2008). Structural insight into the mechanism of substrate specificity and catalytic activity of an HD-domain phosphohydrolase: The 5′-deoxyribonucleotidase YfbR from *Escherichia coli*. *Journal of Molecular Biology, 378*(1), 215–226. https://doi.org/10.1016/j.jmb.2008.02.036

Łusiak-Szelachowska, M., Weber-Dąbrowska, B., Jończyk-Matysiak, E., Wojciechowska, R., & Górski, A. (2017). Bacteriophages in the gastrointestinal tract and their implications. *Gut Pathogens, 9*(1), 44. https://doi.org/10.1186/s13099-017-0196-7

Żbikowska, K., Michalczuk, M., & Dolka, B. (2020). The use of bacteriophages in the poultry industry. *Animals, 10*(5), 872. https://doi.org/10.3390/ani10050872